Brain homeostasis in the context of the endocannabinoid system and trauma-induced disorders

Dissertation submitted in fulfillment
of the requirements for the academic degree of

Doctor in natural sciences

from the faculty of Biology of the

Presented by:

Diego Pascual Cuadrado
Born on April 16th, 1990 in Madrid, Spain

Tag der mündlichen Prüfung: 28 / May / 2020

A mi familia, por todo el apoyo y cariño que me han brindado durante estos años.

Y a todos aquellos que han estado a mi lado y me han dado fuerzas durante este largo viaje.

Table of contents

1. Summary / Zusammenfassung

1.1 Summary

Biological homeostasis is a dynamic equilibrium in which internal physiological parameters, such as pH, osmotic pressure or temperature, are actively kept within a specific range in the organism. The homeostatic range is not fixed and may change throughout the lifespan of an individual. However, the homeostatic state can also be transiently modified in the presence of internal or external perturbations. The aim of this new homeostasis, or also called allostatic state, is to facilitate the adaptability of the organism.

Brain homeostasis should ensure the optimal conditions for an efficient and correct flow of information within the nervous system and, as a consequence, the survival of the individual. However, neurons are very sensitive cells that require a tight control of their neuronal activity to avoid cellular damage and maladaptive responses. The endocannabinoid system (ECS) is a major neuromodulatory signaling system and has fundamental roles in restoring neuronal homeostasis once the neural signal has been transmitted. Furthermore, the high and widespread abundance of the ECS across different brain regions and cell populations suggests its relevance for the optimal functioning of the brain as a whole. One of the aims of this thesis was to characterize the hippocampal transcriptome of mice lacking the cannabinoid type 1 receptor (CB1), the main receptor of the ECS, in either glutamatergic or GABAergic neurons. The consequence of these genetic manipulations is an excess of excitatory and inhibitory neurotransmission at the synapses, respectively. Under basal, non-stressed conditions, these mutant mice are very similar in their behavioral phenotype as compared to their wild-type controls, yet their neuronal morphology is strongly altered. However, upon external challenges, the transcriptome was observed to react very differently in each conditional CB1 mutants and, partly, even in a dichotomic manner. These observations suggest that the brains of these two conditional CB1 mutants have adopted different allostatic states in response to an excess of excitation and inhibition, respectively, as compared to the wild-type control mice. Understanding how to reach and modulate these allostatic states could be relevant for specific pathologies, such as epilepsy or stress-related disorders.

There is a plethora of factors that influences brain homeostasis, such as developmental stage, past experiences and genetics. As a consequence thereof, two individuals cannot have an identical brain homeostasis, which has important implications in psychiatric

disorders, such as depression and stress-related pathologies. We hypothesize that the wide dispersion of behavioral responses observed in populations exposed to the same stressor or traumatic experience is a result of differences in the individual's brain homeostasis. Thus, these differences would translate in different stress coping abilities, with individuals classified as either resilient, when they can successfully deal with the stressor, or susceptible, when they develop serious disorders. In this context, we developed a single-trauma stress model to induce posttraumatic stress disorder (PTSD)-like behaviors in mice. Our first aim was to study the behavior of trauma-exposed mice and determine which of them showed a resilient or susceptible phenotype, using for this purpose a set of pre-defined features based on the diagnostic criteria of human PTSD patients. Our final goal was to characterize different brain regions from the resulting phenotypes at different molecular levels and search for putative mechanisms that could explain the behavioral differences. This approach is proposed to improve the segregation of trauma-exposed mice into the resilient and susceptible phenotypes and, thus, should help to understand the underlying neurobiological mechanisms.

1.2 Zusammenfassung

Die biologische Homöostase ist ein dynamisches Gleichgewicht, welches durch interne physiologische Parameter wie pH-Wert, osmotischer Druck oder Temperatur im Organismus aktiv in einem bestimmten Bereich gehalten wird. Dieser homöostatische Bereich ist nicht statisch und kann sich, über die Lebensspanne eines Individuums hinweg, ändern. Der homöostatische Zustand kann jedoch auch, durch das Auftreten interner oder externer Störungen, vorübergehend modifiziert werden. Ziel dieser neuen Homöostase, auch allostatischer Zustand genannt, ist es die Anpassungsfähigkeit des Organismus zu ermöglichen.

Die Homöostase des Gehirns sollte die optimalen Bedingungen für einen effizienten und korrekten Informationsfluss innerhalb des Nervensystems und folglich für das Überleben des Individuums gewährleisten. Neuronen sind jedoch sehr empfindliche Zellen, die eine strenge Kontrolle ihrer neuronalen Aktivität erfordern, um Zellschäden und Fehlanpassungen zu vermeiden. Das Endocannabinoidsystem (ECS) ist ein wichtiges neuromodulatorisches Signalsystem und spielt eine grundlegende Rolle bei der Wiederherstellung der neuronalen Homöostase, nachdem das neuronale Signal übertragen wurde. Darüber hinaus legt die hohe Präsenz des ECS über verschiedene Hirnregionen und Zellpopulationen hinweg nahe, dass es für eine optimale Funktionsweise des gesamten Gehirns von Bedeutung ist. Eines der Ziele dieser Arbeit war die Charakterisierung des Hippocampus-Transkriptoms von Mäusen, denen der Cannabinoid-Typ-1-Rezeptor (CB1), der Hauptrezeptor des ECS, entweder in glutamatergen oder in GABAergen Neuronen fehlt. Die Folge dieser genetischen Manipulationen ist ein Übermaß an exzitatorischer, respektive inhibitorischer Neurotransmission an den Synapsen. Unter basalen, nicht gestressten Bedingungen weisen diese Mausmutanten einen Verhaltensphänotyp auf, welcher dem der Wildtyp-Kontrollmäusen sehr ähnelt; die Morphologie der Dendriten zeigt hingegen starke Veränderungen auf. Es wurde auch gezeigt, dass das Transkriptom auf extern induzierte Anforderungen in jeder konditionalen CB1-Mutante sehr unterschiedlich und teilweise sogar dichotomisch reagiert. Diese Beobachtungen legen nahe, dass die Gehirne dieser beiden konditionalen CB1-Mutanten im Vergleich zu den Wildtyp-Kontrollmäusen in unterschiedliche allostatische Zustände, als Reaktion auf ein Übermaß an Erregung bzw. Hemmung, übergegangen sind. Das Verständnis, wie diese allostatischen Zustände erreicht und moduliert werden können, könnte für bestimmte Pathologien, wie Epilepsie oder stressbedingte Störungen, relevant sein.

Es gibt eine Vielzahl von Faktoren, die die Homöostase des Gehirns beeinflussen, wie z. B. das Entwicklungsstadium, vergangene Erfahrungen und Genetik. Infolgedessen

werden zwei Individuen keine identische Hirnhomöostase aufweisen, was wichtige Auswirkungen auf psychiatrische Störungen wie Depressionen und stressbedingte Pathologien hat. Wir nehmen an, dass die große Streuung der Verhaltensreaktionen, welche in Populationen, die demselben Stressfaktor oder derselben traumatischen Erfahrung ausgesetzt sind, auf Unterschiede in der Hirnhomöostase des Individuums zurückzuführen ist. Diese Unterschiede würden sich somit in unterschiedlichen Stressbewältigungsfähigkeiten niederschlagen, wobei Personen entweder als belastbar eingestuft werden, wenn sie erfolgreich mit dem Stressor umgehen können, oder als anfällig, wenn sie schwerwiegende Störungen entwickeln. In diesem Zusammenhang haben wir ein Single-Trauma-Stressmodell entwickelt, um posttraumatische Belastungsstörungen (PTBS) bei Mäusen zu induzieren. Unser erstes Ziel war es, das Verhalten traumatisch exponierter Mäuse zu untersuchen und zu bestimmen, welche davon einen widerstandsfähigen oder anfälligen Phänotyp aufweisen. Zu diesem Zweck verwendeten wir eine Reihe vordefinierter Merkmale, basierend auf diagnostischen Kriterien menschlicher PTBS-Patienten

Unser Endziel war es, verschiedene Hirnregionen aus den resultierenden Phänotypen auf verschiedenen molekularen Ebenen zu charakterisieren und nach potentiellen Mechanismen zu suchen, die die Verhaltensunterschiede erklären könnten. Dieser Ansatz soll die Trennung traumatisch exponierter Mäuse in die belastbaren und anfälligen Phänotypen optimieren und somit zum Verständnis der zu Grunde liegenden neurobiologischen Mechanismen beitragen.

2. Introduction

2.1 Physiological homeostasis

Life is an obviously complex process in which various elements combine and interact with each other to construct layer upon layer of ever-increasing complexity. These layers are organized hierarchically, and they interact with each other to construct the organism. However, organisms need to push constantly against the natural laws of thermodynamics, which drive any system to a static equilibrium point, where its entropy, or "disorder", is at its maximum. Therefore, organisms must be capable to regulate themselves in order to keep all their inner components and interactions functioning in the most optimal conditions, in order to thrive and survive. These optimized conditions are what is called homeostasis, or the state of steady internal physical and chemical conditions maintained by living organisms.

Throughout history, there has been numerous attempts to give "life" an interdisciplinary definition, although it has remained an elusive task [1]. Classic overlapping definitions of life include "the maintenance of internal homeostasis, within a functionally and structurally integrated entity, against changes in the environment, with the ability to adapt in response to external stimuli, as well as feedback mechanisms that regulate the responses" [2–4]. The interdisciplinary study of cybernetics was defined in 1948 by Norbert Wiener as "the scientific study of control and communication in the animal and the machine" [5], or, simplified, how organisms and machines control themselves and communicate with each other. According to cybernetics, the main regulatory mechanism within a system is the negative feedback loop, in which any deviation of a certain parameter from the optimal range generates a counteraction of a proportional magnitude. This mechanism has been found in all species examined so far [6–8] and ensures that the higher the parameter deviates from the optimal range the stronger the response of the negative feedback and, subsequently, the faster that parameter is stabilized and maintained within an optimal range. This theory of cybernetics led to a definition of life as a set of living individuals, each of them composed of unique networks of negative feedbacks subordinated to a superior positive feedback, which is self-sustaining and self-reproducing. The whole complex of negative feedbacks within an organism act as regulatory mechanisms on and across different hierarchical levels, being all interconnected directly or indirectly. Thus, this implies that one negative feedback can influence a parameter that functions as an element of another negative feedback on the same or on a different level of hierarchy [9]. A homeostatic mechanism (e.g. thermoregulation) to function requires at least three fundamental independent elements:

a sensor (e.g. thermoreceptors), a control center (e.g. hypothalamus) and an effector (e.g. sweat glands or behavioral centers in the brain) [10] (Figure 1). In biology, homeostatic mechanisms are essential to regulate a plethora of biological processes, such as ion or oxygen levels in the inner fluids, internal pH, neurotransmission or even gene expression patterns.

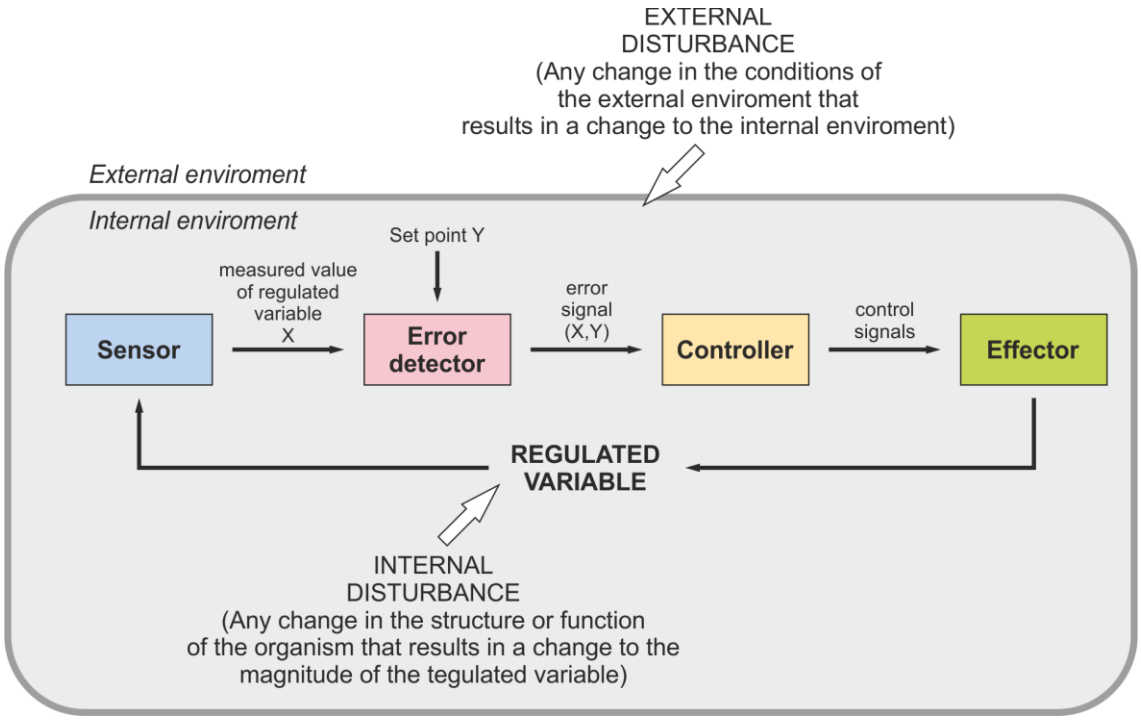

Figure 1. Schematic representation of a homeostatic control mechanism. The disturbance of a regulated variable due to external or internal stimuli is received and measured by a sensor (value X). This sensor sends the information to the control center where X is compared against the pre-set target value (value Y). The control center generates an error signal, whose magnitude is proportional to the deviation between X and Y. Lastly, the information is passed on to an effector, which elicits the behavioral, physiological or biochemical response. Taken from Modell et al (2015).

Physiological homeostasis is the internal state of dynamic equilibrium in which an organism functions in the most optimal way for best survival. This process includes many parameters being kept within pre-set limits, or homeostatic range, as well as the internal mechanisms to respond to internal or external insults. Although it might sound as if organisms act to keep their basal inner state completely static over their lifespan, nothing could be farther from the truth, as the constant influence of the environment forces changes in the homeostatic range in order to adapt to the new conditions (allostasis). Although most of the allostatic changes are transient (e.g. adequate stress response), sometimes different factors require an allostatic state, or a homeostasis significantly different to most of the conspecifics, in order to survive. Furthermore, almost every biological process is stochastic and, therefore, noisy (e.g. biochemical signaling, gene expression, etc.). This noise leads to substantial fluctuations that are regulated and kept

within particular range by a plethora of homeostatic processes. Moreover, the homeostatic range can suffer allostatic processes and change depending on different factors, such as developmental context or external stimuli, so it is bold to assume that two identical organisms will have the exact same internal state. As an example, it has been observed that two identical neurons, under the same activity patterns, display heterogeneities in their conductance profiles, an intrinsic property of the neuron that is homeostatically regulated, even when the cells are coupled [11].

All homeostatic mechanisms are fundamental in general cellular processes within the organism, but they are especially important in the central nervous system (CNS). The role of neurons in information processing, as well as their organization in highly connected multicellular networks, makes brain homeostasis a very interesting research topic, as neurons need to be tightly regulated in order to maintain an efficient flow of information. The essential function of neurons in information processing means that these cells must regulate their biophysical properties to satisfy specific constraints, which might change through their lifespan. Neurons modify their intrinsic properties through different compensatory mechanisms, such as the transcriptional [12] and post-transcriptional regulation of ion channels [13,14], neurotransmission-associated proteins [15], proteins involved in synaptic modulation [16,17], or by modulating their firing rate [18]. Furthermore, neurons are integrated in complex, highly interconnected, multicellular circuits, meaning that regulatory adjustments within individual cells have knock-on effects that influence other components of the circuit and even the organism as a whole [19]. Given the peculiarities of the CNS and the hierarchical structure of homeostatic mechanisms, it is not inconceivable that certain types of homeostatic compensations arise merely as a consequence of the collective, low-level regulation of the neuron´s basic components [20–22]. Emergent properties are a characteristic specific of complex systems in which a property arises through the coordinated action of all the components, with none of single parts possessing that trait beforehand. The emergence of homeostatic mechanisms in the CNS is likely a consequence of the interaction across hierarchical levels of different regulatory mechanisms, as well as the intrinsic complexity of the brain, and responds to the necessity of the CNS to regulate itself as a whole, instead of each of its single parts [23].

Homeostasis in the CNS is of utmost importance for an organism, as the brain is the main control center for most of the behavioral and physiological responses. The high complexity of the CNS matches the equally high complexity of its homeostatic mechanisms, from the low-level regulation of gene and protein expression, to the regulation of the intrinsic properties of neurons and up to the modulation of synaptic

activity by glial cells to regulate entire neuronal networks. The dysregulation of homeostatic processes in the brain can lead to a cascade of maladaptive responses that can jeopardize the survival of the organism and, therefore, they must be finely regulated to ensure the present and future adaptation of the organism.

2.2 The stress response

The environment (both exogenous and endogenous) presents organisms with a multitude of challenges, such as temperature changes, the need to obtain food and water, potential attacks by conspecifics and predators, or the need to find a mate. In order to overcome these challenges and to survive, organisms must have evolved a transient, adaptive response that allows them to react quickly to a potential threat in order to promote their chances of survival at any cost. The biological stress response consists on a set of behavioral, metabolic and physiological changes, triggered in a stressful situation, defined as when environmental demands exceed the natural coping resources of the organism [24]. The key point of this definition is that the trigger for the stress response is the external demand for change [25], thus linking stress and homeostasis. From a homeostatic point of view, the stress response shifts the pre-set homeostatic ranges of all the inner systems implicated to a new temporary allostatic state, i.e. a set of homeostatic ranges for internal parameters different from the basal homeostatic range. However, maintaining the allostatic state is very costly energetically and, therefore, the basal homeostatic state must be restored once the stressor is no longer present. The stress response not only occurs in response to what it is typically considered negative stimuli, such as predation or threat, but also in response to what is regarded as positive and that requires energy mobilization, such as sexual behaviors [24].

The perception of the stressor, a stimulus capable of eliciting a biological stress response, and the psychological state, or stress, triggered as a consequence is highly subjective and unique for each individual, as it depends on a myriad of factors, such as the intensity, valence, and other properties of the stressor, as well as early experiences and the learning processes associated, including habituation and sensitization. The process of identifying a stimulus as a stressor depends on innate and learning mechanisms, as well as the interactions between them. These stimuli may be internal or external, systemic (normally not impinging on consciousness) or psychogenic (associated with the anticipation of a stressor although there is no current threat). Therefore, it is important to distinguish between “reactive responses”, primarily to internal stimuli (e.g. pain, inflammatory or homeostatic signals), and “anticipatory responses”, usually to external stimuli (e.g. predators, social challenges), as well as memory programs [26]. Studies of fear conditioning have helped elucidate the circuitry and the main

brain regions associated to fear and the fear response, showing that stimuli are analyzed at various neural levels in a hierarchical manner [27]. Visual and auditory stimuli are first processed in the thalamus, from where information is relayed through two pathways. An initial, basic analysis of the stimulus occurs in the amygdala, a brain region fundamental in the mediation of the stress response. The lateral amygdala (LA) is the sub-region that receives sensory inputs from other brain areas, whereas the central nucleus of the amygdala (CeA) is the main output gateway (Figure 2). The CeA sends the processed information to other regions in order to mount the endocrine and motor autonomic responses. This thalamoamygdala pathway is quick but at the expense of providing only raw information, unfiltered by any higher cognitive function. A second, slower pathway involves reciprocal thalamocortical and amygdaloid projections, connecting the thalamic regions with the amygdala and polysensory cortical areas, as well as the prefrontal cortex (PFC). These cortical areas not only send sensory information to be processed in the amygdala, but also modulate its response (Figure 2). The infralimbic subregion of the PFC can inhibit the amygdala output, playing an important role in the extinction of fear memories [27]. These reciprocal interactions allow for higher order cognitive processes (e.g. emotion, imagination, rumination, etc.) to influence the function of the amygdala and its output. Besides these brain regions and their role in processing stressful stimuli, the hippocampus has projections reaching the amygdala (LA and basal nucleus of the amygdala) and the PFC to provide information about the context of the stimulus. The amygdala integrates all the information from different brain regions and delivers an output to specific centers in the brain, such as the hypothalamus, which regulates the slow endocrine response to stress, or the striatum, which mediates behavioral instrumental responses such as avoidance or escape. Additionally, the amygdala also activates the sympathetic nervous system (SNS) to mobilize quickly energy resources, as well as triggering the initial stage of alarm [28] and the fight-or-flight response [29].

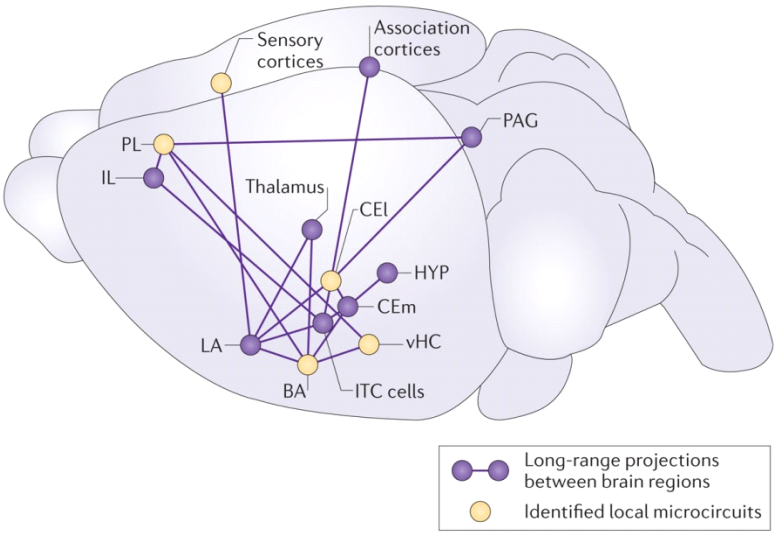

Figure 2. Relevant brain areas and circuits during the stress response. The perception of threats or stressors involves long-range excitatory and inhibitory connections between different brain regions, as well as local microcircuits within some of these regions. The basal (BA) and lateral (LA) amygdala areas are central in the modulation of whether an external element is perceived as a threat or not, based on inputs from cortical regions. Regions such as the prelimbic (PL) and infralimbic (IL) cortices, as well as the ventral hippocampus (vHC) provide additional layers of modulation to ensure an adequate response mediated by the hypothalamus (HYP). PAG, periaqueductal grey; CEl, central lateral amygdala; CeM, central medial amygdala; ITC, intercalated cells. Modified from Tovote et al. (2015).

2.2.1 Pathways of the stress response

The stress response strongly alters the internal physiology of the organism to increase adaptability to the current situation, usually a threat. In order to do so, the amygdala induces the stress response using two different mechanisms, involving different systems and organs across the whole organism: the hypothalamic-pituitary-adrenal (HPA) axis (Figure 3, right) and the sympathetic nervous system (SNS), including the sympathoadrenal-medullary (SAM) axis (Figure 3, left).

After the information about the stressor or potential threat has been integrated in the amygdala, the CeA signals the output response to the brain steam, increasing the release of noradrenaline from sympathetic nerve endings, and activating the SNS and the adrenal medulla. The activation of the SNS leads to an increase of noradrenaline in the blood stream, as well as glucocorticoids, estrogen and testosterone; whereas the SAM axis releases catecholamines (mostly adrenaline) also into the blood stream [30]. Besides the increase of these signaling molecules, the overall effect is the increase in arousal and vigilance, i.e. enhanced processing of external cues. Furthermore, the SNS innervates peripheral organs via the sympathetic ganglia, increasing blood pressure and heart rate, as well as diverting energy resources to the musculature and away from vegetative functions. The main goal of the SNS action is to adapt quickly the organism for the fight-or-flight response, in which the animal will either fight or flee to an immediate threat to survival [31]. Once the stress response is terminated, the parasympathetic system

returns the internal systems of the organism to their basal homeostasis, in order to avoid potential tissue damage.

Simultaneous to these events, a second mechanism against the stressor is acting in a slower manner. The hypothalamus is activated indirectly by the amygdala, via the bed nucleus of the stria terminalis (BNST) [26], releasing corticotropin-releasing hormone (CRH) from the paraventricular nucleus (PVN) and ensuing the activation of the HPA axis. CRH acts on the anterior pituitary by binding to the receptor CRH-R1, found abundantly in the pituitary and throughout the rest of the brain (e.g. limbic areas), and working synergistically with vasopressin [32]. Once the signal has reached the pituitary, proopiomelanocortin is cleaved into β-endorphins and adrenocorticotropic hormone (ACTH). ACTH is released into the blood circulation, in order to stimulate the synthesis of glucocorticoids (GC) (i.e. cortisol and corticosterone) in the adrenal cortex, leading to the release of GCs into the blood. GCs exert their effects via cytoplasmic, high-affinity mineralocorticoid (MR) and low-affinity glucocorticoid (GR) receptors [33], and their pharmacological blockade within the brain leads to the reduction of endocannabinoid (eCB) levels associated to the stress response [34]. Activated MRs and GRs translocate to the cell nucleus, where they serve as transcription factors to induce specific hormone-response genes, and to inhibit other transcription factors, such as NF-kB [32]. GCs stimulate the release of stored energy by glycolysis, lipolysis or proteolysis, and suppresses the highly demanding metabolic processes of the immune system [35]. Overall, GCs have profound effects on various brain processes, such as synaptic physiology, circuit responsiveness to stress and, ultimately, behavior [36]. The final goal of the activation of the HPA axis is to promote the physiological and behavioral adaptability of the organism.

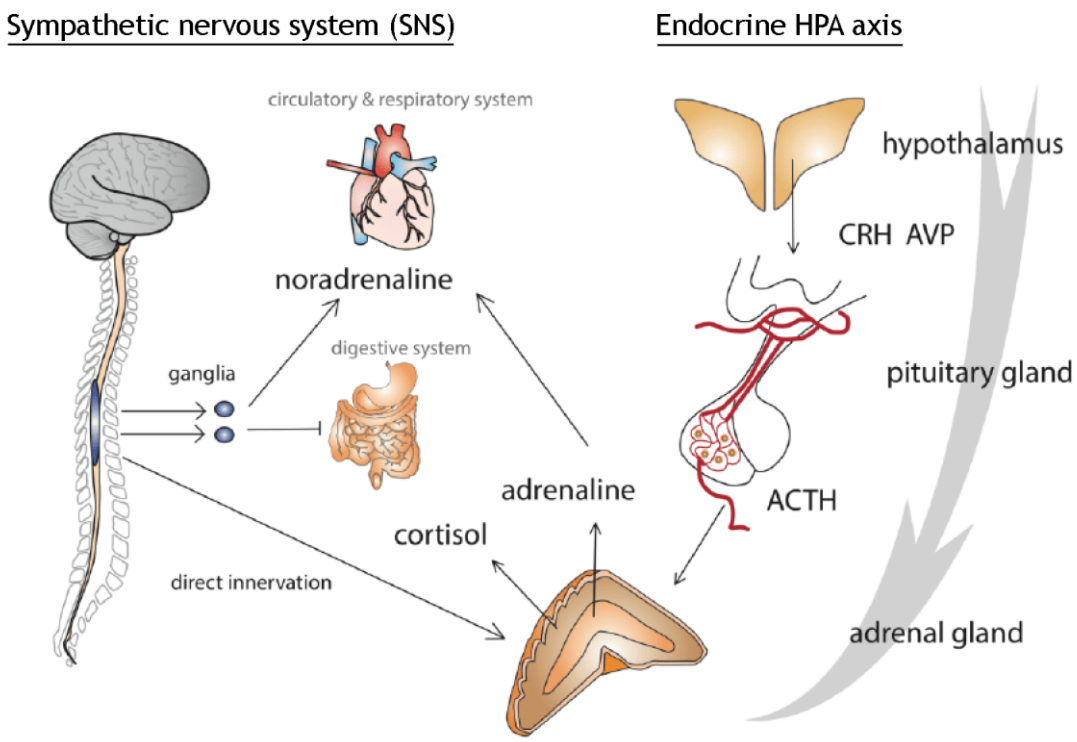

Figure 3. Stress response pathways from the autonomic nervous system and the endocrine system. Once the stress response is triggered, the sympathetic nervous system (SNS; left side) acts quickly to mobilize energy resources and direct them to the heart, lungs and muscles in case sudden bursts of exercise are necessary. Meanwhile, the slower HPA axis (right side) sends neuroendocrine signals from the hypothalamus to the pituitary gland and from there to the adrenal glands to produce stress hormones that will not only help the SNS in its function, but also promote long-term adaptations. CRH, corticotropin-releasing hormone; AVP, arginine vasopressin; ACTH, adrenocorticotropic hormone, Adapted from Ulrich and Herman, 2009.

Brain-stem structures mediate the response to stressors, both external and systemic, and allow for an integrated response of the HPA and the SNS. These two systems interact, and this interaction is essential for a correct stress response. Noradrenaline injections into the PVN stimulate CRH-containing cells via α1-adrenoreceptors [37], triggering the production of ACTH in the pituitary and creating a positive feedback loop. Reciprocally, CRH injections in the locus coeruleus increase the electrophysiological activity of noradrenergic neurons [38] and the levels of noradrenaline [39], as observed by *in vivo* microdialysis [37].

Due to the high toll imposed on the internal systems by the stress response, it is of utmost importance that the stress response is terminated whenever the stressor is gone. GCs acts as a negative feedback loop by inhibiting the hypothalamus and the pituitary, therefore suppressing the release of CRH, vasopressin, and the cleavage of proopiomelanocortin into ACTH. The goal of this negative feedback mechanism is to restore homeostasis quickly and avoid the potential damage to the internal systems associated to hyperactivity of the HPA and the SNS. A dysregulated stress response,

due the intensity, valence and/or duration of the stressor, can alter the internal homeostasis in the long-term and cause severe damage to some body systems. However, chronic stressors (or chronic administration of exogenous GCs) have been linked with hippocampal atrophy [40,41], HPA increased activity and reactivity [42], and mood disorders [43]. They are also the main suspects for the comorbidity of cardiovascular diseases with stress-related disorders [44].

2.2.2 Stress and the organism´s challenges

All organisms known to date have some sort of physiological response to stressful situations [45]. This prevalence indicates that the stress response must contain a positive, helpful value for survival throughout the history of life. However, the stressors are not the same now as they were millions of years ago. Evolution has played an essential role in shaping the stress response, so that its advantages outweigh its costs. Indeed, one of the consequences of this selective pressure is the appearance of “programs” in the stress response, with subtle differences that makes them specific for certain situations, such as facing a predator, fighting an infection, or facing a conspecific for mating or food, among others [45]. In the natural environment, the stress response is normally triggered by acute, physical stressors, with stress being a psychological feeling to trigger the alarm state of the organism. In a natural situation, the stress response works perfectly, as it quickly mobilizes the energy reserves to the muscles and increases heart rate and oxygen absorption in preparation for sudden bursts of exercise. Furthermore, it increases the general awareness of the organism, as well as it enhances cognitive functions (e.g. learning and memory) to increase adaptability in future encounters. This response is transient and, once the stressor is gone, the homeostatic state is quickly restored to avoid harmful side effects. However, the environment where most humans currently live differs enormously from the world in which our ancestors lived.

Nowadays, most of the human population lives in industrialized cities and faces an array of stressors, many of which are specific to modern societies. Contrary to the stressors faced by communities of hunter-gatherers in the past, stress in big conglomerates of people have mostly a social and/or psychological origin and tend to last longer in time, even becoming chronic. Unfortunately, the stress response has not evolved in parallel to respond to these new conditions, meaning that the dysregulation of homeostasis caused by stress may be triggered by stressors that do not require a physical response, such as deadlines and schedules, online harassment and abuse, discrimination, etc., or that the stress-induced dysregulation becomes chronic, causing a heavy toll on the organism. Although psychological stress is a phenotypic state necessary for mankind’s survival, its chronification has been characterized as an immune-altering factor associated with a

wide range of allergic, cardiovascular, autoimmune, and other inflammatory-related diseases [46].

An atypical stress response due to physical, mental or emotional stress can carry short- and long-term physiological consequences that cause impairments in the daily life, such as chronic migraines, asthma attacks, increased risk for hypertension and heart strokes, inflammation in the coronary arteries, dysregulated endocrine system with increased levels of stress hormones, bloating, nausea and fertility problems, among others [47]. Besides the physiological effects of stress in the organism, emotional and mental impairments are also of high relevance, as they can develop into chronic mental health disorders. These disorders are defined in the "Diagnostic and statistical manual of mental disorders, fifth edition" (DSM-5) as stress-related disorders. However, before explaining the most common stress-related disorders, it is important to clarify the differences between stressful and traumatic experiences.

2.2.3 Stress is not trauma

The consequences of a maladaptive stress response are very different across individuals and depend, not only on intrinsic properties of the stressor, but also on the past experiences and the own perception of the individual. Stress-induced pathologies appear most commonly after chronic periods of stress, although single stressful events are also known to trigger this type of disorders, but less frequently. Most of the stressors that an individual will face in their lifetime, induce a canonical stress response, which turns pathological under special circumstances of the individual, e.g. life experiences or developmental stage, or when the response extends too long in time, either because the stressor is still present or the inability of the organism to return to homeostasis.

However, certain stressors or their chronification can induce psychological traumas, a damage to the mind as a result of a distressing event that makes the individual unable to cope with or integrate the emotions related to that experience. Trauma is defined in DSM-5 as the "exposure to actual or threatened death, serious injury, or sexual violence" [48], and the manual specifies that the exposure to the event can mean directly experiencing it, witnessing it in person, learning about it when it involves a close person, or being exposed often to the aftermath of such experiences (like in the case of first responders). The events that trigger traumas are emotionally painful, intense and distressing and generally outside of the scope of daily human experiences (e.g. murder, rape), although chronic stress can also become traumatic (e.g. bullying, discrimination). Traumatic events trigger an emotional response on top of the general stress response, with unique psychological long-term consequences [49]. People with traumas often

develop involuntary recurring memories, or flashbacks, in which they re-experience explicit and intense moments of the traumatic event, causing intense fear, helplessness or horror [50]. These flashbacks damage the own image of self and safety, and induce severe symptoms, such as hyperarousal and panic attacks, the abuse of psychoactive substances, emotional detachment and dissociation, sleep deprivation, and mood disorders, such as anxiety and depression [51–53]. In addition, constant re-experiencing of the trauma has been linked to neurophysiological changes, such as slowed myelination, abnormalities in synaptic pruning, shrinking of the hippocampus, and cognitive and affective impairments [54,55]. The number and severity of symptoms varies a lot between different individuals and depends on different factors, such as developmental stage, past life experiences, type of trauma, emotional support they receive, and resilience mechanisms intrinsic to that person, among many other factors.

Like with the stress response, the physiological and emotional reactions to traumatic events help the individual cope with the distressing experience and move on with life. Thus, the trauma response must be transient and have a termination point to avoid a chronic dysregulation and the potential psychological damage associated with. Surprisingly, only 5-15% of the people exposed to trauma will develop severe long-term impairments, such as posttraumatic stress disorder (PTSD), whereas the rest will recover from the experience and move on with their lives. This observation highlights the high variability found in stress- or trauma-induced disorders and indicates the presence of internal resilience mechanisms to cope with distressing situations.

2.3 Stress-related disorders

As mentioned above, the feeling of stress (and its consequences thereof) is highly subjective and depends on a lot of environmental, genetic and developmental factors that are specific for each individual. This fact makes the boundaries of psychiatric disorders thin and hard to limit. Therefore, several attempts have been made to standardize the definition, diagnosis and treatment of stress-related disorders. The two most commonly used examples are the DSM-V [56], by the American psychiatry association, and the “ICD-10 Classification of mental and behavioral disorders”, by the world health organization. These manuals help to unify the definition and symptomatic panel for a wide variety of psychiatric disorders, and provide diagnostic criteria based on empirical evidence. Although both manuals have been extremely helpful, each of them has drawn criticism and controversy in certain aspects, showing the lack of consensus that exists for the criteria of some psychiatric disorders.

2.3.1 Anxiety disorders

Anxiety disorders are a group of mental disorders characterized by intense, and normally chronic, feelings of anxiety, or worry about future events, and fear, as a reaction to current events. Each year, about 12% of the people are affected by an anxiety disorder and between 5% and 30% are affected over a lifetime. They generally begin before the age of 25 and affect women twice as often as males [57]. The most common cause for triggering anxiety disorders is stress, although genetics, medical conditions and substance abuse (e.g. alcohol, drugs, caffeine, etc.) can increase susceptibility towards them [58–60]. Anxiety disorders are usually triggered by moments of high stress and are accompanied by physiological symptoms, such as headache, muscle spasms, sweating, tachycardia and hypertension. Moreover, in about 50% of patients with generalized anxiety there is comorbidity with depression or other anxiety disorder [61]. As for the neurobiological causes of anxiety, low levels of γ-aminobutyric acid (GABA) have been linked to increased anxiety [62,63], and the use of selective serotonin reuptake inhibitors have proved useful as a first line treatment [64]. Furthermore, the amygdala is fundamental to the processing of fear and anxiety, and neural dysregulations in the basolateral amygdala (BLA) are known to increase anxiety levels [65,66]. Unfortunately, there are no known objective biomarkers associated with anxiety disorders, and their diagnoses relies on long-lasting symptoms (> 6 months) instead [48].

Among the different disorders englobed under anxiety, generalized anxiety disorder (GAD) is the most commonly associated to the public concept of anxiety. GAD is characterized by excessive, uncontrollable, and often irrational worry about events or activities, causing restlessness, trouble sleeping, irritability, and trembling among others. GAD also interferes with daily life functioning and causes social, cognitive and emotional impairments to the sufferer [67]. However, there are many other (and even more common) anxiety disorders besides GAD, such as specific phobias, panic disorders, agoraphobia, social or separation anxiety, obsessive-compulsive disorder, selective mutism or PTSD.

2.3.2 Major depressive disorder

Major depressive disorder (MDD), also simply known as depression, is one of the most prevalent mental health disorders of modern times [68]. MDD is often accompanied with low self-esteem, loss of interest in activities that would normally be enjoyable (anhedonia), low energy and pain without reason. Depression is very variable across patients, with some people having sporadic episodes separated by years, whereas others suffer from the symptoms almost constantly. In both cases, during depressive episodes, the negative effects on the patient´s daily life is severe, affecting even eating habits, personal hygiene and general health [69]. Between 2% and 8% of adults diagnosed

with MDD die by suicide, whereas 50% of those who commit suicide had depression or another mood disorder [70]. Globally, the prevalence of MDD is ~3% of the world population. However, developed nations have higher lifetime rates (15%) when compared to developing countries (11%) and the percentages vary significantly between geographical regions [71]. Typical onset time of depression is at the age of 20-30 years and affects women almost twice as often as men. Typically, treatment options consist on anti-depressant medication and counseling, such as cognitive behavioral therapy or interpersonal therapy [72,73]. The medication appears to be effective, although its efficacy is highly variable among patients [73], and it is not proven that it affects the risk of suicide [74]. When therapy does not work, other more invasive options such as electroconvulsive therapy may be considered.

The pathophysiology of MDD is not fully understood, although current studies revolve around monoaminergic systems [75], circadian rhythm, immunological [76] and HPA axis dysfunction [77,78], as well as structural and functional abnormalities of neural circuits related to reward and emotion [79,80]. The main issue to study the physiological consequences of depression is the high heterogeneity of data found among patients. Insufficient activity of monoaminergic systems in depressed patients have been extensively studied and, for a long time, it was the main theory to explain the biology of depression. It has been observed that acute depletion of tryptophan, a necessary precursor of the monoamine serotonin, can cause depression in patients with predisposition [75,81], and there is a correlation between the depression risk and polymorphisms found in the gene of serotonin receptors (5-HTTLPR). An increased activity of monoamine oxidase, the enzyme to degrade monoamines, has also been associated to depression [82]. Despite these observations, the heterogeneity of symptoms and therapy efficacy found across patients, as well as new studies, have brought into question the monoamine theory as the only cause for depression [83]. Currently, the research scope for depression has expanded to include epigenetic mechanisms, such as histone deacetylation or methylation [84], on gene networks relevant to brain function (e.g. the brain- and glia-derived neurotrophic factors BDNF and GDNF, respectively) or the stress response (e.g. GR and genes of the HPA axis) [85–87].

2.3.3 Other stress-related disorders

Stress induces many other pathological phenotypes in patients exposed to chronic and traumatic stressors, as well as acute stressors that repeat episodically. Acute stress disorder is the most common response to intense physical or psychological stressors and shares similarities with the general stress response which generally subside within hours or days, depending on the individual´s coping mechanisms. If the symptoms of the

acute stress disorder prolong long enough (> 1 month), it is then considered PTSD, a severe stress-related disorder with unique peculiarities which will be covered most extensively on Chapter 4 of this thesis.

2.4 Resilience and susceptibility to stress

The different stimuli and stressors that an individual encounters throughout its life shape core parameters of such individual. Early-life stress is particularly relevant later on in life, as it may induce permanent changes in gene expression profiles, neural circuitries and physiology, all of which will have an impact during adulthood. One of the resulting consequences is the appearance of individual heterogeneities at the behavioral, neurobiological and physiological level when stressed. The response to stress is especially interesting, because the individual outcomes from a population exposed to a stressful experience will differ significantly, meaning some individuals will cope with the situation and continue with their lives, whereas others will develop some form of mental health disorder and suffer severe impairments. This observation settled the basis for a new approach to stress-related disorders: the study of psychological resilience and its internal mechanisms, as a way to prevent mental health disorders [88,89].

Although the stress response is normally protective, it can become severely damaging if it is dysregulated or if it fails to cease once the exposure to the stressor is terminated. Upon exposure to any stressor that exceeds the individual´s coping capacity, e.g. traumatic stress, different internal mechanisms actively try to counter negative physiological effects derived from a dysregulated stress response. Such putative resilience mechanisms act on different levels and tissues within the organism and help the individual restore its physical, emotional and psychological homeostasis to ensure no long-term deleterious effect. Stress resilience is not something one is born with, although genetic predisposition to stress is well documented [90], but rather something that is developed throughout life and shaped by the environment and previous life experiences. When resilience mechanisms fail to cope with the stress, the resulting imbalances within the organism´s biology increase the likelihood of developing mental health disorders. Importantly, stress resilience does not grant immunity against stress, but rather provides physiological and psychological mechanisms to cope with it. However, significant individual differences arise across individuals in the type of strategies used and the way to use them when facing stressors [91], which increases the difficulty to establish causal relations. This observed heterogeneity also complicates the replication of experiments and causes contradictory findings [92]. Therefore, more research is required to unravel and confirm potential resilience mechanisms (Figure 4).

2.4.1 Psychological phenotype of resilience and susceptibility

Although the molecular and neurobiological basis for resilience and susceptibility have been studied for around two decades now, research on the topic started in the early 1970s from a psychological point of view [88]. The motivation was to understand the protective factors that explain the capabilities of certain individuals to adapt and cope with stress. These mental processes and behaviors allowed individuals within a population exposed to a stressor to remain calm during the incident and to move on without long term negative consequences.

From the psychological perspective, three bases (among many others) for resilience are mainly discussed: self-confidence, self-esteem and self-concept. However, resilience processes are not limited to characteristics of the individual, but also to environmental factors that increase the sense of protection, such as a good family, community or social policies [93]. Resilient individuals commonly correlate with personality traits of openness, positive emotionality, which promotes

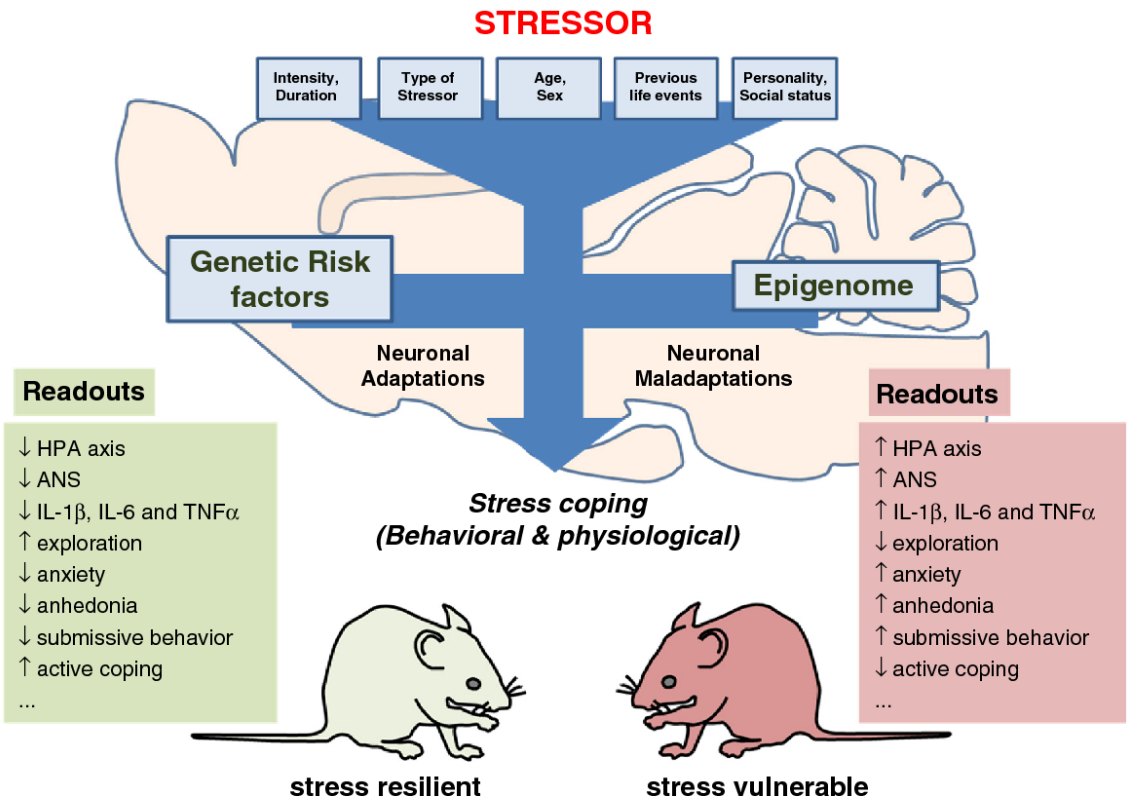

Figure 4. Schematic illustration of the effects of gene x environment interactions in stress resilient and susceptible individuals. Intrinsic properties of the stressor (intensity, duration, type, etc.) and individual differences (age, sex, previous life events, etc.) interact with genetic risk factors and the epigenome to shape the physiological response to stress and, therefore, the coping capacity of the individual. The outcome will be an internal environment that favors resilience or susceptibility to stress. Adapted from Ebner and Singewald, 2017.

cognitive flexibility and problem solving in the face of adversity, and grit, or the individual perseverance of effort combined with the passion for a particular long term goal or end

state [94]. These individuals tend to engage and confront the world with confidence in success and a fair value of self-directedness [95]. Positive emotions have also physiological consequences, as they have been associated to improved functionality of the immune system [96], among many other benefits. On the contrary, susceptible individuals correlate with negative personality traits, such as neuroticism and negative emotionality, and also tend to see and react to the world as threatening, problematic and distressing, as well as seeing themselves as vulnerable [95].

2.4.2 Molecular and physiological findings of resilience and susceptibility

The response to stress, and the arising resilience mechanisms to counter its deleterious effects, depends on many different variables. Although the environment and developmental stage are important factors, some genetic findings suggest there is some degree of predisposition [90]. Although current findings consist on candidate genes with relatively weak associations, such as *fkbp5*, *npy*, *crhr1*, *adcyap1r1* or *slc6a4*^{LRP} [97–99], the field is moving consistently towards genome-wide analysis with large cohorts, which increases the chances of finding causal relationships between different alleles and the individual's resilience status. Some of these genes are important for the proper function of the HPA axis. Furthermore, the sensitivity and reactivity of the HPA axis and the autonomic nervous system are being studied as potential predictive biomarkers, as it has been observed that individuals suffering from mental health disorders have a more hyperactive stress response [100]. However, contradictory findings in MDD and PTSD patients currently make the relationship between HPA axis and stress resilience unclear. Within the neuroendocrine system, GRs and MRs are very interesting as they can regulate corticosterone and cortisol (in mice and humans, respectively) signaling and modulate the behavioral response to stress. Indeed, genes related to GR signaling have been shown to be differentially expressed in the amygdala and hippocampus using genome-wide analyses [101]. Similarly, MRs appear to be up- or down-regulated in different brain regions upon chronic social defeat, and the phenotypic outcome depends on the brain region where the MR gene is dysregulated. For example, lower expression of MR in the hippocampus was described to increase stress susceptibility [102], whereas overexpression of MR in the medial PFC results in decreased anxiety-like behavior and suppressed HPA axis response [103].

Other molecules have also been found to play a major role in increasing the resilience or susceptibility to stress. Dehydroepiandrosterone (DHEA), a precursor for the synthesis of anabolic steroids, is released from the adrenal cortex during stress to counter the effects of cortisol and to exert antioxidant and anti-inflammatory effect. The DHEA-to-cortisol ratio has been associated to resilience and increased coping [104], but

one study had previously linked DHEA to increased suicide rate in patients with PTSD [105]. Neuropeptide Y (NPY), a peptide neurotransmitter, might be protective under high stress conditions, with higher levels being predictive of decreased psychological distress and dissociative symptoms [106]. Although not directly related to the HPA axis and the stress response, blockade of hippocampal BDNF signaling induces vulnerability, and this phenotype can be reversed by intrahippocampal infusions of a BDNF mimetic [107]. Although polymorphisms and other genetic factors are relevant in the study of resilience and susceptibility to stress, research is recently moving towards uncovering their epigenetic basis in the search of potential therapeutic targets and predictive markers [108,109].

The modulation of the stress response and the systems involved is not the only mechanism to cope with stress. The immune system heavily influences neurobiological and neuroendocrine responses. In individuals characterized by stress-related disorders, increased concentrations of pro-inflammatory interleukins, such as IL-6, IL-1ß, and TNFα, have been observed in blood samples, as well as monocyte infiltration through the blood-brain barrier and microglial activation [110]. Furthermore, modifications of the intrinsic properties of neurons and circuits have also been associated to resilient or susceptible phenotypes, although it is not yet clear whether these changes are active mechanisms or part of a compensatory effect due to stress-induced neuronal over-activation. How the changes in neuronal properties will affect the behavioral and physiological outcome depend on which neuronal population and brain region are affected. However, the modulation of intrinsic excitability is mediated , among others, via potassium (K^+) channels that regulate the firing rate of the neuron [111–114].

2.4.3 Neural circuits involved in resilience/susceptibility

During the stress response, different brain regions activate and interact with each other to modulate and/or to regulate the behavioral, emotional and physiological responses. In studying resilience, these brain regions and associated neural circuits are a valuable trove of information, as alterations in their functionality can induce a dysregulated response, increasing the likelihood of stress-related disorders, or the opposite, to restore partially or fully the homeostatic state.

The hippocampus is central in the regulation and termination of the stress response via a GR-mediated negative feedback loop. However, the hippocampus is modulated itself by glucocorticoids, which normally induce beneficial effects unless the stress becomes detrimental [115]. This region has also direct and indirect connections to the PVN, one of the main centers for the stress response and essential for its initiation. Dysfunctions of

hippocampal glutamatergic neurotransmission, maladaptive structural and functional changes in hippocampal circuitry, and decreased hippocampal volume have been observed in stress-related conditions [116], whereas facilitated glutamatergic plasticity in the dentate gyrus (DG) enhances exploratory behaviors [117]. Thus, glutamatergic transmission appears to be central to the regulatory function of the hippocampus (Figure 5). Indeed, different alterations in neuronal and glial glutamate transport and reuptake have been observed between basal and stress conditions [118,119]. Glutamate receptors, such as NMDA and AMPA receptors, are also modulated by glucocorticoids. AMPA receptors are particularly interesting, as vulnerable individuals have fewer GluR1 subunits, but higher number of GluR2 subunits in CA1 and DG subregions of the dorsal hippocampus [120]. Additionally, BDNF is both necessary and sufficient to increase resilience, as its overexpression in the adult DG blocks the anhedonic effects of stress, while its knockdown in young animals elevates corticosterone levels and induces depressive-like behaviors [121,122].

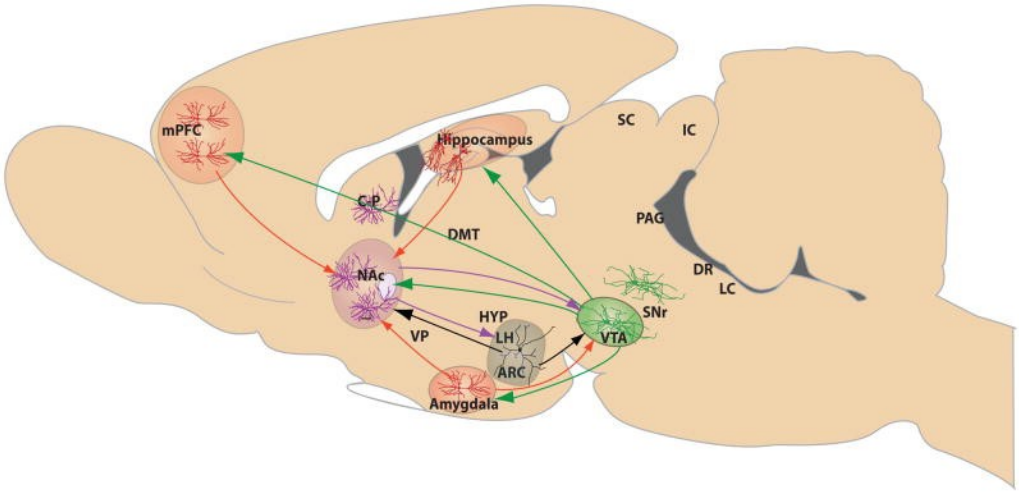

Figure 5. Brain regions and circuits involved in stress resilience and susceptibility processes. Depicted are the major brain structures in mood–related circuits that are altered by stress in animal models of depression or implicated in human depression. The red solid lines represent excitatory glutamatergic afferents to NAc from mPFC, amygdala, and hippocampus, and glutamatergic innervation of VTA by amygdala. GABAergic afferents, shown in purple, are inhibitory circuits, and include connections from NAc to VTA and hypothalamus. Dopamine neurons (shown in green solid lines) project from VTA to a range of limbic targets, including NAc, mPFC, amygdala, and hippocampus. Peptidergic pathways through which the hypothalamus (e.g., ARC, arcuate nucleus, and LH, lateral hypothalamus) alters neurotransmission in NAc and VTA are shown in solid black lines. Each structure contains specialized neuronal cell types thought to regulate stress responses, including resilience. These cell types, color–coded to reflect the transmitter signal they convey, include amygdala, PFC and hippocampal glutamatergic neurons (red), GABAergic NAc medium spiny neurons (purple), hypothalamic peptidergic neurons (black), and VTA dopaminergic neurons (red). CP, caudate-putamen; DMT, dorsomedial thalamus; SC, superior colliculus; IC, inferior colliculus; VP, ventral pallidum; SNr, substantia nigra; PAG, periaqueductal gray; DR, dorsal raphe; and LC, locus ceruleus. Adapted from Russo et al., 2012.

The medial PFC and its projections are also a target for, and a negative modulator of the stress response, and this brain region has been extensively linked to resilience processes. In susceptible animals, neural activity and expression of activity-dependent genes, such as ΔFosB or c-fos, are dampened in the ventral medial PFC following stress and induces social anxiety and anhedonia. These symptoms can be corrected via optogenetic cortical burst firing [123]. Some pro-resilience effects mediated by the PFC can result from the suppression of activity in the amygdala through reciprocal functional connections [124]. Surprisingly, the PFC is also involved in the acquisition of stress resilience (Figure 5), a complex process involving progressive learning of a coping response. This process is long-lasting, protein synthesis-dependent and mediated by glutamatergic pyramidal cells in the ventral medial PFC, a region involved in self-control [125] Stress resilience can also be acquired via exposure to an enriched environment, although in this case the effect is mediated through the infralimbic cortex, a subregion of the PFC [126].

The reward system and its pathways favor goal-directed and motivated behaviors, decisions, positive actions and emotions, as well as optimism, all of which are pro-resilience processes (Figure 5). The dysregulation of these pathways leads to the appearance of negative thoughts, the reduction of motivation and drive and, ultimately, depression [127]. The reward system is transcriptionally active during stress, with resilience and susceptibility processes having different transcriptional programs in the nucleus accumbens (NAc) and the ventral tegmental area (VTA) [111](Figure 5). Expression levels of the immediate early gene (IEG) ΔFosB in the NAc have a potential predictive value, with higher levels associated to resilience and lower levels to susceptibility to stress ΔFosB functions as a transcription factor and regulates the expression of GluR2, changing the GluR2:GluR1 ratio and modulating neuronal excitability [112].

Lastly, serotonergic circuits are fundamental to regulate mood and emotions. They are known to underlie the etiology of stress-induced affective disorders such as MDD and anxiety [128]. Inhibiting the reuptake of serotonin is to date the best treatment available. Although serotonergic transmission has been studied for a long time, only recently its role in resilience and susceptibility processes has been understood in more details [129].

2.5 The brain-gut-microbiome axis

The gut microbiota consists on all the microorganisms (e.g. bacteria, virus, fungi, etc.) that are found within the gastrointestinal tract of multicellular organisms. These commensal microbes help digestive processes by breaking down molecules, such as dietary fiber, which would be inaccessible to the host otherwise. In exchange, they

provide essential molecules to the host as a “by-product” of their metabolism. Although it was thought that the role of the gut microbiota was restricted to digestive processes, researchers observed in 2004 that depleting the gut microbiome early on in life increased stress responsiveness during adulthood. This effect was partially reversed by microbial colonization, even by just a single species [130]. Since then, the use of different experimental approaches, such as manipulation with antibiotics [131], fecal microbial transplantation [131,132] and probiotic administration [133], or applying germ-free (GF) animal models [130], has revealed a plethora of beneficial effects on host’s physiology mediated by microbiota-derived metabolites, including short-chain fatty acids (SCFA), secondary bile acids (2BAs) and tryptophan metabolites [134,135], as well as neuroactive molecules, such as GABA, serotonin (5-HT), norepinephrine and dopamine [136–138]. These compounds are known to influence not only stress responsiveness, but also modulate anxiety-like and depressive-like behaviors in mice, the nociceptive response, feeding behavior, taste preference and metabolism [139].

The modulation of the CNS by the gut microbiome occurs primarily through neuroimmune and neuroendocrine mechanisms, often involving the vagus nerve [140,141]. However, it is not clear to date whether this bottom-up modulation occurs by acting directly on brain sites or by inducing central responses via long-distance neural signaling (Figure 6). The enteric system plays an essential role by interacting with microbe metabolites and propagating the signals to the CNS. 2BAs and SCFAs derived from microbial metabolism interact with enteroendocrine cells (EECs) to stimulate the secretion of peptide YY and GLP-1, which regulate glucose homeostasis and induce satiety and associated behavioral changes [142,143]. Furthermore, expression of farnesoid X receptor (FXR) in the ileum is induced by 2BAs and triggers the production of fibroblast-growth factor 19 (FGF19). This molecule can penetrate the blood-brain barrier (BBB) and improve the central regulation of energy and glucose metabolism [144,145], as well as suppress HPA axis activity [146]. Surprisingly, the gut microbiome has been shown to induce the expression of neuro-protective molecules directly in the brain [131]. Enterochromaffin cells (ECCs) establish bidirectional interactions between the gut microbiota and the brain. ECCs produce 5-HT, storing around 95% of the organism’s 5-HT together with enteric neurons [147]. 5-HT regulates gastrointestinal motility and secretion, so it is fundamental for gut microorganisms in order to modulate their environment effectively. Plasma metabolite analysis of GF mice show a 2-fold reduction in 5-HT levels [148], and it has been proposed that gut microbiota contribute to the peripheral availability of tryptophan, an essential amino acid and precursor of 5-HT, by modulating its degradation through the kynurenine pathway [149]. The gut microbiota also

interacts with the host's immune system [150]. The use of mouse models of multiple sclerosis has revealed substantial roles for gut microbial regulation of autoimmunity, inflammation and immune cell trafficking [151,152]. Experiments with GF mice have shown that active microbial signaling is required during adulthood to preserve microglial maturation [153]. Lastly, recent evidence suggests direct activation of enteric neurons by gut microbiota via toll-like receptors [154], although it is unclear to what degree microbes make direct contact with neurons.

The brain-gut microbiome axis is bidirectional, so the brain is also able to influence the gut microbial community (Figure 6). The last 40 years of research show the effect of stress on the community structure of the gut flora [155]. The modulation of the gut microbiome by the brain can be achieve via indirect and direct methods. Indirectly, the CNS regulates gut functions through the autonomic nervous system which, in turn, transforms the microbial habitat and influences the composition and activity of the microbiome (Figure 6). One way to achieve this indirect modulation is by regulating gastrointestinal motility, as regional intestinal transit times affect water content, nutrient availability, and bacterial clearance rates [139]. Gut motility is influence by different factors, such as food intake patterns, sleep quality and stress, and increased transit time was shown to causally reduce bacterial biomass and diversity [156]. Another parameter that can be regulated to modulate the gut microbiome is the permeability of the intestinal barrier. Stress is known to cause epithelial barrier defects, which ultimately increase the translocation of gut microbes and metabolites [157]. Direct modulation of epithelial permeability occurs in response to stress and brain signals, causing a proinflammatory environment in the gut due to the higher translocation rate of bacteria. This phenotype has been observed in mice with depressive-like behaviors and has been reversed using antidepressants [158]. Furthermore, the autonomic nervous system controls the secretion of mucus by goblet cells, affecting the thickness and quality of the microbe's environment and creating a less-protective mucus layer. Some stress-induced changes in microbiota composition have been linked to changes in mucoprotein production by the autonomic nervous system [159]. Direct methods to modulate the gut microbiome consist on the luminal release of neurotransmitters by the host's neuroendocrine system. Some of the signaling molecules released by neurons, ECCs and immune cells are catecholamines, 5-HT, dynorphin and cytokines, a process modulated by the CNS [160,161].

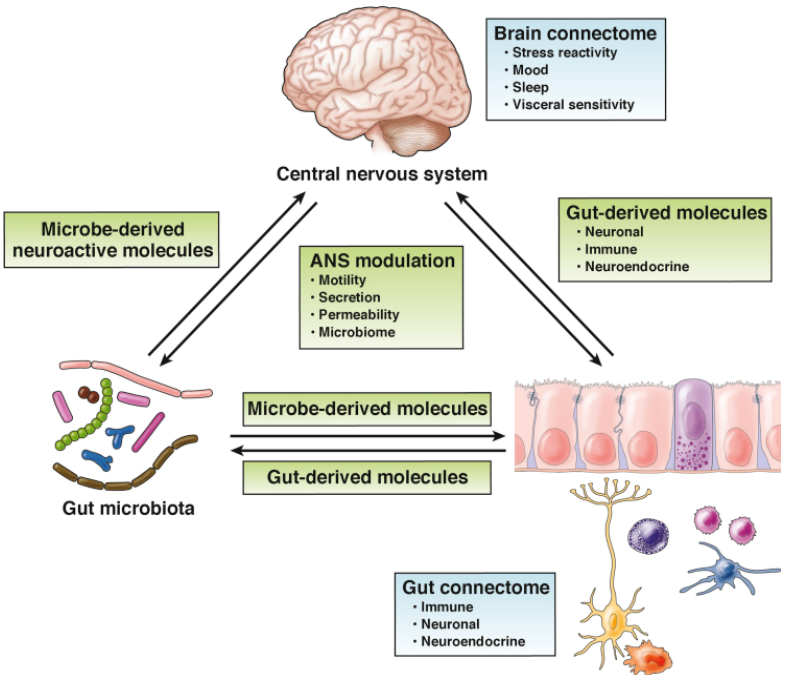

Figure 6. Interactions between the brain, the gut and its microbial community. Schematic representation of the bidirectional interactions between the brain, the gut and the microbiome within. These interactions maintain the homeostatic state and help counter deleterious effects. However, when dysregulated due to physiological aberrations or external factors (e.g. antibiotics, poor diet), the brain-gut-microbiome axis can increase inflammation levels, cause bacterial dysbiosis or even induce physiological changes that would make the individual more susceptible to stress. Adapted from Martin et al., 2018.

Given the relationship between stress and the gut microbiome, the BGM axis has been extensively studied in relation to different diseases and disorders. For example, several studies have reported significant specific changes in gut microbial composition in patients with different subtypes of irritable bowel syndrome [162]. Gut microbiota has a fundamental role in the regulation of appetite and satiety. Indeed, an association between different gut microbial profiles and brain microstructure has been found and used to differentiate obese patients. Moreover, fecal transplantation has been shown to induce phenotypic changes in body weight and food intake on GF mice, being this effect dependent on the donor's lean or obese state [163,164]. In addition, further evidence suggests an important influence of the gut microbiota on psychiatric and neurologic disorders such as Parkinson's disease [165], autism spectrum disorder [166], and mood disorders such as depression and anxiety [167]. Interestingly, the study of gut microbiome dynamics is proving especially useful in stress-related disorders, such as PTSD [168]. Besides a dysregulated HPA axis, which induces higher levels of cortisol, PTSD has been associated to increased pro-inflammatory cytokine levels. This pro-inflammatory phenotype is observed in young mice (and humans) after exposure to early life stress and has been described as a cause for increased susceptibility to stress during adulthood [169,170]. Interestingly, stress during early developmental stages has also been

linked to sex-dependent changes in gut microbiome composition and relative abundance [171,172], with the deleterious effects on emotion and cognition partially or fully reverting upon supplementation with probiotics, fecal microbial transplantation, or gut colonization by complex microbial communities or even single species [131,133]. Therefore, the gut microbiome has become a promising topic for research groups interested in psychiatric pathologies, stress resilience and stress physiology, as it has become a promising and accessible therapeutic target, as well as for preventive treatments aimed at increasing the psychological resilience of the individual.

Despite the promising potential of gut microbiome manipulations, and consequently their effects on the BGM axis and emotional behavior, research on this topic is at a very early stage [139]. There is a translational disconnect between findings made in mice and the small clinical trials performed in humans, which hints at host-specific microbiota interactions, as well as a gender bias, as most of the research is conducted on males despite stress-related disorders having clear sex-specific differences. Moreover, supplementation with probiotics does not seem to alter the microbial composition or distribution of gut communities but induces its effect by transiently altering the transcriptional state of the gut´s microbiome [173]. The lack of translation between animal models and human studies requires a better characterization of the gut microbial communities and their host interactions at different “omics” levels (i.e. transcriptomic, metabolomics, proteomic, etc.), as well as a better modelling of the gut microbiome ecology to further understand how global and regional changes in the gut affect the host´s nervous system and physiology [174].

3. Brain homeostasis and the endocannabinoid system

3.1 Introduction to the endocannabinoid system (ECS)

3.1.1 Discovery of the components of the ECS

Cannabis sativa, also commonly known as marihuana, is an herbaceous flowering plant that has been very intimately intertwined with human agriculture and development since the dawn of civilization. Evidence suggests that the plant originated in the steppes of central Asia around 12.000 years ago. The plant played a key role in the development of agriculture and the transition from hunter-gatherers to permanent settlements [175]. *C. sativa* was cultivated for many purposes, such as fiber production, food, medicine and recreation [176]. Carbon-14 dating techniques pinpoint the first documented use of *C. sativa* in a medicinal manner somewhen around 6.000 years ago [177]. The plant started spreading from central Asia to the rest of the world around 4.000 years ago, following the movement of nomadic tribes and the Silk Road. However, it was not until the XVII

century that it reached South America at the hands of African slaves and, from there, it spread to North America through Mexico in the early XX century [178]. At this time, its use and consumption started to carry negative connotations, which led to the demonization of the plant.

Despite the long shared history between humans and the cannabis plant, one has to wait until 1940 for the first scientific research of the plant, which led to the isolation and identification of cannabidiol [179], a non-psychoactive component found in higher concentrations in hemp, a non-psychotropic version of the plant. It was only in 1964 when the main psychoactive component of marihuana, Δ^9-tetrahydrocannabinol (Δ^9-THC), was identified by the group of Raphael Mechoulam [180]. It was not the only component identified in the study and, to this date, more than 500 molecules have been identified in *C. sativa*, from which 113 are so-called cannabinoids.

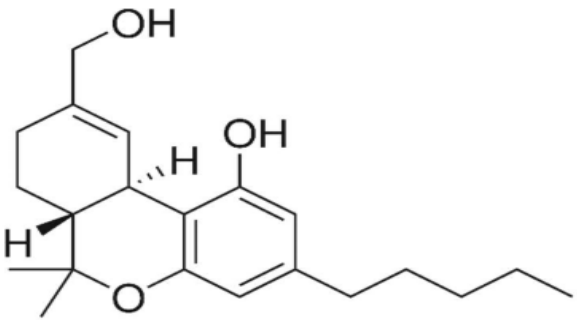

Figure 7. Molecular structure of Δ^9-THC. Water-clear glassy solid when cold, which becomes viscous and sticky if warmed. Δ^9-THC has a very low solubility in water, but good solubility in most organic solvents, specifically lipids and alcohols.

Although Δ^9-THC had been isolated and described (Figure 7), how it acted on the brain remained unknown. However, evidence started to emerge suggesting that the effect of this phytocannabinoid was mediated by an unknown receptor, which could inhibit adenylate cyclase activity in a dose-dependent, stereoselective and pertussis toxin-selective manner. Over 25 years after the discovery of Δ^9-THC, the first cannabinoid receptor (CB1) was identified in the rat brain [181]. A few years later, a second peripheral cannabinoid receptor (CB2) was isolated from macrophages in the spleen [182]. Both proteins were described as classical G-protein coupled receptors (GPCR) containing seven transmembrane helices (Figure 8). CB2 is shorter and only shares 44% of the amino acid sequence with CB1.

In the mammalian brain, CB1 is the most abundant GPCR [183] and can be preferentially found in the presynaptic terminals. However, CB1 is often condensed in perisynaptic portions of the axon [184]. CB1 expression is not uniform across the whole brain. Whereas some brain regions, such as basal ganglia, cerebellum, hippocampus and cerebral

cortex, contain the highest densities for CB1 [185,186], others, such as thalamus, hypothalamus and brainstem, show moderate to low CB1 receptor levels. Although CB1 is expressed by almost all neuronal populations, the level of expression is also different in each of them [187]. Inhibitory GABAergic interneurons (mainly cholecystokinin-positive and parvalbumin-negative) show very high levels of CB1 expression, in contrast with glutamatergic, cholinergic, noradrenergic and serotonergic neurons that have low to moderate expression levels [185,188–190]. In contrast to the almost ubiquitous expression of CB1 in the brain, CB2 is expressed at very low levels in the CNS [191] and has high levels of expression in the immune system [182].

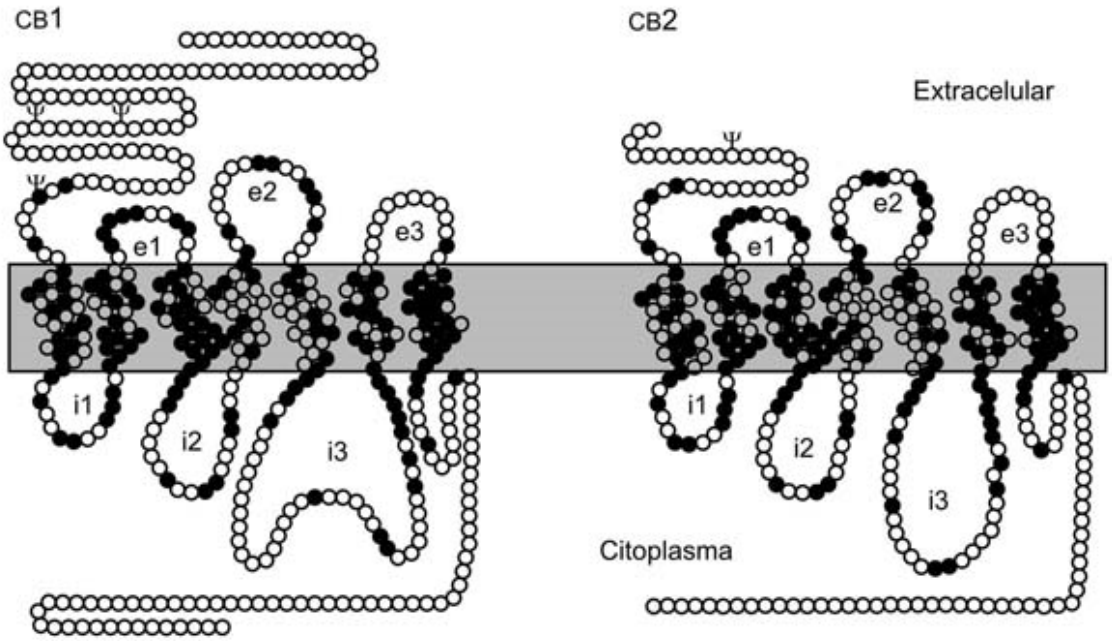

Figure 8. Protein structure of cannabinoid receptors. Both receptors present the classical seven transmembrane conformation with 3 extracellular loops (e1-e3) and 3 intracellular loops (i1-i3). Mouse CB1 receptor is a 473-amino acid G-protein coupled receptor with a human homolog of 472 amino acids. Human CB2 receptor is significantly shorter and it shares only 44% amino acid sequence identity (black circles) with human CB1 receptor (adapted from [192]).

The discovery of a cannabinoid receptor that mediated the pharmacological effects of Δ^9-THC suggested the presence of endogenous molecules that would bind to such a receptor. Shortly after the identification of CB1, its first endogenous ligand, a derivate from arachidonic acid with an inhibitory activity equivalent to that of Δ^9-THC, was isolated and identified as arachidonyl ethanolamide (AEA) [193] (Figure 9), or also called anandamide, the first endocannabinoid (eCB). Applying the same methodology, a second cannabinoid, 2-arachidonoyl glycerol (2-AG), an ester containing arachidonic acid and glycerol, was isolated shortly after and its structure deciphered (Figure 9), which led to the discovery of another endogenous ligand for CB1 with a potency similar to Δ^9-

THC [194]. Afterwards, 2-AG was characterized as a full agonist of CB1 and CB2, whereas AEA was shown to have higher affinity at both receptors, but only acted as a low-efficacy partial CB1 agonist, and with an even lower efficacy at CB2 [195].

After the characterization of the cannabinoid receptors and the isolation of the eCBs, research focused on the metabolism of these lipid compounds and the underlying fundamental biochemical processes. The eCBs were shown to be synthetized on-demand at the synapse from phospholipid precursors, taken from either the cell membrane or adjacent storage sites, in a neuronal activity-dependent manner [196,197]. The enzymes involved in the metabolism of these molecules were elucidated in the early 2000s and, although the biosynthetic routes of 2-AG are well known [198], those of AEA remain not fully understood [199]. Following their release, both eCBs are degraded to arachidonic acid to avoid potential harmful effects due to the over activation of the ECS.

The biosynthesis of 2-AG is catalyzed from arachidonoyl-containing diacylglycerol (DAG) by the enzymes *sn*-1-specific diacylglycerol lipase-α and –β (DAGL-α/β), with the former being dominantly localized in the brain and the latter in the peripheral tissues [200]. Most of the 2-AG that is produced is degraded by the enzyme monoacylglycerol lipase (MAGL) [201]. Additionally, the degradation of the rest of 2-AG has been shown to be performed by the enzymes α-β hydrolase 6 (ABHD6) and α-β hydrolase 12 (ABHD12) in a compartment-selective manner, thereby potentially controlling different pools of 2-AG *in vivo* [202], as well as cyclooxygenase-2 (COX-2) [203]. In the case of AEA, several biochemical routes exist which could potentially synthetize AEA from its precursor, *N*-arachidonoyl phosphatidylethanolamine (NArPE), a derivate from arachidonic acid produced in a Ca^{2+}-dependent manner. The most widely accepted route, probably due to being the most straightforward, is the direct synthesis by the enzyme *N-acyl* phosphatidylethanolamine-selective phospholipase D (NAPE-PLD). AEA is degraded post-synaptically by the enzyme fatty acid amide hydrolase (FAAH) [204].

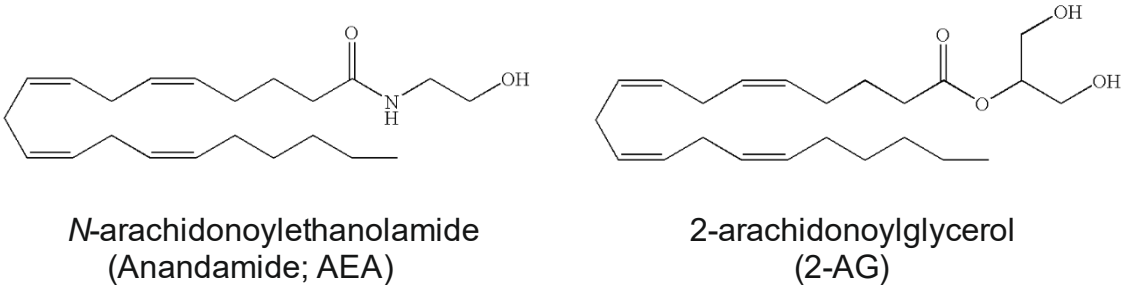

N-arachidonoylethanolamide (Anandamide; AEA)

2-arachidonoylglycerol (2-AG)

Figure 9. Molecular structure of AEA and 2-AG. The endocannabinoids AEA and 2-AG are lipid neuromodulators derived from arachidonic acid and typically synthetized on-demand upon intracellular Ca2+ influx rise.

Further research has shown additional receptors associated with the ECS. The transient receptor potential vanilloid 1 (TRPV1) is only activated by anandamide [205], whereas the orphan receptor GPR55 can be activated by Δ^9-THC and other cannabinoids [206], as well as other molecules without an effect on CB1 and CB2 [207]. On top of those two receptors, the peroxisome proliferator-activated receptor (PPAR) family of nuclear receptors mediates the anti-inflammatory effects of *C. sativa* through the binding of endogenous cannabinoids and Δ^9-THC analogues [208]. Lastly, the $GABA_A$ receptor influences locomotion through the binding of 2-AG, but not AEA [209].

3.1.2 The role of the ECS in the mammalian brain

Neurons, as any other known organism, require very specific and stable conditions to operate in an efficient and healthy manner. They are especially sensitive to over-activation, as neuronal activity causes a momentary, but expensive disruption in the homeostasis of the cell. Therefore, neurons require a feedback mechanism to modulate their response and stop it once the electrical impulse has been passed to the next neuron.

Since the identification of Δ^9-THC and the cannabinoid receptors, the use of genetic and pharmacological tools has revealed the ECS as a molecular system that is fundamental in regulating many homeostatic processes inside and outside of the CNS. In the mammalian brain, the ECS has been shown to function primarily as a neuromodulator at the synaptic level. Anterograde synaptic transmission is well described and is characterized by a Ca^{2+}-triggered release of neurotransmitters upon depolarization of the membrane from the presynaptic zone of a neuron, which sends the “message” to the postsynaptic zone of the next neuron, which receives the “message” [210]. This flow of information in the brain must be tightly regulated, as the general behavior of the organism and many of its core processes are dependent on delivering the correct output for a specific input. Thus, feedback mechanisms are necessary to manage this flow of information across the whole brain [211]. To this purpose, neurons have developed retrograde messengers, molecules that are released from the postsynaptic neuron and travel backwards to modulate the activity at the presynaptic terminal (Figure 10). There are a few molecules that act as retrograde messengers, such as nitric oxide (NO) and arachidonic acid (AA) among others [212,213], but the best characterized and most widespread are the lipid-derived eCBs [214].

In the early 2000s, a form of short-term plasticity in the hippocampus and cerebellum was shown to be mediated by eCBs, suggesting a retrograde eCB signaling. This type of plasticity occurred in both excitatory glutamatergic synapses and inhibitory GABAergic

synapses (containing γ-aminobutyric acid or GABA), and was referred to as depolarization-induced suppression of excitation (DSE) and depolarization-induced suppression of inhibition (DSI), respectively [215–218]. The underlying mechanism for both DSE and DSI has been pinpointed to the rise of intracellular Ca^{2+} thanks to the opening of voltage-gated Ca^{2+} channels (VACCs) in the postsynaptic membrane [219]. This Ca^{2+} influx activates Ca^{2+}-sensitive enzymes that activate DAGL-α and, subsequently, increase the postsynaptic concentration of 2-AG, the main eCB required for activity-dependent retrograde signaling [220]. Alternatively, the activation of type-1 metabotropic glutamate receptors (mGluRs) in the postsynaptic neuron causes a G-protein cascade, starting with the activation of guanine nucleotide-binding protein G(q) subunit alpha ($G\alpha_q$), which leads to the production of the 2-AG precursor diacylglycerol (DAG) from phosphatidylinositol (PI) [219] (Figure 10). Both pathways converge in order to produce 2-AG, which in turn is released into the synaptic cleft [211], where it binds presynaptically located CB1 receptors. The activation of CB1 starts a G-protein signaling cascade that transiently suppresses the release of neurotransmitter via the inhibition of presynaptic VGCCs, most likely through its βγ subunits, and the opening of G protein-activated inwardly rectifying K^+ channels (GIRKs) [184,219].

The role of the second major eCB, AEA, remains harder to be elucidated. Although the synthesis of this eCB has not yet been completely characterized, NAPE-PLD can be found presynaptically in axons and, thus, AEA acts in an anterograde manner on postsynaptic TPRV1 channels [221], before being postsynaptically degraded by FAAH [222] (Figure 10). However, NAPE-PLD has been also found at presynaptic terminals, meaning that AEA, like 2-AG, also acts in a retrograde manner [223]. Both major eCBs, AEA and 2-AG, are necessary at specific synapses in order to fully engage CB1 and cause the transient suppression of neurotransmitter release which, ultimately, leads to an eCB-mediated short-term depression (eCB-STD) at the synapse. This observation gave rise to the idea of CB1 operating as a coincidence detector, integrating different physiological signals that are required to modulate synaptic plasticity [211]. In addition to this phasic and transient modulation of synaptic activity, a tonic eCB-mediated modulation has been observed [224], giving strength to the hypothesis of the ECS as a major homeostatic regulator. A pharmacological blockade of FAAH, which causes chronically elevated levels of AEA throughout the whole brain, is responsible for sustained agonism without downregulating the expression levels of CB1. In contrast to this observation, chronic MAGL blockade, which causes a continuous elevation of 2-AG levels, reduces the expression level of CB1 [225]. These findings imply that 2-AG and AEA mediate different types of signals for synaptic modulation, with 2-AG transmitting a rapid,

transient and point-to-point retrograde signal, whereas AEA may act as a slower modulator in an anterograde and possibly also retrograde manner or even as a TRPV1 agonist.

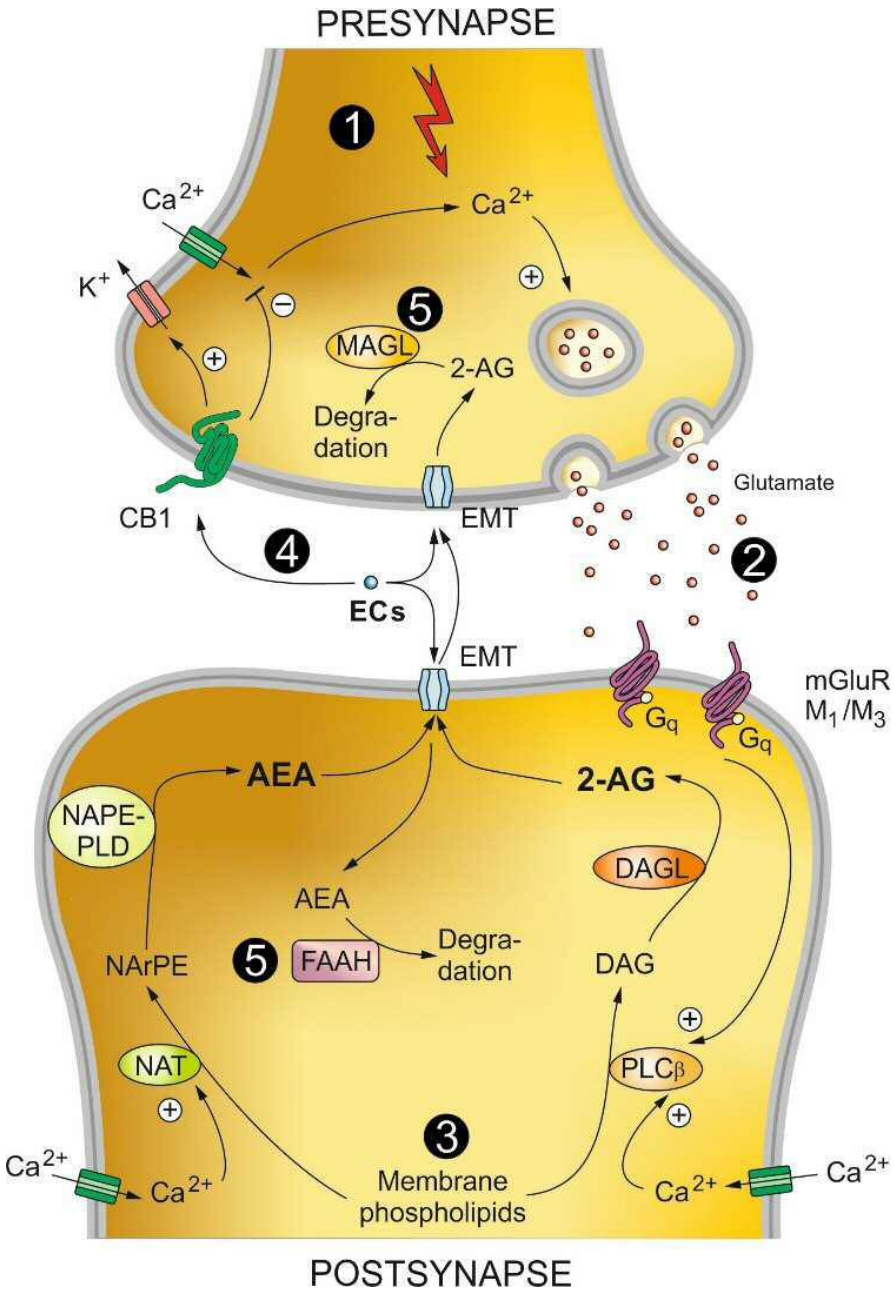

Figure 10. Components of the ECS in the neuronal synapse. Depolarization of the postsynapse leads to an influx of Ca2+ via voltage-gated Ca2+ channels (VGCCs). A rise in intracellular Ca2+ activates sn-1-specific diacylglycerol lipase-α (DAGLα), presumably via Ca2+-sensitive enzymes and production of 2-arachidonyl glycerol (2-AG). After release of glutamate, a simultaneous activation of postsynaptic group I metabotropic glutamate receptors (mGluRs) leads to the activation of phospholipase Cβ (PLCβ), which produces the 2-AG precursor diacylglycerol (DAG) from phosphatidylinositol (PI), and thus, further promotes the production of 2-AG, which is then released into the synaptic cleft via a yet not characterized endocannabinoid membrane transporter (EMT). 2-AG activates cannabinoid receptor type 1 (CB1) and initiates downstream signaling cascades, which lead to opening of G protein-activated inwardly rectifying K+ channels (GIRKs), inhibition of VGCCs, inhibition of adenylyl cyclase (AC) and inhibition of neurotransmitter release (Glu or GABA) until 2-AG gets hydrolyzed by its degrading enzyme monoacylglycerol lipase

(MAGL). The second major endocannabinoid arachidonylethanolamide (AEA) is produced postsynaptically, as well as presynaptically (not depicted) by the enzyme N-acyl phosphatidylethanolamine-selective phospholipase D (NAPE-PLD) from the precursor N-arachidonoyl phosphatidylethanolamine (NArPE), which in turn is produced by a not yet identified Ca2+-dependent transacylase enzyme (TA). AEA therefore can act on CB1 in a retrograde manner according to 2-AG or anterogradely on postsynaptic transient receptor potential cation channel subfamily V member 1 (TRPV1), before getting inactivated by fatty acid amide hydrolase (FAAH), which is located primarily in the postsynapse.

The binding of the major eCB to CB1 at the presynaptic terminals not only induces eCB-STD via the suppression of neurotransmitter release [218] (Figure 10). Stimulation of CB1 inhibits the enzyme adenylyl cyclase (AC) through the action of Gα proteins (from the $G_{i/o}$-family, or $G\alpha_{i/o}$). Consequently, the activity state of downstream targets is affected, including presynaptic cyclic adenosine monophosphate (cAMP) / proteinkinase A (PKA) signaling. This pathway forwards the signal from the CB1 receptor to the release machinery in order to suppress transiently neurotransmitter release. Furthermore, CB1 activates other signaling pathways to induce long-term adaptation processes [196], which constitute the molecular basis for eCB-mediated long-term suppression (eCB-LTD) [226,227]. eCB-LTD is a form of long-term synaptic plasticity that has not been to date fully elucidated. The mechanisms of eCB release from the postsynaptic terminal during the induction of eCB-LTD vary depending on the brain region and experimental conditions, and whether the activation of CB1 alone for several minutes is sufficient to trigger the process is not consistent among studies [184]. Overall, the ECS modulates the balance of excitatory and inhibitory neurotransmission within neuronal circuits to ensure both the homeostatic levels and an efficient flow of information are kept in the brain [189,228].

The complexity of the ECS, involving different signaling molecules with tonic and phasic release, and its role in regulating neuronal activity, with both short- and long-term effects, cause the ECS to differentially modulate homeostatic, short-term, and long-term synaptic plasticity throughout the brain. However, the release of eCBs needs to be highly localized and efficient to avoid detrimental side effects [229]. Given that the flow of information within the CNS ultimately governs the behavior and most of the core processes of the organism, the ECS is a fundamental actor in mammalian physiology and regulates a plethora of processes, such as cognition, appetite [230], pain sensation, mood, and behavior [231]. The ECS also modulates the general sensitivity of the hypothalamic-pituitary-adrenal (HPA) axis, heavily involved in the stress response, through the action of AEA and 2-AG [232], being the ECS central in regulating stress hormone levels. Moreover, the ECS has also been shown to be involved in mediating some of the physiological and cognitive effects of voluntary physical exercise [233], as well as modulating locomotor activity [234] and the motivational salience for rewards. Besides its function in the CNS, the ECS is also involved in other physiological processes, such as immunomodulation [235], energy

metabolism [236] and fertility [237]. It is important to note that the function of the ECS changes depending on the developmental stage of the organism. In the developing brain, the ECS mediates axonal outgrowth and guidance [238], whereas in the adult brain it modulates synaptic strength and adult neurogenesis [239]. The amount and relevance of physiological processes, in which the ECS is tightly involved, proves its role as a fundamental feedback system to maintain homeostasis within the mammalian brain.

3.1.3 Clinical relevance of the ECS

The fact that the ECS is such a core element to keep homeostasis within the brain and the organism makes its correct functioning of special relevance. The dysregulation of the ECS can carry short- and long-term consequences depending on which tissue, brain region or neuronal circuit is affected.

In modern times, the easiest way to alter the function of the ECS is the consumption of the cannabis plant, either inhaling it or consuming it orally. The psychoactive and physiological effects of the plant are dose-dependent and start to arise within minutes of its consumption, lasting for several hours. Some of the most common (and desired) psychoactive effects are a state of muscle relaxation, euphoria (or “high” feeling), perceptual alterations, including the perception of space and time, increased awareness of sensations and increased libido [240,241]. Other cognitive and physiological alterations are impaired short-term memory and attention, hypothermia, analgesia, increased sociability, rapid heart rate, reddening of the eyes and increased appetite [242,243]. Cannabis consumption also affects motor skills by inducing hypolocomotion, reducing reaction time and coordination of movements, as well as many forms of skilled psychomotor activity, and inducing catalepsy, characterized by the lack of voluntary movement [243]. Some effects have been reported mostly at high doses or after chronic consumption, and include auditory and visual illusions, pseudohallucinations, disruption of linear memory, paranoia and/or anxiety, acute psychosis and even dissociative states such as depersonalization and derealization [244,245]. The cannabis-induced effects listed above are just part of a much longer list. The behavioral, perceptual and mood alterations caused by the consumption of cannabis are highly subjective and vary greatly among consumers. This variability comes from a lot of different factors, such as dose received, mode of administration, concurrent drug use, prior experience with cannabis and the “set and setting”, i.e., the user´s expectations, attitude towards cannabis, mood state, and the social setting in which cannabis is used [241,246].

Despite the long list of cannabis-induced alterations, and the severity of some of them, recent research has unraveled the therapeutic potential of the plant [247]. The ECS, the

mediator of the pharmacological effects of marihuana, is gaining more weight as a neuroprotective system in the brain due to its unique ability of buffering neurotransmission and avoiding excitotoxicity. The function of the CNS implies elevated neuronal activity even during the basal state, which, if excessive, can induce neurotoxic effects. In particular, excessive glutamatergic signaling (a key feature of epileptiform seizures) can cause a heavy strain on neurons, leading ultimately to a collapse of the circuit. The ECS through the action of CB1 mediates neuroprotection against excitotoxicity in the hippocampus [196,248]. CB1 dampens the excitability of pyramidal neurons in the hippocampus by hyperpolarization as a rapid on-demand protection. Moreover, CB1 induces intracellular cascades, including ERK phosphorylation and neurotrophins (e.g. BDNF), to generate long-term adaptive cellular changes in response to future excitotoxic stimuli [190,249]. CB1 has also been shown to induce neural progenitor proliferation and neurogenesis upon excitotoxicity [250]. Cannabinoids are also being investigated to treat the symptomatic panels of different diseases and disorders. For example, medical cannabis is reported to be effective in reducing chemotherapy-induced vomiting and nausea for cancer patients [251], as well as for relieving chronic pain in several conditions [252]. Extracts of Δ^9-THC and cannabidiol are being used to treat muscle spasms in multiple sclerosis, Tourette syndrome and epilepsy [253], although the reported spasticity relief is highly subjective. The use of medicinal marihuana to treat psychiatric disorders, such as posttraumatic stress disorder (PTSD), is currently controversial, and there is insufficient evidence to confirm its effectiveness [254]. However, recent research is backing progressively the usefulness of the plant in treating PTSD, as it has been shown to prevent depressive-like symptoms and alterations in BDNF expression in rat models [255].

Lately, an ever-increasing amount of research is showing the neuroprotective [256] and therapeutic potential of the marihuana plant [257] and, thus, of the ECS as a target for therapeutic strategies to treat more and more symptoms and psychiatric disorders [258–260]. Despite this therapeutic potential, the high variability found in the cannabis-induced relief on patients, as well as the subjectivity of some of the reported positive effects (with no objective measurement backing the claim), makes the use of medicinal cannabis highly controversial. Furthermore, the side effects of cannabis consumption and the potential long-term consequences of dysregulating the ECS, be it for recreational or medicinal purposes, are not fully understood and require further investigation before cannabis-based therapies are commercialized and widely available [261].

3.1.4 The role of CB1 in hippocampal homeostasis

Although the neurons in every brain region are highly interconnected with other neurons from the same region and from other parts of the brain, hippocampal neurons are

especially prominent in this aspect. The hippocampus is a part of the limbic system that receives information from almost every brain process and, as such, the neurons within have one of the highest degrees of connectivity in the entire brain [262]. The hippocampus is composed of several curved tubular structures: the *cornu ammonis* (CA) regions (CA1-CA4) and the dentate gyrus (DG), and can be extended to the hippocampal formation, which also includes the entorhinal cortex and the subiculum [263]. The hippocampus functions as an integration hub and, therefore, it is involved in regulating and directing many different brain processes, such as learning and memory, orientation and navigation, stress and anxiety, and decision-making, among others [264]. This variety of functions divides the hippocampus, not only in its anatomical subfields, but also along the anterior-posterior axis [265,266]. Given the high degree of connectivity, the need for an efficient modulatory system is high in order to keep a correct balance between excitation (gluatamate) and inhibition (GABA). This need is more prominent upon exposure to strong external stimuli, such as stressful situations [267].

The use of transgenic mice has been fundamental to elucidate the regulatory role of CB1 within the hippocampus. Glutamatergic circuits in the hippocampal formation have a tendency towards excessive pathological activity. Thus, mice lacking CB1 (CB1-KO) display more susceptibility towards e.g., chemically induced epileptogenic seizures and increased neuronal damage as a consequence of the impairment in CB1-mediated inhibition of excitatory transmission [196,248]. Moreover, the genetic deletion of CB1 affects particularly memory engrams within the hippocampus, impairing learning and memory processes. CB1-KO mice not only show increased contextual fear memory and altered synaptic plasticity under highly adverse conditions [268], but also show strong impairments in short- and long-term extinction of aversive processes [269].

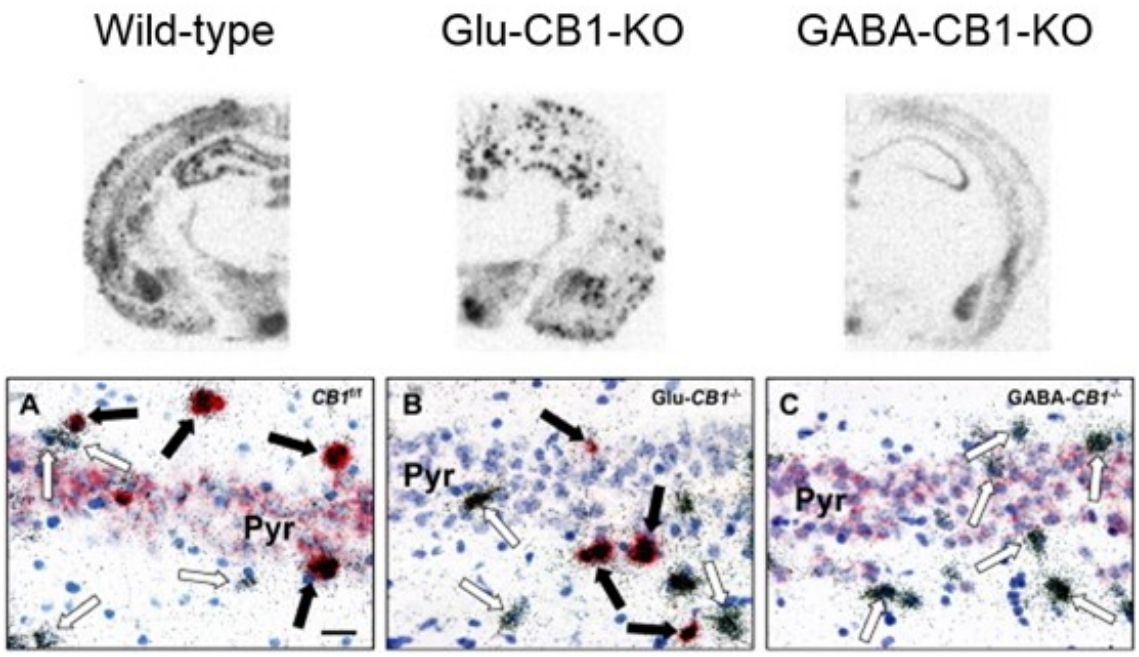

Figure 11. CB1 mRNA expression in conditional CB1-KO mice. In situ hybridization with a specific probe to label CB1 mRNA in a brain section (above) and in the CA3 hippocampal area (below). Lower pictures show CB1 mRNA (red) in closer detail together with GAD65 (silver grains), a marker for GABAergic terminals. **(A)** Micrographs showing CB1 (black dots, upper picture; red, lower picture) and GAD65 (silver grains, lower picture) in WT mice. **(B)** Micrographs showing the same staining in (A) but in Glu-CB1-KO mice, so CB1 is only present at GABAergic terminals. **(C)** Micrographs showing the same staining in (A) but in GABA-CB1-KO mice, so CB1 is only present in glutamatergic terminals. Modified from Monory et al., 2006.

However, given the wide distribution of CB1 in the hippocampus, genetic approaches that involve the total deletion of the receptor might not be the most adequate to elucidate the hippocampal role of CB1. For this purpose, genetically modified mice with a conditional *knock-out* of the CB1 gene were developed, i.e. mice lacking CB1 only in glutamatergic or GABAergic neurons [248], as they are the main excitatory and inhibitory neurotransmitters in the brain, respectively (Figure 11). The consequence of this genetic deletion is the increase of the respective neurotransmitter at the synaptic terminals where CB1 is no longer present. Immunohistochemical studies of these mice show high levels of CB1 protein associated only to a subset of GABAergic interneurons (Figure 11B), whereas CB1 associated to glutamatergic neurons appears with a lower density, but homogenously throughout the pyramidal layer of the hippocampus [248] (Figure 11C). With the use of these conditional mutants, scientists were able to dissect the CB1-induced signaling pathways specific for glutamatergic (Glu-CB1-KO mice) and GABAergic (GABA-CB1-KO mice) neurons [270]. Surprisingly, [^{35}S]GTPγS binding assays demonstrated that, although CB1 is found with higher density in GABAergic interneurons, glutamatergic terminals are several fold more efficiently coupled to the G protein signaling cascade [270]. A dose-dependent biphasic effect of cannabinoids has also been

reported: when injecting low and high concentrations of CB1 agonist, Glu-CB1-KO animals showed increased anxiogenic behavior (compared to WT littermates) with a low dose of CB1 agonist, while GABA-CB1-KO animals showed effects only with high concentrations of CB1 agonist, and displayed a marked anxiolytic response [228]. Recent research has revealed higher levels of AEA and 2-AG in the hippocampus of diet-induced obese mice, as well as higher CB1 immunoreactivity in the CA1 and CA3 areas [271]. The use of conditional CB1-KO animals also showed a potential role for CB1 in GABAergic neurons, as GABA-CB1-KO mice were partly resistant to the diet-induced obesity.

Although conditional CB1-KO mice lack a fundamental piece of the ECS in a specific subset of neurons, compensatory mechanisms and the general plasticity of the brain are able to overcome this deficit. Both Glu-CB1-KO and GABA-CB1-KO animals show almost no phenotypical or behavioral difference in the basal state and require a triggering stimulus (e.g. diet-induced obesity, CB1 agonist injection, etc.) to observe any change. Surprisingly, they do show profound distinctions at the cellular and electrophysiological level [189]. Hippocampal pyramidal neurons from Glu-CB1-KO mice show increased dendritic branching and dendritic spine density in their apical area, whereas GABA-CB1-KO mice show a sharp overall reduction of dendritic branching and spine density (Figure 12). Physiologically, the pyramidal neurons from these two mouse lines show also a dichotomic contrast. Glu-CB1-KO mice displayed increased long-term potentiation (LTP), a form of synaptic plasticity, when compared to WT littermates, whereas GABA-CB1-KO mice showed a decreased response in LTP [189]. All these observations suggest that the brains of Glu-CB1-KO and GABA-CB1-KO mice have reached a completely different homeostatic state, or allostatic state, as compared to wild-type controls in order to adapt to the increase in excitatory and inhibitory neurotransmission, respectively. Therefore, these two mouse lines offer a window to new homeostatic mechanisms that could be regulated via cell type-specific CB1 modulation.

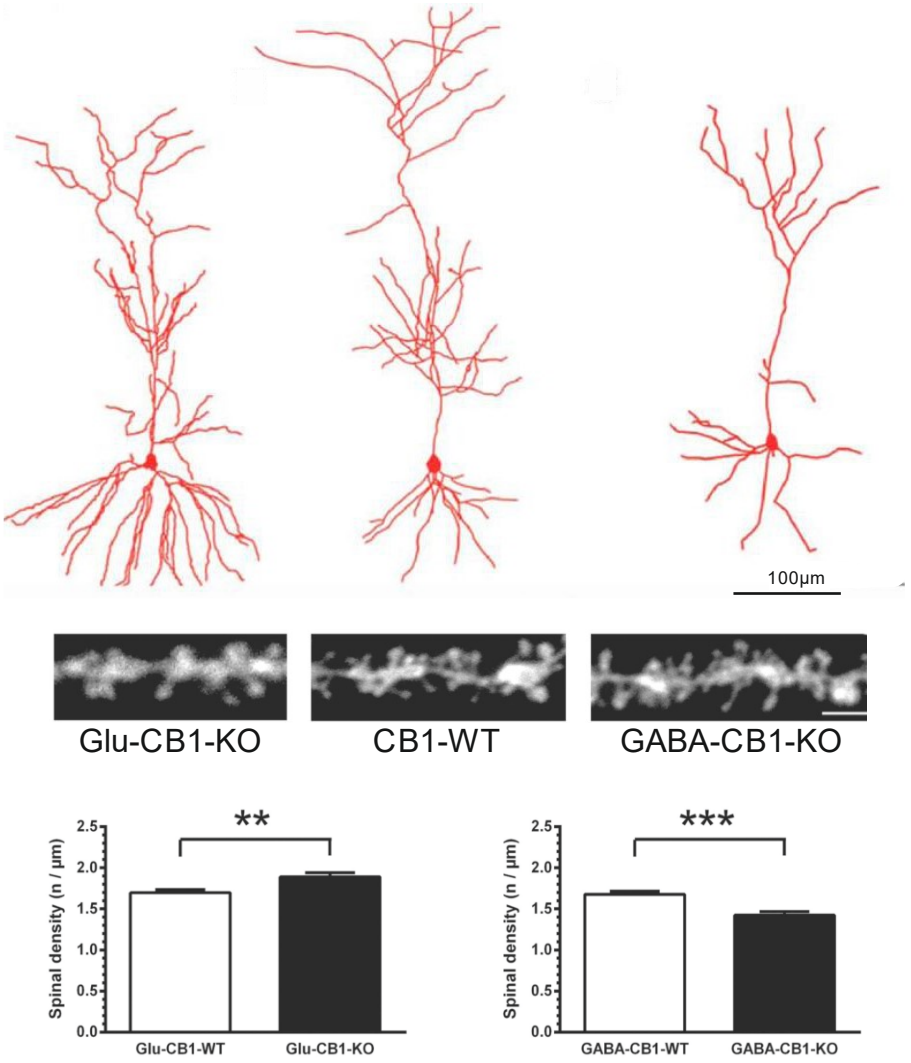

Figure 12. Pyramidal hippocampal neurons in WT and conditional CB1-KO mice. Morphology (above), dendritic spine micrographs (middle) and dendritic spine count in WT and conditional CB1-KO mice. Excess of glutamate (Glu-CB1-KO) or GABA (GABA-CB1-KO) at the synapses induces morphological changes in hippocampal neurons. Neurons in Glu-CB1-KO mice (left) had increased dendritic branching and a higher density of dendritic spines when compared to the WT animals (center). GABA-CB1-KO mice had in contrast reduced dendritic branching and a lower density of dendritic spines. Modified from Monory et al., 2015.

3.2 Aim of the project

A correct functioning of the brain is fundamental for individuals to survive and, thus, keeping brain homeostasis is of utmost importance. Given the plasticity of the brain, its homeostatic range can (and will) moderately change across the lifespan of the individual without developing pathologies. In some cases, the plasticity of the brain allows for drastic changes to the homeostatic state without severe impairments, reaching an allostatic state. The aim of this project is to characterize the transcriptome of 2 different allostatic states, Glu-CB1-KO and GABA-CB1-KO mice, and compare it to the homeostatic state of their respective CB1-WT counterparts to uncover potential compensatory mechanisms at the genetic level. Our focus will be in the hippocampus, a

brain region heavily involved in information processing, spatial navigation, learning and memory, and the stress response, among many other functions. We will focus on the CA hippocampal regions of mice in the basal condition and after exposure to a new environment. With this approach, we will be able to uncover differences between conditional CB1-KO and CB1-WT mice at the transcriptomic level in the basal state and after a mild behavioral activation, so that we can also gather information about how these allostatic states react to stimuli.

3.3 Material and Methods

3.3.1 Mouse lines

In order to study homeostatic processes, we used the Cre-LoxP system to create conditional-KO mouse lines that could help us understand the relevance of the cannabinoid receptor type-1 (CB1) in the maintenance of brain homeostasis. To this end, CB1 was deleted only in two specific cell populations within the whole brain: glutamatergic and GABAergic neurons. These specific populations were chosen because glutamate and GABA are the main neurotransmitters for excitatory and inhibitory signaling respectively. To achieve this specificity in the deletion of CB1, mice expressing Cre-recombinase under the control of the regulatory elements of the genes *Dlx5/6* (for GABAergic deletion) and *NeuroD6* (or *nex1*; for glutamatergic deletion) are crossed with animals that have a *"floxed"* CB1 gene ($CB1^{f/f}$). The resulting mouse lines (dlx-cre x CB1ff and nex-cre x CB1ff) lack CB1 in GABAergic or glutamatergic neurons respectively, which causes an increase of the respective neurotransmitter in the synapses of those neurons as the eCB system is unable to exert its regulatory function. This dysregulation occurs from the moment of birth and forces the brain to adapt to the excess of neurotransmitter at the synapses. These transgenic mice (named Glu- and GABA-CB1-KO) are behaviorally very similar to their wild-type counterparts, although their neuronal morphology and electrophysiology are very different (Monory et al 2015).

3.3.2 Behavioral hippocampal activation

In order to study how the hippocampus, our brain region of interest, from the conditional-KO mice react upon stimulation, we induced neuronal activity by exposing the animals to a new environment: an open field arena, which they could explore undisturbed for 5 minutes (light intensity: 20-30 lux). This simple, yet sufficient, stimulus induces neuronal activity throughout the hippocampus as the animal explores and navigates the arena (40x40x30 cm white box) and drives changes in gene expression that can be later analyzed.

The degree of neuronal activity induced by the exposure to a new environment was analyzed for every sample via RT-qPCR using primers for the *Arc* gene (Life Technologies, Mm01204954_g1), an immediate-early gene that is expressed upon neuronal activity. *ß-actin* was used to normalize the data to the control group (unexposed to the new arena).

3.3.3 Hippocampal microdissection and validation

Given the amount and variety of inputs that the hippocampus has to process on a daily basis, it does not come as a surprise its relatively heterogeneous structure. Therefore, we aimed at analyzing only the hippocampal *Cornu ammonis* (CA) subregions, more involved in stimulus processing as well as learning and memory. In order to micro-dissect only CA1-CA3 from the hippocampus, we first proceeded to remove the dentate gyrus (DG), involved in hippocampal processes, but also in neurogenesis, from the rest of the hippocampus according to the protocol of Hideo Hagihara [272]. The remaining hippocampal regions were then dissected in one piece out of the remaining brain and snap-frozen using dry ice.

The purity of the dissected tissue was validated afterwards via RT-qPCR using *TDO2* (tryptophan 2,3-dioxygenase) and *Lphn2* (latrophilin 2) as dentate gyrus- and CA-specific genes respectively. *ß-actin* was used as a housekeeping gene and the Ct values of both hippocampal sub-regions were compared against each other to determine the relative expression of each gene in the dissected CA regions.

3.3.4 RNA extraction from hippocampal sub-regions

In order to increase the amount and quality of the hippocampal RNA for sequencing, the extraction and purification of RNA was performed as described in Lerner et al. 2018. To summarize, we followed the instructions from the RNeasy Mini kit (Qiagen) with a slight modification during the homogenization step: frozen tissue was homogenized in RLT buffer with 1% ß-mercaptoethanol (as per the manufacturer´s protocol) with the addition of 200 µL chloroform. Apart from this step, there was no other change made. After samples were homogenized, the liquid phase was collected and run through a silica column. Columns were washed to purify RNA and eliminate any other contaminant. While in the column, samples were treated with DNase I to degrade any possible contamination from genomic DNA. Samples were then finally eluted in 30 µL RNase-free water. The working bench and the tools used were cleaned before and during the extraction with RNase away plus (MßP, San Diego, CA, USA) to ensure the good quality of the samples and avoid RNA degradation.

3.3.5 Hippocampal CA1/CA3 RNA-sequencing

The sequencing of the hippocampal transcriptome occurred at the Core Facility Genomics (Institute of Molecular Biology, IMB; Mainz). Next generation sequencing (NGS) library preparation was performed in two steps. First, cDNA was generated using NuGEN´s Ovation RNA-seq system v2, from an input amount of 10ng of total RNA, following the kit´s instructions from 2012 (NuGEN, The Netherlands). Samples were amplified using the single primer isothermal amplification (SPIA) method from NuGEN and the resulting purified cDNA was quantified using the Qubit dsDNA HS assay kit in a Qubit 2.0 Fluorometer (Life Technologies, Germany). Afterwards, the cDNA was profiled on a high sensitivity DNA chip using a 2100 Bioanalyzer (Agilent technologies, Germany) as a quality control. From the total cDNA, 1.5 µg were fragmented using a Covaris S2 focused-ultrasonicator (Covaris, UK), with the following parameters: 1) Duty cycle = 10%; 2) Intensity = 5; 3) Cycles/Burst = 200; 4) Time = 160 seconds; and 5) Water level = 15. After the fragmentation, the resulting material was once again quantified and profiled using a Qubit 2.0 and a 2100 Bioanalyzer, respectively, as described above. This process was repeated as an extra quality control point to ensure an optimal fragmentation.

Secondly, NGS libraries were generated from 100 ng of fragmented cDNA using NuGEN´s Ovation ultralow system v2, following the kit´s manual from 2014 (NuGEN, The Netherlands). Libraries were amplified in 7 PCR cycles and purified using beads. These purified libraries were quantified as described above, and profiled on a DNA 1000 Chip using a 2100 Bioanalyzer as a last quality control. Libraries representing all the experimental groups were pooled into individual pools containing 12 libraries, all of them in equimolar ratio. Each pool was loaded into four lanes of an Illumina´s HiSeq flowcell and ran on a HiSeq 2500 in High-output mode (Illumina, USA), generating single-reads 50 base pairs long with an average yield of 52 million reads per library.

3.3.6 Quantitative polymerase chain reaction (qPCR)

In order to perform qPCR, RNA must be retrotranscribed into complementary DNA (cDNA) first. To this purpose, 1 µg of RNA was used with the high-capacity cDNA reverse transcription kit (Life technologies, Germany). This kit uses random primer for the reverse-transcription step in order to target every RNA strand found in the sample. The resulting cDNA was diluted 1:10 in RNase free water and stored at -80°C.

For the qPCR procedure, the cDNA was amplified using the commercial TaqMan assays (Applied Biosystems) with an ABI7300 real-time PCR cycler (Applied Biosystems). Reactions were performed in duplicates and *ß-actin* was used as a reference gene.

Analysis of the resulting data was performed using the 7300 system SDS software (Applied Biosystems).

Genes, and their respective primers, were selected according to the necessities of the experiment. Arc was used to measure hippocampal activation, whereas TDO2 and Lphn2 were used to prove the validity of the hippocampal microdissection. The rest of the genes (except of the reference gene) were chosen because they appeared as differentially expressed genes in the RNA-seq analysis. A full list of the TaqMan primers used can be found below.

Gene symbol	Gene name	TaqMan primer code
ß-actin	ß-Actin	Mm00607939_s1
Arc	Activity-regulated cytoskeleton-associated protein	Mm01204954_g1
TDO2	Tryptophan 2,3-dioxygenase	Mm00451266_m1
Lphn2	Latrophilin 2	Mm01320597_m1
Npy	Neuropeptide Y	Mm00445771_m1
CRHBP	Corticotropin-releasing hormone binding protein	Mm01283832_m1
Cnr1	Cannabinoid receptor-type 1	Mm01212171_s1
FosB	FBK osteosarcoma oncogene B	Mm00500401
Bdnf (exon V)	Brain-derived neurotrophic factor	Mm04230607
Grm8	Glutamate receptor metabotropic 8	Mm00433840_m1
Rab3b	Member RAS oncogene family	Mm00772238_m1
Nr4a2	Nuclear receptor subfamily 4, group A, member 2	Mm00443060_m1
Cntn4	Contactin 4	Mm00476065_m1
Grin2B	Glutamate receptor ionotropic NMDA-type subunit 2B	Mm00433820_m1

Table 1. List of TaqMan primers used for qPCR. List of TaqMan primers used for qPCR. For each gene, the pair of primers was selected according to the manufacturer´s suggestion and their gene coverage.

3.3.7 Bioinformatic analysis

The bioinformatic analysis of the data was done in collaboration with Charlotte Hewel and Anna Wierczeiko from the group of Susanne Gerber. An initial quality check of the raw sequencing data was done via FastQC (version v0.11.8). Then, bbduk.sh from the BBMap suite of tools (version 38.06) was employed to perform adapter trimming and quality filtering of the raw sequence reads (q30 cutoff). Afterwards, the trimmed and cleaned sequences were mapped against the mouse reference genome mm10 from

UCSC (downloaded via Illumina iGenome: http://support.illumina.com/sequencing/sequencing_software/igenome.html, download date 06/06/18), using the STAR aligner (version 2.6.0a) with default options. Summarized quality results were created by MultiQC (version 1.8.dev0).

Counting of reads per gene was done via featureCounts (version 1.6.2), with the -s 2 option, using the annotation file for the mm10 mouse genome. All following steps were done in R (version 3.4.4). DESeq2 was used for all subsequent DGE analysis. Volcano Plots were realized with ggplot2. And the heatmaps were generated via pheatmap(). Filtering for heatmaps was padj < 0.05 and/or baseMeanExpression > 50. The threshold for significantly differentially expressed genes (DEGs) was defined as p-adjusted < 5 %.

The Gene Ontology (GO) term and KEGG (Kyoto Encyclopedia of Genes and Genomes) pathway analysis were executed by the functions goana() and kegga() from the R package limma, using the standard over-representation test provided there. As the number of differentially expressed genes per condition was rather small, the threshold for the input gene lists was set to a p-adjusted value < 0.2.

EISA (exon-intron split analysis) by Gaidatzis et al., (2016) is a method to predict transcriptional and post-transcriptional gene regulation via differences in intron and exon counts of transcripts [9]. The theory is that intron level changes are associated to transcription and that exon-intron differences are connected to post-transcriptional regulation. The first step necessary for EISA is to obtain an intron-exon annotation. For this, we loaded the annotation _le for mm10 into R with help of the makeTxDbFromGff() function from the GenomicFeatures package. Then, only exons linked to single genes were extracted. Exon-boundaries were padded by 10 bp (bedtools, version v2.26.0), as recommended by the authors. Introns were defined as Gene introns. The resulting annotation was converted to SAF (Simplified Annotation Format) annotation, reads per exon/intron region were counted by featureCounts and counts of exon/introns were summed up per gene. Afterwards, we used the code for EISA provided by Gaidatzis et al. (2016). Briefly, the processed exon/intron counts were filtered by the genes that have a minimum coverage in both exonic and intronic regions. Subsequently, the differentially expressed regions of exons/introns of the 8 defined comparisons were calculated via the edgeR workow. The Pearson correlation of the log2 Fold change between exons and introns was calculated per gene.

3.4 Results

3.4.1 Hippocampal activation via exposure to new environment

Conditional CB1-KO mice, i.e., mice lacking CB1 in a specific neuronal population, have proven to be a useful tool to study the differential role of the ECS in specific neuronal populations. Indeed, studies using mice lacking CB1 in dorsal telencephalic glutamatergic (Glu-CB1-KO) and forebrain GABAergic (GABA-CB1-KO) neurons, the major excitatory and inhibitory neurotransmitter systems, respectively, revealed major differences in the role of CB1 and its signaling pathways within these neuronal subtypes [228,248,270]. Importantly, these observations consistently showed a dichotomic phenotype, such as CB1 mRNA expression levels and severity of epileptic seizures [248], cannabinoid-induced anxiety-like behavior [228], CB1-mediated G-protein coupled signaling cascade [270] and even neuronal morphology and synaptic plasticity processes [189,231].

Next, we wondered whether this opposite effect could also be observed at the transcriptome level in the hippocampus, a brain region central to information processing and crucially involved in spatial memory and navigation. To this end, we investigated the three genotypes Glu-CB1-KO, GABA-CB1-KO and the corresponding WT mice, but in one group of each genotype, the transcriptomic profile was determined in basal conditions (home cage) and in the other group after triggering neuronal activation in the hippocampus via exposure to a new environment. The paradigm used to trigger this neuronal activity was the open field, a behavioral test to study anxiety-like behaviors in rodents. There were no significant behavioral differences between the different genotypes (Figure 13) for the time they spent in the corner (anxiogenic) or center (anxiolytic) area. GABA-CB1-KO and Glu-CB1-KO mice spent more time in the corner (Figure 13A) and center (Figure 13B) area, respectively, than their corresponding WT mice. No significant differences were found either in locomotive behavior (Figure 13C).

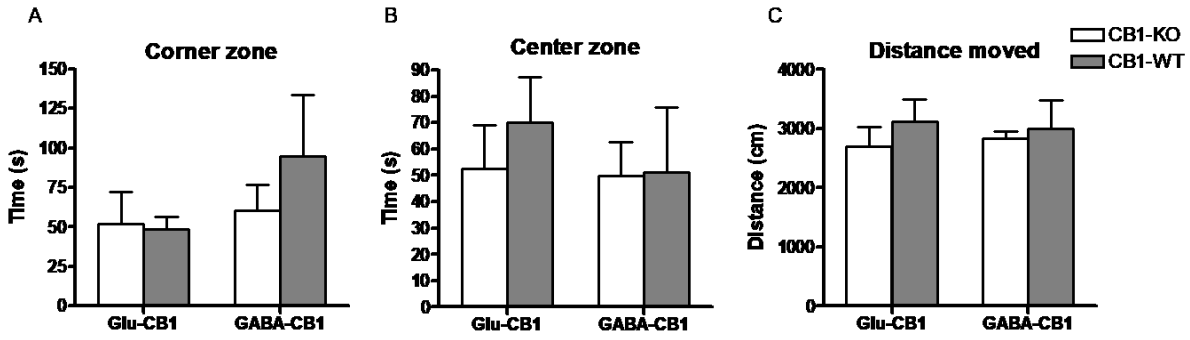

Figure 13. Anxiety-like behavior evaluated in the open field. The open field arena is a simple 40x40x30cm white box where the mice are free to explore for 5 minutes under dim light conditions. As mice prefer closed spaces to avoid predation, they tend to avoid the center of the arena. **(A)** Time spent in the corner areas of the arena, indicative of anxiety-like behavior. **(B)** Time spent in the center zone of the open field, where increased time is

correlated with reduced anxiety. **(C)** Locomotion estimated as distance moved in the 5 minutes of exposure. Data presented as mean ± s.e.m. n=6 per experimental group.

This exposure to a new environment not only corroborated that these mouse lines show barely any differences between KO and WT without applying a strong stimulus beforehand, but also triggered the expression of the neuronal activity-induced *Arc* gene as shown by qPCR data (Figure 14A). The close to 2-fold increase in comparison with non-exposed animals shows that a 5-minute exposure to a new environment is sufficient to induce significant neuronal activity in the hippocampus.

3.4.2 Microdissection of hippocampal subregions

The hippocampus receives a multitude of inputs from different brain regions, reflecting its role in information processing. The hippocampus is also a very complex structure regarding neuroanatomical features and cellular composition. As previous morphological and electrophysiological observations [189] were performed on the Schaffer collateral pathway (axons from CA3 pyramidal cells projecting into CA1), we decided to focus our transcriptomic study to these CA regions, and omit the analysis of the dentate gyrus (DG). To this end, we dissected the CA regions from the mouse brain and validated the tissue purity via qPCR using CA- and DG-specific genes, such as latrophilin-2 (*Lphn2*) and tryptophan 2,3-deoxygenase (*TDO2*), respectively (Figure 14B).

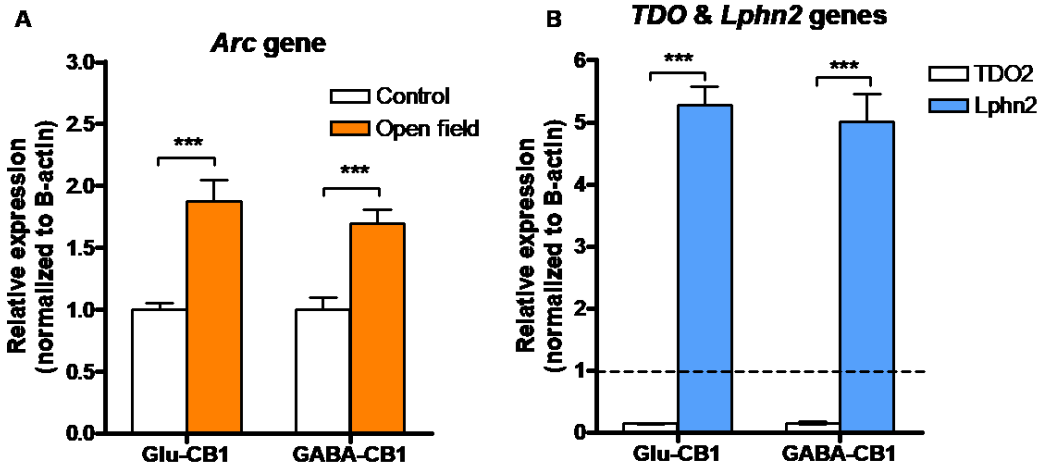

Figure 14. mRNA expression levels determined by qPCR to control sample purity. The expression levels of different genes were measured to evaluate sample purity and the degree of neuronal activity induced by the exposure to the open field arena. **(A)** To evaluate the degree of neuronal activity induced by a new environment, the expression level of Arc, an immediate early gene whose expression is induced by neuronal activity, was measured and compared between control non-exposed animals and mice exposed to the open field arena. **(B)** To validate the quality of the dissection and the purity of the CA and DG samples, the expression levels of Lphn2 (CA-specific) and TDO2 (DG-specific) in CA samples were normalized and compared to DG samples taken from the same mice (represented by a dashed line). Data presented as mean ± s.e.m. n=6 per experimental group. P values calculated using unpaired two-tailed t-test. ***, $p<0.001$.

Tissue purity was estimated by normalizing the relative mRNA expression levels of *Lphn2*, CA-specific GPCR, and *TDO2*, DG-specific and central for the kynurenine pathway, in the CA samples to the expression levels of the DG samples (Figure 14B, dashed line). Results show a 5-fold increase of *Lphn2* in the CA samples, whereas the expression level of *TDO2* is around 10-15% when compared to DG samples. These results show the success of the hippocampal microdissection, as well as the effect on neuronal activity induced by the exposure to the open field arena.

3.4.3 Differential gene expression analysis of conditional CB1-deficient mice

In order to analyze the differential gene expression (DGE) between the different subgroups, two independent approaches were designed to study the data from different perspectives. In the first comparison, samples from the open field and control groups were compared against each other for every genotype, whereas in a second comparison, samples from conditional CB1-KO and CB1-WT mice were compared to both in the basal state and in the open field condition. In both approaches, pair-wise comparisons were done among the different genotypes (comparison 1) or activation status (comparison 2) to uncover as much information as possible.

Comparison 1: Basal state versus Open field exposure

To elucidate the differential changes in gene expression induced by the behavioral exposure to a new environment, the control and open field groups of each genotype were compared. This approach helped us to uncover the different genes that were induced as a result of neuronal activity in each of the allostatic states, i.e. Glu-CB1-KO and GABA-CB1-KO mice, as well as in the basal homeostatic state, i.e. Glu-CB1-WT and GABA-CB1-WT mice. The volcano plots from these comparisons revealed an increased number of DEGs in GABA-CB1-KO neurons when compared to those of Glu-CB1-KO (Figure 15). Furthermore, in the Glu-CB1-KO and GABA-CB1-KO samples there is a rather equal number of up-regulated and down-regulated genes (Figure 15B, D), whereas their WT counterparts have a bias towards up-regulated genes (Figure 15A, C). These observations indicate that hippocampal neurons react to external mild stimuli mainly by inducing the expression of specific genes, and not by suppressing gene expression.

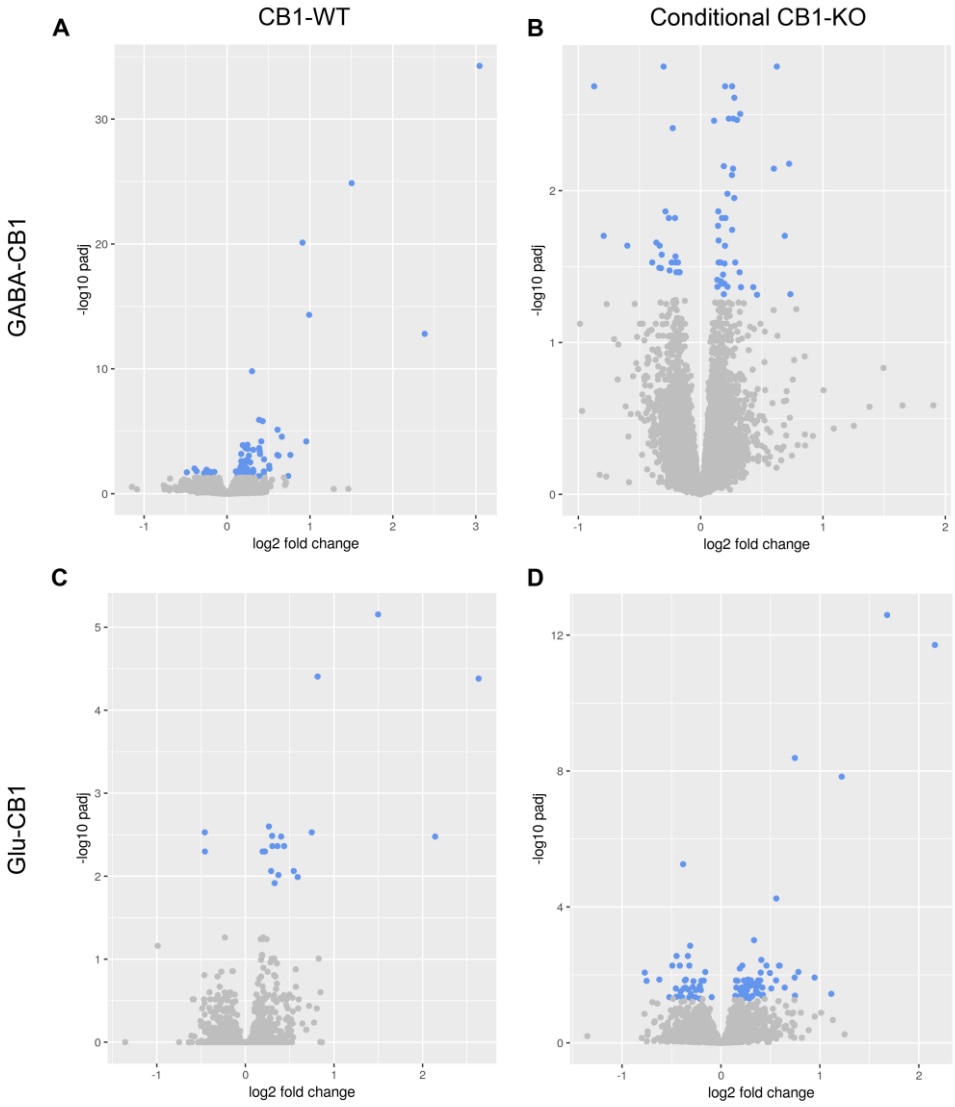

Figure 15. Volcano plots of DEG after comparing the basal state and open field exposure. Each dot in the graph represents a gene. Genes in blue are statistically significant and are defined as DEG, whereas genes in grey do not reach the threshold required for statistical significance. Genes are up-regulated or down-regulated in the open field condition if their log2 fold change is above or below 0, respectively. **(A)** DEG in GABA-CB1-WT mice (18 up-regulated and 2 down-regulated). **(B)** DEG in GABA-CB1-KO mice (63 up-regulated and 37 down-regulated). **(C)** DEG in Glu-CB1-WT mice (89 up-regulated and 11 down-regulated). **(D)** DEG in Glu-CB1-KO mice (41 up-regulated and 22 down-regulated). n=6 per experimental group.

Interestingly, when studying the top20 genes in each comparison (Figure 16) several genes relevant to neuronal activity appeared consistently. Among these genes, there are several members of Fos family, a group that comprises several immediate early genes that act as transcription factors, such as *fosB*, *c-fos* or *c-jun*, among others. Other genes known to be induced by neuronal activity also appear differentially expressed, such as members of the early growth response (EGR) family, that comprises several zinc finger transcription factors, or the nuclear receptor family (Nur), such as *Nr4a1* or *Nr4a2*, which also modulate transcriptional processes. Among the list of DEG, there are also several

genes of interest such as the glucocorticoid receptor (Nr3c1), which plays a central role in the transient shift of homeostasis induced by the stress response.

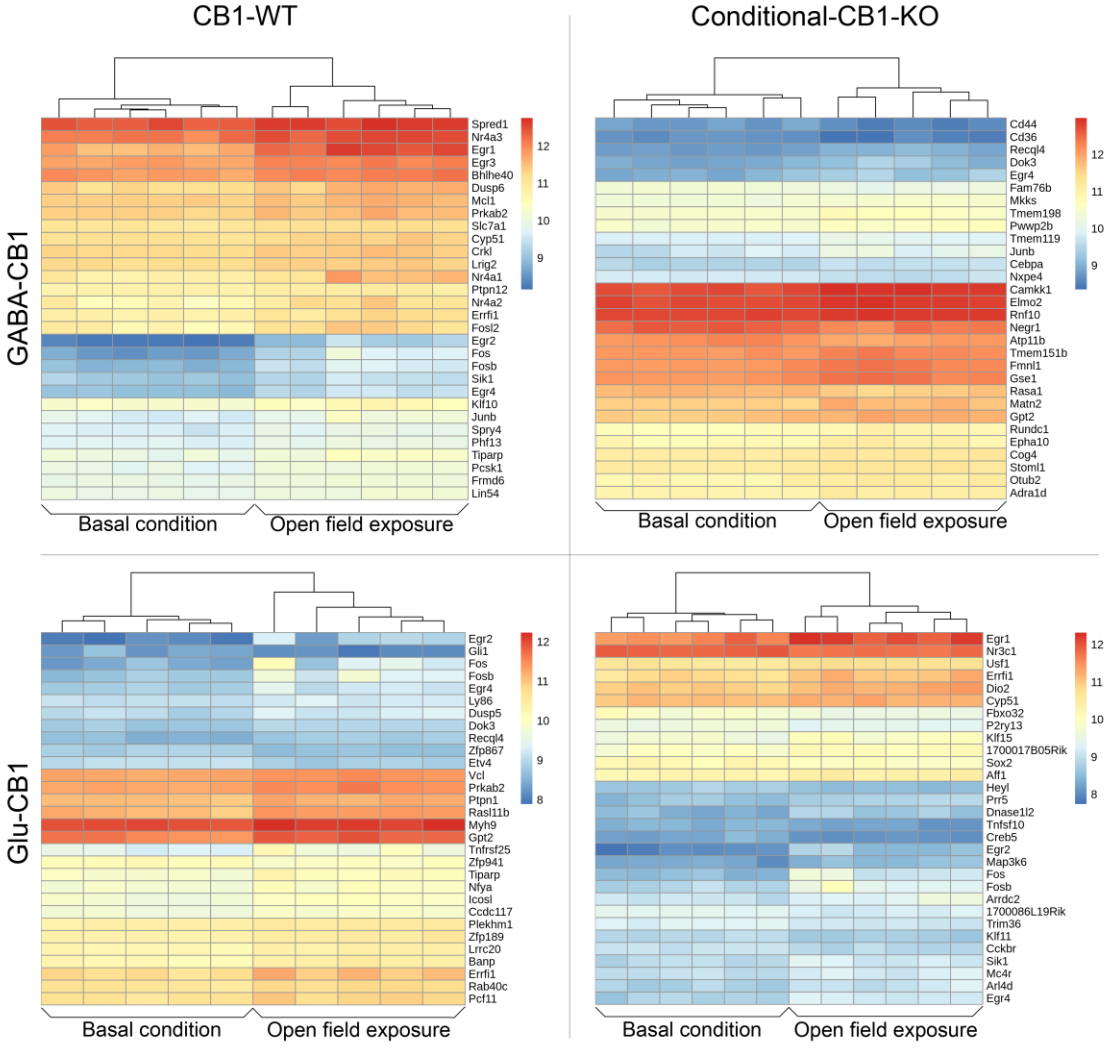

Figure 16. Heatmap of the top20 DEGs for each genotype. The 20 DEGs with the lowest p-value were used to generate heatmaps to compare their expression between groups and within the replicates of each group. Dark red and dark blue represent the highest and lowest expression, respectively. **(A)** Heatmap of the top20 DEGs in GABA-CB1-WT mice. **(B)** Heatmap of the top20 DEGs in GABA-CB1-KO mice. **(C)** Heatmap of the top20 DEGs in Glu-CB1-WT mice. **(D)** Heatmap of the top20 DEGs in Glu-CB1-KO mice. n=6 per experimental group.

Our next question was whether the two conditional CB1-KO would use the same set of genes to respond to the open field exposure or not. A high degree of overlap between them would mean that, although each conditional CB1-KO represents a different allostatic state with severe differences between each other and towards CB1-WT animals, they still respond to the same stimuli using the same genetic programs. For this purpose, we compared the up-regulated and down-regulated genes of Glu-CB1-KO and GABA-CB1-KO samples (Figure 17). Not surprisingly, each allostatic state reacts completely different to neuronal activity. When comparing up-regulated with down-

regulated genes (or vice versa), there are no shared genes between genotypes (Figure 17B, C). The highest number of overlapped genes resulted from comparing the up-regulated genes of each conditional CB1-KO animal (Figure 17A). Most of these genes are actually immediate early genes, such as *Junb*, *Egr1* and *Egr4*, which are expressed upon neuronal activation. The fourth gene is *Gpt2*, a glutamic pyruvate transaminase with an important role in gluconeogenesis and amino acid metabolism. The overlap of the down-regulated genes of each genotype (Figure 17D) has only *Klf11* in common, a zinc-finger transcription factor involved in glucose and neurotransmitter metabolism.

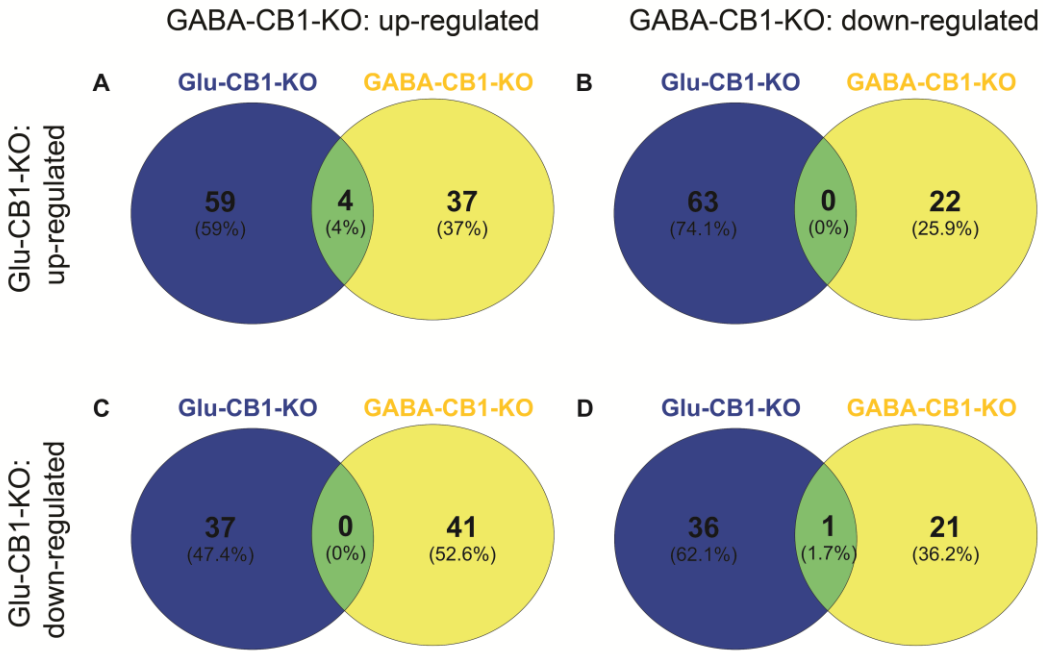

Figure 17. Venn diagram of DEG from Glu-CB1-KO and GABA-CB1-KO mice. Up-regulated and down-regulated genes found in the conditional CB1-KO groups were compared with each other to study the degree of similarity in their response to the open field exposure. **(A)** Diagram showing the overlap between the up-regulated genes of Glu-CB1-KO and GABA-CB1-KO. The common genes correspond to the member of the FOS family JunB, the activity-dependent transcription factors Egr1 and Egr4, as well as the gene Gpt2, an alanine transaminase involved in gluconeogenesis and amino acid metabolism. **(B)** Diagram showing the overlap between the up-regulated genes of Glu-CB1-KO and the down-regulated genes of GABA-CB1-KO. **(C)** Diagram showing the overlap between the down-regulated genes of Glu-CB1-KO and the up-regulated genes of GABA-CB1-KO. **(D)** Diagram showing the overlap between the down-regulated genes of Glu-CB1-KO and GABA-CB1-KO. The gene in common is Klf11, a zinc-finger transcription factor.

Comparison 2: CB1-WT versus conditional CB1-KO

Genotype-induced transcriptomic changes were analyzed by comparing the gene expression profiles of WT and conditional-KO mice in the control and open field conditions separately. These differences might correspond to compensatory mechanisms developed within the brain in order to adapt to the excess of neurotransmitter caused by the lack of CB1. The volcano plots resulting from this comparison showed a variable number of DEGs in the different conditions (Figure 18).

Interestingly, there was a strong difference in the number of DEGs in the basal state between dlx-cre x CB1ff (24 up-regulated and 78 down-regulated) and nex-cre x CB1ff samples (4 up-regulated and 5 down-regulated) (Figure 18A, C). This difference is striking, given the differences in the morphology and functionality observed in basal conditions [189], as it means that Glu-CB1-KO are able to adapt to the excess of glutamatergic drive without requiring strong transcriptomic changes. However, the exposure to the open field arena triggered the expression of different gene profiles in the Glu-CB1-KO and Glu-CB1-WT mice, leading to differences between these mice only when they were challenged (Figure 18D), confirming previous studies that used these animals. On the other hand, mice from the mouse line dlx-cre x CB1ff showed an increased number of down-regulated genes both in the basal conditions and after exposure to the open field arena (Figure 18B, D).

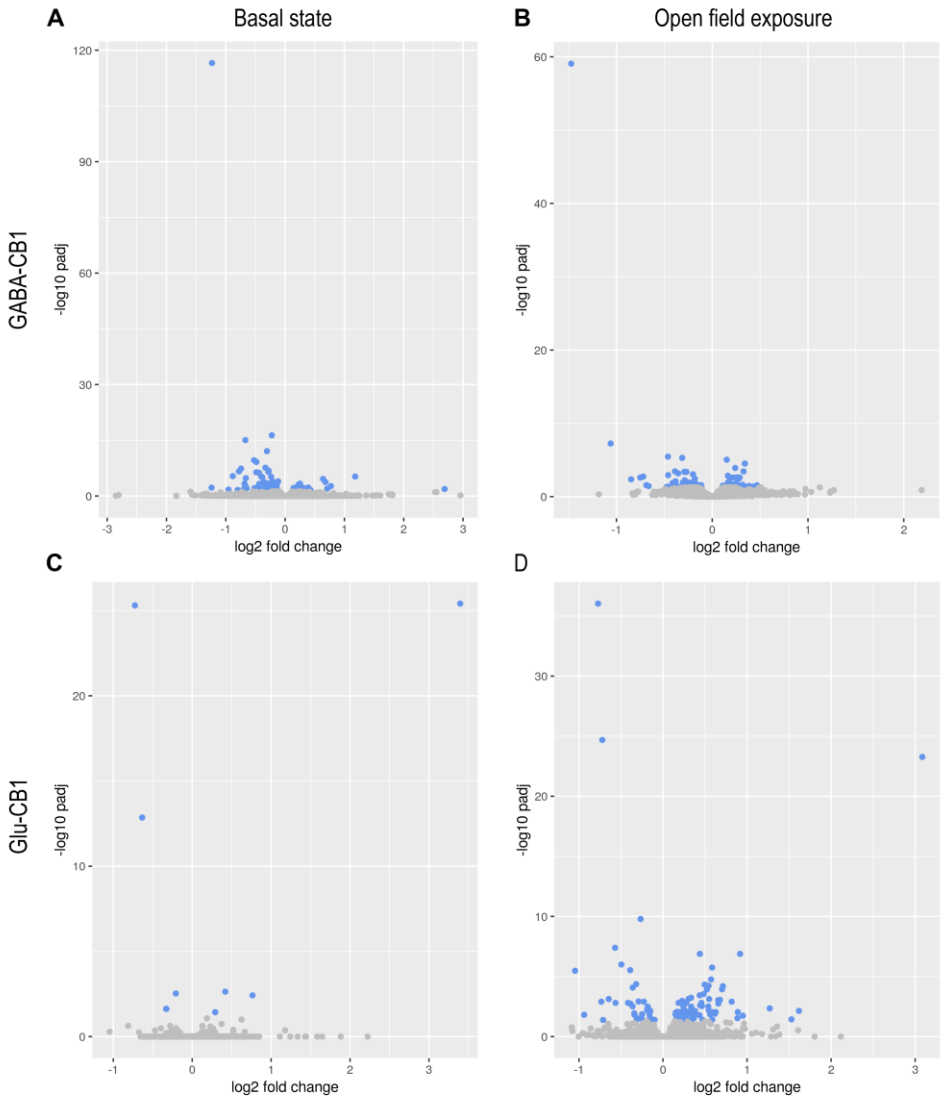

Figure 18. Volcano plots of the comparison 2 for the basal and the activated states. Each dot in the graph represents a gene. Genes in blue are statistically significant and are defined as DEG,

whereas genes in grey do not reach the threshold required for statistical significance. Genes are up-regulated or down-regulated in the conditional CB1-KO group if their log2 fold change is above or below 0, respectively. **(A)** DEG in the basal state of dlx-cre x CB1ff mice (24 up-regulated and 78 down-regulated). **(B)** DEG in the open field condition of dlx-cre x CB1ff mice (49 up-regulated and 60 down-regulated). **(C)** DEG in the basal state of nex-cre x CB1ff mice (4 up-regulated and 5 down-regulated). **(D)** DEG in the open field condition of nex-cre x CB1ff mice (77 up-regulated and 35 down-regulated). n=6 per experimental group.

The heatmaps resulting from the top20 DEGs in these pair-wise comparisons did not show genes appearing consistently in all the graphs. Nevertheless, several genes interesting for neuronal function have appeared in the analysis. Some of these highlighted genes are *npy* or *crhbp*, important during the stress response, and *Pdlim1*, a protein involved in the regulation of the cytoskeleton (Figure 19). This reduced number of common genes could indicate that the differences between conditional CB1-KO and CB1-WT mice are completely different in the basal state and after open field exposure.

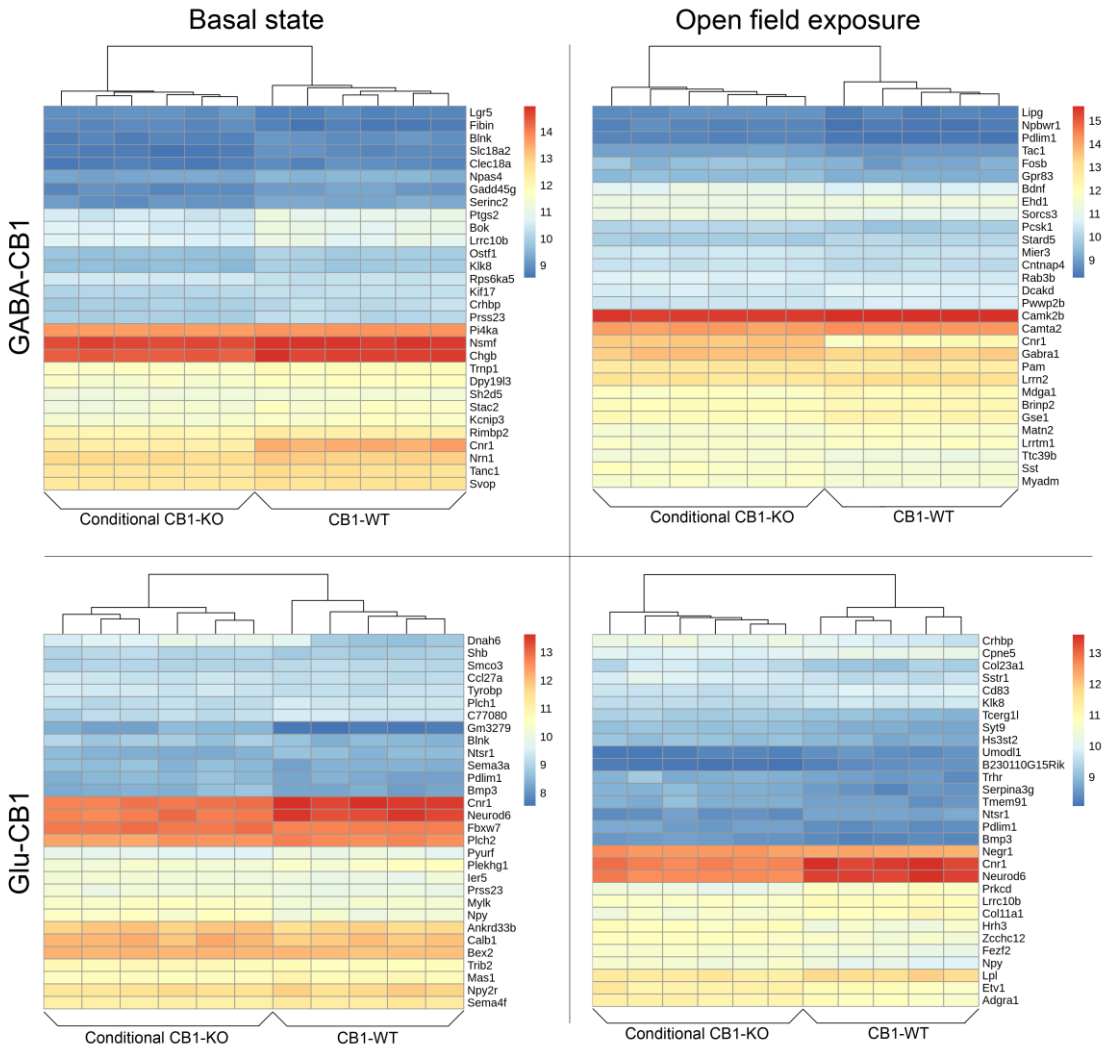

Figure 19. Heatmap of the top20 DEGs in the basal state and the open field condition. The 20 DEGs with the lowest p-value were used to generate heatmaps to compare their expression between groups and within the replicates of each group. Dark red and dark blue represent the highest and lowest expression, respectively. **(A)** Heatmap of the top20 DEGs in the basal state of GABA-CB1-KO and wt mice. **(B)** Heatmap of the top20 DEGs after open field

exposure in GABA-CB1-KO and wt mice. **(C)** Heatmap of the top20 DEGs in the basal state of Glu-CB1-KO and wt mice. **(D)** Heatmap of the top20 DEGs after open field exposure in Glu-CB1-KO and wt mice. n=6 per experimental group.

The overlap of DEGs between the up-regulated and down-regulated genes of the different conditional CB1-KO samples in the open field condition is, once again, not very high (Figure 20). Comparison of only up-regulated genes (Figure 20A) or only down-regulated genes (Figure 20D) showed no overlap, except for CB1 which was, expectedly, down-regulated in both genotypes. However, the cross-comparison between down-regulated genes in Glu-CB1-KO and up-regulated genes in GABA-CB1-KO (Figure 20C) shows one common gene: *Sptb*, a subunit of β-spectrin, an essential protein to keep the structure of the cytoskeleton. The highest degree of overlap was found when comparing up-regulated genes in Glu-CB1-KO and down-regulated genes in GABA-CB1-KO (Figure 20D). Among these genes, there are several genes involved in synaptic processes (*Kcnn2*, *Rab3b*), the regulation of transcription (*Ldb2*, *Pdlim1*), the stress response (*Crhbp*) and neurotransmission (S*st*). Interestingly, the few overlapping genes could help to explain phenotypes previously observed, such as anxiety or neuronal function, among others. Even more interestingly, there were only genes in the cross-comparisons (i.e. down-regulated genes from one genotype to up-regulated genes from another, or vice versa), which could indicate that there are similarities in the genetic programs used by neurons to adapt to the excess of excitatory and inhibitory neurotransmitters, with the only difference being whether they are up-regulated or down-regulated.

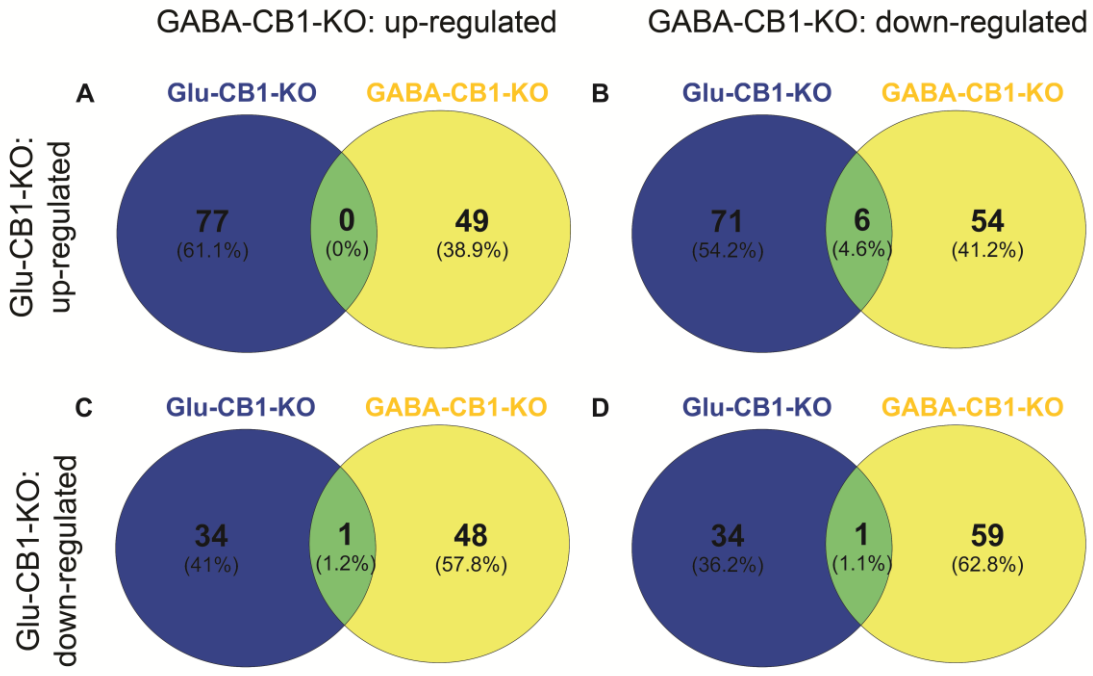

Figure 20. Venn diagram of DEG from Glu-CB1-KO and GABA-CB1-KO mice. Up-regulated and down-regulated DEGs from each genotype found in the open field group were compared with each other to study the similarity of the allostatic states after behavioral neural activation. **(A)** Diagram showing the overlap between the up-regulated genes of Glu-CB1-KO and GABA-CB1-KO. **(B)** Diagram showing the overlap between the up-regulated genes of Glu-CB1-KO and the down-regulated genes of GABA-CB1-KO. The genes in common are related to synaptic processes (Kcnn2, Rab3b), regulation of transcription (Ldb2, Pdlim1), the stress-response (Crhbp) and neurotransmission (Sst). **(C)** Diagram showing the overlap between the down-regulated genes of Glu-CB1-KO and the up-regulated genes of GABA-CB1-KO. Within this comparison, a single gene can be found in common: Sptb, a spectrin involved in the cytoskeleton. **(D)** Diagram showing the overlap between the down-regulated genes of Glu-CB1-KO and GABA-CB1-KO. The only common gene in this comparison is cnr1, which encodes the CB1 receptor.

3.4.4 RNA-sequencing validation of differentially expressed genes via qPCR

The sequencing of genetic material is a stochastic process that potentially adds noise to the samples. Furthermore, the current bioinformatic algorithms and databases are not perfect and, thus, they also add some noise to the final numbers. For this reason, it is necessary to validate sequencing results via other methods, such as quantitative PCR (qPCR). In our study, we used independent samples to validate different genes of interest that we found differentially expressed in our RNA-seq data.

The first gene that needed to be validated as a quality control is *cnr1*, the gene encoding CB1 (Figure 21A). Previous studies suggested that CB1 appeared only in a subset of hippocampal GABAergic neurons, but with higher levels than in glutamatergic neurons, where its expression was faint, but present across all glutamatergic terminals. Our qPCR data showed that GABAergic neurons contain around 60% of the total hippocampal CB1, whereas CB1 in glutamatergic synapses accounts for just 40% of the total mRNA in the CA hippocampal regions. These results validated the data obtained in the RNA-sequencing procedure. In addition, mRNA levels of several other genes were measured. These genes were chosen as they are involved in neuronal activity (Figure 21B), neurotransmission and homeostasis (Figure 21C), and stress response (Figure 21D). Furthermore, these genes showed a dichotomic feature, meaning they are up-regulated in Glu-CB1-KO or GABA-CB1-KO mice and down-regulated in the opposite. Out of these genes, the characteristics of *FosB* is very interesting, as it shows an increased level of neuronal activity in Glu-CB1-KO mice when compared to GABA-CB1-KO mice (Figure 21B), most likely as a result of the excess of excitatory neurotransmitter. The alterations of *Npy* and *Crhbp* could be a result of this overexcitation, as both genes are known to be involved in homeostatic processes and stress modulation [273,274]. Genes with this dichotomic feature are important because they can potentially uncover genetic "switches" that could allow to shift between the allostatic and the homeostatic state by modulating the intensity and direction of change.

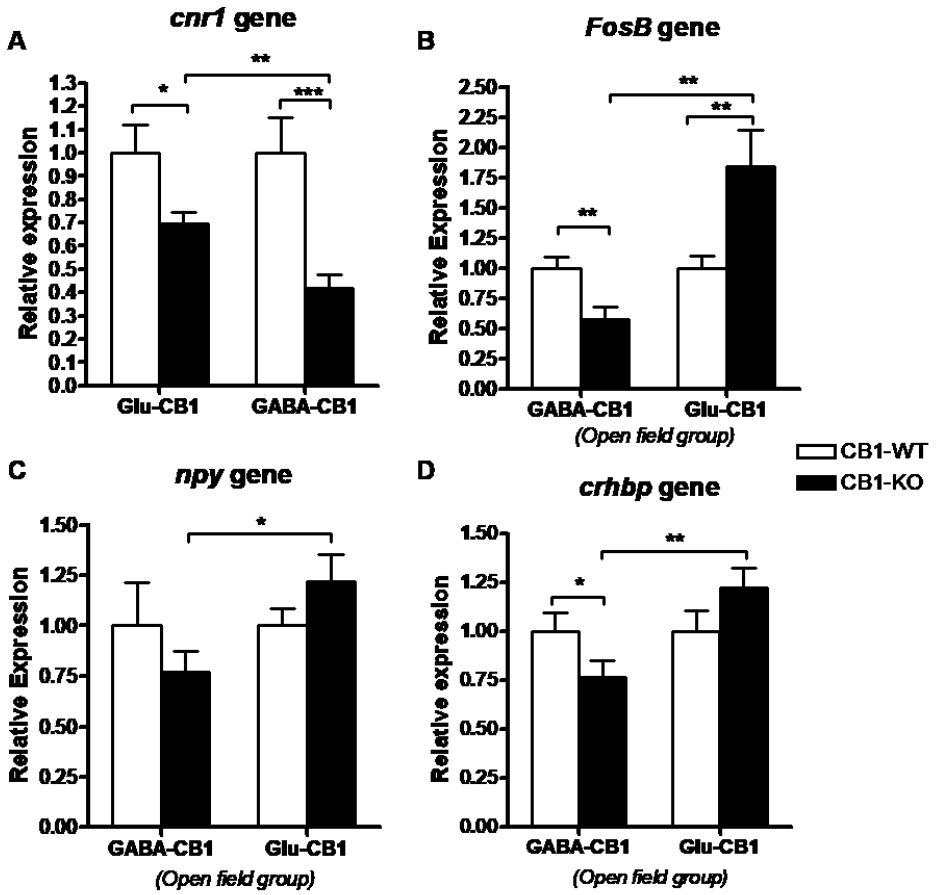

Figure 21. qPCR data to validate the mRNA expression of certain DEGs. Quantitative PCR of CB1 gene and other genes with dichotomic behavior. Graphs show the relative expression of conditional CB1-KO samples in the open field condition to their CB1-WT counterparts. However, the graph for CB1 is an exception, as it shows the relative expression of conditional CB1-KO mice to their CB1-WT conspecifics but merging the samples from basal condition and open field exposure. **(A)** Graph showing the relative expression of the cnr1 gene (CB1) in conditional CB1-KO and CB1-WT samples. **(B)** Graph showing the relative expression of FosB, an immediate early gene induced upon neuronal activation. **(C)** Graph showing the relative expression of the npy gene, a neuropeptide involved in neurotransmission, reduction of stress and anxiety and homeostasis. **(D)** Graph showing the relative expression of the crhbp gene, a neuromodulator important in the inhibition of crh and the regulation of the stress response. There are 6 replicates in each experimental group. P value was estimated using one-way ANOVA analysis. *, $p<0.05$; **, $p<0.01$; ***, $p<0.001$.

Several other genes were also measured, although these ones did not show the dichotomic behavior previously observed (Figure 22). These genes also appeared as DEGs in the RNA-sequencing data in some pair-wise comparisons. These genes were selected because they are involved, directly or indirectly, in neurotransmission and synaptic processes. There were a few statistically significant differences between both conditional CB1-KO genotypes (marked by *) and between one conditional CB1-KO in the open field group and the dashed line (marked by $), which symbolizes either their respective CB1-WT counterpart (Figure 22A) or the same conditional CB1-KO genotype in the basal state (Figure 22B). Among these genes, *Grm8* is quite interesting as it has

been linked to protection against excitotoxicity [275], a likely consequence for the neurons of Glu-CB1-KO mice. Moreover, the accumulation of inhibitory neurotransmitter in the GABA-CB1-KO brain could help explain the differences in *BDNF V* and *Grin2B*, as both genes are normally induced by excitatory signals and repressed by prolonged neuronal inhibition.

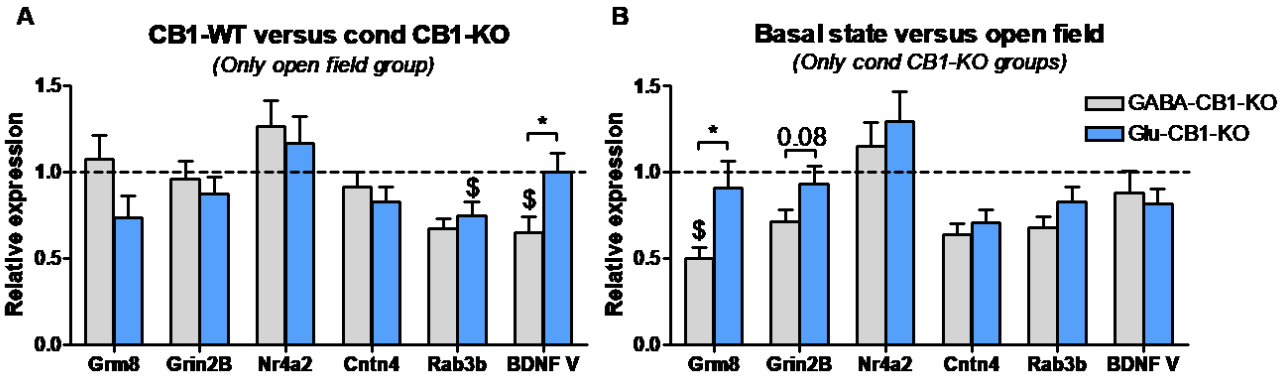

Figure 22. qPCR data of different genes to validate the sequencing data. Quantitative PCR of different genes of interest found to be differentially expressed in the RNA-sequencing experiment. Relative expression for Glu-CB1-KO and GABA-CB1-KO samples is normalized to the dashed line, which represents either CB1-WT samples from the open field group (A) or the same conditional CB1-KO group in the basal state. A star symbol (*) indicates a comparison between Glu-CB1-KO and GABA-CB1-KO, whereas the dollar symbol ($) indicates a comparison between one group and their normalized baseline (dashed line). **(A)** Relative expression of different genes resulting from comparing CB1-WT and conditional CB1-KO samples in the open field group. **(B)** Relative expression of different when comparing the conditional CB1-KO in the control and open field groups. N=6 for all experimental groups. P value was estimated using unpaired two-tailed t-test. *, $p<0.05$; $, $p<0.05$.

3.4.5 Gene ontology (GO) and pathway analysis of conditional CB1-deficient mice

The list of DEGs, resulting from comparing different experimental conditions, can then be used to uncover different gene ontology (GO) terms that provide information about cell compartments, molecular functions or biological processes that might have been affected by deletion of CB1 in specific neuronal populations. Furthermore, we performed a KEGG (Kyoto Encyclopedia of Genes and Genomes) pathway analysis in search of cellular pathways affected by the excess of neurotransmitter at the synaptic terminals.

Comparison 1: Control vs Open field

In a first approach, we analyzed the DEGs found in Glu-CB1-KO and GABA-CB1-KO animals when comparing their transcriptomes in the basal state and after open field exposure. The GO analysis of the Glu-CB1-KO group (Table 2) showed up-regulated terms related to cellular metabolic processes, the nucleus, and transcription. Given that this comparison provided information about the effect of the open field exposure, it does not come to a surprise that some of the up-regulated terms found in Glu-Cb1-KO mice are related to the cellular response to stimulus and hormones. Surprisingly, the cellular

response to glucocorticoids was down-regulated in Glu-CB1-KO animals, together with processes of cell adhesion, transcription and apoptosis.

	Open field effect on Glu-CB1-KO --- GO terms	N	P-value
Up-regulated	intracellular part	170	1.32E-16
	cellular metabolic process	139	1.60E-16
	cellular macromolecule metabolic process	115	4.85E-13
	binding	156	9.30E-11
	response to hormone	22	1.64E-08
	nucleus	91	2.08E-07
	cellular response to chemical stimulus	47	2.11E-06
	response to stimulus	109	3.23E-06
	transcription regulator activity	31	3.30E-06
	DNA binding transcription factor activity	26	5.38E-06
Down-regulated	cell-cell adhesion	14	1.42352E-06
	biological adhesion	18	6.36609E-06
	response to glucocorticoid	5	1.68867E-05
	programmed cell death	19	0.000304361
	negative regulation of cellular biosynthetic process	19	2.25611E-05
	DNA binding transcription factor activity	16	2.68765E-05
	RNA polymerase II transcription factor activity, sequence-specific DNA binding	12	0.000101954
	cell-cell junction	9	0.000143415
	regulation of apoptotic process	17	0.000188778
	nervous system development	21	0.000405182

Table 2. GO terms after comparing the basal and open field state in Glu-CB1-KO mice. GO terms after comparing the basal and open field state in Glu-CB1-KO mice. List of selected GO terms that resulted from analyzing the up-regulated and down-regulated genes of Glu-CB1-KO mice after brief exposure to a new environment (open field), in comparison to their basal state. GO terms are color coded as green or red for up-regulated and down-regulated terms, respectively. The two additional columns on the right side indicate the number of DEGs for each term and the statistical significance of the GO term (as P-value).

On the other hand, the up-regulated GO terms of GABA-CB1-KO mice related to protein binding and kinase activity, the organization of cellular components and its regulation, and the regulation of cellular processes in the cytoplasm and nucleus when comparing their basal and activated state (via open field) (Table 3). Similarly to Glu-CB1-KO animals, the exposure to a new environment induced genes involved in cellular metabolic processes. Contrary to Glu-CB1-KO mice, GABA-CB1-KO animals showed apoptotic processes up-regulated. The excess of the inhibitory neurotransmitter GABA induced by the neuronal activity had, however, consequences for GABA-CB1-KO mice. The exposure to the open field down-regulated genes related to the synapses and their assembly, as well as genes involved in ion binding and the activity of ionotropic glutamate receptors. Additionally, GO terms related to homeostatic processes, such as cellular chemical homeostasis and ion homeostasis appeared down-regulated.

Interestingly, GABA-CB1-KO animals had significantly down-regulated genes involved in behavior, which would correspond with previous observations of behavioral changes induced by external manipulations [228].

	Open field effect on GABA-CB1-KO --- GO terms	N	P-value
Up-regulated	cytoplasm	180	1.39E-16
	protein binding	151	2.69E-12
	regulation of cellular component organization	58	3.31E-09
	cellular metabolic process	149	4.71E-09
	negative regulation of cellular process	85	7.60E-08
	nucleus	112	8.41E-08
	cellular component organization	99	2.76E-07
	regulation of cell death	33	5.46E-04
	negative regulation of response to endoplasmic reticulum stress	6	3.34E-06
	kinase activity	24	4.16E-06
Down-regulated	homeostatic process	35	1.028E-06
	cellular chemical homeostasis	21	2.05343E-06
	behavior	20	2.70473E-06
	ion binding	75	3.07512E-06
	synapse assembly	9	8.80448E-06
	ion homeostasis	20	1.00409E-05
	somatodendritic compartment	22	1.6723E-05
	ionotropic glutamate receptor activity	4	1.9237E-05
	synaptic membrane	12	2.21281E-05
	synapse	22	2.55883E-05

Table 3. GO terms after comparing the basal and open field state in GABA-CB1-KO mice. GO terms after comparing the basal and open field state in GABA-CB1-KO mice. List of selected GO terms that resulted from analyzing the up-regulated and down-regulated genes of GABA-CB1-KO mice that had been briefly exposed to a new environment (open field), in comparison to their basal state. GO terms are color coded as green or red for up-regulated and down-regulated terms, respectively. The two additional columns on the right side indicate the number of DEGs for each term and the statistical significance of the GO term (as P-value).

The KEGG pathway analysis showed the different pathways that were affected due to the exposure to the open field arena (Figure 23). Among the results, there are several molecular pathways of importance to brain function, such as the MAP kinase (MAPK) signaling pathway and pathways for the regulation of glucose metabolism (e.g. FoxO and glucagon signaling pathways). Furthermore, the interactions between neuroactive ligands and their receptors, which are mainly up-regulated and down-regulated in Glu-CB1-KO and GABA-CB1-KO mice, respectively, also appeared as significantly altered. The processing of proteins in the endoplasmic reticulum is also a common pathway up-regulated in both conditional CB1-KO groups. Interestingly, Glu-CB1-KO mice showed a down-regulation of tight junctions, fatty acid metabolism and the synthesis and secretion of cortisol. Meanwhile, GABA-CB1-KO mice down-regulated pathways were all involved

in synaptic function (Figure 23B), such as glutamatergic transmission, cAMP signaling, axon guidance and cell adhesion molecules.

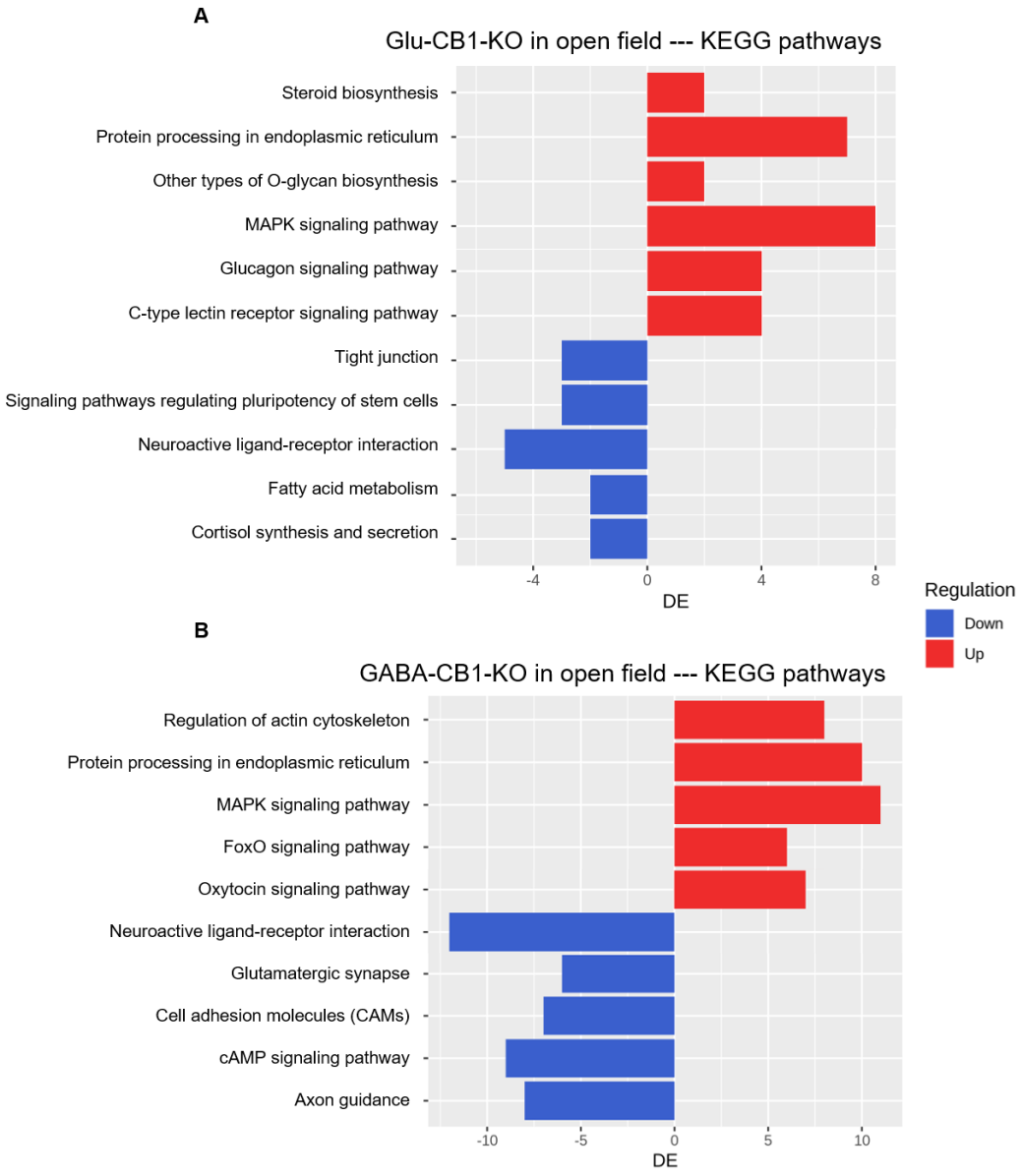

Figure 23. GO terms after comparing the basal and open field state in GABA-CB1-KO mice. Representative images of the number of DEGs for each of the KEGG terms that were significantly changed between CB1-WT mice and the respective conditional CB1-KO animals. These two genotypes were compared after the exposure to the open field arena to study the effect of neuronal activation, and subsequent neurotransmitter excess, in Glu-CB1-KO and GABA-CB1-KO mice. **(A)** Graph showing the different KEGG terms that resulted from comparing the Glu-CB1-WT and Glu-CB1-KO genotypes after the open field exposure. **(B)** Graph showing the different KEGG terms that resulted from comparing the GABA-CB1-WT and GABA-CB1-KO genotypes after the open field exposure.

Comparison 2: CB1-WT vs Conditional-CB1-KO

Next, we analyzed the GO terms and KEGG pathways that were significantly different between CB1-WT and conditional CB1-KO animals. GABA-CB1-KO in the basal state showed down-regulated GO terms relating to the synaptic terminals (e.g. neuron

projection, axon, presynapse), synaptic function (e.g. cell-cell signaling, signal transduction) and cognition (e.g. learning and memory, behavior) (data not shown). Many of these GO terms involved in synaptic function were also down-regulated in Glu-CB1-KO mice. However, the low number of DEGs in the basal state of Glu-CB1-KO animals complicated the GO analysis and the conclusions that can be drawn from this group. Interestingly, both conditional CB1-KO mice showed terms related to cell communication and cell-cell binding as up-regulated during the basal state.

The exposure to the open field arena caused an excess of excitatory and inhibitory neurotransmitter at the synapses of Glu-CB1-KO and GABA-CB1-KO mice, respectively. The excess of glutamate induced the expression of genes related to behavior, synaptic transmission and various neuron-specific compartments (e.g. dendrite, synapse, somatodendritic compartment) in Glu-CB1-KO mice (Table 4). Glutamate transmission as well as the activity of certain glutamate receptors were also up-regulated in Glu-CB1-KO animals. Contrary to the observed phenotype of Glu-CB1-KO mice, GABA-CB1-KO individuals showed GO terms related to neuron differentiation and the development of neuronal projections as up-regulated (Table 5). Other interesting GO terms were also up-regulated, such as synaptic signaling, lipid homeostasis and cellular metabolic processes.

	Glu-CB1-KO after open field --- GO terms	N	P-value
Up-regulated	somatodendritic compartment	29	3.12E-15
	neuron projection	33	2.84E-14
	behavior	21	6.83E-11
	dendrite	19	4.36E-10
	synapse	23	5.85E-10
	regulation of cell communication	39	3.66E-08
	chemical synaptic transmission	18	4.31E-08
	synaptic transmission, glutamatergic	7	5.71E-07
	glutamate receptor signaling pathway	6	2.08E-06
	adenylate cyclase inhibiting G-protein coupled glutamate receptor activity	3	4.74E-06
Down-regulated	cellular developmental process	30	1.05774E-07
	neuron projection development	14	3.76123E-07
	positive regulation of apoptotic process	11	5.22369E-07
	plasma membrane	31	6.44724E-07
	cell periphery	31	1.13798E-06
	positive regulation of cell death	11	1.347E-06
	regulation of neuron projection development	10	1.62935E-06
	neuron differentiation	15	3.63387E-06
	synaptic signaling	11	4.06205E-06
	regulation of response to stimulus	23	2.03472E-05

Table 4. GO terms after comparing CB1-WT and Glu-CB1-KO mice exposed to the open field. GO terms after comparing CB1-WT and Glu-CB1-KO mice exposed to the open field. List of selected GO terms that resulted from analyzing the up-regulated and down-regulated genes of Glu-CB1-KO mice that had been briefly exposed to a new environment (open field). GO terms are color coded as green or red for up-regulated and down-regulated terms, respectively. The two additional columns on the right side indicate the number of DEGs for each term and the statistical significance of the GO term (as P-value).

Interestingly, the GO terms associated to neuronal developmental processes that appeared up-regulated in GABA-CB1-KO mice were shown to be down-regulated in Glu-CB1-KO animals (Table 5). Furthermore, GO terms such as apoptotic processes, the regulation of the response to stimuli and synaptic signaling also appeared down-regulated. This last GO term is especially interesting as signaling processes between neurons was up-regulated in Glu-CB1-KO. This contradiction could indicate that the excess of glutamate induces both an increase in neuronal transmission and a compensatory mechanism, most likely to avoid excitotoxicity. On the other hand, GABA-CB1-KO mice predominantly showed GO terms related to synaptic transmission, and especially GABAergic neurotransmission, as down-regulated (Table 5). Moreover, GO terms associated to the regulation of the membrane potential, the cell junctions of the synapses, and behavior were also found down-regulated in GABA-CB1-KO mice upon exposure to a new environment.

	GABA-CB1-KO after open field --- GO terms	N	P-value
Up-regulated	cytoplasm	147	3.31E-09
	protein binding	128	1.62E-08
	intracellular membrane-bounded organelle	133	2.23E-06
	neuron differentiation	31	1.67E-05
	lipid homeostasis	8	2.10E-05
	cell projection	41	4.28E-05
	neuron projection development	24	5.03E-05
	cellular metabolic process	121	8.64E-05
	synaptic signaling	19	1.17E-04
	neuron projection morphogenesis	17	1.35E-04
Down-regulated	neuron part	43	3.3914E-11
	synapse	31	2.02366E-10
	binding	154	3.51527E-09
	cell junction	33	8.12448E-09
	chemical synaptic transmission	24	2.52207E-08
	synaptic signaling	24	2.65626E-08
	synaptic transmission, GABAergic	7	1.38512E-07
	behavior	22	1.82068E-07
	regulation of membrane potential	16	4.3913E-07
	modulation of chemical synaptic transmission	17	2.40398E-06

Table 5. GO terms after comparing CB1-WT and GABA-CB1-KO mice exposed to the open field. GO terms after comparing CB1-WT and GABA-CB1-KO mice exposed to the open field. List of selected GO terms that resulted from analyzing the up-regulated and down-regulated genes of GABA-

CB1-KO mice that had been briefly exposed to a new environment (open field). GO terms are color coded as green or red for up-regulated and down-regulated terms, respectively. The two additional columns on the right side indicate the number of DEGs for each term and the statistical significance of the GO term (as P-value).

The analysis of the KEGG pathways revealed interesting pathways that could be affected in the different allostatic states. The results of the basal state in Glu-CB1-KO mice (Figure 24A) showed an up-regulation of pathways involved in the control of appetite, e.g. the apelin and adipocytokine pathways. The NF-κβ pathway, which is essential for cognitive and cellular stress processes, was also positively regulated in Glu-CB1-KO mice. The signaling of the ECS and axon guidance processes seemed to be down-regulated in Glu-CB1-KO mice. However, the low number of DEGs in this comparison made impossible to draw strong conclusions. GABA-CB1-KO mice also showed the signaling of the ECS as down-regulated (Figure 24B), together with various signaling pathways (e.g. MAPK, oxytocin and apelin) and metabolic processes involving glycerolipids and glutamate. Furthermore, different signaling pathways, such as the Wnt, prolactin, cAMP and adipocytokine signaling pathways, were all up-regulated in the basal state of GABA-CB1-KO mice. The interaction between neuroactive ligands and their receptors was also up-regulated in the basal state of GABA-CB1-KO.

The exposure to the open field arena initiated differential changes in gene expression, and subsequently cellular pathways down the line, in Glu-CB1-KO and GABA-CB1-KO mice (Figure 25). Both conditional CB1-KO groups showed an up-regulated cAMP signaling pathway in comparison to CB1-WT mice, surprisingly. Interestingly, some terms, e.g. glutamatergic synapse and neuroactive ligand-receptor interaction, showed a dichotomic feature by being up-regulated in Glu-CB1-KO and down-regulated in GABA-CB1-KO. On top of the down-regulation of genes present in the glutamatergic synapse, GABA-CB1-KO mice showed a down-regulation of the GABAergic synapse, but an up-regulation of the dopaminergic system (Figure 25B). Moreover, elements involved in the gap junction were down-regulated in GABA-CB1-KO animals, whereas cell adhesion molecules were up-regulated in Glu-CB1-KO mice. Surprisingly, genes involved in LTP and calcium signaling pathways were down-regulated in the Glu-CB1-KO genotype, maybe as a reaction to the excess of glutamate and neuronal activity. Another possible consequence of this excess of glutamate could be the simultaneous up-regulation and down-regulation of genes involved in axon guidance processes (Figure 25A). The up-regulated genes could be those induced by normal neuronal activity, which is known to promote the development of neuronal projections, whereas those down-regulated could correspond to either excitotoxicity or compensatory mechanisms induced by an excess of glutamate. Lastly, various signaling pathways

involved in brain function (e.g. Rap1, Ras, etc.) were also differentially regulated in Glu-CB1-KO and GABA-CB1-KO mice.

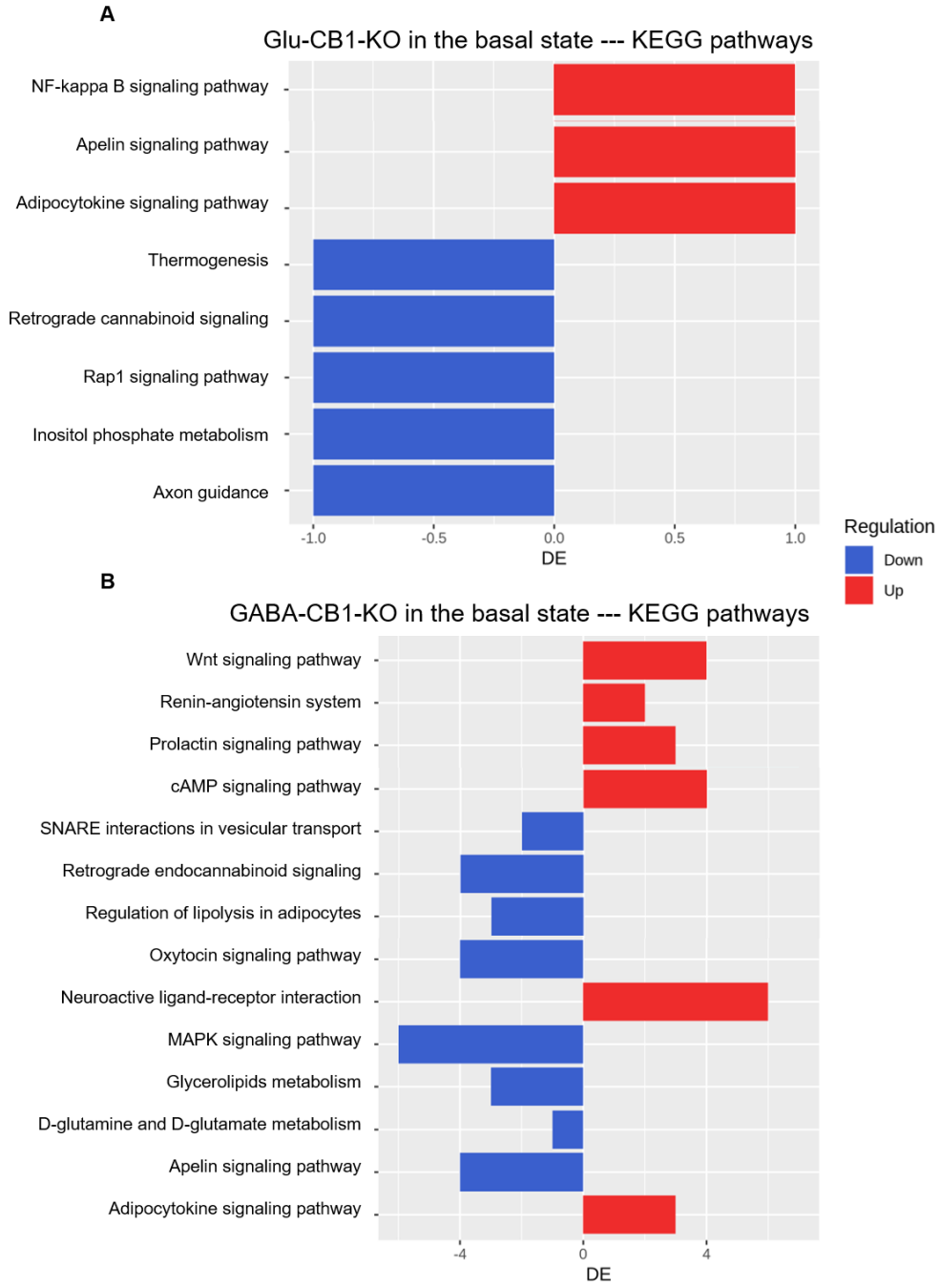

Figure 24. KEGG pathways of Glu-CB1-KO and GABA-CB1-KO mice in the basal state. Representative images of the number of DEGs for each of the KEGG terms that were significantly changed between CB1-WT mice and the respective conditional CB1-KO animals. These two genotypes were compared in the basal state (before the exposure to the open field arena) to study the transcriptomic differences between Glu-CB1-KO and GABA-CB1-KO mice in their resting state. **(A)** Graph showing the different KEGG terms that resulted from comparing the Glu-CB1-WT and Glu-CB1-KO genotypes in the basal state. **(B)** Graph showing the different KEGG terms that resulted from comparing the GABA-CB1-WT and GABA-CB1-KO genotypes in the basal state.

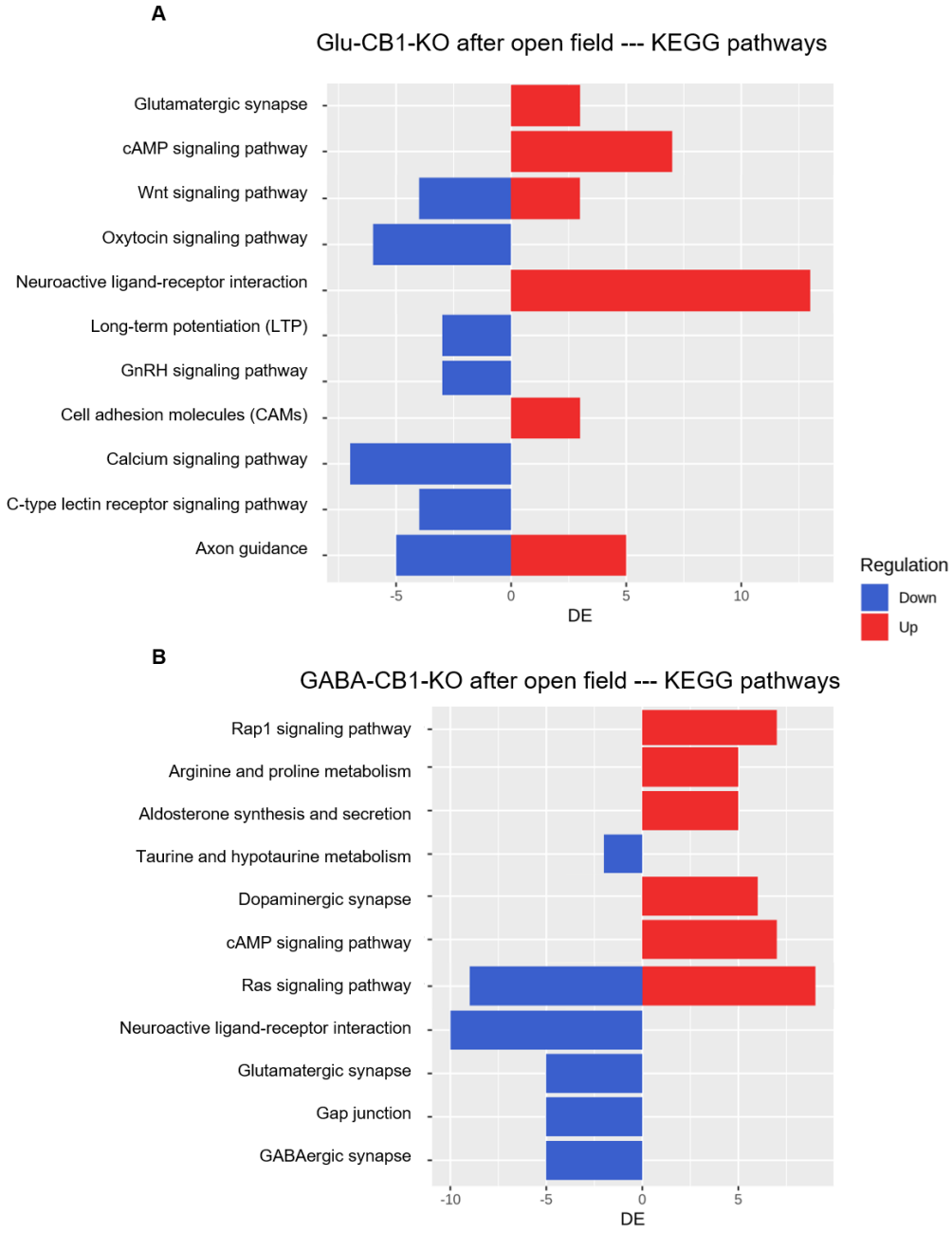

Figure 25. KEGG pathways of conditional CB1-KO mice after exposure to open field. Representative images of the number of DEGs for each of the KEGG terms that were significantly changed between CB1-WT mice and the respective conditional CB1-KO animals. These two genotypes were compared after the exposure to the open field arena to study the effect of neuronal activation, and subsequent neurotransmitter excess, in Glu-CB1-KO and GABA-CB1-KO mice. **(A)** Graph showing the different KEGG terms that resulted from comparing the Glu-CB1-WT and Glu-CB1-KO genotypes after the open field exposure. **(B)** Graph showing the different KEGG terms that resulted from comparing the GABA-CB1-WT and GABA-CB1-KO genotypes after the open field exposure.

3.4.6 Exon-intron split analysis (EISA) of CB1-deficient mice

Changes in the expression levels of a gene can be caused by several molecular mechanisms. Mainly, these mechanisms can act at the transcriptional or post-transcriptional level. The control of the gene expression is fundamental to keep internal parameters within homeostatic range, as well as to interact with other cells or tissues

towards the proper functioning of the organism. Neurons are particularly interesting in this regard, as they respond to external stimuli by modulating their gene expression profile with changes being transient or staying in the long term. Interestingly, neurons do not only modulate their mRNA pool by regulating transcription, but they also extensively use at the synapses post-transcriptional mechanisms on available mRNAs, but translationally repressed, for a fast and local adaptive response to incoming signals [276,277].

The exon-intron split analysis (EISA) is a bioinformatic analysis of RNA-seq data developed by the group of Michael B. Stadler (Basel), which aims at extracting additional information on the origin of the observed changes in gene expression [278]. Basically, by comparing the difference between experimental conditions in the number of reads mapped to introns (Δ intron) versus exons (Δ exon), it is possible to estimate whether expression changes are due to transcriptional or post-transcriptional mechanisms, respectively. The rationale behind is that introns are only present in pre-mRNA (nucleus), whereas exons are found in both pre-mRNA and mature mRNA (cytoplasm). This fact means that changes in intronic reads that correlate with changes in exonic reads are due to transcriptional mechanisms. On the other hand, genes that show changes in exonic reads and keep a constant number of intronic reads are mainly under the control of post-transcriptional mechanisms.

Comparison 1: Control vs Open field

The exposure to the open field triggered changes in the expression levels of some genes, both in CB1-WT and in conditional CB1-KO mice. However, it remained undetermined whether these changes were the consequence of transcriptional or post-transcriptional mechanisms. Therefore, we performed this analysis by performing the same pair-wise comparisons as for the DGE analysis.

We started comparing the basal state and the open field groups for each genotype, as a way to explore whether the gene expression changes associated with hippocampal activity were mostly transcriptional or post-transcriptional (Figure 26). Interestingly, both conditional CB1-KO groups showed opposite reactions: while GABA-CB1-KO mice (Figure 26B) had a higher correlation value than the CB1-WT groups, Glu-CB1-KO animals were below the values observed in CB1-WT mice. These results indicate that transcriptional processes are more relevant in the hippocampal response of GABA-CB1-KO mice than in Glu-CB1-KO mice. However, the correlation value is far from 1, which means that there are important post-transcriptional processes influencing the gene expression patterns. On the other hand, the CB1-WT of each mouse line had a very

similar correlation factor, as expected (Figure 26A, C). This observation showed that the CB1-WT animals within each mouse line responded similarly when exposed briefly to the open field arena.

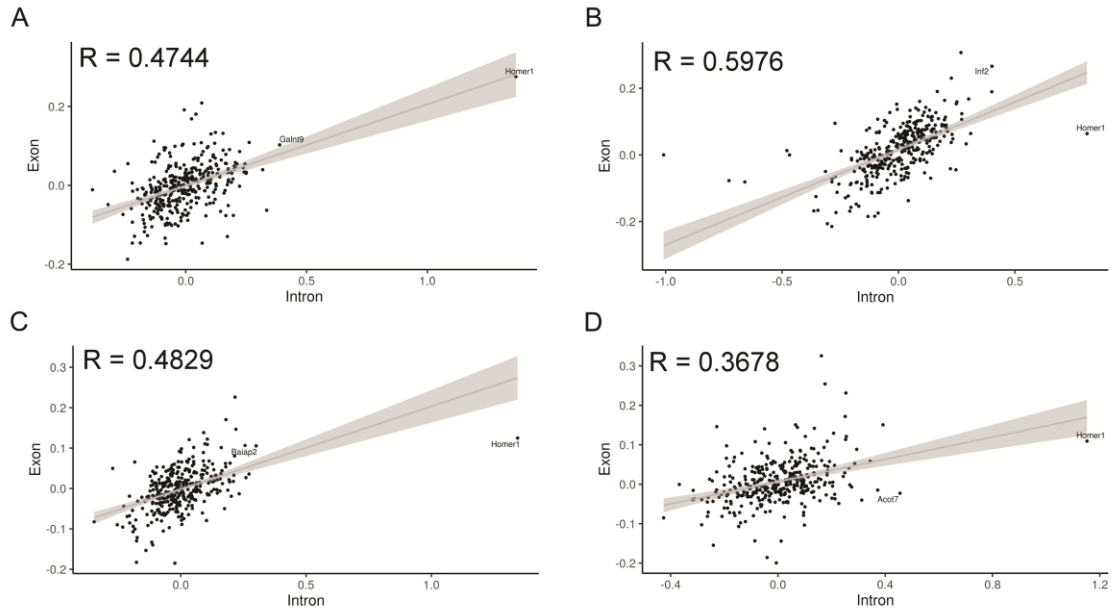

Figure 26. Correlation between the number of exonic and intronic reads in different conditions. Correlation plots comparing the differences in intronic and exonic counts between the experimental groups "basal state" and "open field" for the different genotypes. A correlation coefficient (R) of 1 means that the changes in intronic counts are matched by the changes in exonic counts, which is indicative of transcriptional processes modulating gene expression. **(A)** Graph showing the correlation between intronic and exonic reads in GABA-CB1-WT mice, R=0.4744. **(B)** Graph showing the correlation between intronic and exonic reads in GABA-CB1-KO animals, R=0.5976. **(C)** Graph showing the correlation between intronic and exonic reads in Glu-CB1-WT mice, R=0,4829. **(D)** Graph showing the correlation between intronic and exonic reads in the Glu-CB1-KO genotype, R=0.3678. n=6 per experimental group.

Comparison 2: CB1-WT vs Conditional-CB1-KO

Our next step was to perform pair-wise comparisons between each conditional CB1-KO group and their respective CB1-WT for the basal state and the open field groups (Figure 27). Interestingly, the differences between Glu-CB1-KO and GABA-CB1-KO appeared clearly in the form of very different correlation coefficients (Figure 27A, C), when they were compared to the respective CB1-WT in the basal state. These data suggests that Glu-CB1-KO mice rely more on post-transcriptional mechanisms to maintain their allostatic state than GABA-CB1-KO animals. On the other hand, GABA-CB1-KO mice in the basal state seem to use both transcriptional and post-transcriptional processes to maintain their internal allostasis (Figure 27C). After exposure to the open field, the gene expression differences found between CB1-WT and the respective conditional CB1-KO are more the consequence of transcriptional mechanisms, as indicated by an increased correlation coefficient (Figure 27B, D).

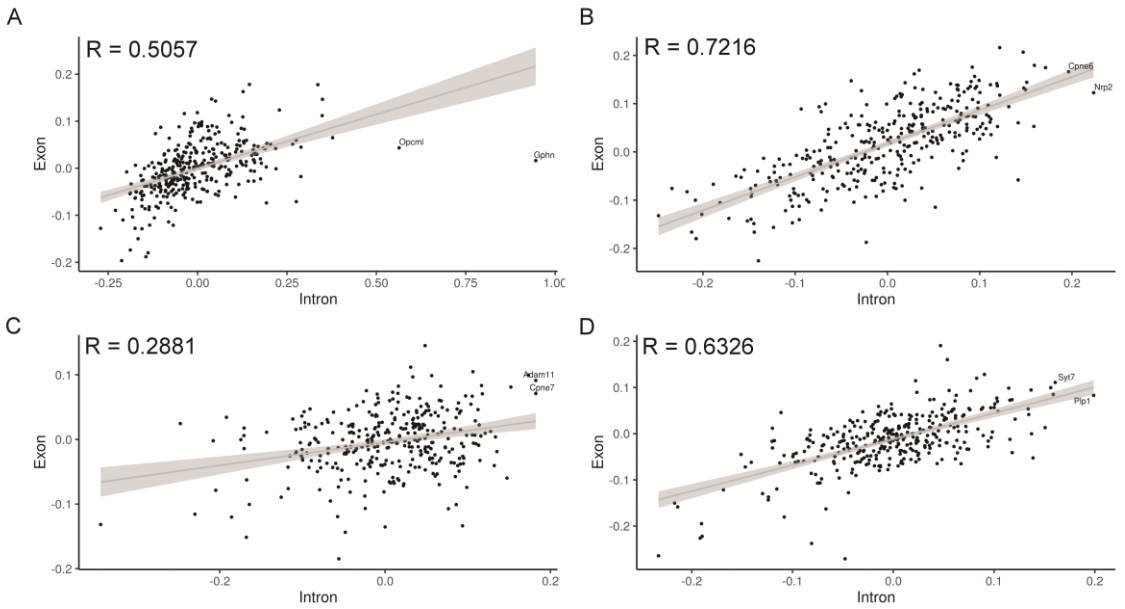

Figure 27. Correlation between the number of exonic and intronic reads in different conditions. Correlation plots comparing the differences in intronic and exonic counts between the genotypes CB1-WT and the respective conditional CB1-KO for the different experimental conditions. A correlation coefficient (R) of 1 means that the changes in intronic counts are matched by the changes in exonic counts, which is indicative of transcriptional processes modulating gene expression. **(A)** Graph showing the correlation between intronic and exonic reads in the basal state of GABA-CB1 mice, R=0.5057. **(B)** Graph showing the correlation between intronic and exonic reads after open field exposure in GABA-CB1 mice, R=0.7216. **(C)** Graph showing the correlation between intronic and exonic reads in the basal state of Glu-CB1 mice, R=0.2881. **(D)** Graph showing the correlation between intronic and exonic reads after open field exposure in the Glu-CB1 animals, R=0.6326. n=6 per experimental group.

The results from EISA provide valuable information about the molecular processes responsible for the observed changes in gene expression and highlight the differences between genotypes and experimental groups. In line with previous research using these conditional CB1-KO mouse lines, a dichotomic behavior could be observed when comparing the different genotypes. For example, although the CB1-WT genotypes showed similar results after comparing the control and open field groups (Figure 26A, C), the Glu-CB1-KO and GABA-CB1-KO genotypes showed opposing results (Figure 26B, D), with the former having a lower correlation coefficient than the latter. These results indicate that Glu-CB1-KO mice depend less on transcriptional processes when exposed to a new environment, in contrast to GABA-CB1-KO animals that displayed a correlation coefficient higher than the control and Glu-CB1-KO groups, which is indicative of a higher involvement of transcriptional processes in the hippocampus after the exposure to a new environment. Interestingly, the comparison of CB1-WT and their respective conditional CB1-KO group showed a similarly high correlation coefficient only in animals exposed to the open field arena (Figure 27B, D), which adds relevance to the observation that open field induces changes in gene expression mainly via transcriptional mechanisms. In contrast, the same comparison (CB1-WT versus the respective

conditional CB1-KO) in the basal state shows a very low correlation coefficient in the Glu-CB1 mouse line (Figure 27C) but not for the GABA-CB1 (Figure 27A).

These results suggest that Glu-CB1-KO mice use less transcriptional processes to modulate their gene expression profile for keeping their internal allostasis, whereas GABA-CB1-KO seem to induce even more transcriptional mechanisms than their CB1-WT counterparts. This dichotomic use of transcriptional processes to modulate gene expression patterns could be a compensatory mechanism for brains with an excess of neurotransmitter at synapses: with an excess of glutamate (excitatory) the neuron suffers excitotoxic damage and, therefore, needs to reduce its activity and excitability, whereas with an excess activity of GABAergic (inhibitory) neurons become less excitable and develop a smaller dendritic branching.

3.5 Discussion

Brain homeostasis is fundamental to ensure an efficient and correct flow of information within the CNS. Neurons are highly specialized cells that require an optimal environment to generate the action potential and, thus, to communicate with each other. The ECS regulates neurotransmission at the synapses, and it is one of the main modulators of synaptic function. Given its role and the abundance of its components in the mammalian brain, the ECS has an essential role in keeping physiological parameters within the homeostatic range in the brain.

We studied the hippocampal transcriptomes of two different allostatic states by using conditional CB1-KO mice, i.e. different stable homeostatic state than the homeostatic state of CB1-WT animals. These allostatic states were induced by the deletion of CB1 on specific neuronal populations and the subsequent excess of excitatory and inhibitory neurotransmitter at the synapses of Glu-CB1-KO and GABA-CB1-KO mice, respectively. Several studies have shown dichotomic characteristics between these two genotypes, although only upon external stimulation in most cases [189,228,248]. Based on these previous observations, we analyzed the transcriptomic profile of these genotypes in the basal state and upon mild external stimulation via short exposure to a new environment (i.e. open field arena).

Our results revealed very different gene expression profiles in Glu-CB1-KO and GABA-CB1-KO individuals, both in the basal state and after behavioral activation. Interestingly, the mRNA levels for some genes showed the dichotomic pattern previously observed in behavioral and morphological studies. These genes are particularly interesting because they are commonly dysregulated in both Glu-CB1-KO and GABA-CB1-KO genotypes, but they are modulated in opposite directions within each conditional CB1-KO group.

Genes with this dichotomic feature are very interesting for brain homeostasis, as they have the potential to modulate the directionality of the shift from an allostatic state back into the homeostatic state. The majority of these dichotomic genes were found to be up-regulated in Glu-CB1-KO mice and down-regulated in GABA-CB1-KO animals, upon exposure to the open field arena. These genes are known to be involved in synaptic processes (*Kcnn2*, *Rab3b*), the regulation of transcription (*Ldb2*, *Pdlim1*, *FosB*), the stress response (*Crhbp*, *npy*), and neurotransmission (*Sst*, *npy*). Interestingly, these genes could help explaining previous dichotomic phenotypes observed in these mouse lines, such as anxiety-like behavior [279], neuronal morphology, and LTP [189]. Additionally to these genes, there were a few more genes that showed the dichotomic feature: *Sptb*, a gene encoding the cytoskeletal β-spectrin, was found to be up-regulated in GABA-CB1-KO mice and down-regulated in Glu-CB1-KO animals after open field exposure. Moreover, B-cell linker (*Blnk*) and myosin light-chain kinase (*Mylk*) were up-regulated in Glu-CB1-KO replicates and down-regulated in GABA-CB1-KO mice, but only in the basal state.

Further analysis revealed GO terms and pathways that were dysregulated between CB1-WT and conditional CB1 mutants. The excess of excitatory neurotransmission in Glu-CB1-KO mice caused by the exposure to open field induced processes related to communication between cells, neuronal projections, and glutamatergic transmission. These observations correspond to the expected effects of glutamate on neuronal cells [280,281]. However, the excess of glutamate causes excitotoxicity and, as such, Glu-CB1-KO aims at avoiding overexcitation and the possible subsequent neuronal damage. Indeed, genes related to LTP and synaptic signaling, calcium signaling pathways, and neuronal projections were shown to be down-regulated in Glu-CB1-KO mice. The simultaneous down-regulation and up-regulation of genes and GO terms closely related to synaptic function might be indicative of compensatory mechanisms within the brains of Glu-CB1-KO mice.

The excess of inhibition in the brain of GABA-CB1-KO mutants had a very distinct effect. GO terms and pathways related to synaptic function, such as synaptic signaling and transmission, behavior, and the regulation of membrane potential were shown to be down-regulated after open field exposure. Interestingly, both glutamatergic and GABAergic transmission were, unlike the dopaminergic system, down-regulated as a consequence of the excess of GABA. On the other hand, genes related to lipid homeostasis, protein binding and cellular metabolic processes were up-regulated in GABA-CB1-KO mice upon neuronal activation. Genes and terms involved in synaptic signaling and the development of neuronal projections were also up-regulated after

behavioral activation, possibly as a compensatory mechanism in response to the increased inhibition due to CB1 deletion. Interestingly, GABA-CB1-KO mutants showed an up-regulation of pro-inflammatory genes both in the basal state and after open field exposure. These observations are congruent with previous findings in this mouse line [282].

Next, we tried to identify the nature of these changes in gene expression by analyzing the correlation between the numbers of intronic and exonic reads (EISA) [283]. Increased correlation values indicate transcriptional processes and lower correlation values may correspond to post-transcriptional mechanisms, although the latter requires a closer inspection of the data because long non-coding RNAs and alternative splicing can interfere with the analysis. This approach revealed that GABA-CB1-KO mice use more transcriptional processes to keep their allostatic state in basal conditions than Glu-CB1-KO mutants. However, both groups showed similar correlation factors after the exposure to the open field arena, most likely as a consequence of neuronal activity-induced expression of new genes. Although EISA provides a new perspective and interesting information, further analysis and validation experiments are required to reach definitive conclusions about the origins of the changes in gene expression.

Taken together, our results show very different transcriptomes in the hippocampal CA regions of Glu-CB1-KO and GABA-CB1-KO mice. The former shows signs of excitotoxicity induced by an excess of glutamatergic transmission, whereas the latter correlates to a hypoactive state of the brain as a result of a strong inhibitory drive. Some of the DEGs display the dichotomic feature that was previously reported at different paradigms when using these conditional CB1-KO mouse lines. Indeed, genes related to synaptic function, neurotransmission, and the stress response, as well as some transcription factors were found to show this dichotomy. Most of these common genes were found to be up-regulated in Glu-CB1-KO mice and down-regulated in GABA-CB1-KO mutants, suggesting a possible mechanistic underpinning in the excess of excitatory and inhibitory neurotransmission. Furthermore, our results also indicate the presence of compensatory mechanisms to counteract the excess of excitation and inhibition in Glu-CB1-KO and GABA-CB1-KO mutants, respectively.

Despite the promising results from the transcriptomic analysis, further work needs to be done to understand the underlying mechanisms in the context of brain homeostasis, and to uncover specific pathways involved in the maintenance of the new allostatic state. Furthermore, the study of compensatory mechanisms at the neuronal level could prove useful for the research and treatment of specific pathologies that affect brain

homeostasis, such as epilepsy. The characterization of the transcriptome could be complemented using the assay for transposase-accessible chromatin (ATAC) paired with in-depth sequencing. With ATAC-seq it is possible to characterize and analyze open regions of the chromatin. This information would uncover which elements of the genome (e.g. promoters, enhancers, etc.) interact to regulate specific genes. Knowing how to "open" or "close" specific genomic areas would help developing strategies to modify the chromatin state in specific regions of the genome. This effect could be achieve, for example, by using the clustered regularly interspaced short palindromic repeats (CRISPR) system paired with enzymes that modulate the chromatin status via histone marks or DNA methylation [284,285]. Using this system, it could be possible to regulate the expression of specific genes and, thereby, to shift between the homeostatic state and new allostatic states.

4. Behavioral and molecular characterization of resilient and susceptible mice after a single traumatic exposure

4.1 Introduction to posttraumatic stress disorder (PTSD)

The progress and development of human societies has inevitably been accompanied by the exposure of individuals and communities to traumatic experiences, such as war, exploitation and famine, among many others. Although the nature of the trauma that a hunter-gatherer in the Paleolithic, a slave in the Middle Ages or an individual in modern times may be completely different, the emotional consequences and long-term impairments were very similar. The first epic written by humankind, the tale of Gilgamesh, already described posttraumatic symptoms in great detail, such as panic attacks and personality changes due to the sudden loss of a beloved friend. However, it was not until the battle of Marathon (440 BC) that Herodotus reported for the first time the case of chronic mental symptoms caused by a sudden fright in the battlefield. Interestingly, he described how these mental symptoms were not caused by physical wounds, but by the emotional distress of the battle and the vision of killed comrades, and how they persisted in the long-term. Old Icelandic literature (e.g. *Gísli Súrsson Saga*) and chronicles from the Hundred Years´ War by Jean Froissart described the cases of soldiers that were awakened at night by frightening dreams, where they vividly re-experienced past battles to the point of changing their behavior [286].

During the industrial revolution and the rise of modern psychiatry, physicians focused on traumatic symptoms. Psychiatrist Philippe Pinel used his experiences with civilians shocked by trauma (e.g. train crash) and in the French Revolutionary wars and Napoleonic wars [287], where army physicians described how soldiers collapsed into protracted stupor after shells passed by them, even though they were left physically unscathed. He was the first one to precisely describe war neuroses and posttraumatic states, although he used different terms. At this time, two theories were put forward to explain the origin of these symptoms: the organic theory stated that it was microscopic lesions of the brain or spine, whereas an alternative theory suggested that the cause was the emotional shock and the symptoms were hysterical in nature. The German physician Hermann Oppenheim used the term “traumatic neurosis” for the first time in 1884 after analyzing cases of railway and workplace accidents. Another German doctor, Georg Honigmann, coined the term “war neurosis” in 1907 after his experience during the Russian-Japanese war, and highlighted the similarity between his cases and those of Oppenheim [288].

World War I (WWI) was the tipping point for the study and advancement of psychiatric research, of traumatic disorders in particular. The use of massive industrial resources for the war effort led to an unexpected high number of psychiatric casualties, as described by authors from all warring parties. The use of heavy artillery caused these psychiatric casualties to appear very early in the war and to increase constantly throughout its duration. At first, they were evacuated to the rear for psychological treatment but, as the war progressed, physicians noticed that soldiers treated close to the frontline (forward treatment) had a higher likelihood of returning to their military unit, whereas patients who were evacuated worsened and displayed chronic symptoms. Forward treatment became the standard procedure along with five key principles summarized for the first time by Thomas W. Salmon in 1917, although all warring parties reached the same conclusions independently [289]. Despite the advancement in the field, the question whether the origin of the symptoms was somatic or psychological remained a controversial topic after the war.

World War II (WWII) introduced the dreadful concept of “total war”, which involved the systematic targeting of civilian populations. This concept was exemplified in the millions of civilian casualties caused by the Holocaust, the air raids on populated areas and the atomic bombs dropped on Japan. Most of the knowledge about psychiatric casualties was forgotten by all warring parties. However, it was soon clear that the syndrome had to be treated immediately to avoid the consolidation and chronification of the impairments, which led to the appearance once more of forward treatment stations [290]. This time, the interest for trauma-related psychiatric disorders did not disappear after the war, and the origin and chronic nature of the symptoms were extensively studied in WWII survivors. The knowledge gained was successfully applied during the Vietnam War, which saw a reduction in the number of psychiatric casualties during combat operations (although the incidence of alcoholism and drug abuse was high). Despite the effort to prevent psychiatric casualties, the delayed and chronic nature of posttraumatic stress disorder (PTSD) caused that almost a quarter of all soldiers sent to Vietnam required psychological help once they returned to their homeland. This event ultimately led to the adoption of PTSD as a diagnostic category in 1980 in the third edition of the Diagnostic and Statistical Manual (DSM-III) of the American psychiatry association (APA)[291]. The distinction between PTSD, with symptoms often delayed and separated from the trauma by a latency period, and acute stress disorder, a short-lived natural reaction to trauma, was done with the publishing of DSM-IV in 1994 [292].

4.1.1 Current definition and symptomatic panel of PTSD

PTSD is a mental health disorder that develops after an individual is exposed to a traumatic experience, such as warfare, deadly traffic or train accidents, sexual violence, shooting, etc. The symptoms associated to the disorder cause a severe chronic impairment of the individual´s daily life. Furthermore, PTSD can lead to personality changes that can also severely affect the social relationships of the individual and, ultimately, lead to suicide. In contrast to other stress- and trauma-induced disorders, the symptoms of PTSD are delayed in time and appear only after an incubation period of a minimum of one month.

In 2013, the DSM-V was published, and PTSD was moved from the category of "anxiety disorders" to the newly created category of "stress- and trauma-related disorders". Moreover, the DSM-V includes for the first time different subtypes of PTSD, such as preschool PTSD, for children aged 6 years old or younger, dissociative PTSD, when the disorder includes feelings of depersonalization or derealization, and delayed PTSD, for cases where the diagnostic criteria are not met for at least 6 months since the exposure to the trauma occurred. The DSM-V [48] summarizes the diagnostic criteria in eight different blocks:

Criterion A: Stressor

The person was exposed to: death, threatened death, actual or threatened serious injury, or actual or threatened sexual violence, in one of the ways these ways:

- Direct exposure.
- Witnessing, in person.
- Indirectly, by learning that a close relative or close friend was exposed to trauma. If the event involved actual or threatened death, it must have been violent or accidental.
- Repeated or extreme indirect exposure to aversive details of the event(s), usually in the course of professional duties (e.g. first responders, social workers, medics). This does not include indirect non-professional exposure through electronic media, television, movies or pictures.

Criterion B: Intrusion

The person experiences at least one of the following intrusive symptoms associated with the traumatic event:

- Recurrent, involuntary and intrusive recollections.
- Traumatic nightmares.
- Dissociative reactions (e.g. flashbacks), which may occur on a continuum from brief episodes to complete loss of consciousness.
- Intense or prolonged distress after exposure to traumatic reminders.
- Marked physiological reactivity after exposure to trauma-related stimuli.

Criterion C: Avoidance

Persistent effortful avoidance of distressing trauma-related stimuli after the event, in at least one of the following ways:

- Trauma-related thoughts or feelings.
- Trauma-related external reminders, such as people, places, conversations, objects, activities or situations.

Criterion D: Negative alterations in cognition and mood

Negative thoughts or feelings that began or worsened after the trauma, requiring at least two of the following ways:

- Inability to recall key features of the traumatic event not due to head injury, alcohol or drugs (dissociative amnesia).
- Persistent and often distorted negative beliefs and expectations about oneself or the world.
- Persistent distorted blame of self or others for causing the traumatic event or for resulting consequences.
- Persistent negative trauma-related emotions, such as fear, horror, anger, anger, guilt or shame.
- Markedly diminished interest in pre-traumatic significant activities.
- Feeling alienated from others (e.g. detachment or estrangement).
- Constricted affect or persistent inability to experience positive emotions.

Criterion E: Alterations in arousal and reactivity

Trauma-related alterations in arousal and reactivity that began or worsened after the traumatic event, in at least two of the following ways:

- Irritable or aggressive behavior.
- Self-destructive or reckless behavior.
- Hypervigilance.
- Exaggerated startle response.
- Problems in concentration.
- Sleep disturbance.

Criterion F: Duration

Persistence of given symptoms from criteria B to E for more than one month.

Criterion G: Functional significance

Significant symptom-related distress or functional impairment (e.g. social, physical, occupational, etc.).

Criterion H: Exclusion

Symptoms are not due to medication, substance abuse or other illness.

PTSD is diagnosed when a patient meets all criteria listed in the DSM-V. However, the high comorbidity of PTSD with anxiety and depressive disorders makes it a rather heterogeneous disorder and complicates both its diagnosis and treatment, which has led some scientists to consider PTSD a spectrum disorder with different pathological phenotypes that can be distinguished symptomatically and psychobiologically [293,294].

Despite the severity of traumatic experiences, only a fraction of the affected population will develop PTSD after a period of time. The global prevalence of PTSD is calculated to be 3-4%, although the responses of affected individuals can greatly vary between 5% and 20%, depending on the trauma and its context. Conflict-exposed communities have the highest prevalence at around 15-20% [295]. This is a relatively low percentage of individuals (when compared to the total population) that are unable to cope with the emotional distress of the trauma and that develop the pathology. However, the underlying causes of this susceptibility are still poorly understood. Although genetic risk factors have been proposed to explain this phenomenon, twin studies have demonstrated a hereditability risk of 30-40% [296], but the environmental influence via gene x environment interactions might modify the influence of genetic risk factors.

4.1.2 PTSD-like models in animal research

Animal models are an invaluable research tool for understanding the biological mechanism underlying the pathology, and for developing and testing of novel treatments. However, effective and translational animal models are difficult to develop in psychiatric research, because psychopathologies tend to have high variability among patients and require fluent communication in order to assess the emotional status of the patient. It was originally thought that PTSD would be easy to model because it starts with a single, well-defined traumatic event (although in some cases the stressor is chronic in nature). Despite the interest to develop robust animal models for PTSD, they still suffer severely from the lack of translatability. This is mainly the result of research bias (e.g. research only on males, averaging the group response, or insufficient diagnostic power) and the intrinsic heterogeneity of PTSD.

Several animal models have appeared over the years [297]. Given that PTSD mostly starts with a traumatic event, the different models have focused on the type of trauma employed. The initial and most common model used has been Pavlovian fear conditioning, using a single inescapable electric shock, which has provided useful insights on the brain regions and neural circuits that are dysregulated in PTSD [298]. Stress-enhanced fear learning is another PTSD-like model in which the pre-exposure to

repeated mild foot shocks in one context produces an enhancement of conditioned freezing to cues associated with a single traumatic shock that was delivered in another distinct context [299]. Long-duration (>2h) restraint stress has also been used as a severe psychological stressor [300], in combination, or not, with other procedures, such as forced swim and exposure to ether vapors, to enhance PTSD-like symptoms [301]. Less conventional or chronic traumatic stressors have also been used, such as the exposure to a predator or its odor [302], underwater trauma [303], or chronic stress models that use one or several stressors over several days [304]. The rationale behind all these models is that when exposed to a sufficiently traumatic experience, animals will develop a PTSD-like pathology. There is no need to focus on a single type of traumatic stressor, because in humans, markedly different types of trauma are associated with the development of PTSD. However, it is important to consider that the intrinsic characteristics of the traumatic experience (intensity, duration, repetition, etc.) will modulate the behavior of the animals within the spectrum of PTSD, as well as the conclusions that can be drawn from the observed behavioral response.

Although all stress models mentioned above induce changes in the animal´s behavior, there are some requirements that need to be met before considering it a model for PTSD-like behavior. These requirements are based on the idea that, whatever the effect the trauma has on the animals, this effect has to correlate with observations made with human cohorts, including: i) symptoms must be present in the long-term (>1 month) without further exposure to the stressor, ii) a wide dispersion of the behavioral response(s) of the trauma-affected group, iii) the core symptoms of PTSD, such as increased startle response, fear generalization and persistent fear memory, must be present. Even if a stress model meets all the required criteria, the conclusions that can be drawn from it have to be critically viewed, as they will be influenced by the sex of the animals (ideally, these studies are done in both male and females to avoid a sex bias), by genetic risk factors present in transgenic mouse lines, by the type of trauma and by which behaviors will be measured. Furthermore, it is essential that the individual behavioral responses are analyzed and compared in the very detail. Given the heterogeneity observed in PTSD symptomology and the wide dispersion of the behavioral responses, averaging the responses of the trauma-exposed group would simply eliminate valuable and essential information (e.g. resilience or susceptible phenotypes) and, thus, cripple the conclusions that can be taken.

4.1.3 Long-term neuroanatomical and molecular alterations in PTSD

Stress, and especially traumatic stress, is an external agent capable of shifting the homeostatic state of the individual to promote survival. However, when stress induces

maladaptive changes and becomes pathological, this transient shift of homeostasis translates into permanent neuroanatomical and molecular changes within different brain regions, neural circuits, and gene expression profiles [305,306]. Here, we will review some of the neuroanatomical and molecular changes induced by traumatic stressors that have been observed in human patients and PTSD-like animal models.

The dysregulation of the HPA axis is characteristic of stress- and trauma-induced disorders. In the case of PTSD, an abnormal increase of CRH in plasma and cerebrospinal fluid (CSF) has been observed in comparison to healthy individuals [307,308]. These high CRH levels could result in a dysregulated activation of CRH1R that is known to induce an increased startle response and sensorimotor gating [309], as well as over-consolidation of fear memories [310], all of them characteristic of PTSD. In response to stress, plasma levels of ACTH increase to induce the production of corticosteroids in the adrenal glands. For PTSD patients, the plasma levels of ACTH are lower than healthy individuals in the basal state [311], but are higher after exposure to a stressor, and it is not followed by a noradrenaline peak [312]. This feature is likely a consequence of the reduction of the pituitary gland volume observed in PTSD patients. Interestingly, plasma levels of corticosteroids negatively correlate with PTSD severity [313] and are decreased in individuals suffering from PTSD [314]. Corticosteroids not only shift the homeostatic state to face a stressor, they also interact with GRs to negatively modulate the release of ACTH and CRH. For this reason, the pharmacological activation of GR could help to restore the balance to the HPA axis and to facilitate fear extinction, without influence on fear acquisition in PTSD cohorts [315].

The abnormally high levels of CRH, and subsequent impaired glucocorticoid negative feedback, can also be explained by an insufficient control of the PVN in the hypothalamus. Within this brain region, there are different cell populations. Non-neurosecretory parvocellular neurons project to the brainstem and spinal cord, controlling sympathetic activity [316], and they widely express CRH1R and glutamate decarboxylase (GAD67), the precursor for the production of GABA [317,318]. This observation suggests an influence of the GABAergic system within the PVN in the dysregulated HPA axis. Indeed, treatment and co-treatment with baclofen, a GABA receptor type B ($GABA_BR$) agonist, alleviates many PTSD symptoms [319,320]. Studies with pharmacological interventions in the PVN to stimulate glutamatergic neurons (via injections of NMDAR agonists or glutamate) provoked an increase in ACTH release, HPA axis activity and noradrenergic tone, but it did not increase corticosterone levels. The blockade of the GABA receptor type A ($GABA_AR$) produced a significant increase in corticosteroid release, showing the relevance of the inhibitory activity of GABAergic

neurons within the PVN [321]. When considering the low levels of corticosteroids in PTSD patients, it seems that an imbalance between glutamate and GABA in the PVN highly contributes to the dysregulation of the HPA axis due to an insufficient inhibitory control on glutamatergic neurons. Indeed, the levels of GABA in plasma negatively correlates with the severity of PTSD symptoms [322], and lower concentration of GABA in plasma has been linked to increased susceptibility to develop PTSD symptoms [323,324]. This imbalance of neurotransmitters in the PVN may be mediated by the trauma-induced downregulation of CB1 in this brain region [325], which might be one of the reasons why medical marihuana is being explored as a palliative treatment. On the case of glutamatergic neurotransmission, one of the causes of its dysregulation during stress might be the restructuring of NMDA channels and their increased excitability [326]. This observation fits with reports from clinical trials about the effectiveness of NMDA antagonists, such as memantine and ketamine [327,328].

In has been proposed that intrusive memories in PTSD patients might depend on learning from both the hippocampus, which mediates a context-based representation, and the amygdala, which induces a sensation-based representation [329]. Given shrinkage of the hippocampus observed in PTSD [330–332], it might be possible that the context-based representation is impaired and overtaken by the amygdala-based memory, evoking a conditioned fear response regardless of the context. This reduction of hippocampal volume might either predispose to stress-related disorders [331,333] or be a consequence of abnormal CRH levels [334]. Within the lesioned hippocampus of trauma-exposed rats, a reduction in MR and GR levels, as well as in the ratio MR/GR were observed [335]. Glutamatergic transmission modulates BDNF-induced neural plasticity, shown to be reduced in postmortem PTSD patients [336], and has a key role in hippocampal LTP and LTD. The metabotropic glutamate receptor $mGluR_5$ mediates LTP and LTD, along with metaplasticity and contextual fear extinction [337]. Interestingly, the different members of the mGluR family seem to be selectively modulated depending on the stimulus, as contextual fear conditioning in rats increased the expression levels of $mGluR_5$ but not $mGluR_1$, suggesting therapeutic potential for the former [338]. Furthermore, $mGluR_2$ and $mGluR_3$ may alleviate hypoglutamatergic conditions by lowering the threshold for the induction of LTP in the CA1 region, and promoting memory formation [339]. The ECS is the most important modulator of neurotransmission in the hippocampus, and traumatic stressors induce a tonic reduction of AEA. The inhibition of FAAH and subsequent increase in AEA levels, together with extinction training, could consolidate the extinction of fear memories [340]. It has also been proposed that eCB deficiency may contribute and/or predispose to the development of trauma-related disorders, such as PTSD [341].

Thus, marihuana-based therapies might potentially restore the normal activity of the ECS and alleviate some PTSD symptoms.

In PTSD studies, an enhanced amygdala-dependent memory (sensation-based) as a result of a hyperactive amygdala has been observed [342]. This brain region is central in stress-related disorders, as it stores and associates unconditioned and conditioned stimuli, and evokes the retrieval of conditioned fear [343]. In the BLA, GABAergic interneurons modulate glutamatergic pyramidal neurons [344], but stress was shown to reduce GABAergic activity and the sensitivity of $GABA_AR$ in the BLA [345], leading to a hyperactive amygdala. Interestingly, administration of $GABA_AR$ agonists into the CeA, adjacent and connected to the BLA, blocked fear retrieval [346]. Furthermore, decreased levels of $GABA_AR$ have been positively correlated with PTSD [347]. The ECS also modulates the activity of the BLA, and animal studies have shown an AEA-induced increase of the LTP via long-term depression (LTD) of inhibitory synapses [348,349]. Moreover, exposure to trauma up-regulates CB1 expression in the BLA [350], which corresponds to observations in PTSD patients [351]. CB1 agonists are known to decrease memory consolidation in the CA1 region of rats, preventing an increase in GR and CB1 expression in the CA1 and BLA [352]. Some cannabinoid-based treatments appear to be promising therapeutic options for alleviating PTSD symptoms when administered before sleep [353]. Although this effect of cannabinoids is not fully understood, it is hypothesized that the administration of cannabinoids in patients with PTSD during sleep hours may influence the consolidation and reorganization of memories that occur during sleep [354], and possibly enhance the extinction and/or attenuate the retrieval of the traumatic memory [355]. A correct balance in neurotransmission is also essential for a correct function of the amygdala. Serotonin receptor $5\text{-}HT_{2C}$ was upregulated in the amygdala of trauma-exposed rats [356] and has been shown to mediate the stress-induced consolidation of fear memories [357]. Furthermore, tonic activity of serotonin via $5\text{-}HT_{1A}$ receptors correlates with a positive stimulation of hippocampal neurogenesis and partially explain the effectiveness of SSRIs in PTSD [358]. Stress-induced hallucinations occurring in severe PTSD cases are correlated to the activation of the receptor $5\text{-}HT_{2A}$, although studies on post-mortem human samples have shown that it might also be associated to glutamatergic transmission and $GluR_{2/3}$ activation [359,360]. Neurotransmission involving noradrenaline is also enhanced in PTSD, and the activation of β-adrenergic receptors potentiates further activity in the amygdala [361]. This hyperactivity of the amygdala was shown to be reduced after activation of alfa-7 containing nicotinic cholinergic receptors via an increased inhibitory input from GABAergic interneurons in the BLA [362]. Indeed, treatment with propofol, a $GABA_AR$ agonist, coupled with memory reactivation was

shown to impair selectively the retrieval of the emotionally negative phase of the reactivated memory after 24 hours, while leaving non-reactivated memories intact [363].

Several brain regions involved in stress-related disorders (e.g. amygdala, hippocampus, PVN, etc.) are bidirectionally connected to the prefrontal cortex (PFC), a key region for fear extinction and stress processing. In fact, the inhibition of the PVN region, and CRH release subsequently, is mediated by the PFC in a CB1-dependent manner [325]. Furthermore, the ventromedial region of the PFC (vmPFC) inhibits the conditioned response from the amygdala, and the activity of the vmPFC has been found to be negatively correlated with PTSD [364]. Therefore, GABAergic transmission is a key component in PFC function and a reduction of $GABA_AR$ in this region has been highly correlated to PTSD [365]. Moreover, a general decrease of GABA was observed in plasma samples from PTSD patients [366]. Current observations support the hypothesis that the abnormal level of noradrenaline found in PTSD is associated with a higher conversion of dopamine to noradrenaline [367], which activates α_1-adrenergic receptors in the PFC that mediate stress-induced cognitive impairments [368]. The PFC was shown to suffer atrophy upon chronic stress exposure. Studies using animal models of PTSD have shown a reduction in GAD67, the enzyme responsible for GABA synthesis, in the PFC and the hippocampus. The subsequent insufficient GABAergic transmission could induce excitotoxicity and oxidative stress resulting in the atrophy of these brain regions [369,370]. Furthermore, a reduction of the number of dendrites in the infralimbic cortex (a subregion of the vmPFC) has been observed in trauma-exposed animals that show a susceptible phenotype. Interestingly, within the same study, trauma-exposed animals that displayed a resilient phenotype showed a reduction of dendrites in the prelimbic cortex, another subregion of the vmPFC, but an increase of dendritic branching in the infralimbic cortex [371]. This observation seems to confirm the central role of the vmPFC in fear processing and trauma-related disorders.

Other areas of the brain have been linked to PTSD and stress-related disorders. For example, an increased excitation of noradrenergic pathways from the locus coeruleus (LC) has been implicated in overconsolidation of memories and a hyperresponsive state, both characteristic of PTSD [372]. This effect has been shown to be alleviated by the action of GCs in the amygdala, which inhibit the CRH-dependent activation of noradrenergic neurons in the LC [372]. Estrogens are also known to increase noradrenaline levels in the LC, as well as to enhance the sensitivity of CRH_1R in females, which could explain the almost 2-fold prevalence of PTSD in women [373]. The periaqueductal gray (PAG), deeply involved and freezing behavior and other responses to threat or danger [374], is

hypothesized to reinforce the fear response and, thus, to trigger it by subliminal and/or generalized cues, as it has been observed in PTSD patients [375].

4.2 Aim of the project

PTSD is one of the most impairing psychological disorders due to the severity of the symptoms and their duration. Despite this fact and the prevalence of PTSD in the world, there is insufficient knowledge about the molecular basis underlying the pathology. The gap in research is most likely a result of the difficulty to define and model PTSD-like behavior on animals, as PTSD symptomology is very variable between patients, and also because research until recently has focused on the average response of the group, rather than on analyzing the full spectrum of individual behavioral responses. The aim of this project is to provide a new approach to model PTSD in mice, as well as to characterize the resulting long-lasting phenotypic alterations that could emerge from the high variability within the trauma-exposed animals. Our approach consists on a single strong traumatic experience, and, after one month, followed by a battery of behavioral tests, which should correlate with the symptomatic panel of PTSD. Furthermore, we combine this battery of tests with behavioral profiling, a set of predefined criteria to classify stress-exposed individuals according to their behavioral performance, in order to characterize individuals that are resilient or vulnerable to stress at the molecular level. This approach should provide new helpful information about the molecular basis of stress resilience and susceptibility.

4.3 Material and methods

4.3.1 Mouse line

All experimental procedures were done using a double *knock-in* mouse line (Arc-CreER^{T2} x R26-CAG-LSL-Sun1-sgGFP-myc; from now on referred to as “Arcnu”). The first transgenic construct (Arc-CreER^{T2}) consists on the regulatory elements of the *Arc* gene, an immediately early gene expressed upon neuronal activation, fused to a specially modified Cre-recombinase. This version of Cre-recombinase contains the human estrogen receptor ligand-binding domain with a triple mutation (G400V / M543A / L544A). The resulting protein is inactive in basal conditions, as it cannot translocate to the nucleus. Cre-ER^{T2} requires the binding of tamoxifen (a selective estrogen receptor modulator) to translocate to the nucleus and excise the genetic code between two loxP sites (34-bp sequences that are recognized and targeted by Cre) (Figure 28). The use of CreER^{T2} provides both spatial and temporal control, as it is expressed only in activated neurons and requires the presence of tamoxifen to catalyze the recombination in the nucleus. The second transgene (R26-CAG-LSL-Sun1-sgGFP-myc) is found in the

ubiquitously expressed *Rosa26* locus with a CAG promoter to ensure high levels of GFP expression. The construct also contains a *floxed* STOP cassette (LSL; loxP-STOP-loxP) and elements of the SUN1 gene to guide GFP expression to the nuclear membrane. The GFP of this transgene is a superfolder version of the protein (sfGFP) that reduces protein misfolding and, therefore, increases the fluorescence signal. All experimental mice were heterozygous for both transgenes. Adult male mice (8±1 weeks of age) were single-housed 2 weeks before the start of the experiment. Food and water were provided *ad libitum* and mice were subjected to a 12-hour light-dark cycle (07:00-19:00).

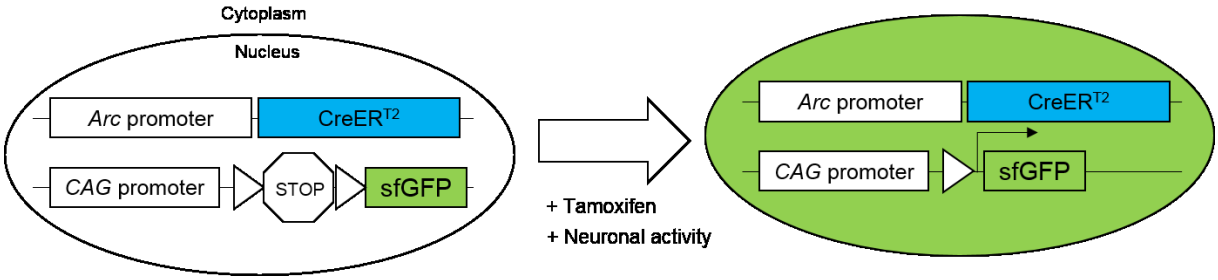

Figure 28. Schematic representation of the double transgene system of Arcnu mice. In order to induce the expression of sfGFP in the nuclear membrane of the neuron, there are two previous requirements that need to be met. First, neuronal activity is required to be sufficiently strong to trigger the expression of CreERT2, which is under the control of the immediate-early gene Arc. Second, tamoxifen needs to be simultaneously present at the time of neuronal activity so that CreERT2 can translocate to the nucleus and perform the recombination of the LoxP sites. This recombination triggers the expression of sfGFP at the nuclear membrane.

4.3.2 Tamoxifen preparation and injection

Mice were injected i.p. with a tamoxifen solution (10 mg/mL in 90% corn oil, 10% ethanol) 5 hours prior to the foot-shock to label the nuclei of neurons activated during the trauma exposure. Mice spent the next 2 days in a dark room (except when they received the foot-shock) to avoid as many stimuli as possible while tamoxifen was metabolized. After this period, animals were returned to the colony room.

The tamoxifen solution was prepared fresh every time. To prepare it, tamoxifen (Sigma) was adjusted to room temperature for 15 minutes. Pure ethanol, pre-heated to 55° C, was then added to the tamoxifen and mixed by shaking until most of the compound was dissolved. This solution was then added to corn oil (Sigma) to reach a final concentration of 10 mg/mL and incubated in a water bath at 37° C for 15 minutes. All tamoxifen solutions were protected from the light to avoid degradation.

4.3.3 Trauma model

To induce a strong and reliable PTSD-like phenotype in our animals, we used a modified version of the protocol from Carsten Wotjak [376]. In summary, mice were introduced in the shock chamber and left to habituate for 3 minutes with lights on. After this time, 2 foot-

shocks (1,5 mA; 2 seconds) were delivered to the paws through the bottom grid, with 1 minute of rest in between each shock. After the last electric shock, mice were left for one more minute in the chamber before being returned to their home cage. The shock chamber was cleaned after every round with 1% acetic acid to avoid triggering episodic memories during the behavioral tests, in which 70% ethanol was used to clean the different arenas. The behavior of the animals during the foot-shock protocol was constantly monitored using video cameras.

4.3.4 Behavioral longitudinal study

To assess the severity of the behavioral dysregulation caused by the exposure to trauma, mice were subjected to a battery of behavioral tests. The paradigms were chosen according to the symptomatic panel of stress-related disorders:

Acoustic startle response (ASR)

In this paradigm, mice are introduced in a small cage inside a soundproof box, where they are not fully restrained, but their movements are heavily restricted. The animals are habituated in this cage for 5 minutes before being exposed to 120 acoustic stimuli of four different intensities: 75 dB, 90 dB, 105 dB and 115 dB. The order in which the different stimuli were presented was pseudorandomized and the interval between the stimuli was randomized (12-18 seconds). This setup is designed so that the mouse cannot predict when the next tone will come or which intensity will it have and, therefore, have a genuine startle response.

This startle reflex can then be measured, as the cage stands on top of piezoelectric materials, which generate an electric current upon receiving physical pressure. This measurement (in mV) of the startle response is a good indicator of the vigilant state of the animal. Therefore, this paradigm is a good test to evaluate the hypervigilant behavior observed in PTSD and many other stress-related disorders.

Holeboard test (HbT)

To assess the anxiety levels induced by trauma exposure, mice were placed in an open field box (40x40x30 cm) with four small holes in the center (diameter 1.8 cm; depth 7.5 cm) for the mouse to explore (Figure 29). The diameter of the holes allowed for the mouse to poke its head through, but not to escape the arena. Mice were always placed in the same position between corners and were able to explore the arena for 10 minutes. The behavior of each individual mouse was recorded and was analyzed using EthoVision XT 8.5 (Noldus). The main measurement used to evaluate anxiety was the number of exploratory head pokes through the holes. Additionally, other parameters were

considered such as the time spent in the corners, in the center and the time animals explored the holes with the nose (without dipping in). Locomotive behavior was also assessed using total distance moved and average velocity.

This paradigm lies in the category of conflict test, whereby the experimental subject´s tendency to seek out a positive stimulus is confronted by an opposite impulse of avoidance due to innate fear (Mullan, 2003). Mice present thigmotaxis (tendency to remain close to walls and corners; negative stimulus) (Simon et al., 1994) but also naturally tend to explore new unknown environments (positive stimulus). Therefore, higher levels of exploration of the open space (center) and through the holes are indicative of reduced anxiety and *vice versa*.

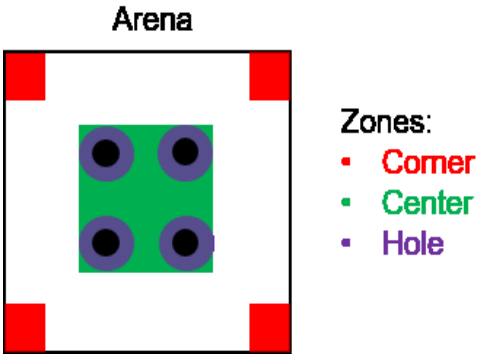

Figure 29. Layout of the holeboard test arena. The arena for the HbT, a 40x40x30cm white box with 4 holes (black dots) in its center area, was divided according to how anxiogenic each of the zones are: corners (anxiolytic), center area (anxiogenic) and the area around the holes (very anxiogenic).

Sucrose preference test (SPT)

Given the comorbidity rates of PTSD and depressive disorders, a paradigm to evaluate hedonic behavior was introduced in the longitudinal study. This test is based on the diminished interest in engaging in pleasurable activities (anhedonia) of patients with depression and the preference of mice to drink sucrose water over normal water. To this end, mice were habituated to have two drinking bottles in their home cage the day before the experiment started. On the next day, the body weight of each mouse was measured and one of the bottles was substituted for a bottle containing a 4% sucrose (m/v) solution. On each of the next 3 days, both bottles were measured, and their positions were swapped to avoid any potential effects due to the placement of the bottles. On the last day of the experiment, mice were changed to a new home cage with only the normal water bottle. The measurements of each day were then averaged and used to calculate a preference index as follows:

$$Preference\ Index = \left(\frac{Sucrose\ consumption * 100}{Total\ liquid\ consumption}\right) / Body\ weight$$

Social interaction test (SIT)

This paradigm is based on the innate sociability of mice and other rodents. Mice are exposed twice for 5 minutes to an open field arena (40x40x30 cm white box), where there is a circular cage on one of the sides (Figure 30). During the first exposure, or habituation phase, the cage is empty, whereas in the second exposure, or social phase, the cage contains a wt/wt mouse born around the same time, but without previous contact with the experimental subject to avoid any possible interference. During both phases, the experimental animals are allowed to explore freely the arena and their behavior is analyzed. Besides the usual locomotion parameters (distance moved and velocity), the time spent in the opposite corners to the cage was measured as a sign of avoidance behavior. To measure sociability, the time spent around the cage and the time exploring the cage with the nose was measured. These parameters were used to calculate a sociability index as follows:

$$Sociability\ Index = \left(\frac{time\ in\ zone\ (social\ phase)}{total\ time\ in\ zone\ (both\ phases)} * 100 \right) - 50$$

This formula gives values within a range of 50 and -50, which indicate preference or avoidance respectively during the social phase of the protocol. This equation was used for the three different zones that were studied as a measure of preference/avoidance behavior for each of the areas. However, only the time exploring the cage with the nose is considered as the standard sociability index.

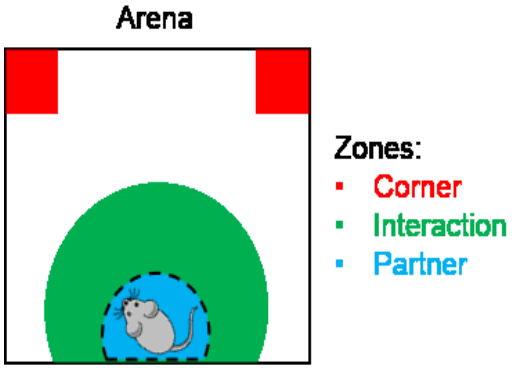

Figure 30. Layout of the social interaction test arena. The arena for the SIT consisted of a 40x40x30cm box with a cage (dashed line) on one side. The arena was divided into 3 zones to represent the social behavior of the mouse: corners (avoidance of social interaction), Interaction area (mild form of sociability) and partner area (full social interaction). The time in the partner area was only counted when the test subject explored it with its nose, rather than just being close to the zone.

Generalized fear

Generalization, or using past experiences in present situations of learning if the context is similar enough, plays a key role in learning processes. Fear generalization occurs when fears learned in the past are associated to similar situations in the present.

However, if it becomes maladaptive (overgeneralization of fear), these learned fears are associated to harmless situations unrelated to the original traumatic context. In order to test whether our PTSD-like model induced an overgeneralization of fear to new contexts, the immobility time in new environments/arenas was calculated using EthoVision XT 8.5 (pixel lower threshold = 1%). GF was measured in the Hb and SI arenas, as both were unrelated to the original trauma context but still were sufficiently different between them.

Contextual fear (CF)

To measure the strength of the trauma-induced fear memory, mice were placed for 5 minutes in the same shock chamber where they received the trauma. The fear response of mice, or freezing behavior, was recorded and was measured using the software TopoWatch (v 0.3) and TopoWatch Analyzer (v 1.1.1). Freezing behavior was defined as the lack of muscle movement except for those required for breathing. The software parameters were set to Background-to-mouse threshold = 246, noise level = 22 and freezing threshold = 30 in order to identify and quantify the immobility time that fits to the definition of freezing. After the 5 minutes exposure, mice were placed back in their home cages and the shock chamber was cleaned using a 1% acetic acid solution.

4.3.5 Sample collection

In order to study the changes in gut microbiota composition and the physiological alterations that occur upon experiencing a traumatic event, blood and stool samples were collected before and after the exposure to the foot-shock.

Blood was collected from the facial vein using a lancet into 1 mL EDTA-coated tubes (KABE Labortechnik). For every time point, 4-5 drops of blood were collected per mouse and the animal was afterwards returned to its home cage. Two 20 µL droplets from this blood were pipetted on a FTA DMPK-C card (Sigma-Aldrich, Cat# WHAWB129243), which lyse cells and denature proteins on contact to preserve lipid molecules, and left to dry under a hood for 3-4 hours. These dried blood spots (DBS) were then stored in hermetic bags at -80° C. The rest of the blood was centrifuged (~10000 g, 10 minutes) and the plasma was collected and immediately frozen on dry ice.

Stool samples were collected on the same day as the blood was collected. Before the blood extraction, mice were placed in an empty cage and left undisturbed. Mice were removed from the cage and prepared for blood extraction once they had defecated 2-3 times at least, which usually took around 5-10 minutes. Feces were collected with sterile tweezers and immediately frozen in dry ice. Both the tweezers and the empty box were thoroughly cleaned with ethanol to avoid any possible contamination between samples.

4.3.6 Mouse perfusion

Mice were anesthetized by injecting i.p. 200 µL pentobarbital (15mg/mL) and 100 µL buprenorphine (0,015 mg/mL). To test the depth of the anesthesia, we checked whether the interdigital reflex was present by pinching the interdigital membrane with forceps. Once the mouse completely lost this reflex, the perfusion procedure commenced.

The unresponsive animal was laid face-up and its limbs were fixed with needles to the operation table. Afterwards, a median incision through the linea alba was performed to expose the inner organs. To drain all the blood from the animal, PBS was injected with a needle through the left ventricle of the heart, while the right auricle was cut open to allow the release of fluid from the circulatory system. After approximately 5 minutes, PBS was switched with PFA (4%) to fixate the animal. Once the tail of the mouse started to get stiff (approx. 5-10 minutes), the perfusion was ended and the brain was dissected out of the skull and placed in PFA (4%) overnight. On the next day, the brains were transferred to a sucrose solution (30% sucrose in 1x PBS with 0.02% NaN_3) until they sunk to the bottom (approx. 1 day) and then were frozen at -20°C.

4.3.7 Immunohistochemistry

Before performing any immunostaining, it is necessary first to cut the brain in sections. For this purpose, we used a Leica CM3050S cryostat. A drop of tissue freezing medium (Leica) was placed on the specimen block to bind the brain and make it more stable during the cutting procedure. The whole brain was cut in 40µm sections and section was placed in the well of a 96-plate with a few milliliters of 1x PBS.

From these free-floating sections spanning the whole brain, one every six was used for GFP immunostaining. In summary, the sections were washed for 5 to 10 minutes in 1x PBS with 0.2% Triton at room temperature (RT). Next, sections were blocked for 15 minutes using the same buffer containing 4% goat serum (immunobuffer) and incubated overnight at 4°C with the primary antibody (rabbit anti-GFP 1:500; homemade) in immunobuffer. On the next day, sections were washed 3 times as in the previous day and incubated afterwards for 1 hour with the secondary antibody (Alexa-546 anti-rabbit 1:1000) in immunobuffer. After this step, sections were washed one time and counterstained for 5 minutes with DAPI (1:5000 in PBS), before being washed a last time. All the steps from day 2 were carried out at RT and in the dark to avoid bleaching of the antibodies. Finally, sections were transferred onto glass slides, using Moviol (Sigma-Aldrich) as mounting medium.

4.3.8 Image acquisition and post-processing

Images were taken using a spinning disc confocal microscope (Visitron systems, CSU-W1, Yokogawa) based on an inverted microscope (Nikon Ti2) with a motorized stage controlled by the VisiView software (v4.4). A 10x air objective (NA 0.45, CFI Plan Apo Lambda; Nikon) was used to magnify the specimens and the resulting light was captured using two sCMOS BSI cameras (Photometrics). Fluorescence activation was achieved using a 561 nm laser (intensity: 70%) with a long-pass filter (570LP) for the signal from the secondary antibody (Alexa 546). DAPI fluorescence was also activated with a 405 nm laser and the emission was selected with a band-pass filter for DAPI (ET460/50). DAPI images were exclusively used find the correct brain regions. Binning was kept at 1 and exposure time was 100 ms. In total, 16 different (2 µm thick) Z-series were acquired for each image.

Image post-processing was performed using Fiji ("Fiji Is Just ImageJ"). First, the brightness and contrast of every Z-section in the image were adjusted to automatic values and the Z-stack image was changed to 8-bit. Then, the whole Z-stack was 2-D projected using a "Maximum" approach, i.e. for a specific pixel within the original image, the highest value across all Z-stacks will be used in the final image. Lastly, GFP+ nuclei were manually counted with the add-on "Cell counter".

4.3.9 Dual extraction of RNA and lipids from brain regions

The simultaneous extraction of RNA and lipids from the same sample was performed according to the instructions from the original publication [377]. In summary, the dissected brain tissues were weighted and inserted into cold 2 mL precellys tubes with RNase-free ceramic beads and a mix of 600 µL of RLT buffer from the RNeasy® mini kit (Qiagen, Germany) with 1% β-mercaptoethanol. 200 µL of chloroform was added. This solution was spiked with a 10 µL mixture of internal standards (ISTD) (Avanti Polar Lipids, Inc.) for different lipidic molecules to reach a final concentration of 0.5 ng/mL for each standard (Table 6). The samples were homogenized using a precellys tissue homogenizer (Bertin, France) and transferred to a new tube. Upon centrifugation of the samples, two phases could be observed: an upper transparent phase containing the RNA and a lower chloroform phase with the lipids. Each phase was then transferred to new tubes for further processing.

The upper transparent phase was used for RNA extraction following the instructions of the RNeasy® mini kit (Qiagen, Germany), including DNase I treatment for the removal of genomic DNA. In the end, total RNA from the sample was eluted in 30 µL of RNase-free water. The lower phase with the lipids was collected and mixed with 800 µL of methyl

tert-butyl ether (MTBE)/methanol (MeOH), in a 10:3 v/v proportion, and 250 µL of ice-cold 0.1% formic acid. Samples were vortexed for 30 minutes at 4°C and centrifuged afterwards 15 minutes at 13000 rpm. The organic phase was removed, and any leftover was evaporated using a gentle stream of nitrogen. Samples were then reconstituted in 90 µL MeOH and 18 µL of this solution was mixed with 2 µL water before injecting the sample into the mass spectrometer. For the analysis of eCBs and polyunsaturated fatty acids (PUFAs), 27 µL of the final solution were evaporated once more and dissolved in 30 µL of acetonitrile (ACN) mixed with water (1:1 v/v).

Internal standards (ITSD)	
Molecular name	**Abbreviation**
phosphatidylcholine 17:0/14:1	PC 17:0/14:1
phosphatidylglycerol 17:0/14:1	PG 17:0/14:1
phosphatidylethanolamine 17:0/14:1	PE 17:0/14:1
phosphatidylserine 17:0/14:1	PS 17:0/14:1
phosphatidic acid 17:0/14:1	PA 17:0/14:1
phosphatidylinositol 17:0/14:1	PI 17:0/14:1
lysophosphatidylcholine 17:0/0:0	LPC 17:0
lysophosphatidic acid 17:0/0:0	LPA 17:0
sphingomyelin d18:1/12:0	SM d18:1/12:0
ceramide d18:1/17:0	CER d18:1/17:0
ceramide-1-phosphate d18:1/12:0	C1P d18:1/12:0
sphingosine d17:1	SPH d17:1
sphingosine-1-phosphate d17:1	S1P d17:1

Table 6. List of internal standards used for the lipidomic profiling of resilient and susceptible mice. List of internal standards used for the lipidomic profiling of resilient and susceptible mice. Different lipidic species were added to each sample as internal standards with a final concentration of 0.5 ng/mL. These ITSD are used to estimate the percentage of recovery for each molecule after the extraction protocol. This information improves the quantification of lipids and provides a better estimate of their original concentration.

4.3.10 Lipidomic quantitative profiling from brain tissue

Targeted lipid profiling throughout this study was invariably carried out in polarity switching using a 5500 QTrap triple-quadrupole linear ion trap mass spectrometer (AB SCIEX, Darmstadt, Germany), interfaced with an Agilent 1200 series LC system (degasser, pump, and thermostated column compartment; Agilent, Waldbronn, Germany). The LC conditions were set as recently described [377,378]. Briefly, chromatographic separation of lipids was achieved using an Ascentis Express 2.7 µm C18 column, 100 mm x 2.1 mm (Supelco, Sigma-Aldrich, München, Germany) applying two different experiment. For PL and sphingolipid analysis the column was thermostated

at 45°C and the mobile phase A consisted of methanol/water (1:1; v/v) containing 0.2 % formic acid, 7.5 mM ammonium formate and 0.1% TEA and the mobile phase B consisted of methanol/isopropanol (2:8; v/v) containing 0.2 % formic acid, 7.5 mM ammonium formate and 0.1% trimethylamine (TEA). The flow rate was 200 µL/min. Gradient elution began at 40% B, held for 3 min and was then linearly increased over 42 min to 90% B, then linearly increased to 99% B in 1 min, held there for 7 min and decreased over 2 min to 40% B. For eCBs and PUFA analysis the mobile phase A consisted of 0.1 % formic acid and phase B of 100% ACN containing 0.1% formic acid. The flow rate was set to 300µL/min. Gradient elution began at 20% B, held so for 1 min, then linearly increased over 4 min to 50% B, maintained so for 7 min, linearly increased to 90% B over 1 min, held for 4 min, decreased over 0.5 min to 20% B. The column was then re-equilibrated at 20% B for 2.5 min.

Quantification of lipids was conducted via Analyst 1.6.2 software and MultiQuant 3.0 quantitation package (AB SCIEX, Darmstadt, Germany). The obtained values were normalized to the tissue weight.

4.3.11 Extraction of bacterial DNA from stool samples

To characterize the mouse gut microbiota, we used the QIAmp Fast DNA Stool mini kit (Sigma) following the instructions from the manufacturer. In summary, 1-3 feces were homogenized in InhibitEX buffer (Sigma) by vortexing. Next, the homogenate was centrifuged at full speed for 1 minute and 600 µL of the supernatant were transferred to a tube containing 25 µL of proteinase K to digest any protein in the sample. Buffer AL (600 µL) was added to the mix and a 10-minute incubation at 70°C was performed to ensure the lysis of all cells and the denaturation of proteins. Afterwards, 600 µL of ethanol were added to the lysate and mixed. This mixture was then passed through a QIAamp column (Qiagen) and washed with different buffers (AW1, AW2) until it was eluted using 200 µL nucleic acid-free water. Each sample was measured twice using Nanodrop to determine the concentration and purity of the DNA extraction.

4.3.12 Library preparation and sequencing from stool samples

Microbiome analysis via next generation sequencing (NGS) requires the sequencing of amplicons belonging to highly conserved regions within the bacteria genome. In contrast to other sequencing analysis, DNA samples need to be amplified before being processed for library preparation. Shortly described, the DNA samples were amplified via polymerase chain reaction (PCR) using a primer combination (515F and 806bR) specific for the hypervariable region V4, found within the bacterial 16S ribosomal RNA (rRNA) sequences. The region V4 is one of the nine hypervariable regions found within the 16S

region (V1-V9) and one of the most reliable for microbiome analysis (Yang et al 2016). The degree of conservation is not same across the different hypervariable regions, with more conserved regions correlating to higher-level taxonomy and the less conserved ones to lower levels, such as genus and species (Gray et al 1984; Yang et al 2016). The amplicons generated via PCR were then used for library preparation as per the manufacturer´s instructions (Illumina, USA). Among other steps, two Illumina adapters were ligated to the sequences of interest to provide a forward and backward reading frame (GGCTGACTGACT and ACAATTACCATA respectively) and spiked with PhiX control v3 library (Illumina, USA) in order to balance the base composition and improve the quality of the run.

Libraries were then pooled and loaded in a flowcell to be processed in an Illumina MiSeq sequencer. All 72 samples were sequenced in the same flowcell, which gave a yield of 20-30 million reads in total (including ~25% of PhiX library). Reads were 300 nucleotides long to cover all of the 16S V4 region and paired-end, meaning they were read starting from both extremes, which increases the alignment quality of the read.

4.3.13 Lipid extraction from dried blood spots

The procedure for the extraction of lipids from dried blood spot samples is not yet disclosed due to pendant patent.

4.3.14 Bioinformatic analysis of gut microbiome data

The bioinformatic analysis of the microbiome samples was performed in collaboration with Hristo Todorov from the group of Susanne Gerber. In summary, sequencing data were processed using mothur v1.40.5. Briefly, reads were merged into contigs, sequences with any ambiguous bases or homopolymers longer than 8 bases were removed. Sequences were then aligned to the SILVA reference alignment and chimeras were removed using VSEARCH. Taxonomy was assigned using the Greengenes database. Sequences with identical taxonomy were grouped to operational taxonomic units (OTUs). Statistical analysis and visualization were then performed using the *phyloseq* R package. Alpha diversity was estimated by rarefying each sample to the smallest library size and calculating the diversity index. This procedure was repeated 1000 times and the average over all runs was reported as the final diversity estimate. Beta diversity was calculated based on Bray-Curtis dissimilarity and Jaccard distance and visualized using unconstrained and constrained analysis of principal coordinates. Changes in taxonomic composition between phenotypes at each time point were evaluated using the non-parametric Kruskal-Wallis test followed by Dunn’s post hoc test in case of significant results. Longitudinal changes within each phenotype were

statistically evaluated with the non-parametric Friedman test followed by Nemenyi post-hoc test in case of significant results.

4.4 Results

4.4.1 Behavioral characterization of trauma-exposed (+FS) and control (-FS) mice

In order to assess the behavioral effect of the traumatic foot-shock, mice were tested in a behavioral battery four weeks after the exposure to trauma (Figure 31A). The paradigms in this study were chosen based on the relation to the symptoms found in human patients with PTSD. These tests not only included test for PTSD-specific dysregulations, such as hyperarousal, generalized fear and a strong fear memory, but also for mood disorders that often show comorbidity with PTSD, such as anxiety and depressive-like behaviors. The idea of this experimental setup is to classifiy trauma-exposed mice to the resilient or susceptible phenotype according to their behavior (Figure 31B). Starting before the traumatic shock and during the whole duration of the experiment, the body weight of the mice was measured weekly (Figure 31C) to study potential effects of stress-induced alterations in eating behavior. However, no differences in body weight were found in any of the time points investigated.

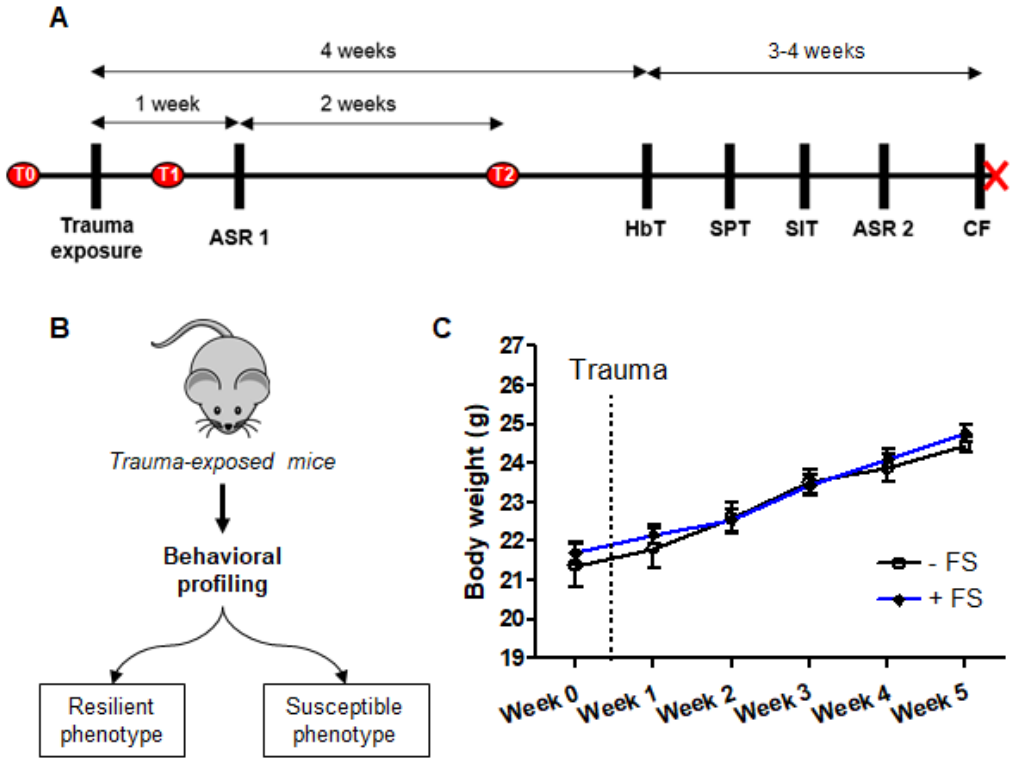

Figure 31. Experimental setup and body weight measurements. (A) Experimental timeline for the PTSD model, which includes a single, strong trauma followed after four weeks by a battery of behavioral tests. Red circles represent the three different time points for the collection of blood and fecal samples (T0, T1 and T2, respectively). **(B)** Animals exposed to the trauma are then profiled according to a set of predetermined behavioral criteria. The final goal is to separate two distinct subgroups based on their coping abilities towards trauma. **(C)** Body

weight evolution of –FS (n=6) and +FS (n=32) mice during the experiment. Measurements were taken on a weekly basis starting one day before the first collection of blood and fecal samples. ASR: acoustic startle response; HbT: holeboard test; SPT: sucrose preference test; SIT: social interaction test; CF: contextual fear. P value was estimated using two-way ANOVA with repeated measurements. Points in the graph represent mean ± s.e.m.

The first behavioral test to be performed was the acoustic startle response (ASR), a paradigm designed to measure hyperarousal in rodents (Figure 32). This test was done just one week after the trauma (in contrast with the rest of the behavioral tests), because its protocol is not very stressful and does not include strong habituation processes, thus, it can be performed a second time. The reason to evaluate the animals twice in this paradigm (one and four weeks after the trauma) was to uncover potential short-term behavioral effects that could already indicate a resilient or vulnerable phenotype. No differences between stressed (+FS) and naïve (-FS) mice were observed at this time point. Nevertheless, +FS animals displayed a wider dispersion in their behavioral response than unstressed controls, making possible the stratification into the resilient and susceptible phenotypes, respectively.

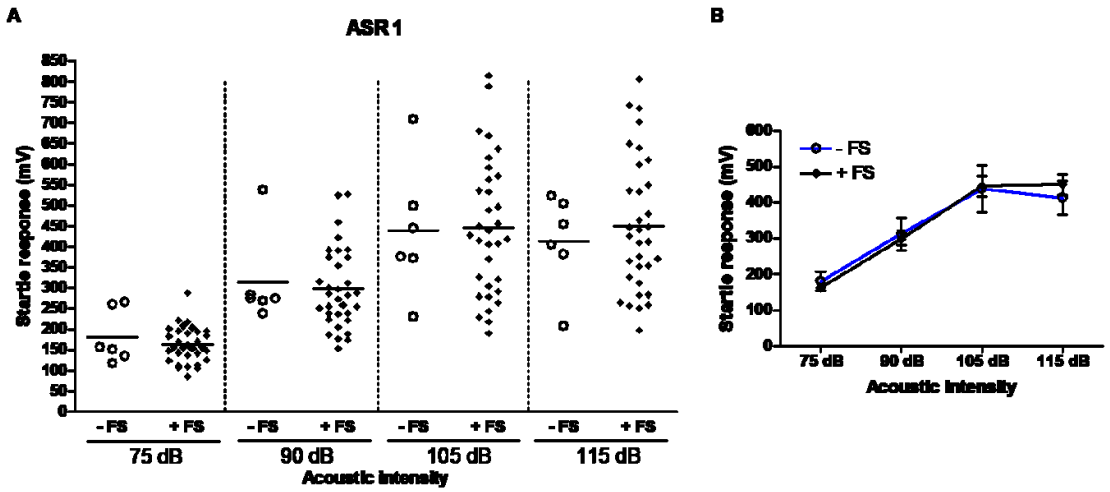

Figure 32. Hyperarousal behavior measured by ASR. Behavioral data showing the startle response of trauma-exposed (+FS; n=32) and control (-FS; n=6) mice. **(A)** Data dispersion for each of the different acoustic intensities tested in this paradigm. **(B)** Graph representing the same data as in (A), but showing the mean ± s.e.m instead of every single data point. Statistical analysis was done using two-way ANOVA.

One month after the exposure to the trauma, mice were first investigated in the holeboard test (HbT), a paradigm designed to study anxiety-like behaviors (Figure 33). Results for this test showed the characteristic wide dispersion of the behavioral response in the +FS group, matching observations done in human cohorts. Furthermore, there were significant statistical differences between groups in the number of head pokes (Figure 33A) and the latency to perform the first head poke (Figure 33B), parameters which are inversely and directly, respectively, correlated to anxiety levels. Locomotion was also significantly reduced in the trauma-exposed animals (Figure 33C), indicating increased

levels of distress and fear as a consequence of the trauma. These results clearly indicate the existence of a long-term behavioral dysregulation as a consequence of the trauma exposure.

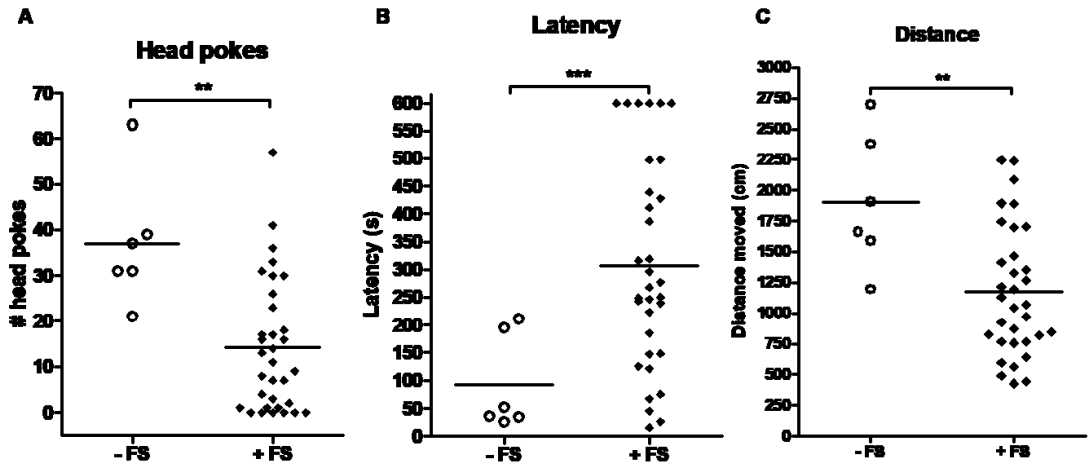

Figure 33. Anxiety-like behavior measured by holeboard test (HbT). Dot plots showing different parameters measured in the HbT that correlate with anxiety-like behavior in –FS (n=6) and +FS (n=32) mice. **(A)** Head pokes mean the number of times that animals explored 4 small-sized hole in the middle of the arena by poking their complete head through it. This measurement inversely correlates with anxiety-like behavior. **(B)** Latency to the first head poke, which directly correlates to anxiety-like behavior. **(C)** Graph showing the locomotor behavior measured as the distance moved. P value was calculated using unpaired two-tailed t-test. ***, $p<0.001$; **, $p<0.01$.

Next, anhedonia and social behavior were analyzed using sucrose preference test (SPT) (Figure 34A) and social interaction test (SIT) (Figure 34B), respectively. Although patients with PTSD often develop anhedonia (a sign of depressive-like behavior) and reduced sociability, the prevalence of these symptoms is lower when compared with other more PTSD-specific dysregulations, such as intrusive memories, hyperarousal and a strong fear memory of the trauma. For both of these paradigms, no significant differences between experimental groups could be observed. However, the characteristic wide dispersion of the data is still present in both tests, making it possible to classify +FS mice into different phenotypes. Moreover, although in SIT no differences were observed in the time they spent in the interaction and partner zones, -FS mice spent less time in the corners during the social interaction phase, meaning –FS mice displayed less anxiety and were more open to explore the arena and other conspecifics. The lack of statistically significant differences between the groups is most likely a result of the individual variability in the behavioral response, as well as the fact that anhedonia and reduced sociability are not present in every patient suffering from PTSD.

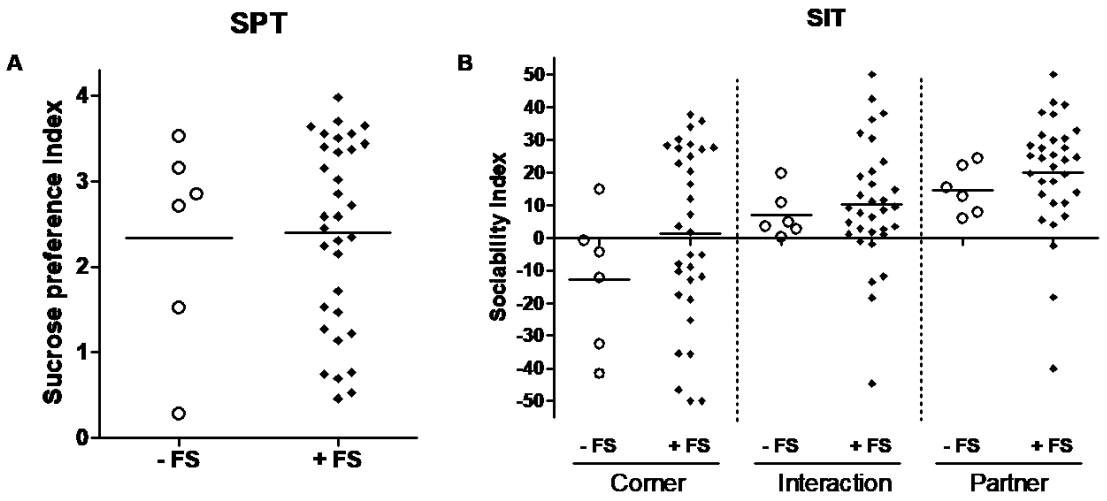

Figure 34. Results analyzing anhedonia and social behavior in control and stressed mice. Graphs showing anhedonia and sociability in –FS (n=6) and +FS (n=32) mice. These two behaviors are known to be dysregulated in some PTSD patients. **(A)** Anhedonia as measured by the sucrose preference test (SPT), in which mice have the option to drink either normal or 4% sucrose water. Increased preference indices indicate normal behavior (i.e. preference for sucrose water), whereas a low index is related to anhedonia. **(B)** Graph showing social behavior as measured by social interaction test (SIT), a paradigm in which mice explore two times the same arena with an empty circular cage and then with the same cage containing an unknown mouse (of the same strain). Increased sociability index (>0) is indicative of higher exploration time during the phase where the conspecific is present. Statistical significance was analyzed using unpaired two-tailed t-test for SPT and two-way ANOVA for SIT.

The next paradigm performed during the behavioral testing was a second session of ASR (Figure 35). Surprisingly, there were barely any differences between both time points, although during the repetition of the ASR paradigm the two experimental groups behaved more differently, but without clear statistical significance. The scattering of the data of the stressed mice (+FS) showed that part of that cohort still suffers from a long-term behavioral maladaptation observed also in PTSD patients, even more than four weeks after the trauma exposure (Figure 35A).

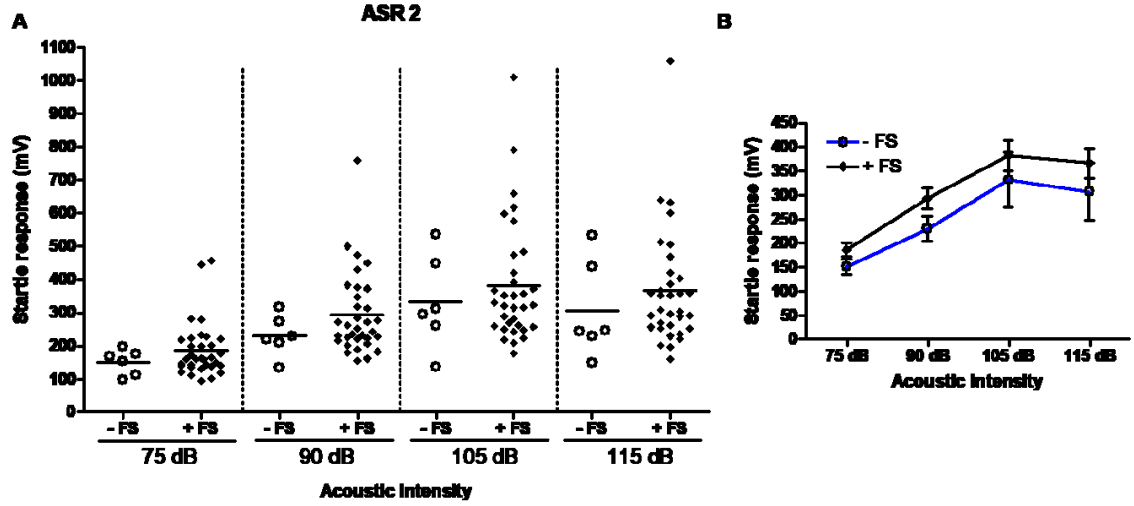

Figure 35. Hypera rousal behavior measured by ASR. Behavioral data showing the startle response of trauma-exposed (+FS; n=32) and control (-FS; n=6) mice. **(A)** Data dispersion for each of the different acoustic intensities tested in this paradigm. **(B)** Graph representing the same data as in (A), but showing the mean ± SEM instead of every single data point. Statistical analysis was done using two-way ANOVA.

Lastly, the final behavior we analyzed was the fear memory itself. Some studies suggest that the onset and/or development of PTSD is due to an excessively strong fear memory that induces other fear-related symptoms, such as fear generalization (or displaying a fear response in response to harmless cues or environments), intrusive memories or the incapacity to extinguish the traumatic memory. For our behavioral profiling we also analyzed the immobility of mice when exposed to new environments (Figure 36A), such as HbT or SIT, as a way to study the generalization of the fear response to harmless environments. Moreover, we measured the strength of the contextual fear (CF) memory by exposing the mice to the traumatic context and analyzing the time that mice spent freezing ("absence of movements except for those of breathing") (Figure 36B), which is the typical display of fear in rodents. The results indicate that in general trauma-exposed mice suffer more from fear generalization when exposed to a new environment than their naïve counterparts, as seen by the increased immobility time in the HbT arena. In the SIT arena, +FS mice also showed a slightly increased immobility time, although the similarities between both arenas (white 40x40x30cm boxes) could account for this difference not being statistically significant (Figure 36A). The strength of the fear response is significantly higher in the trauma-exposed group when compared to the –FS mice, as seen by an increase of over 2-fold in the freezing time (Figure 36B). For both paradigms, the characteristic dispersion of individual behaviors in the +FS group was also present, highlighting once more the intrinsic variability of mice in studies related to stress-induced pathologies. These results showed the persisting long-term dysregulation of the fear response in trauma-exposed mice and their consequently maladaptive behaviors, such as the generalization of the fear memory to harmless environments or cues unrelated to the trauma context.

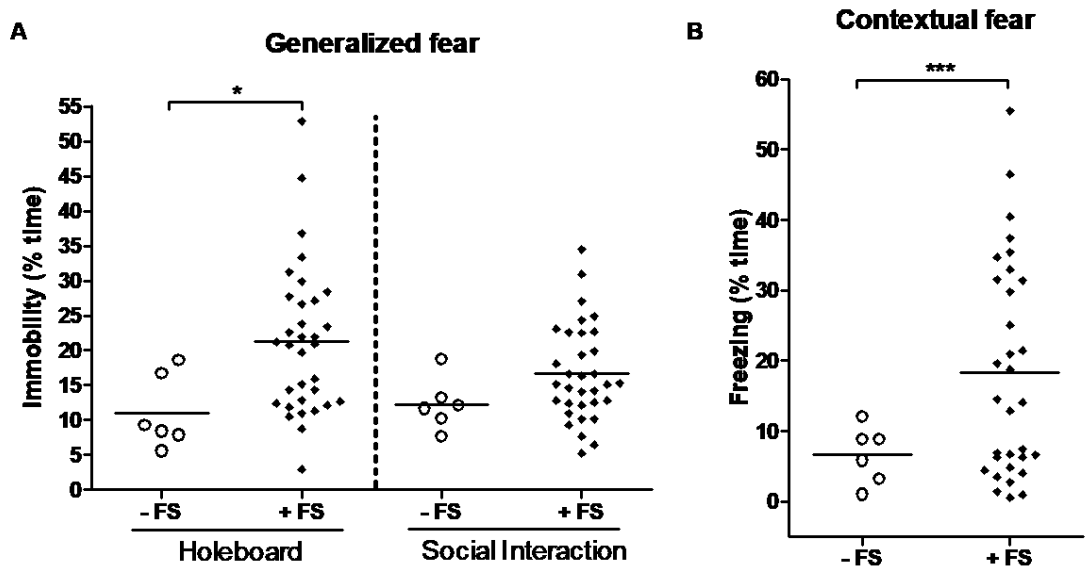

Figure 36. Fear response measured in a novel and in the trauma context. Graphs showing the fear response of –FS (n=6) and +FS (n=32) mice when exposed to a novel unrelated arena or to the traumatic context. **(A)** Immobility time measured during the exposure of the animals to a new environment. The display of the fear response in arenas unassociated to the trauma is indicative of fear generalization. **(B)** Freezing time measured upon a second exposure to the context where the traumatic experience took place. An increased fear response can be indicative of stress-induced psychopathologies. P values were calculated using unpaired two-tailed t-test. *, $p<0.05$; ***, $p<0.001$.

4.4.2 Behavioral profiling of trauma-exposed mice (+FS)

There is no clear consensus among the scientific community as to what a resilient phenotype is. Currently, there are many different approaches to classify mice within a large cohort according to their behavioral performance in one or more behavioral tests. Based on the characteristics of the experimental plan and stress model applied here, we decided to perform a behavioral profiling. The classification method is based on the assumption that “normal” behavior is defined according to the performance of a control, non-exposed group of mice. Following this assumption, the behavior of the trauma-exposed animals is classified into resilient (R+) and non-resilient (R-) depending on whether their performance is within or out of the boundaries of the “normal” behavior, respectively. As different parameters can be measured in each behavioral test, it must also be decided beforehand which of those measurements will be used for the behavioral profiling, paying attention always to the specifications of each paradigm. For this project, we established three criteria to be followed in order to characterize mice according to their resilience or susceptibility status:

1. “Normal” behavior is defined as the confidence interval ($\alpha = 0.15$) calculated from the data of the control, non-exposed group.

2. Each mouse is classified as resilient (R+) or non-resilient (R-) for each behavioral test according to the specifications and measurable parameters of the paradigm.

3. For a mouse to have the R+ or R- phenotype, respectively, it must be classified as such in 4 (out of 7) behavioral paradigms within the longitudinal study. Furthermore, the animal can only be classified as the opposite phenotype in maximum one behavioral test to still obtain a final R+ or R- status, respectively.

We designed these criteria based on the intrinsic symptomatic heterogeneity found among human patients exposed to trauma. For this reason, we decided that mice should be able to show anomalies in their behavior when compared to the rest of their assigned group, i.e. a resilient mouse being assigned to the non-resilient group in one test, or *vice versa*. Following these criteria, around 10-20% of the total trauma-exposed mice were assigned to the non-resilient (R-) group across different batches in an unbiased manner. The percentage of mice affected by PTSD correlates well with human findings by the world health organization [379].

4.4.3 Behavioral data of resilient (R+) and non-resilient (R-) mice

After applying the criteria for resilience and susceptibility to the trauma-exposed group, there were 6 and 4 individual animals classified as resilient (R+) and vulnerable (R-), respectively (Table 7). Although these numbers are not big, they respectively represent around 18% and 12% of the total cohort. The behavioral data of R+ and R- mice was then re-graphed to study how different both groups were, as a way to study the behavioral differences between the R+ and R- phenotypes.

Mouse Nr.	ASR 1	HbT	GF	SPT	SIT	ASR 2	CF	Final phenotype
2526								R+
2547								R+
2552								R-
2561								R+
2582								R+
2607								R+
2625								R-
2627								R-
2632								R+
2671								R-

Table 7. Results of the behavioral profiling from the R+ and R- mice. Results of the behavioral profiling from the R+ and R- mice. The individual outcomes for each behavioral paradigm are analyzed independently to determine whether mice display resilient (green) or susceptible (red)

behavior. Sometimes, mice cannot be classified in one paradigm due to contradicting or insufficiently clear behavior (marked with a slash). In the final step, all behaviors are considered to classify mice into the R+ (dark green) or R- (dark red) phenotypes. ASR, acoustic startle response; HbT, holeboard test; GF, generalized fear; SPT, sucrose preference test; SIT, social interaction test; CF, contextual fear.

Trauma-exposure did not induce significant differences in the body weight of resilient and vulnerable mice. Although the latter group showed a lower, but non-significantly (p>0,1), body weight across most of the measurements (Figure 37B). Given that there were no differences between control and trauma-exposed mice before the behavioral profiling and the low variability found in their body weight distribution (Figure 31B), the lack of statistical differences was expected. However, the lower body weight of the R- animals was surprising and could potentially lead to differences across groups when working with larger cohorts of animals or when analyzing the body weight for longer periods of time, as it seems the differences in body weight between R- and the R+ and –FS groups were becoming more pronounced each week after the trauma.

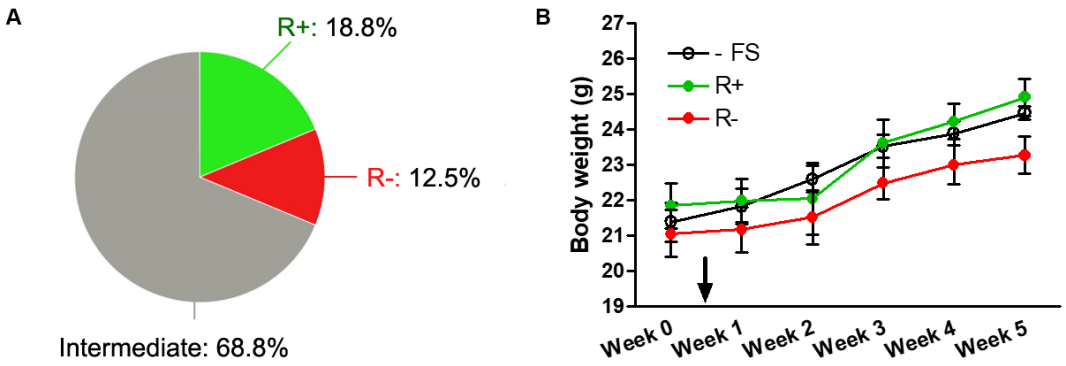

Figure 37. Percentage of resilient (R+) and vulnerable (R-) mice and their body weight. (A) Pie chart showing the resulting percentages of R+ and R- mice after the behavioral profiling. **(B)** Mice were weighted once a week starting before the trauma exposure (black arrow). There was no significant difference between experimental groups in any of the time points, suggesting that mice were not sufficiently affected by the stressor to change food intake and metabolism. P values were estimated using two-way ANOVA with repeated measurements. To study the differences in a specific time point, a one-way ANOVA analysis was performed.

Our PTSD-like model did not seem to elicit any kind of dysregulation of the startle response, as seen by the similar behavior of the –FS and +FS mice (Figure 32B). However, after the behavioral profiling, and the subsequent classification of mice into R+ and R- phenotypes, differences within the +FS can be observed already during the first exposure to ASR (Figure 38). Mice classified as R- showed an increased startle response, with statistically significant differences in the response to loud stimuli (105 dB and 115 dB) (Figure 38B) when compared to both –FS animals and mice classified as R+. These results show that our stress model and behavioral profiling criteria function well to divide stressed populations into different subgroups according to their behavior, even if the initial analysis with the original population did not suggest so. Furthermore,

the results also support the notion of focusing research on the extreme values of a population instead of the average value, as this new approach can uncover subgroups with significantly different behaviors (e.g. R+ and R-). Complementing traditional research methods with the study of the extreme responders could help unraveling the underlying causes of stress-related disorders, as well as the mechanisms behind the individual differences observed in this type of psychopathologies.

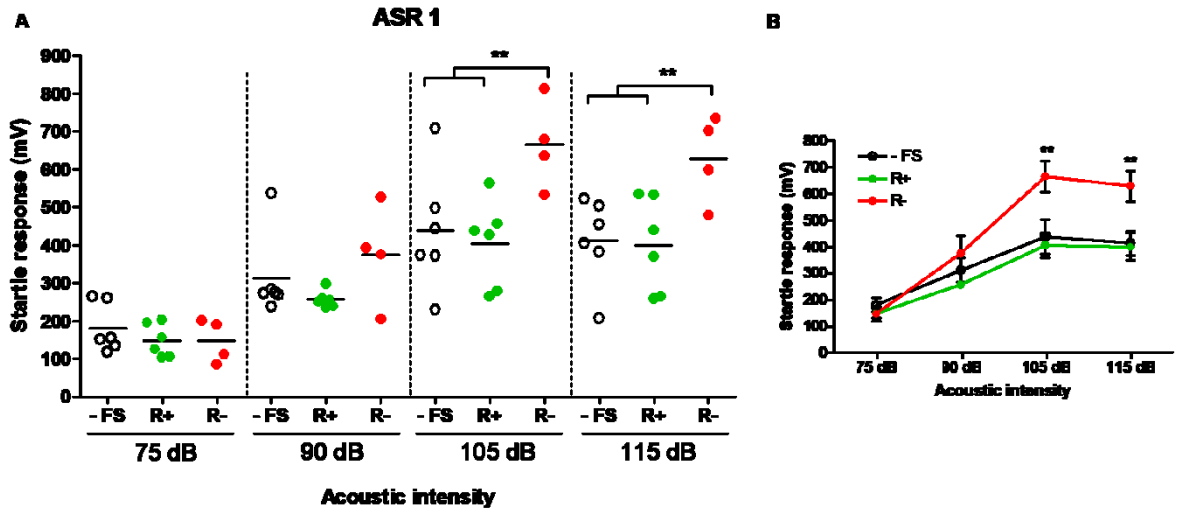

Figure 38. Data from the first exposure to ASR after the behavioral profiling of +FS mice. Upon behavioral profiling, differences arise within the trauma-exposed group. Mice classified as either R+ or R- differed significantly between them only when exposed to acoustic stimuli of high intensity. Only the R- mice (and not the R+) were significantly different to the -FS group. **(A)** Dispersion of the startle response in control (-FS), resilient (R+) and vulnerable (R-) mice. **(B)** Graph representing the same data as in (A), but showing the mean ± SEM instead of every single data point. Statistical differences were analyzed using two-way ANOVA analysis. **, $p<0.01$.

The results of the HbT showed a strong difference between +FS and –FS mice, indicative of increased anxiety levels in mice exposed to a traumatic experience. After applying the criteria for the behavioral profiling, R- show significant differences to the –FS group in the number of head pokes performed, but not in the latency for the first head poke (Figure 39A, B). On the other hand, R+ mice show no statistical differences to the –FS mice in any of the measured parameters. However, their behavioral response stands in the middle between –FS and R- animals for all parameters, but without significant differences to the R- mice. Ambulatory behavior also showed differences between –FS and R- animals, but not between R+ mice and any of the other experimental groups. These results showed that trauma-exposed mice that failed to cope with the stressor have higher levels of anxiety when compared with non-exposed animals. Furthermore, the response of the resilient mice is quite variable, with mice within the R+ group split between those with anxiety-like behavior similar to the –FS group, and those with a response similar to R- animals. This observation is consistent with data from PTSD

studies in human cohorts, where some patients develop anxiety and depressive behaviors together with (or as a consequence of) PTSD [380,381].

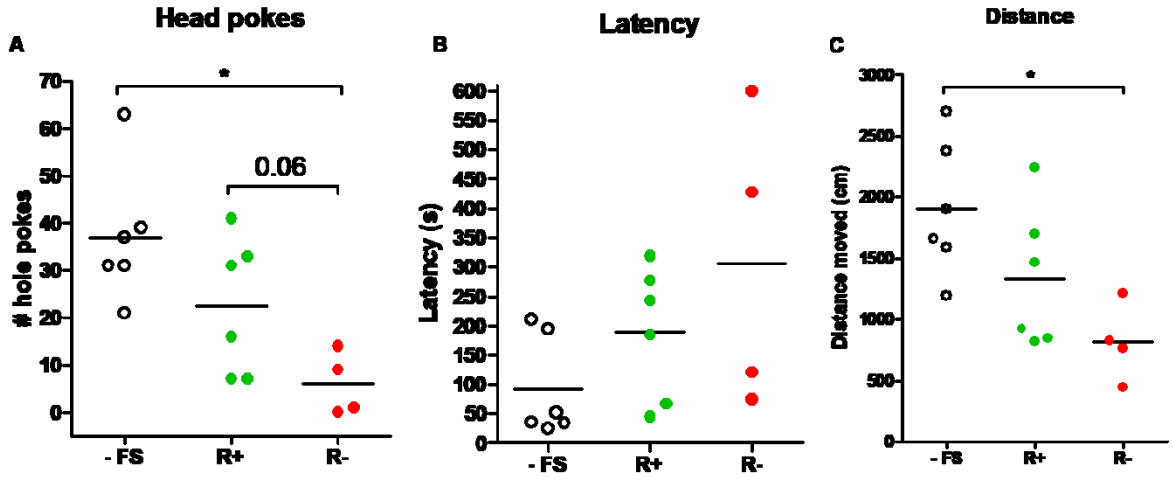

Figure 39. Anxiety-like behavior of R+ and R- animals as measured by HbT. Graphs showing different parameters related to anxiety-like behaviors, as measured during the HbT. **(A)** Number of head pokes represent the exploration of a new location and correlates inversely with anxiety. **(B)** Latency to the first head poke. **(C)** Locomotor behavior measured as the distance moved while performing HbT. P values were calculated using one-way ANOVA and the Mann-Whitney t-test. *, $p<0.05$.

Anxiety is not the only psychopathology that affects patients of PTSD. Depressive disorders are also often comorbid with PTSD and other stress-related disorders. Moreover, the ability to socially interact with other conspecifics is also impaired in a percentage of the PTSD-affected population. The analysis of anhedonic (Figure 40A) and social behavior (Figure 40B) in R+ and R- mice did not reveal any statistical differences between the different experimental groups. However, it is important to mention that R+ mice had an increased preference for sucrose and were more social than their R- counterparts. Although these results are not statistically significant, the tendency of R+ animals to behave more similar to the –FS (or better) than the R- helps to validate our PTSD model and our criteria for behavioral profiling. Taken together with the data from the HbT, our results indicate that the resilient mice were able to cope better with the trauma, as their behavioral performance was better than observed in vulnerable mice in paradigms involving anxiety, anhedonia and sociability, all of which are important to the pathology of PTSD, but not central to it.

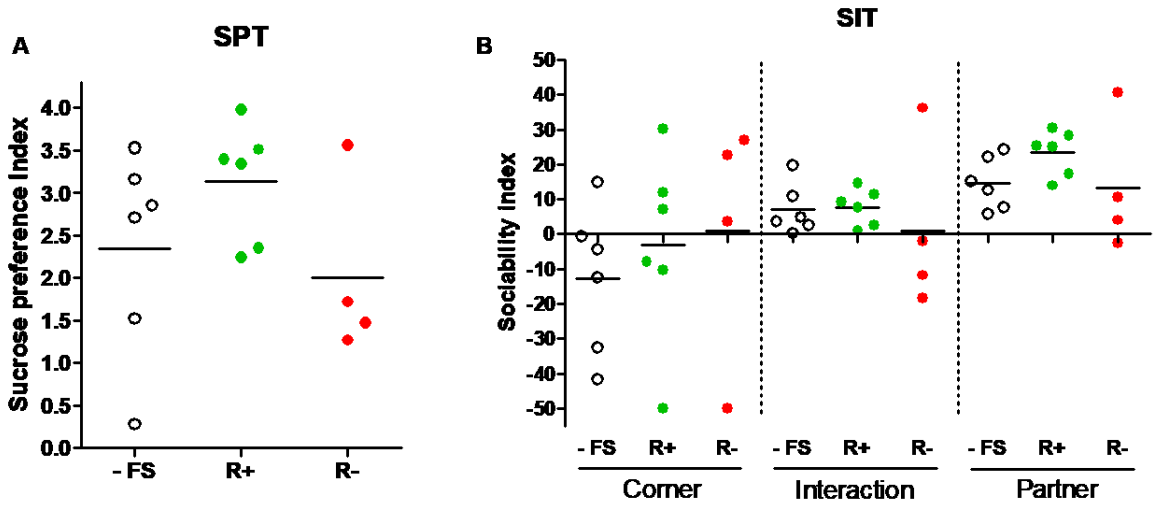

Figure 40. Anhedonic and social behavior of R+ and R- mice. Anhedonia and social behavior did not show strong differences between groups. However, R+ animals showed a tendency towards reduced anhedonia, which correlates with depressive-like behavior, and increased sociability. **(A)** Anhedonia, or lack of motivation towards rewarding stimuli, as measured by the sucrose preference test. The sucrose preference index is based on the proportion of sucrose water taken, in comparison to normal water, and normalized to the weight of the mice. **(B)** Social behavior measured during social interaction test. Values above 0 indicate preference for a specific zone of the arena during the phase in which an external mouse is also present. Statistical significance was analyzed using one-way ANOVA analysis.

Data from the second exposure to the ASR paradigm showed stronger differences between the R+ and R- groups than in the first performance of ASR (Figure 41). The statistical differences in the startle response to the two highest intensities (105 dB and 115 dB) became more significant than one month after the traumatic experience. Moreover, R- mice also showed a significantly increased startle response to the 90 dB stimulus (Figure 41A) compared to both -FS and R+ animals. These data suggest that increasing the time after trauma might exacerbate the behavioral dysregulation in susceptible individuals.

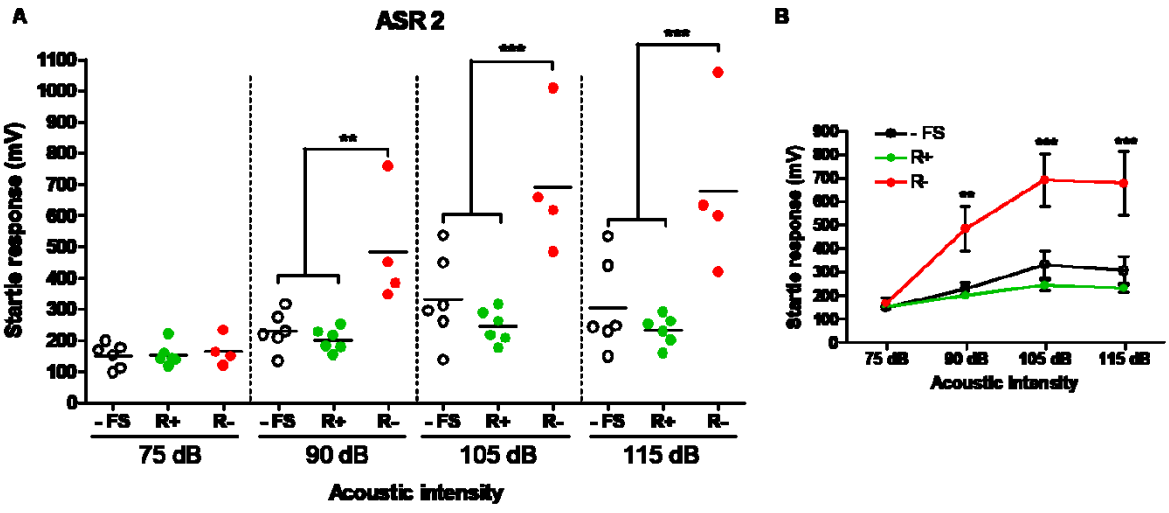

Figure 41. Hyperarousal of R+ and R- animals as measured by ASR. During the second exposure to the ASR paradigm, differences between groups became more significant. R- mice are statistically different in the 3 highest acoustic intensities, when compared to the other two experimental groups (-FS and R+). **(A)** Dispersion of the startle response in control (-FS), resilient (R+) and vulnerable (R-) mice. **(B)** Graph representing the same data as in (A), but showing the mean ± SEM instead of every single data point. P values were calculated using two-way ANOVA analysis with Bonferroni post-test. **, p<0.01; ***, p<0.001.

Regarding the fear response, several statistical differences were observed in the fear response of +FS and -FS mice (Figure 42). After the behavioral profiling, R- animals kept being significantly different to the -FS group in the shock context (Figure 42B) and when presented to a new environment only for the first time (Figure 42A). On the other hand, R+ mice did not differ significantly from the -FS animals, but had nevertheless a higher fear response in both paradigms. Interestingly, R+ animals were not significantly different to their R- counterparts in the generalization of the fear response, but there were statistical differences in the strength of the original fear memory (Figure 42B). These observations indicate that resilient mice are not "immune" to stressors, but rather they cope better with them than vulnerable animals. The low variability within the R- group in the contextual fear response could also point to an aberrantly strong fear memory playing a central role in the onset and development of PTSD.

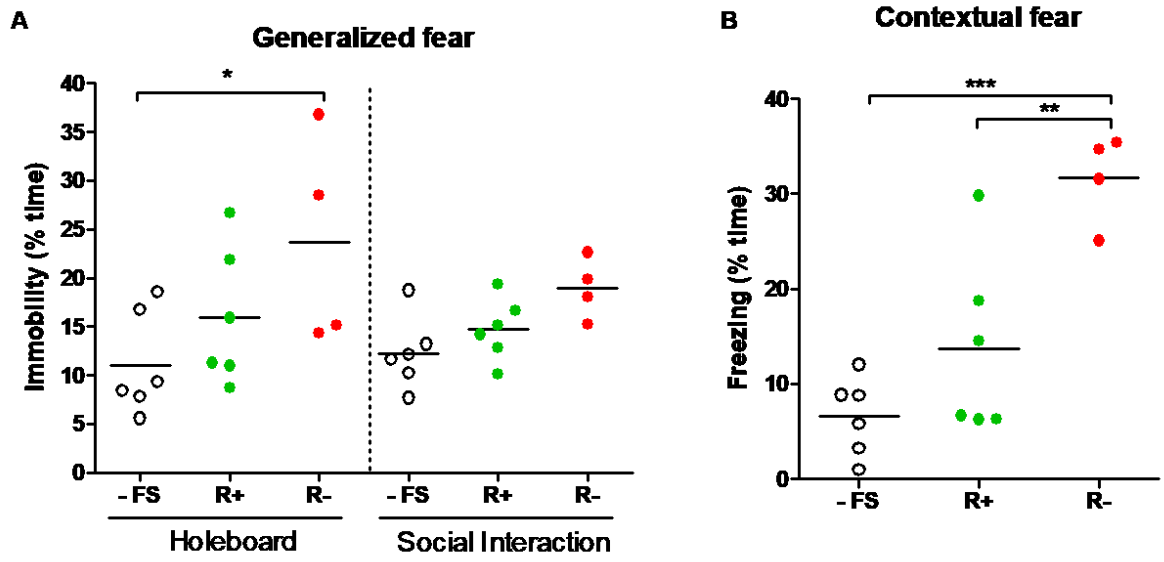

Figure 42. Fear response of R+ and R- mice to new environments and to the trauma context. Maladaptive behaviors related to the fear response include the generalization of fear to new environments, unrelated to the traumatic context, as well as abnormally strong long-lasting fear memories that are resistant to extinction processes. **(A)** Generalization of the fear response as measured by the immobility time of the animals when presented to new environments (holeboard and social interaction test arenas). **(B)** Evaluation of the strength of the contextual fear memory as measured by the freezing time when mice were exposed to the context where they received the traumatic foot-shock. *, p<0.05; **, p<0.01; ***, p<0.001.

4.4.4 Immunohistological analysis of ARC-nucl GFP mice

Quality control of the reporter transgene

Regulated reporter gene expression is a very valuable tool in molecular genetics, as it contains the potential to tag any cell type or cell structure within a specific time window. However, in reality, inducibilty and specificity of gene expression are generally a challenge depending on the transgenic mice used. In order to test the specificity of our mouse model, we performed an immunohistological staining on ARCnu mice that were exposed either to a traumatic stressor (i.e. strong foot-shock) or to the context without the stressor. To test whether the presence of tamoxifen (TAM) is necessary to induce GFP expression, half of the animals were injected with TAM and the other half with a saline solution (Figure 43). Our analysis showed that the presence of tamoxifen was absolutely necessary to induce any GFP expression at all (Figure 43A, B), whereas the intensity of the stimulus was directly correlated to the number of GFP+ nuclei counted (Figure 43B, C). These results suggest a high specificity of the reporter transgene in our animal model, as the expression of GFP stringently required the presence of TAM together with a strong stimulus to induce the recombination of the transgene in a significant number of cells (Figure 43B).

GFP expression analysis of brain regions involved in traumatic experiences

Once the quality control of the reporter GFP transgene was performed, we wondered whether there were any differences between mice resilient to the stress exposure (R+) and mice that developed stress-induced pathologies (R-). For this purpose, we perfused a few mice that were classified into the R+ or R- phenotype according to behavioral criteria and prepared the brains for immunostaining. Several regions involved in the stress response and PTSD, such as the hippocampus, the amygdala and the nucleus accumbens (NAc), were analyzed by counting the total number of GFP+ nuclei (i.e. neurons activated due to the trauma exposure) in respective brain sections.

As a consequence of its role in information processing, the hippocampus is functionally a very heterogeneous structure within the brain [265,266,382]. Due to this reason, we decided to analyze the degree of neuronal activity in R+ and R- mice along the longitudinal axis of the hippocampus (Figure 44D and E) and within different hippocampal subregions. Our analysis revealed increased neuronal activity in the hippocampi of R- mice when compared to R+ animals (Figure 44A). This difference in the number of GFP+ nuclei was

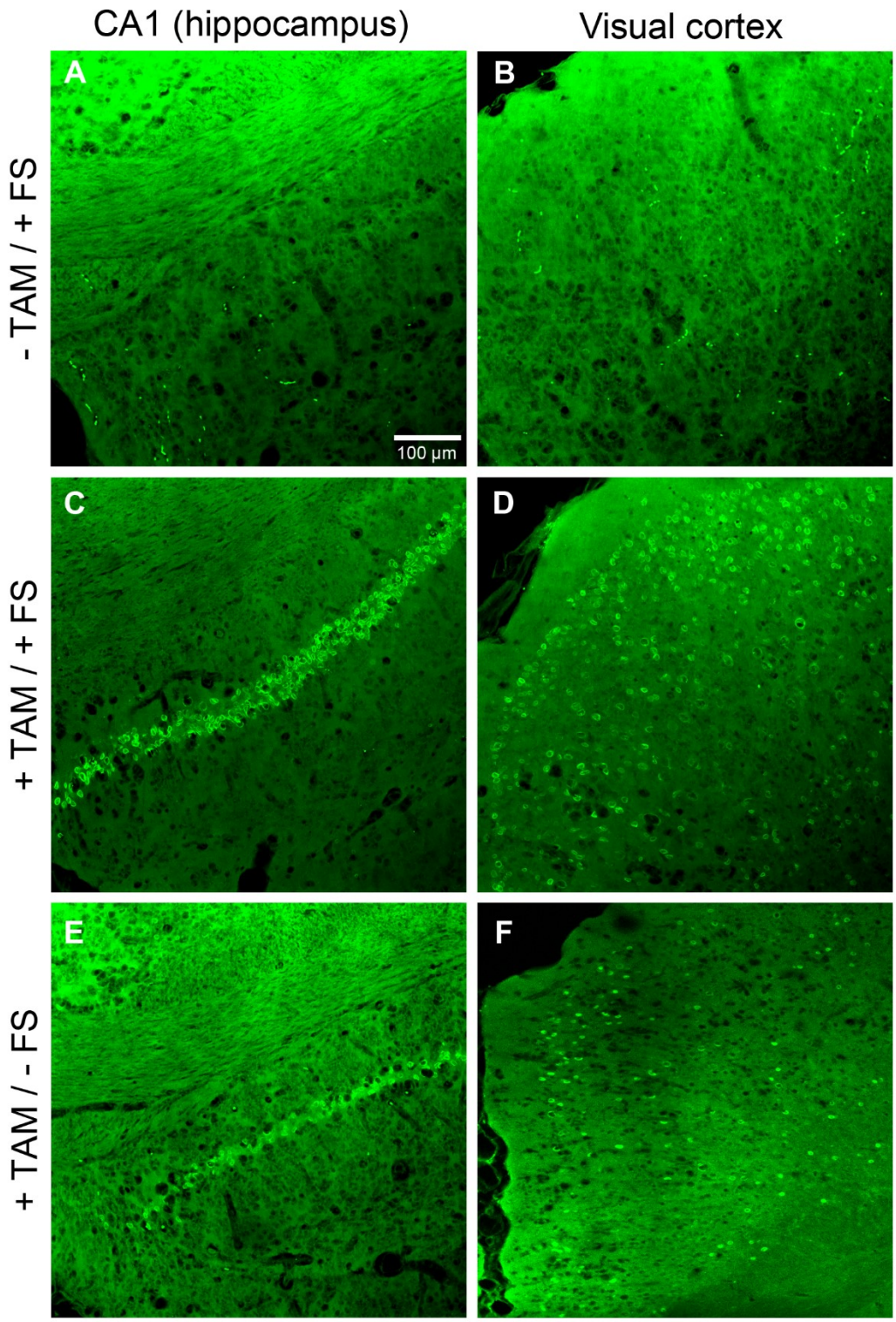

Figure 43. Tamoxifen and neuronal activity are necessary for nuclear GFP expression. To induce the expression of GFP in the nuclear membrane of activated neurons, the presence of tamoxifen (TAM) is necessary. Moreover, to induce GFP expression in a significant population of cells, a strong stimulus, e.g. foot-shock (FS), is also required. **(A-B)** GFP immunostaining of the CA1 hippocampal area and visual cortex from mice exposed to FS but without TAM. **(C-D)** GFP immunostaining of the CA1 hippocampal area and visual cortex from mice exposed to FS and injected with TAM. **(E-F)** GFP immunostaining of the CA1 hippocampal area and visual cortex from mice exposed to a new environment without FS but injected with TAM. Bars indicate 100 µm and the scale is the same for all images. All images were done with 20x magnification.

found to have an origin mainly in the CA1 area, and to a lesser extent in the CA3 subregion, but not in the DG (Figure 44B). Next, we analyzed the hippocampal subregions at their anterior and posterior sides to search for possible differences along the hippocampal long axis. The increased number of GFP+ nuclei found in the hippocampi of R- mice was also observed in the anterior and posterior sides of the CA1 subregion, but only in the posterior side of the CA3 area (Figure 44C). Unfortunately, these differences did not reach statistical significance. Interestingly, the neuronal activity induced by the traumatic experience was the lowest in the CA3 area, when compared to the CA1 and the DG, with less than half of the number of GFP+ nuclei than the other hippocampal subfields analyzed.

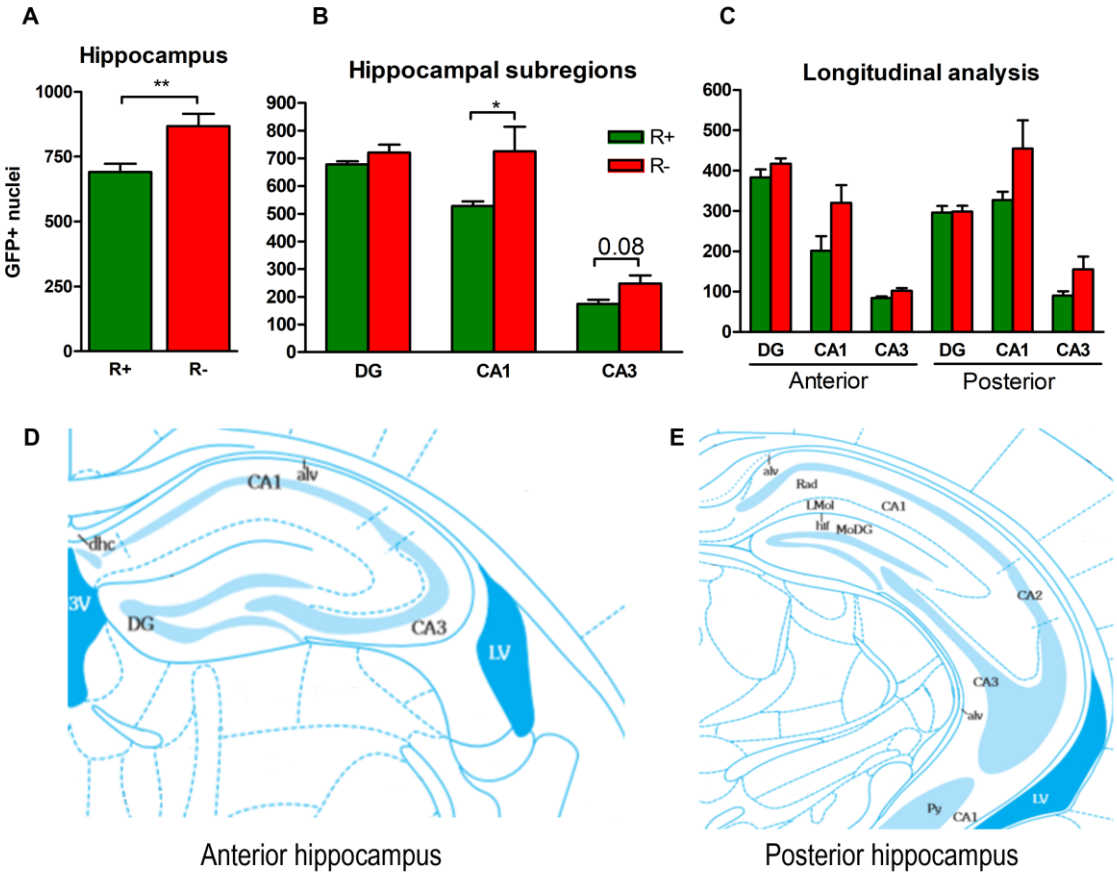

Figure 44. Number of hippocampal GFP+ nuclei in R+ and R- animals. Representative images of the anterior and posterior area of the mouse hippocampus and associated graphs showing the number of GFP+ nuclei counted in each of the hippocampal subregions. The number of positive events was calculated by counting 3 Z-stacks images (16 planes, 2 µm thick) from each replicate. For this experiment, 2 R+ and 3 R- mice were used. **(A)** Bar graph representing the total number of GFP+ nuclei found in the hippocampi of R+ and R- mice. **(B)** Bar graph showing the number of GFP+ nuclei of each phenotype in each of the different hippocampal subregions. **(C)** Bar graph showing the longitudinal differences in the number of GFP+ nuclei for each hippocampal subregion. **(D)** Representative image of the anterior hippocampus and its subregions. **(E)** Representative image of the posterior hippocampus and its subregions. P-values were calculated by performing an unpaired two-way ANOVA with Bonferroni post-test. Bar graphs represent mean ± s.e.m. *, $p<0.05$; **, $p<0.01$.

Additionally to the hippocampus, we also analyzed two other regions that are deeply involved in stress-related disorders: the amygdala (Figure 45C) and the nucleus accumbens (NAc) (Figure 45D). The amygdala is a brain structure that belongs to the limbic system and has a primary role in the processing of memory, decision-making and emotional responses [383,384], whereas the NAc is part of the mesolimbic pathway and is involved in motivation, aversion (including fear), reward and reinforcement [385,386]. These brain regions also modulate the behavioral and physiological response to threats or stressors, so they have lately gained attention in stress resilience and susceptibility research.

Both the amygdala and the NAc showed a lower number of GFP+ nuclei in comparison with the hippocampus. Furthermore, there were no apparent differences between R+ and R- mice in any of the subregions of the NAc, although R- animals had slightly more GFP+ nuclei altogether (Figure 45B). The same observation was done in amygdala, where R- showed a slightly increased total number of GFP+ nuclei than their R+ counterparts (data not shown). However, there were differences between both phenotypes in each of the subregions of the amygdala (Figure 45A). Trauma-induced neuronal activity appeared to be increased in the central amygdala (CeA) of R- mice when compared to the R+ phenotype, although the difference was close to statistical significance ($p \sim 0.07$). As the CeA is the main output center of the amygdala, an aberrant pattern of neuronal activity could dysregulate other brain regions involved in stress and fear processing and cause maladaptive behaviors. Interestingly, R+ mice showed a slight increase in the number of GFP+ nuclei in the basolateral amygdala (BLA), the main input center of this brain region, although this difference was not statistically significant.

4.4.5 Characterization of the lipidome of R+ and R- animals

Lipidomic profiling from brain samples

During the extraction of RNA from brain samples, we purified simultaneously the lipids contained in the same brain regions. From the whole set of lipid molecules that conform the brain lipidome, we focused on eCBs and related molecules, phospholipids (PL), and polyunsaturated fatty acids (PUFA) for this study given their relevance in psychiatric disorders and as potential biomarkers [387–390]. We analyzed the dorsal region of the DG and CA area within the hippocampus, and the PFC, as all of them are relevant brain regions involved in stress and resilience processes.

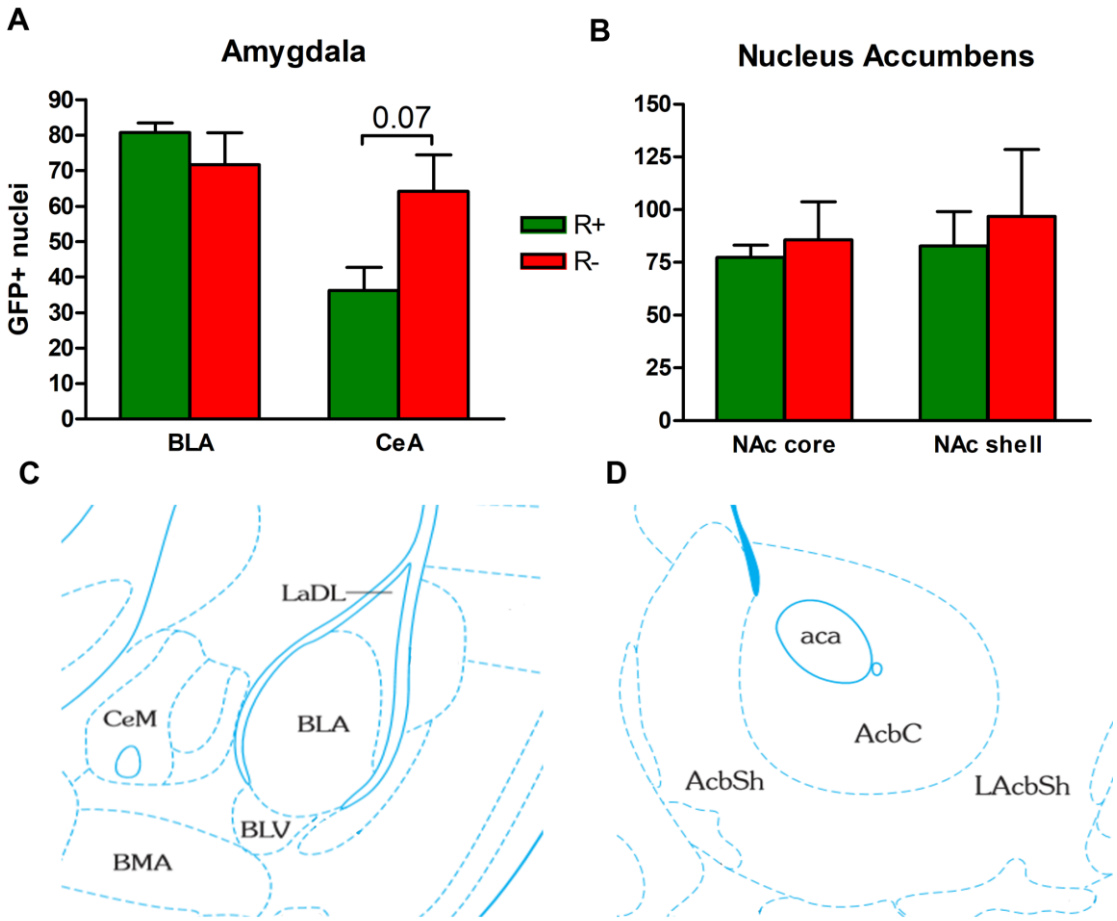

Figure 45. Number of GFP+ nuclei in the amygdala and the nucleus accumbens (NAc). Representative images of the NAc and amygdala, as well as the associated graphs showing the number of GFP+ nuclei counted in each of the brain regions. The number of positive events was calculated by counting 3 Z-stacks images (16 planes, 2 µm thick) from each replicate. For this experiment, 2 R+ and 3 R- mice were used. **(A)** Bar graph representing the number of GFP+ nuclei found for the different phenotypes in the basolateral amygdala (BLA) and the central amygdala (CeA), two major subregions of the amygdala. **(B)** Bar graph showing the number of GFP+ nuclei found for each phenotype in the core and shell subregions of the NAc. **(C)** Representative image of the amygdala and its 2 main subregions: the BLA (LaDL + BLA + BLV) and the CeA (CeL + CeC + CeM). **(D)** Representative image of the NAc and its two main subregions: the core (AcbC) and the shell (AcbSh + LAcbSh). P-values were calculated by performing an unpaired two-way ANOVA with Bonferroni post-test. Bar graphs represent mean ± s.e.m.

We observed the highest number of statistical differences in the dorsal CA region of the hippocampus (Figure 46), when compared to other brain areas. Among the lipids that were found to be significantly different between R+ and R- mice, there were different species of phosphatidylcholine (PC), phosphatidylglycerol (PG) and phosphatidylethanolamine (PE) which were increased in R- mice as compared to R+ animals (Figure 46A, B, E). Moreover, lysophosphatidic acid 20:4 (LPA) was also shown to be increased in R- replicates, although the difference in this case was only close to statistical significance (Figure 46F). On the other hand, some lipid species were

increased in R+ mice, such as sphingomyelin (SM) 34:1 and sphingosine-1-phosphate (S1P) (Figure 46C, D).

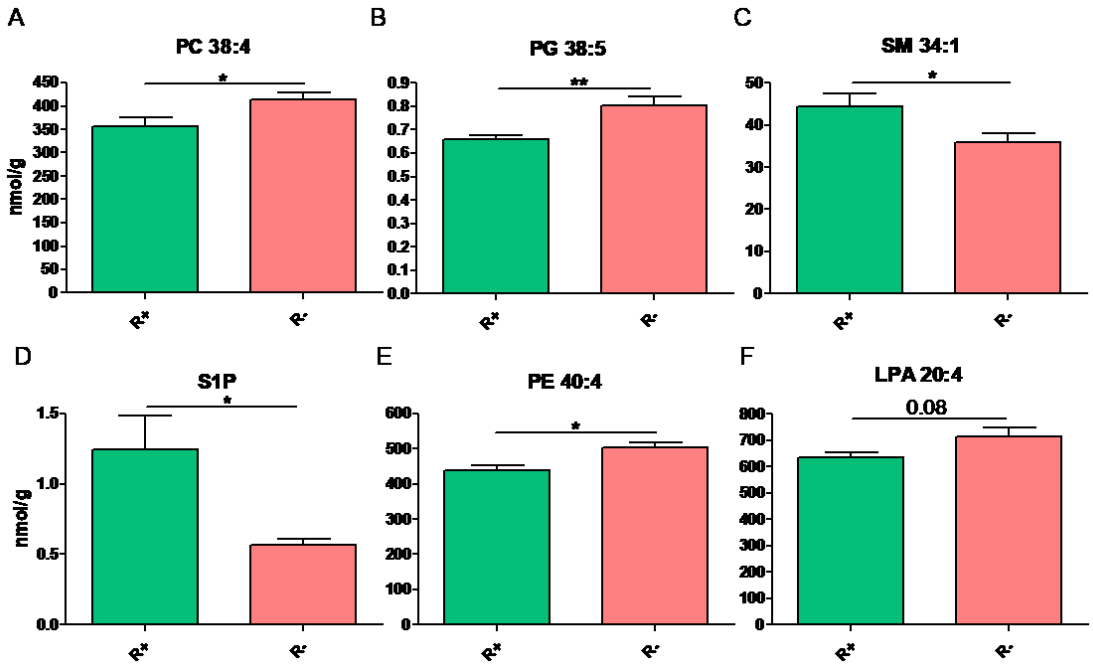

Figure 46. Levels of different phospholipids (PL) in the dorsal CA region of the hippocampus. From all the lipids that were measured, these species were found to be statistically significant (or close to) between R+ and R- mice only in the dorsal CA area of the hippocampus. The abbreviations above each graph indicate the type of lipid, and the numbers correspond to the number of carbon atoms and double bonds, respectively. **(A)** Concentration of phosphatidylcholine (PC) 38:4. **(B)** Levels of phosphatidylglycerol (PG) 38:5. **(C)** Concentration of sphingomyelin (SM) 34:1. **(D)** Levels of sphingosine-1-phosphate (S1P). **(E)** Concentration of phosphatidylethanolamine (PE) 40:4. **(F)** Levels of lysophosphatidic acid (LPA) 20:4. Bar graphs represent mean ± s.e.m. P-values were calculated using unpaired double-sided t-test. *, $p<0.05$; **, $p<0.01$. 6 replicates per group.

Several lipids also showed significant differences between R+ and R- mice in the dorsal DG (Figure 47C). Interestingly, our results revealed that PG 38:5 and PE 40:4 were also dysregulated in this brain region (Figure 47C, E). However, the concentration of lipid molecules was increased in R+ mice unlike in the CA area, where R- animals showed the highest levels, although the differences in PE 40:4 levels did not reach statistical significance. Additionally, two different species of phosphatidylserine (PS) and one lipid species of lysophosphatidylinositol (LPI) were found to be increased in R+ mice as compared to R- animals (Figure 47A, B, D). Lastly, there were differences between R+ and R- mice in one species of phosphatidylinositol (PI), although they were not statistically significant (Figure 47F).

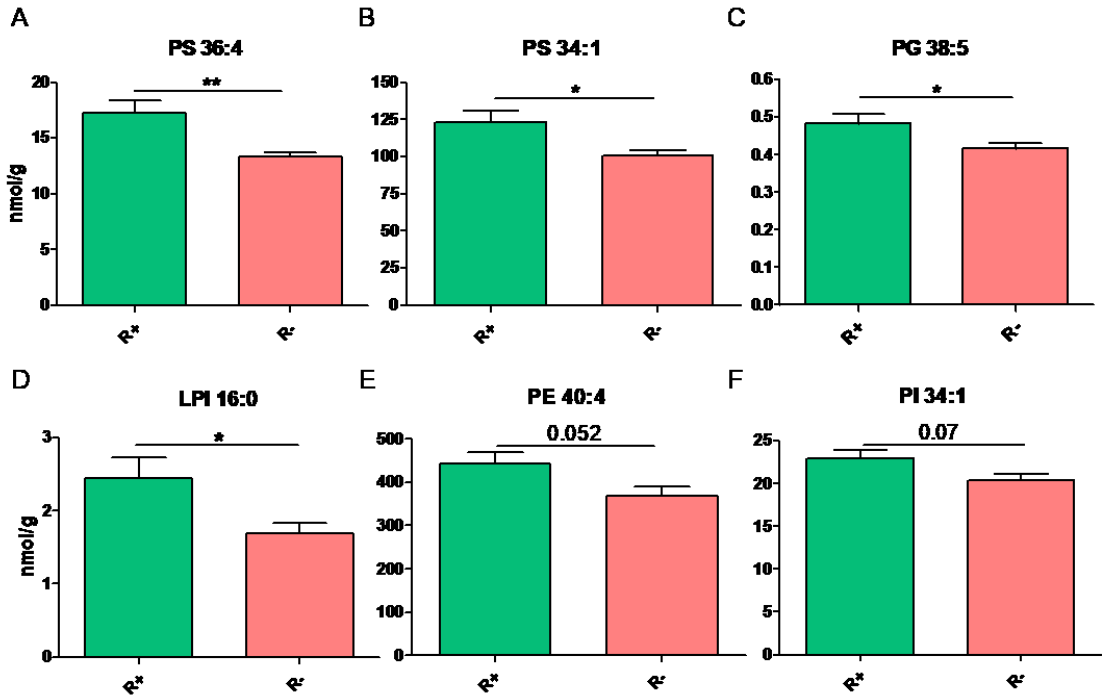

Figure 47. Concentration of different phospholipids (PL) in the dorsal DG of R+ and R- mice. From all the lipids that were measured, these species were found to be statistically significant (or close to) between R+ and R- mice only in the dorsal DG. The letters above each graph indicate the type of lipid, whereas the numbers correspond to the number of carbon atoms and double bonds, respectively. **(A-B)** Concentration of the species of phosphatidylserine (PS) 36:4 and 34:1. **(C)** Levels of phosphatidylglycerol (PG) 38:5. **(D)** Concentration of lysophosphatidylinositol (LPI) 16:0. **(E)** Levels of phosphatidylethanolamine (PE) 40:4. **(F)** Levels of phosphatidylinositol (PI) 34:1. Bar graphs represent mean ± s.e.m. P-values were calculated using unpaired double-sided t-test. *, $p<0.05$; **, $p<0.01$. 6 replicates per group.

Our analysis of the lipidome in the PFC yielded no statistically significant differences between the R+ and R- groups (Figure 48). However, several lipids did show an apparent increase in R+ mice, such as ceramide (CER), lysophosphatidylcholine (LPC) 20:4 and LPI 16:0, although it did not reach statistical significance. Curiously, the variability within the R+ group appears to be higher than in other brain regions, and it could explain that no statistical significance was found between groups.

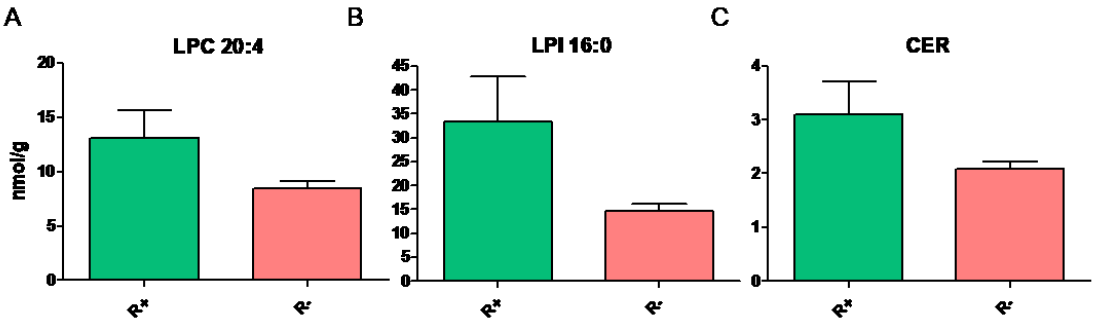

Figure 48. Concentration of different phospholipids (PL) in the PFC of R+ and R- mice. Representative lipids that showed differences in the PFC of R+ and R- animals, although they were not statistically significant. The letters above each graph indicate the type of lipid, whereas the numbers correspond to the number of carbon atoms and double bonds,

respectively. **(A)** Concentration of lysophosphatidylcholine (LPC) 20:4. **(B)** Levels of lysophosphatidylinositol (LPI) 16:0. **(C)** Concentration of ceramide (CER) in the PFC. Bar graphs represent mean ± s.e.m. 6 replicates per group.

Additionally to the phospholipids, we also measured the concentration of the major eCBs, e.g. AEA and 2-AG, and of arachidonic acid (AA), a lipid involved in eCB metabolism (Figure 49). There were no differences between groups for 2-AG or AA in any of the brain regions analyzed. In the case of AEA, R- animals showed increased levels when compared to R+ mice in the PFC (Figure 49A), but not in the dorsal DG or CA. Interestingly, the levels of AEA in the PFC were much reduced in comparison to the other regions analyzed. However, the concentration of 2-AG and AA remained very similar across the different brain regions. Lastly, we analyzed the ratio between AEA and 2-AG, because imbalances between both molecules might disrupt the proper functioning of the ECS. Yet, there were no differences between R+ and R- phenotypes in any of the brain regions analyzed.

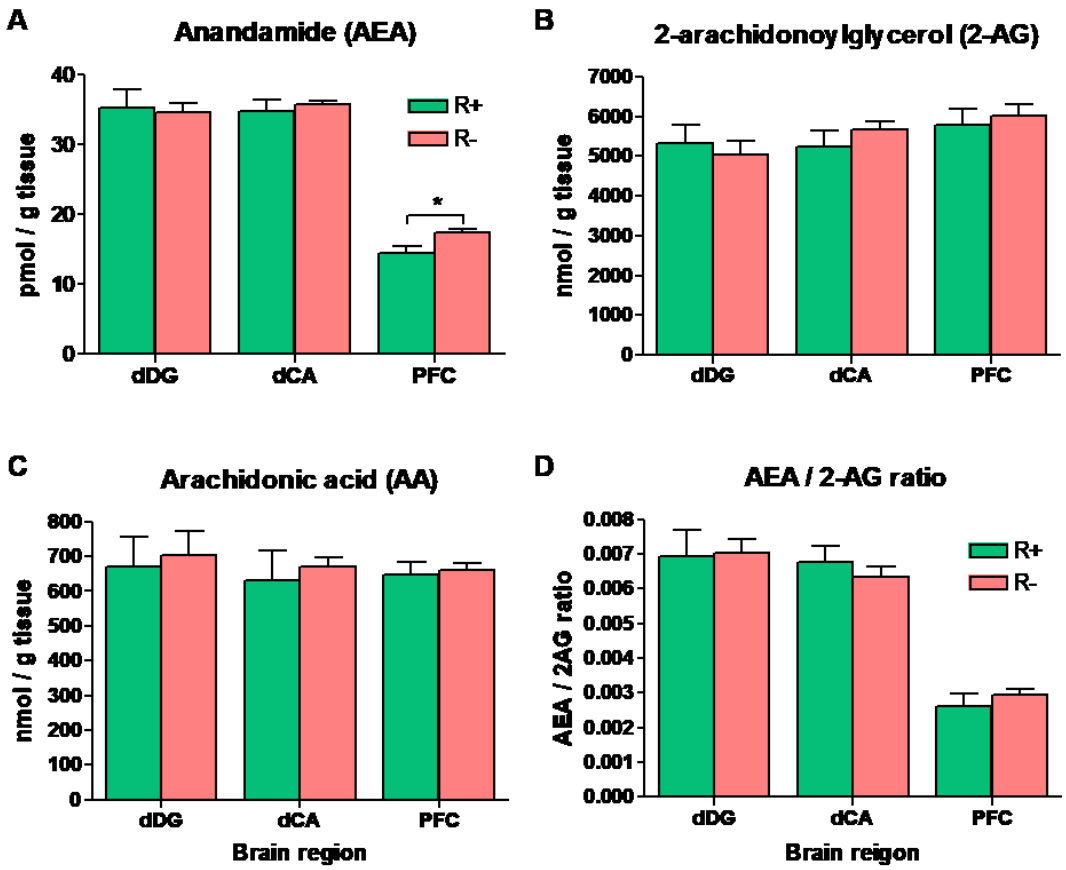

Figure 49. Concentration of eCBs and AA in different brain regions. Representative lipids that showed differences in the PFC of R+ and R- animals, although they were not statistically significant. **(A)** Concentration of anandamide (AEA), one of the major eCBs, in the analyzed brain regions. **(B)** Levels of 2-AG, another major eCB, in different brain regions. **(C)** Concentration of AA, a precursor and by-product of eCB metabolism. **(D)** Ratio between AEA and 2-AG as a measurement of correct ECS function. Bar graphs represent mean ± s.e.m. P-values were calculated using unpaired t-test. *, $p<0.05$. 6 replicates per group.

Lipid analysis from blood samples

Additionally to the characterization of different brain regions, we analyzed blood samples from R+ and R- mice taken at different time points before and after the traumatic exposure. Blood sampling provides insights into parameters of the internal physiology of the animal and are useful to confirm different pathologies, as they are cheap, efficient and basically non-invasive. However, we focused in our study on searching for molecules that could potentially hold predictive value in PTSD. Hence, we analyzed the blood levels of the major eCBs (Figure 50), as well as AA and palmitoylethanolamide (PEA), a non-cannabinergic derivative of AEA (Figure 51), before (T0) and after (T1 and T2) the exposure to the trauma.

We observed significant changes in eCB levels between +FS and –FS groups, as well as between the R+ and R- phenotypes, in contrast to our lipid analysis of different brain regions. The concentration of AEA increased gradually with time for both +FS and –FS groups (Figure 50C), whereas the levels of 2-AG increased right after the trauma (T1) but were reduced almost to the pre-trauma levels after 2 weeks (T2). There were no statistical differences between the +FS and –FS groups for both molecules at any time point. The ratio between AEA and 2-AG (Figure 50A) was also very similar between groups across the different extraction times.

The comparison between the circulating levels of eCBs of the R+ and R- phenotypes revealed some interesting observations. Although the gradual increase in the concentration of AEA could be observed in both subgroups, R- mice had increased levels of AEA when compared to R+ individuals after trauma (Figure 50D). Moreover, the highest difference was found right after trauma, although it was only close to significance (p-value = 0.06). On the other hand, the concentration of 2-AG remained very stable for R- mice across time, whereas the R+ phenotype had significantly increased levels of 2-AG right after the trauma, but not at later time points (Figure 50F). This is indeed a very interesting observation, as 2-AG has been associated to increased stress resilience [391,392]. Furthermore, the eCB balance, or ratio between AEA and 2-AG (Figure 50B), was found to be significantly different between R+ and R- mice only after trauma. Surprisingly, these differences remained 3 weeks after the traumatic experience, which indicates that the ratio between AEA and 2-AG could potentially predict the resilience status of trauma-exposed individuals.

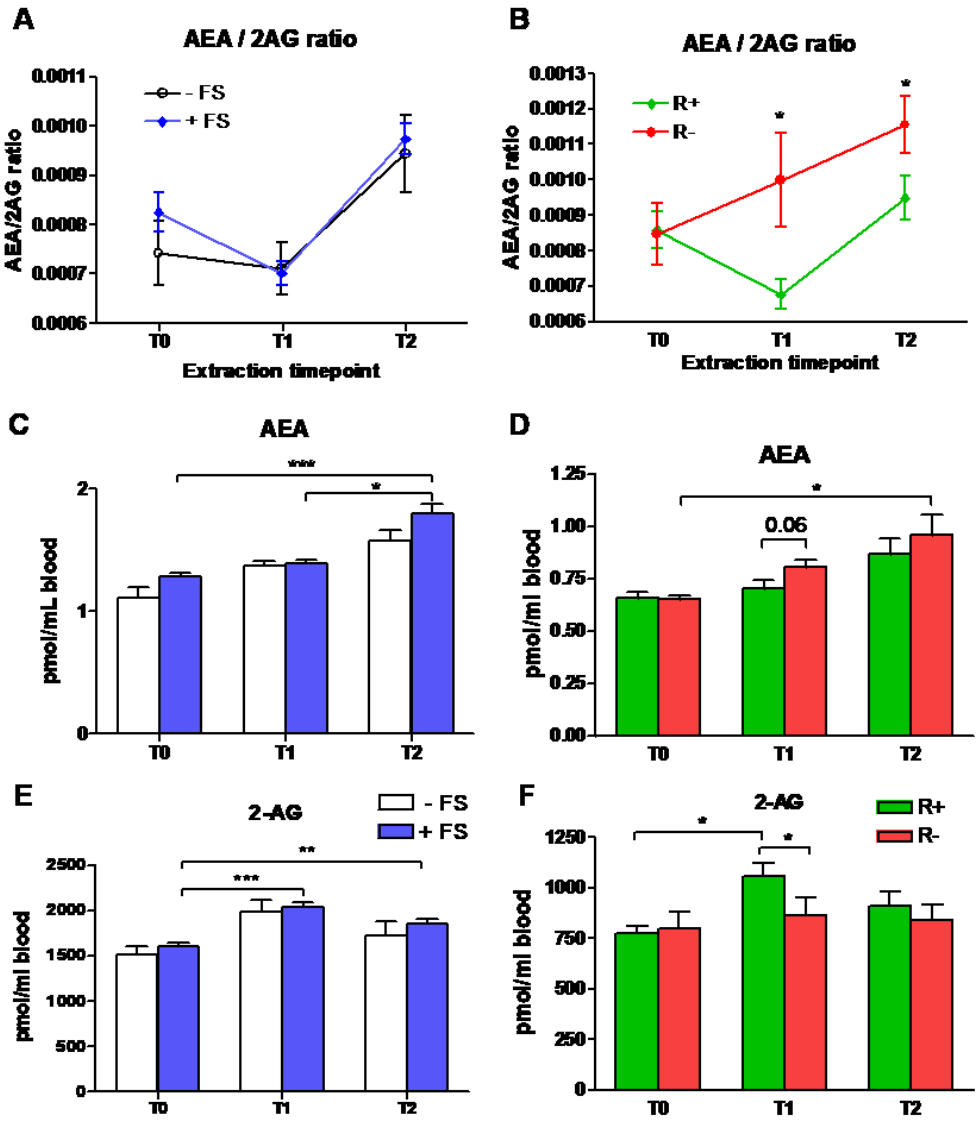

Figure 50. Concentration of the major eCBs in plasma during the development of PTSD. Circulating levels of AEA and 2-AG were measured using liquid chromatography-mass spectrometry. Samples were collected on dried blood spots, from where the lipids were extracted at a later time point. **(A-B)** Ratio between AEA and 2-AG in before and after applying the behavioral profiling criteria to the +FS group. **(C-D)** Concentration of AEA in blood before and after classifying the mice into R+ and R- phenotypes. **(E-F)** Circulating levels of 2-AG before and after applying the behavioral profiling criteria to the +FS group. Bars show mean ±s.e.m. P-values were calculated using two-way ANOVA analysis (including repeated measurements) with Bonferroni post-test. *, p<0.05; **, p<0.01; ***, p<0.001. 6 replicates per group.

The analysis of AA and PEA showed very stable circulating levels of these two molecules across the different time points (Figure 51), although with small fluctuations. Moreover, there were no differences between the +FS and –FS groups, or between the R+ and R- phenotypes in any of the measured time points.

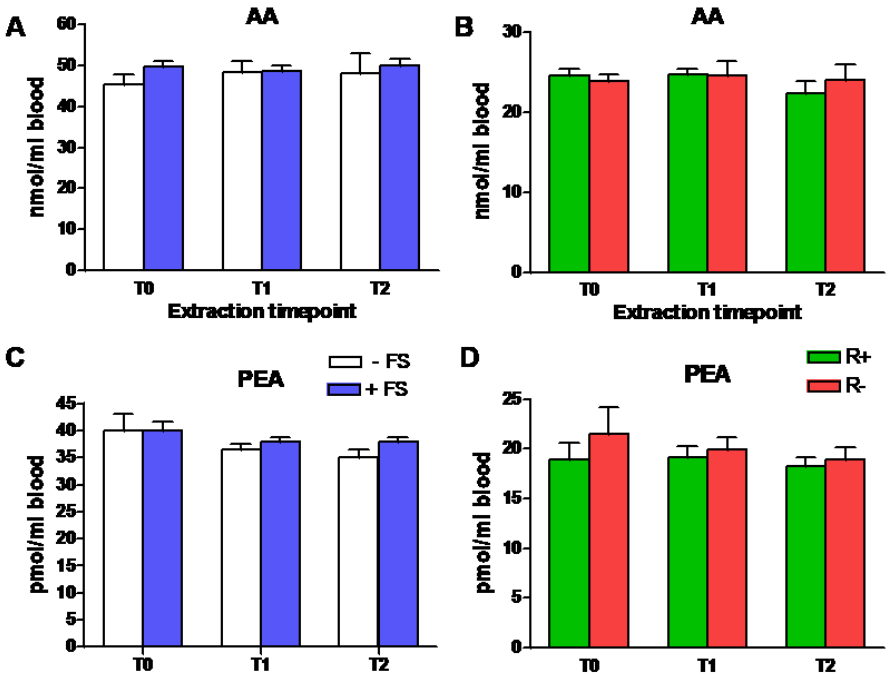

Figure 51. Circulating levels of AA and PEA during the development of PTSD. Blood levels of AA and PEA were measured using liquid chromatography-mass spectrometry methods after extracting all lipid molecules from dried blood spots. In contrast to the eCBs, there were no strong differences across time or between groups. **(A-B)** Circulating levels of AA before and after classifying trauma-exposed mice into their respective behavioral phenotypes. **(C-D)** Circulating levels of PEA before and after the behavioral profiling, which differentiated the +FS group into different behavioral phenotypes. Bars show mean ±s.e.m. P-values were calculated using two-way ANOVA analysis with Bonferroni post-test. 6 replicates per group.

4.4.6 Characterization of the gut microbiome

The analysis of the gut microbiome focuses on studying both the diversity and the abundance of the different microbial species that reside within the gut lumen. These two factors have been associated in different studies to obesity [393,394], metabolic disorders [395,396] and behavioral deficits [397,398], among other pathologies. The diversity of the gut microbial community can be estimated by calculating the alpha-diversity, which accounts for the richness and evenness of the different operational taxonomical units (OTUs), and the beta-diversity, which analyzes the taxonomical abundance profiles between different samples.

Alpha-diversity is usually estimated by analyzing two different indices: the Chao1 index to estimate richness, i.e. the total amount of OTUs present in the sample, and the Shannon index to estimate evenness, i.e. how evenly each OTU is represented (Figure 52A, B). The variability within each group and time point was relatively high, although the R- phenotype showed the lowest variability. This observation could explain the lack of statistical differences between R+ and R- mice, and between different time points, in any of the indices. This result was nevertheless expected, as significant changes in alpha-diversity would reflect a drastic redistribution of the composition of the gut

microbiome, which can usually be accomplished only by direct interventions (e.g. antibiotic or probiotic treatment, among others) and not by a single stress exposure.

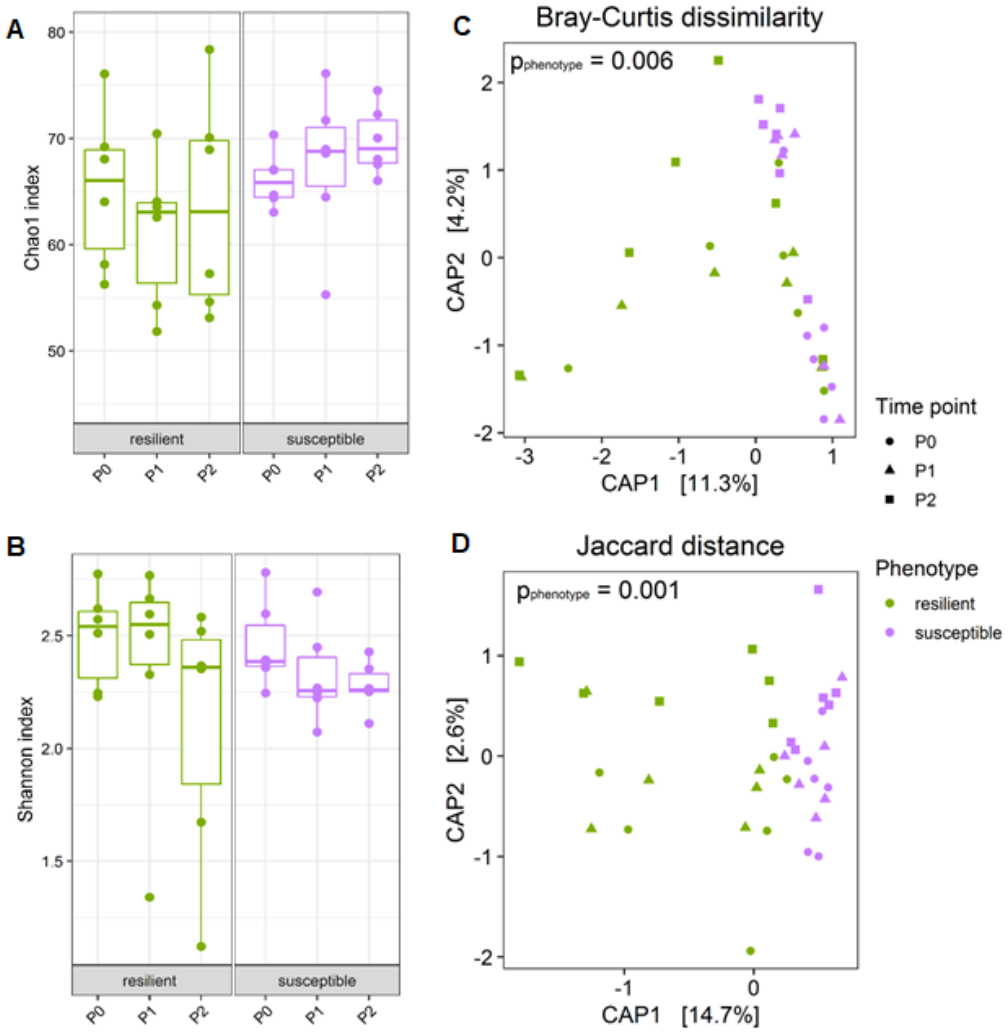

Figure 52. Diversity indices from microbiome samples of R+ and R- mice. Alpha-diversity is used to estimate the richness and evenness of the microbial community within one sample, whereas Beta-diversity estimates the difference in taxonomic abundance between different samples. **(A)** Boxplot showing the Chao1 index, which accounts for the richness, or number of OTUs, of one sample. **(B)** Distance map showing Bray-Curtis dissimilarity, which calculates the difference in microbial abundance, or read count, of different OTUs. **(C)** Boxplot showing the Shannon index, which indicates the evenness of OTUs, or how the different OTUs are distributed, in one sample. **(D)** Distance map showing Jaccard distance, based on the presence or absence of OTUs without using any information on the abundance, therefore providing information about the differences in microbial composition between two samples. 6 replicates per group and time point.

Beta-diversity is normally estimated using also two different parameters: the Bray-Curtis dissimilarity, which calculates the differences in microbial abundance, and the Jaccard distance, which is solely based on the presence or not of OTUs (Figure 52C and D). The analysis of beta-diversity was constrained, meaning both the experimental group and sampling time were considered when calculating distances between samples. The Bray-Curtis dissimilarity showed both phenotypes overlapping each other. Interestingly,

samples from the R- group were more closely grouped than those of the R+ group. Furthermore, R- samples clustered in two distinct subgroups and, very surprisingly, one of these subgroups appeared to correlate with the time point P0 (pre-trauma), as it contained 5 out of the 6 R- individuals. On the other hand, the Jaccard distance showed samples from the R+ and R- phenotypes grouped and without overlap, although both clusters were extremely close to each other. Once again, the R- group was more tightly packed, but without signs of any subcluster. A permutational analysis of variance revealed a strong effect of the phenotype on the distribution of the data, which adds validity to our behavioral profiling. This significance was not present when the dataset was analyzed in a longitudinal manner, i.e. across time points.

Next, we performed a differential analysis of the abundance of the different OTUs. At the phylum level, we found time or group differences in 3 phyla: Bacteroidetes (Figure 53A), Proteobacteria (Figure 53B) and Deferribacteres (Figure 53C). In the case of Bacteroidetes, both R+ and R- phenotypes saw a significant increase between the basal state (P0) and the last time point measured 3 weeks after the trauma (P2). Although the abundance of Bacteroidetes in the R- phenotype appeared to be reduced compared to the R+ group, there was no statistical significance. The abundance of Proteobacteria significantly increased after the trauma (P1) in the R+ phenotype compared to P0, and decreased to almost basal levels at P2. There were also statistical differences between R+ and R- mice at the time points P0 and P1 for this phylum. Interestingly, the abundance of Proteobacteria in the R- phenotype seemed to increase gradually along the experiment. Contrary to this observation, the abundance of Deferribacteres in the R- group decreased gradually with time and there were statistical differences between the abundance of this phylum at P0 and at P2.

There were also differences at deeper taxonomic levels between the R+ and R- phenotypes (Figure 54). The abundance of different OTUs was significantly different at specific time points, although some of these OTUs were also close to significance at additional time points. In the basal state (P0) (Figure 54A), R- mice lacked *Akkermansia muciniphila*, one of the main bacteria that influences the gut mucosa. Interestingly, a reduction in the relative abundance of this species has been associated with a susceptible phenotype after chronic social defeat [399].

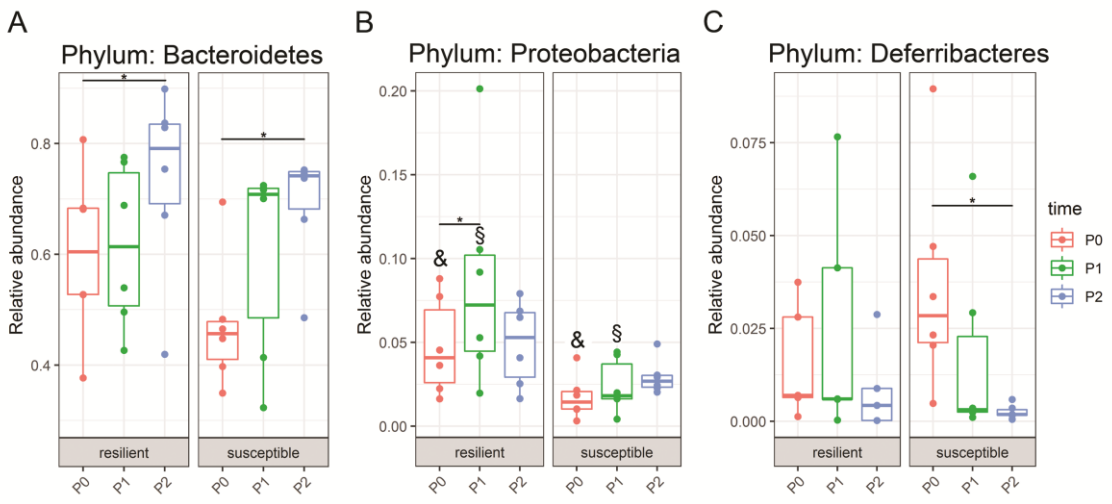

Figure 53. Relative abundance of different OTUs at the phylum level. Bioinformatic analysis of the 16S sequencing data shows 3 OTUs with statistically significant differences at the phylum level. **(A)** Boxplot showing the different experimental groups and time points for the phylum Bacteroidetes. **(B)** Boxplot showing the different experimental groups and time points for the phylum Proteobacteria. Letters indicate statistical significance across different phenotypes. & and § indicate statistical differences between R+ (resilient) and R- (susceptible) groups at different time points. **(C)** Boxplot showing the different experimental groups and time points for the phylum Deferribacteres. *, $p<0.05$. 6 replicates per group and time point.

Mice associated to a R- phenotype also had a higher relative abundance of the family Ruminococcaceae, part of the order Clostridiales, and deeply involved in homeostatic processes within the gut lumen [400]. Interestingly, there was also an increase in the abundance of *Anaerofustis stercorihominis* (Figure 54B) and the genus *Lactobacillus* (Figure 54C) at P1 and P2, respectively, in R- mice. Bacteria from the genus *Anaerofustis* have been correlated to a susceptible phenotype [401]. The same study showed an increase in the abundance of *Lactobacillus* in mice vulnerable to stress, although previous studies have shown this genus to be decreased in mice showing despair behavior upon exposure to chronic stress [149].

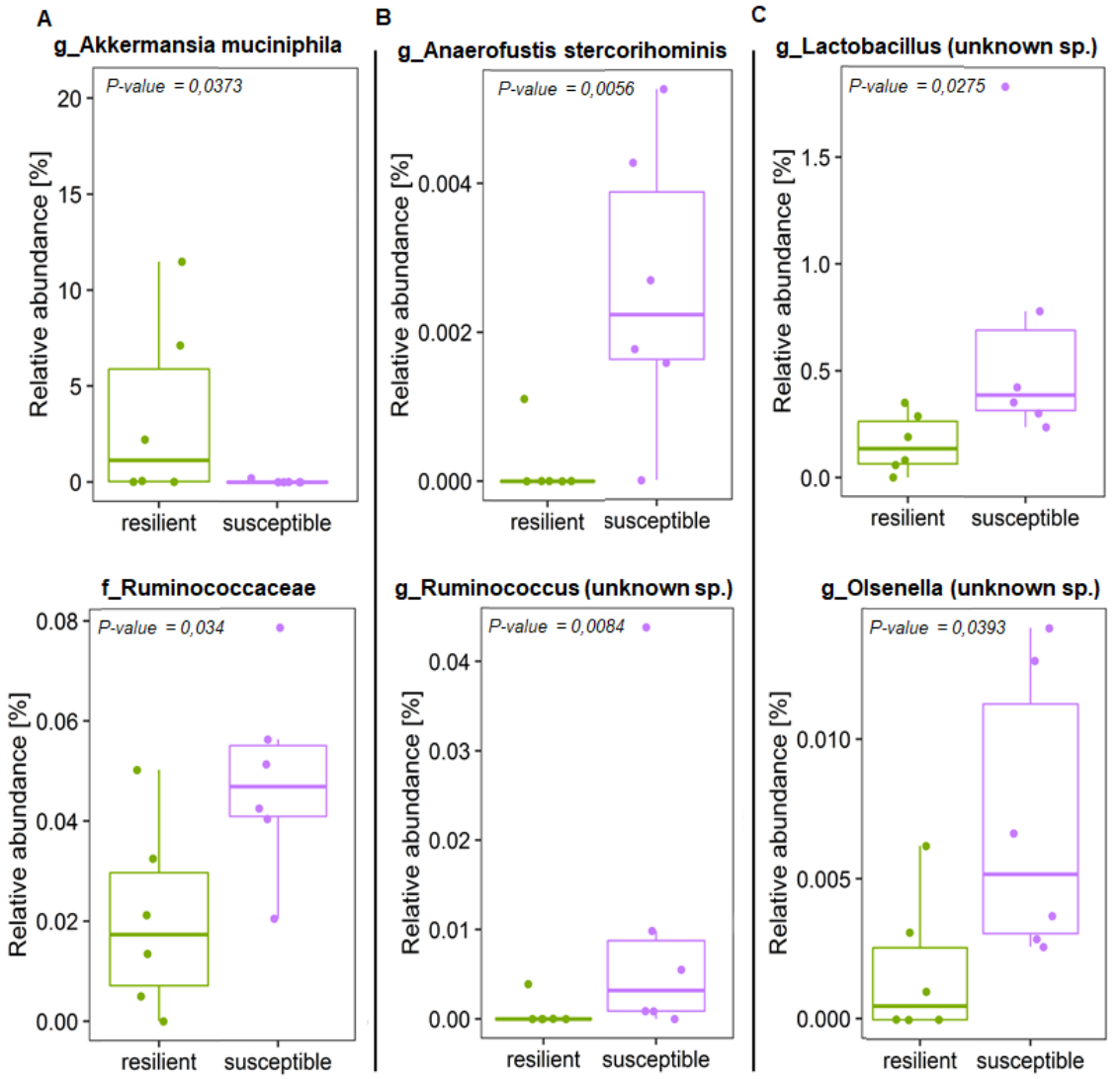

Figure 54. Differential abundance of OTUs in R+ and R- animals at different time points. Boxplots representing the relative abundance of different OTUs for which statistical differences were found between the R+ and R- phenotypes. The letters before the names of each graph indicate the taxonomical level of the word to which they are connected: g (genus), f (family). P-values for each specific OTU are shown on the top left corner of each graph. **(A)** Boxplots showing two OTUs that were significantly different at P0. **(B)** Boxplot showing examples of differentially abundant OTU at P1. **(C)** Boxplot representing the difference in abundance between R+ and R- mice at P2 for different OTUs. 6 replicates per group.

4.5 Discussion

Stress is a natural mechanism that promotes adaptability and survival upon encountering threats in an ever-changing environment. The stress response induces a transient shift of homeostasis that alters the internal physiology and metabolism of the organism, in order to quickly mobilize resources to promote either an adequate response to the challenge. However, the chronification and/or dysregulation of the stress response can originate serious disorders and the appearance of maladaptive behaviors, which cause severe impairments in the individual´s mental health and daily life. Despite the relevance and prevalence of trauma-induced disorders, their neurobiological basis remains poorly understood.

One of the challenges to study stress-related disorders resides in the difficulty to model the pathology using animal models, as individual factors, past experiences and the stressor itself have a strong influence over the outcome of mental health disorders.

PTSD, a trauma-induced disorder, is especially complicated to model, as the maladaptive behaviors must be present in the long term (4+ weeks) and the individual responses must widely scatter, as observed in human PTSD patients [297]. Furthermore, PTSD appears often co-morbidly with other disorders and, thus, its symptoms are very variable across patients.

We developed a single trauma model that induces long term behavioral maladaptations and the dispersion of the individual outcomes in trauma-exposed mice. This scattering of the data appeared in all the behavioral paradigms that were tested. Moreover, a single exposure to a traumatic experience (strong foot-shock) was sufficient to induce higher levels of anxiety, and a stronger and generalized fear memory, both common symptoms of PTSD [402].

The behavioral data suggests that our PTSD-like model effectively induces long-term dysregulations and maladaptive behaviors upon a single exposure to a traumatic experience. Furthermore, the individual behavioral responses of trauma-exposed animals scatter widely, which resembles the human pathology. With the adequate behavioral characterization, our model can provide a comprehensive basis to study the spectrum of PTSD endophenotypes.

After a traumatic event, most individuals develop some form of stress-related disorder for a few days or weeks while they integrate and cope with the emotional information of the experience. However, only about 10-20% of the affected population develops PTSD, depending on the type of trauma and socioeconomic factors related to the trauma-exposed individuals [403]. This ability to cope with the trauma, i.e. stress resilience,

depends on a myriad of genetic, socioeconomic, and psychological factors that are still not fully explored or understood. Therefore, the resilience or susceptibility of an individual towards stress is unique. We hypothesized then that brain homeostasis may influence the outcome after experiencing traumatic or stressful experiences.

Despite the current focus on stress resilience, there is still no clear consensus on the definition of the resilient or susceptible phenotypes. One of the most common strategies to classify trauma-exposed animals involve studying a naïve control group once to establish cut-off values. These thresholds are then applied to successive batches of stressed animals in usually just one behavioral test. Although the basic idea behind this approach is correct, applying it just to one or two behavioral paradigms does not reflect the symptomatic complexity and heterogeneity of stress-related pathologies. Therefore, we chose to perform an exhaustive behavioral profiling comprising enough behavioral paradigms to represent most of the symptomatic panel of human PTSD patients. We selected six distinct behavioral tests to evaluate core PTSD symptoms (e.g. hyperarousal, generalized fear and a strong fear memory) and other symptoms that are often, but not always, observed in PTSD patients (anxiety, anhedonia and impaired sociability).

Our criteria for behavioral profiling clearly revealed two distinct subgroups within the trauma-exposed mice. On one hand, the subgroup defined as resilient (R+) showed no statistical differences with the control no trauma-exposed group in any of the behaviors that were measured, which indicates a similar behavior in spite of the trauma suffered by the resilient animals. On the other hand, the subgroup defined as susceptible (R-) showed strong differences only in paradigms associated to the core symptoms of PTSD (e.g. ASR, CF and generalized fear), whereas these differences were not statistically significant for the rest of the paradigms. This lack of statistical significance could be explained by the comorbid and variable nature of the symptoms that these paradigms represent (e.g. anxiety, anhedonia, and impaired sociability). However, these paradigms could define different endophenotypes within the R+ and R- subgroups, provided that a sufficiently large cohort of individuals is used. Although the number of mice used in this study is relatively low, this project serves as a proof of concept and offers an alternative method for the research of trauma-induced disorders, as well as the resilient and susceptible phenotypes that arise as a consequence.

Lipids have been shown to play an increasingly recognized role in the CNS. Most of the brain lipids can be found in the plasma membrane, where they regulate the localization and function of membrane proteins and, thus, modulate synaptic output in specific

neuronal populations and brain regions. Furthermore, membrane lipids also act as both intracellular and extracellular messengers and modulate exo- and endocytic processes [387,404].

Due to their relevance in brain function, we focused on two specific lipid classes, PLs and eCBs, to characterize part of the brain lipidome. Several PLs showed significant differences between R+ and R- mice and, interestingly, some of these molecules were also common between the different brain regions that were analyzed. R- animals showed significantly increased levels of PC (38:4), PG (38:5) and PE (40:4), whereas the increase of LPA (20:4) was close to statistical significance. Previous studies have shown that stress induces the synthesis of PC, PE and PG [405–407], thus, our data hints at potential pro-resilience strategies revolving around the normalization of these lipids. On the other hand, SM (34:1) and S1P levels were increased in the dorsal CA of R+ animals. These molecules have been correlated with increased homeostatic capacity [408], faster memory extinction [409] and are known to be reduced in neurodegenerative diseases [410,411]. Surprisingly, PG 38:5 and PE 40:4 also showed significantly different levels between groups in the dorsal DG, although in this brain region they were increased in the R+ phenotype, which highlights the heterogeneity of the hippocampal formation and its distinct subregions. Furthermore, PS species (36:4 and 34:1), known to exert neuroprotective effects towards cellular and chronic stress [412], and LPI (16:0), which has been linked to increased permeability of the blood-brain barrier through the action of GPR55 [413], were also increased in the DG of R+ mice. These results together suggest that there might be specific pro-resilience mechanisms involving phospholipids within the different hippocampal subregions.

Additionally to the dorsal CA and DG regions, we analyzed the lipid profile of the PFC, another important region in stress-related disorders and resilience processes. Unfortunately, no significant changes were found between R+ and R- mice in any of the molecules analyzed due to high variance, but our data suggest that some of the lipidic species could be statistically different by increasing the number of replicates or via dissection specific subregions of the PFC.

The ECS is involved in the stress response and the levels of eCBs are known to fluctuate upon exposure to different stressors (Morena et al. 2016, Dlugos et al. 2012). Furthermore, dysregulations in the eCB balance can modulate the symptomatology of stress-related disorders [341,415], which makes the ECS a good candidate to study stress-induced maladaptations and resilience processes.

Our analysis of circulating lipids revealed a stress-induced reduction in 2-AG levels in the R- phenotype when compared to R+ individuals, which could indicate a pro-resilience role for this molecule. Further studies should focus on whether restoring 2-AG levels could reduce the long-term effects of trauma exposure. Moreover, we showed that the ratio between AEA and 2-AG could be used as a predictive marker for the onset of stress-related disorders, although the differences were only significant after trauma. However, more research is required to confirm the predictive accuracy of this parameter. Additionally, the analysis of eCB levels in different brain regions six weeks after exposure to the traumatic experience showed differences only in the concentration of AEA in the PFC between R+ and R- mice. This observation suggests that the imbalance in eCB levels found shortly after trauma is not sustained in the long-term with our model, or that these changes do not originate in the brain regions we analyzed.

Although the study of the gut microbiome in the R+ and R- phenotypes did not show broad changes in microbial diversity, several taxa showed differences in abundance. The phylum Proteobacteria was significantly less abundant in R- mice than in R+ animals before and after the trauma. This phylum has been associated with an increased inflammatory state, both systemically and within the gut [416–418]. Increased inflammation is usually one of the consequences of an aberrant stress response and, as such, it is associated with the development of stress-related disorders. Therefore, our data might suggest a new pro-resilience effect of the phylum Proteobacteria. However, further research is needed to confirm whether members of this phylum can actually promote resilience to stress and, if yes, which specific microbes are responsible for this effect. We also observed significant differences in the abundance of various OTUs at deeper taxonomic levels. *Akkermansia muciniphila* is a bacterial species that showed differences in abundance across the different extraction time points. This bacterium is known to modulate the properties of the gut mucosa and, thus, to influence the microbiome´s environment and composition [419,420]. The lack of *A. muciniphila* in R- mice at P0 (pre-trauma) suggests a predisposition of these mice towards the pathological effects of stress, which would correlate with previous findings about the role of this bacterium in stress resilience [164,399]. Contrary to *A. muciniphila*, the increased abundance of the family Ruminococcaceae in R- individuals before the exposure to the trauma (P0) is indicative of a potential influence in the individual susceptibility to stress by members of this taxa. Post-trauma time points revealed significant differences in the abundance of *Anaerofustis stercorihominis* at P1 and the genus *Lactobacillus* at P2. The former OUT has been associated with susceptible phenotypes to stress, whereas there are contradictory findings for the latter [149,401,421].

The results of the microbiome analysis look very interesting and correspond to some previous findings by others, but the high variability within groups, characteristic of this type of experiments, prohibits strong conclusions. A larger number of replicates is needed to confirm our results and to perform correlation studies that could statistically associate specific OTUs to the resilient or susceptible phenotype with a high degree of certainty. Moreover, additional experiments are required to elucidate and understand how these specific microbes influence and communicate with the CNS.

6. References

1. Tsokolov, S. A. Why Is the Definition of Life So Elusive? Epistemological Considerations. *Astrobiology* **9**, 401–412 (2009).
2. Muller, H. J. Life. *Science (80-.).* **121**, 1–9 (1955).
3. Prigogine, I. *From being to becoming: time and complexity in the physical sciences*. (1980).
4. Koshland, D. E. Special essay. The seven pillars of life. *Science (80-.).* (2002). doi:10.1126/science.1068489
5. Wiener, N. Cybernetics. *Sci Am* 14–18 (1948).
6. Lee, T. I. *et al.* Transcriptional regulatory networks in Saccharomyces cerevisiae. *Science (80-.).* **298**, 799–804 (2002).
7. Shen-Orr, S. S., Milo, R., Mangan, S. & Alon, U. Network motifs in the transcriptional regulation network of Escherichia coli. *Nat. Genet.* **31**, 64–68 (2002).
8. Tsang, J., Zhu, J. & van Oudenaarden, A. MicroRNA-Mediated Feedback and Feedforward Loops Are Recurrent Network Motifs in Mammals. *Mol. Cell* **26**, 753–767 (2007).
9. Korzeniewski, B. Cybernetic formulation of the definition of life. *J. Theor. Biol.* **209**, 275–286 (2001).
10. Modell, H. *et al.* A physiologist's view of homeostasis. *Adv. Physiol. Educ.* **39**, 259–266 (2015).
11. Abbott, L. F. & LeMasson, G. Analysis of Neuron Models with Dynamically Regulated Conductances. *Neural Comput.* (1993). doi:10.1162/neco.1993.5.6.823
12. Vastagh, C., Solymosi, N., Farkas, I. & Liposits, Z. Proestrus Differentially Regulates Expression of Ion Channel and Calcium Homeostasis Genes in GnRH Neurons of Mice. *Front. Mol. Neurosci.* **12**, 137 (2019).
13. MacLean, J. N., Zhang, Y., Johnson, B. R. & Harris-Warrick, R. M. Activity-independent homeostasis in rhythmically active neurons. *Neuron* **37**, 109–120 (2003).
14. Levitan, I. B. Signaling protein complexes associated with neuronal ion channels. *Nature Neuroscience* **9**, 305–310 (2006).
15. McNair, L. F. *et al.* Deletion of Neuronal GLT-1 in Mice Reveals Its Role in Synaptic Glutamate Homeostasis and Mitochondrial Function. *J. Neurosci.* **39**, 4847–4863 (2019).
16. Bridi, M. C. D. *et al.* Two distinct mechanisms for experience-dependent homeostasis. *Nat. Neurosci.* **21**, 843–850 (2018).
17. Henry, F. E. *et al.* A Unique Homeostatic Signaling Pathway Links Synaptic Inactivity to Postsynaptic mTORC1. *J. Neurosci.* **38**, 2207–2225 (2018).
18. Miller, P. & Cannon, J. Combined mechanisms of neural firing rate homeostasis. *Biological Cybernetics* **113**, 47–59 (2019).
19. Marder, E. & Tang, L. S. Coordinating different homeostatic processes. *Neuron* **66**, 161–163 (2010).
20. O'Leary, T. & Wyllie, D. J. . Neuronal homeostasis: time for a change? *J. Physiol.* **589**,

4811–4826 (2011).

21. Deco, G. *et al.* How Local Excitation-Inhibition Ratio Impacts the Whole Brain Dynamics. *J. Neurosci.* **34**, 7886–7898 (2014).
22. Jonke, Z., Legenstein, R., Habenschuss, S. & Maass, W. Feedback Inhibition Shapes Emergent Computational Properties of Cortical Microcircuit Motifs. *J. Neurosci.* **37**, 8511–8523 (2017).
23. Triesch, J. A gradient rule for the plasticity of a neuron's intrinsic excitability. in *Lecture Notes in Computer Science (including subseries Lecture Notes in Artificial Intelligence and Lecture Notes in Bioinformatics)* 65–70 (2005). doi:10.1007/11550822_11
24. Koolhaas, J. M. *et al.* Stress revisited: A critical evaluation of the stress concept. *Neuroscience and Biobehavioral Reviews* **35**, 1291–1301 (2011).
25. Selye, H. The general adaptation syndrome and the diseases of adaptation. *J. Allergy* **6**, 117–230 (1946).
26. Herman, J. P. *et al.* Central mechanisms of stress integration: Hierarchical circuitry controlling hypothalamo-pituitary-adrenocortical responsiveness. *Front. Neuroendocrinol.* **24**, 151–180 (2003).
27. Phelps, E. A. & LeDoux, J. E. Contributions of the amygdala to emotion processing: From animal models to human behavior. *Neuron* **48**, 175–187 (2005).
28. Selye, H. Stress and the general adaptation syndrome. *Br. Med. J.* **1**, 1383–1392 (1950).
29. Cannon, W. B. *The wisdom of the body, 2nd ed. The wisdom of the body, 2nd ed.* (1939).
30. Cannon, W. B. Bodily Changes in Pain, Hunger, Fear and Rage; An Account of Recent Researches into the Function of Emotional Excitement. *Science* **19**, 100–101 (1915).
31. Jansen, A. S. P., Van Nguyen, X., Karpitskiy, V., Mettenleiter, T. C. & Loewy, A. D. Central command neurons of the sympathetic nervous system: Basis of the fight-or-flight response. *Science (80-.).* **270**, 644–646 (1995).
32. Tsigos, C. & Chrousos, G. P. Hypothalamic-pituitary-adrenal axis, neuroendocrine factors and stress. *J. Psychosom. Res.* **53**, 865–871 (2002).
33. De Kloet, E. R., Joëls, M. & Holsboer, F. Stress and the brain: From adaptation to disease. *Nat. Rev. Neurosci.* **6**, 463–475 (2005).
34. Morena, M., Patel, S., Bains, J. S. & Hill, M. N. Neurobiological Interactions Between Stress and the Endocannabinoid System. *Neuropsychopharmacology* **41**, 80–102 (2016).
35. Besedovsky, H. O., Lajtha, A. & Galoyan, A. *Handbook of Neurochemistry and Molecular Neurobiology*. *Handbook of Neurochemistry and Molecular Neurobiology* (2009). doi:10.1007/978-0-387-30410-6
36. Myers, B., McKlveen, J. M. & Herman, J. P. Glucocorticoid actions on synapses, circuits, and behavior: Implications for the energetics of stress. *Frontiers in Neuroendocrinology* **35**, 180–196 (2014).
37. Dunn, A. J. & Swiergiel, A. H. The role of corticotropin-releasing factor and noradrenaline in stress-related responses, and the inter-relationships between the two systems. *European Journal of Pharmacology* **583**, 186–193 (2008).

38. Valentino, R. J., Foote, S. L. & Aston-Jones, G. Corticotropin-releasing factor activates noradrenergic neurons of the locus coeruleus. *Brain Res.* **270**, 363–367 (1983).
39. Lavicky, J. & Dunn, A. J. Corticotropin-Releasing Factor Stimulates Catecholamine Release in Hypothalamus and Prefrontal Cortex in Freely Moving Rats as Assessed by Microdialysis. *Journal of Neurochemistry* **60**, 602–612 (1993).
40. Watanabe, Y., Gould, E. & McEwen, B. S. Stress induces atrophy of apical dendrites of hippocampal CA3 pyramidal neurons. *Brain Res.* **588**, 341–345 (1992).
41. Sapolsky, R. M. Glucocorticoids and hippocampal atrophy in neuropsychiatric disorders. *Archives of General Psychiatry* **57**, 925–935 (2000).
42. Zhu, L. J. *et al.* The different roles of glucocorticoids in the hippocampus and hypothalamus in chronic stress-induced HPA axis hyperactivity. *PLoS One* **9**, e97689 (2014).
43. Khan, S. & Alam, R. Chronic Stress Leads to Anxiety and Depression. *Ann. Psychiatry Ment. Heal.* **5**, 1090–1093 (2017).
44. Jokinen, J. & Nordström, P. HPA axis hyperactivity and cardiovascular mortality in mood disorder inpatients. *J. Affect. Disord.* **116**, 88–92 (2009).
45. Nesse, R. M., Bhatnagar, S. & Ellis, B. Evolutionary Origins and Functions of the Stress Response System. in *Stress: Concepts, Cognition, Emotion, and Behavior: Handbook of Stress* (2016). doi:10.1016/B978-0-12-800951-2.00011-X
46. Brenner, S. L. *et al.* Evolutionary Mismatch and Chronic Psychological Stress. *J. Evol. Med.* **3**, 235885 (2015).
47. Schneiderman, N., Ironson, G. & Siegel, S. D. Stress and Health: Psychological, Behavioral, and Biological Determinants. *Annu. Rev. Clin. Psychol.* **1**, 607–628 (2004).
48. Earle, W. J. DSM-5. *Philos. Forum* (2014). doi:10.1111/phil.12034
49. McFarlane, A. C. The long-term costs of traumatic stress: Intertwined physical and psychological consequences. *World Psychiatry* **9**, 3–10 (2010).
50. Carlson, E. B., Garvert, D. W., Macia, K. S., Ruzek, J. I. & Burling, T. A. Traumatic Stressor Exposure and Post-Traumatic Symptoms in Homeless Veterans. *Mil. Med.* **178**, 970–973 (2013).
51. Klaric, M., Klarić, B., Stevanović, A., Grković, J. & Jonovska, S. Psychological consequences of war trauma and postwar social stressors in women in Bosnia and Herzegovina. *Croat. Med. J.* **48**, 167–176 (2007).
52. Frommberger, U., Angenendt, J. & Berger, M. Post-traumatic stress disorder - A diagnostic and therapeutic challenge. *Dtsch. Arztebl. Int.* **111**, 59–65 (2014).
53. Steel, Z. *et al.* Psychiatric status of asylum seeker families held for a protracted period in a remote detention centre in Australia. *Aust. N. Z. J. Public Health* **28**, 527–536 (2004).
54. Bremner, J. Traumatic stress: effects on the brain. *Dialogues Clin Neurosci* **8**, 445–461 (2006).
55. Osuch, E., Willis, M., Bluhm, R., Ursano, R. & Drevets, W. Neurophysiological responses to traumatic reminders in the acute aftermath of serious motor vehicle collisions using

[15O]-H2O positron emission tomography. *Biol Psychiatry* **64**, 327–335 (2008).

56. Kangas, M. DSM-5 trauma and stress-related disorders: Implications for screening for cancer-related stress. *Front. Psychiatry* (2013). doi:10.3389/fpsyt.2013.00122
57. Kessler, R. C. *et al.* Lifetime prevalence and age-of-onset distributions of mental disorders in the World Health Organization's World Mental Health Survey Initiative. *World Psychiatry* **6**, 168–176 (2007).
58. Calleo, J. & Stanley, M. Anxiety disorders in later life: Differentiated diagnosis and treatment strategies. *Psychiatr Times* 24 (2008).
59. McLaughlin, K. A. & Hatzenbuehler, M. L. Stressful Life Events, Anxiety Sensitivity, and Internalizing Symptoms in Adolescents. *J. Abnorm. Psychol.* **118**, 659–669 (2009).
60. Gottschalk, M. G. & Domschke, K. Genetics of generalized anxiety disorder and related traits. *Dialogues Clin. Neurosci.* **19**, 159–168 (2017).
61. Hirschfeld, R. M. A. The Comorbidity of Major Depression and Anxiety Disorders: Recognition and Management in Primary Care. *Prim. Care Companion J. Clin. Psychiatry* **3**, 244–254 (2001).
62. Nemeroff, C. B. The role of GABA in the pathophysiology and treatment of anxiety disorders. *Psychopharmacol. Bull.* **37**, 133–146 (2003).
63. Lydiard, R. B. The role of GABA in anxiety disorders. *Journal of Clinical Psychiatry* **64**, 21–27 (2003).
64. Dunlop, B. W. & Davis, P. G. Combination Treatment With Benzodiazepines and SSRIs for Comorbid Anxiety and Depression. *Prim. Care Companion J. Clin. Psychiatry* **10**, 222–228 (2009).
65. Etkin, A., Prater, K. E., Schatzberg, A. F., Menon, V. & Greicius, M. D. Disrupted amygdalar subregion functional connectivity and evidence of a compensatory network in generalized anxiety disorder. *Arch. Gen. Psychiatry* **66**, 1361–1372 (2009).
66. Mitra, R., Ferguson, D. & Sapolsky, R. M. SK2 potassium channel overexpression in basolateral amygdala reduces anxiety, stress-induced corticosterone secretion and dendritic arborization. *Mol. Psychiatry* **14**, 847–855 (2009).
67. National Institute of Mental Health, N. Generalized Anxiety Disorder: When Worry Gets Out of Control. *Institute of Mental Health, National* (2016).
68. Krishnan, V. & Nestler, E. J. The molecular neurobiology of depression. *Nature* **455**, 894–902 (2008).
69. Strakowski, S. M. & Nestler, E. J. *Major Depressive Disorder*. (2015).
70. Bachmann, S. Epidemiology of suicide and the psychiatric perspective. *International Journal of Environmental Research and Public Health* **15**, E1425 (2018).
71. Kessler, R. C. & Bromet, E. J. The Epidemiology of Depression Across Cultures. *Annu. Rev. Public Health* **34**, 119–138 (2013).
72. Driessen, E. & Hollon, S. D. Cognitive behavioral therapy for mood disorders: Efficacy, moderators and mediators. *Psychiatric Clinics of North America* **33**, 537–555 (2010).
73. Fournier, J. C. *et al.* Antidepressant drug effects and depression severity: A patient-level

meta-analysis. *JAMA - Journal of the American Medical Association* **303**, 47–53 (2010).

74. Braun, C., Bschor, T., Franklin, J. & Baethge, C. Suicides and Suicide Attempts during Long-Term Treatment with Antidepressants: A Meta-Analysis of 29 Placebo-Controlled Studies Including 6,934 Patients with Major Depressive Disorder. *Psychother. Psychosom.* **85**, 171–179 (2016).
75. Ruhé, H. G., Mason, N. S. & Schene, A. H. Mood is indirectly related to serotonin, norepinephrine and dopamine levels in humans: A meta-analysis of monoamine depletion studies. *Molecular Psychiatry* **12**, 331–359 (2007).
76. Krishnadas, R. & Cavanagh, J. Depression: An inflammatory illness? *Journal of Neurology, Neurosurgery and Psychiatry* **83**, 495–502 (2012).
77. Varghese, F. P. & Brown, E. S. The Hypothalamic-Pituitary-Adrenal Axis in Major Depressive Disorder: A Brief Primer for Primary Care Physicians. *Prim. Care Companion J. Clin. Psychiatry* **3**, 151–155 (2001).
78. Lopez-Duran, N. L., Kovacs, M. & George, C. J. Hypothalamic-pituitary-adrenal axis dysregulation in depressed children and adolescents: A meta-analysis. *Psychoneuroendocrinology* **34**, 1272–1283 (2009).
79. Price, J. L. & Drevets, W. C. Neural circuits underlying the pathophysiology of mood disorders. *Trends in Cognitive Sciences* **16**, 61–71 (2012).
80. Drevets, W. C., Price, J. L. & Furey, M. L. Brain structural and functional abnormalities in mood disorders: Implications for neurocircuitry models of depression. *Brain Structure and Function* **213**, 93–118 (2008).
81. Dunlop, B. W. & Nemeroff, C. B. The role of dopamine in the pathophysiology of depression. *Archives of General Psychiatry* **64**, 327–337 (2007).
82. Meyer, J. H. *et al.* Elevated monoamine oxidase A levels in the brain: An explanation for the monoamine imbalance of major depression. *Arch. Gen. Psychiatry* **63**, 1209–1216 (2006).
83. Andrews, P. W., Bharwani, A., Lee, K. R., Fox, M. & Thomson, J. A. Is serotonin an upper or a downer? The evolution of the serotonergic system and its role in depression and the antidepressant response. *Neuroscience and Biobehavioral Reviews* **51**, 164–188 (2015).
84. Sun, H., Kennedy, P. J. & Nestler, E. J. Epigenetics of the depressed brain: Role of histone acetylation and methylation. *Neuropsychopharmacology* **38**, 124–137 (2013).
85. Heim, C. & Binder, E. B. Current research trends in early life stress and depression: Review of human studies on sensitive periods, gene-environment interactions, and epigenetics. *Experimental Neurology* **233**, 102–111 (2012).
86. Toyokawa, S., Uddin, M., Koenen, K. C. & Galea, S. How does the social environment “get into the mind”? Epigenetics at the intersection of social and psychiatric epidemiology. *Soc. Sci. Med.* **74**, 67–74 (2012).
87. Menke, A. & Binder, E. B. Epigenetic alterations in depression and antidepressant treatment. *Dialogues Clin. Neurosci.* **16**, 395–404 (2014).
88. Werner, E. E., Bierman, J. M. & French, F. E. *The children of Kauai*. (1971).

89. Garmezy, N. Competence and Adaptation in Adult Schizophrenic Patients and Children at Risk. in *Research in the Schizophrenic Disorders* 69–112 (1985). doi:10.1007/978-94-011-6338-5_3
90. Derijk, R. H. Single nucleotide polymorphisms related to HPA axis reactivity. *NeuroImmunoModulation* **16**, 340–352 (2009).
91. Ebner, K. & Singewald, N. Individual differences in stress susceptibility and stress inhibitory mechanisms. *Current Opinion in Behavioral Sciences* **14**, 54–64 (2017).
92. Sarrionandia, A., Ramos-Díaz, E. & Fernández-Lasarte, O. Resilience as a mediator of emotional intelligence and perceived stress: A cross-country study. *Front. Psychol.* **9**, 2653 (2018).
93. Peters, R. D., Leadbeater, B. & McMahon, R. J. *Resilience in children, families, and communities: Linking context to practice and policy. American Psychologycal Association* (2005).
94. Duckworth, A. L., Peterson, C., Matthews, M. D. & Kelly, D. R. Grit: Perseverance and Passion for Long-Term Goals. *J. Pers. Soc. Psychol.* **92**, 1087–1101 (2007).
95. Reich, J. W., Zautra, A. J. & Hall, J. S. *Handbook of adult resilience*. *Zhurnal Eksperimental'noi i Teoreticheskoi Fiziki* (2010). doi:10.1007/s13398-014-0173-7.2
96. McCraty, R., Atkinson, M., Tiller, W. A., Rein, G. & Watkins, A. D. The effects of emotions on short-term power spectrum analysis of heart rate variability. *Am. J. Cardiol.* **76**, 1089–1093 (1995).
97. Binder, E. B. *et al.* Association of FKBP5 polymorphisms and childhood abuse with risk of posttraumatic stress disorder symptoms in adults. *JAMA - J. Am. Med. Assoc.* **299**, 1291–1305 (2008).
98. Polanczyk, G. *et al.* Protective effect of CRHR1 gene variants on the development of adult depression following childhood maltreatment: Replication and extension. *Arch. Gen. Psychiatry* **66**, 978–985 (2009).
99. Domschke, K. *et al.* Neuropeptide S receptor gene converging evidence for a role in panic disorder. *Mol. Psychiatry* **16**, 938–948 (2011).
100. Mikolajczak, M., Roy, E., Luminet, O. & De Timary, P. Resilience and hypothalamic-pituitary-adrenal axis reactivity under acute stress in young men. *Stress* **11**, 477–482 (2008).
101. Daskalakis, N. P., Cohen, H., Cai, G., Buxbaum, J. D. & Yehuda, R. Expression profiling associates blood and brain glucocorticoid receptor signaling with trauma-related individual differences in both sexes. *Proc. Natl. Acad. Sci.* **111**, 13529–13534 (2014).
102. Schmidt, M. V. *et al.* High susceptibility to chronic social stress is associated with a depression-like phenotype. *Psychoneuroendocrinology* **35**, 635–643 (2010).
103. Rozeboom, A. M., Akil, H. & Seasholtz, A. F. Mineralocorticoid receptor overexpression in forebrain decreases anxiety-like behavior and alters the stress response in mice. *Proc. Natl. Acad. Sci.* **104**, 4688–4693 (2007).
104. Yehuda, R., Brand, S. R., Golier, J. A. & Yang, R. K. Clinical correlates of DHEA

associated with post-traumatic stress disorder. *Acta Psychiatr. Scand.* **114**, 187–93 (2006).

105. Butterfield, M. I. *et al.* Neuroactive steroids and suicidality in posttraumatic stress disorder. *Am. J. Psychiatry* **162**, 380–382 (2005).
106. Enman, N. M., Sabban, E. L., McGonigle, P. & Van Bockstaele, E. J. Targeting the neuropeptide Y system in stress-related psychiatric disorders. *Neurobiology of Stress* **1**, 33–43 (2015).
107. Duclot, F. & Kabbaj, M. Epigenetic mechanisms underlying the role of brain-derived neurotrophic factor in depression and response to antidepressants. *J. Exp. Biol.* **218**, 21–31 (2015).
108. Lopizzo, N., Zonca, V., Cattane, N., Patiante, C. & Cattaneo, A. miRNAs in depression vulnerability and resilience: novel targets for preventive strategies. *J. Neural Transm.* 1–18 (2019).
109. Blacker, C. J., Frye, M. A., Morava, E., Kozicz, T. & Veldic, M. A review of epigenetics of PTSD in comorbid psychiatric conditions. *Genes* **10**, E140 (2019).
110. Menard, C. *et al.* Social stress induces neurovascular pathology promoting depression. *Nat. Neurosci.* **20**, 1752–1760 (2017).
111. Krishnan, V. *et al.* Molecular Adaptations Underlying Susceptibility and Resistance to Social Defeat in Brain Reward Regions. *Cell* **131**, 391–404 (2007).
112. Vialou, V. *et al.* ΔfosB in brain reward circuits mediates resilience to stress and antidepressant responses. *Nat. Neurosci.* **13**, 745–752 (2010).
113. Friedman, A. K. *et al.* KCNQ channel openers reverse depressive symptoms via an active resilience mechanism. *Nat. Commun.* **7**, 11671 (2016).
114. Franklin, T. B., Saab, B. J. & Mansuy, I. M. Neural Mechanisms of Stress Resilience and Vulnerability. *Neuron* **75**, 747–61 (2012).
115. De Kloet, E. R., Joëls, M. & Holsboer, F. Stress and the brain: From adaptation to disease. *Nature Reviews Neuroscience* **6**, 463–75 (2005).
116. Sanacora, G., Treccani, G. & Popoli, M. Towards a glutamate hypothesis of depression: An emerging frontier of neuropsychopharmacology for mood disorders. *Neuropharmacology* **62**, 63–77 (2012).
117. Saab, B. J. *et al.* NCS-1 in the Dentate Gyrus Promotes Exploration, Synaptic Plasticity, and Rapid Acquisition of Spatial Memory. *Neuron* **63**, 643–656 (2009).
118. Raudensky, J. & Yamamoto, B. K. Effects of chronic unpredictable stress and methamphetamine on hippocampal glutamate function. *Brain Res.* **1135**, 129–135 (2007).
119. Zink, M., Vollmayr, B., Gebicke-Haerter, P. J. & Henn, F. A. Reduced expression of glutamate transporters vGluT1, EAAT2 and EAAT4 in learned helpless rats, an animal model of depression. *Neuropharmacology* **58**, 465–473 (2010).
120. Schmidt, M. V. *et al.* Individual Stress Vulnerability Is Predicted by Short-Term Memory and AMPA Receptor Subunit Ratio in the Hippocampus. *J. Neurosci.* **30**, 16949–16958 (2010).

121. Taliaz, D. *et al.* Resilience to Chronic Stress Is Mediated by Hippocampal Brain-Derived Neurotrophic Factor. *J. Neurosci.* **31**, 4475–4483 (2011).
122. Taliaz, D., Stall, N., Dar, D. E. & Zangen, A. Knockdown of brain-derived neurotrophic factor in specific brain sites precipitates behaviors associated with depression and reduces neurogenesis. *Mol. Psychiatry* **15**, 80–92 (2010).
123. Covington, H. E. *et al.* Antidepressant Effect of Optogenetic Stimulation of the Medial Prefrontal Cortex. *J. Neurosci.* **30**, 16082–90 (2010).
124. Myers-Schulz, B. & Koenigs, M. Functional anatomy of ventromedial prefrontal cortex: Implications for mood and anxiety disorders. *Molecular Psychiatry* **17**, 132–141 (2012).
125. Wang, Perova, Z., Arenkiel, B. R. & Li, B. Synaptic Modifications in the Medial Prefrontal Cortex in Susceptibility and Resilience to Stress. *J. Neurosci.* **34**, 7485–7492 (2014).
126. Lehmann, M. L. & Herkenham, M. Environmental Enrichment Confers Stress Resiliency to Social Defeat through an Infralimbic Cortex-Dependent Neuroanatomical Pathway. *J. Neurosci.* **31**, 6159–6173 (2011).
127. Pizzagalli, D. A. *et al.* Reduced caudate and nucleus accumbens response to rewards in unmedicated individuals with major depressive disorder. *Am. J. Psychiatry* **166**, 702–710 (2009).
128. Stockmeier, C. A. Neurobiology of serotonin in depression and suicide. *Ann. N. Y. Acad. Sci.* **836**, 220–232 (1997).
129. Savitz, J., Lucki, I. & Drevets, W. C. 5-HT1A receptor function in major depressive disorder. *Progress in Neurobiology* **88**, 17–31 (2009).
130. Sudo, N. *et al.* Postnatal microbial colonization programs the hypothalamic-pituitary-adrenal system for stress response in mice. *J. Physiol.* **558**, 263–275 (2004).
131. Bercik, P. *et al.* The intestinal microbiota affect central levels of brain-derived neurotropic factor and behavior in mice. *Gastroenterology* **141**, 599–609 (2011).
132. Collins, S. M., Kassam, Z. & Bercik, P. The adoptive transfer of behavioral phenotype via the intestinal microbiota: Experimental evidence and clinical implications. *Current Opinion in Microbiology* **16**, 3 (2013).
133. Bravo, J. A. *et al.* Ingestion of Lactobacillus strain regulates emotional behavior and central GABA receptor expression in a mouse via the vagus nerve. *Proc. Natl. Acad. Sci.* **108**, 16050–16055 (2011).
134. Tolhurst, G. *et al.* Short-chain fatty acids stimulate glucagon-like peptide-1 secretion via the G-protein-coupled receptor FFAR2. *Diabetes* **61**, 364–371 (2012).
135. Yano, J. M. *et al.* Indigenous bacteria from the gut microbiota regulate host serotonin biosynthesis. *Cell* **161**, 264–276 (2015).
136. Asano, Y. *et al.* Critical role of gut microbiota in the production of biologically active, free catecholamines in the gut lumen of mice. *Am. J. Physiol. Liver Physiol.* **303**, 1288–1295 (2012).
137. Shishov, V. A., Kirovskaya, T. A., Kudrin, V. S. & Oleskin, A. V. Amine neuromediators, their precursors, and oxidation products in the culture of Escherichia coli K-12. *Appl.*

Biochem. Microbiol. **45**, 550–554 (2009).

138. Barrett, E., Ross, R. P., O'Toole, P. W., Fitzgerald, G. F. & Stanton, C. γ-Aminobutyric acid production by culturable bacteria from the human intestine. *J. Appl. Microbiol.* **113**, 411–417 (2012).
139. Martin, C. R., Osadchiy, V., Kalani, A. & Mayer, E. A. The Brain-Gut-Microbiome Axis. *CMGH* **6**, 133–148 (2018).
140. Wang, Y. *et al.* An intestinal commensal symbiosis factor controls neuroinflammation via TLR2-mediated CD39 signalling. *Nat. Commun.* **5**, 4432 (2014).
141. Singh, V. *et al.* Microbiota Dysbiosis Controls the Neuroinflammatory Response after Stroke. *J. Neurosci.* **36**, 7428–7440 (2016).
142. Samuel, B. S. *et al.* Effects of the gut microbiota on host adiposity are modulated by the short-chain fatty-acid binding G protein-coupled receptor, Gpr41. *Proc. Natl. Acad. Sci.* **105**, 16767–16772 (2008).
143. Cani, P. D. *et al.* Gut microbiota fermentation of prebiotics increases satietogenic and incretin gut peptide production with consequences for appetite sensation and glucose response after a meal. *Am. J. Clin. Nutr.* **90**, 1236–1240 (2009).
144. Fu, L. *et al.* Fibroblast growth factor 19 increases metabolic rate and reverses dietary and leptin-deficient diabetes. *Endocrinology* **145**, 2594–2603 (2004).
145. Ryan, K. K. *et al.* Fibroblast growth factor-19 action in the brain reduces food intake and body weight and improves glucose tolerance in male rats. *Endocrinology* **154**, 9–15 (2013).
146. Perry, R. J. *et al.* FGF1 and FGF19 reverse diabetes by suppression of the hypothalamic-pituitary-adrenal axis. *Nat. Commun.* **6**, 6980 (2015).
147. Kim, D.-Y. & Camilleri, M. Serotonin: a mediator of the brain-gut connection. *Am. J. Gastroenterol.* **95**, 2698–2709 (2004).
148. Wikoff, W. R. *et al.* Metabolomics analysis reveals large effects of gut microflora on mammalian blood metabolites. *Proc. Natl. Acad. Sci.* **106**, 3698–3703 (2009).
149. Marin, I. A. *et al.* Microbiota alteration is associated with the development of stress-induced despair behavior. *Sci. Rep.* **7**, 43859 (2017).
150. Fung, T. C., Olson, C. A. & Hsiao, E. Y. Interactions between the microbiota, immune and nervous systems in health and disease. *Nature Neuroscience* **20**, 145–155 (2017).
151. Ochoa-Repáraz, J. *et al.* Role of Gut Commensal Microflora in the Development of Experimental Autoimmune Encephalomyelitis. *J. Immunol.* **183**, 6041–6050 (2009).
152. Winek, K. *et al.* Depletion of Cultivatable Gut Microbiota by Broad-Spectrum Antibiotic Pretreatment Worsens Outcome After Murine Stroke. *Stroke* **47**, 1354–1363 (2016).
153. Erny, D. *et al.* Host microbiota constantly control maturation and function of microglia in the CNS. *Nat. Neurosci.* **18**, 965–977 (2015).
154. Barajon, I. *et al.* Toll-like receptors 3, 4, and 7 are expressed in the enteric nervous system and dorsal root ganglia. *J. Histochem. Cytochem.* **57**, 1013–1023 (2009).
155. Tannock, G. W. & Savage, D. C. Influences of dietary and environmental stress on

microbial populations in the murine gastrointestinal tract. *Infect. Immun.* **9**, 591–598 (1974).

156. Tottey, W. *et al.* Colonic transit time is a driven force of the gut microbiota composition and metabolism: In vitro evidence. *J. Neurogastroenterol. Motil.* **23**, 124–134 (2017).
157. Santos, J., Yang, P. C., Söderholm, J. D., Benjamin, M. & Perdue, M. H. Role of mast cells in chronic stress induced colonic epithelial barrier dysfunction in the rat. *Gut* **48**, 630–636 (2001).
158. Varghese, A. K. *et al.* Antidepressants Attenuate Increased Susceptibility to Colitis in a Murine Model of Depression. *Gastroenterology* **130**, 1743–1753 (2006).
159. Houlden, A. *et al.* Brain injury induces specific changes in the caecal microbiota of mice via altered autonomic activity and mucoprotein production. *Brain. Behav. Immun.* **57**, 10–20 (2016).
160. Mayer, E. A., Savidge, T. & Shulman, R. J. Brain-gut microbiome interactions and functional bowel disorders. *Gastroenterology* **146**, 1500–1512 (2014).
161. Stephens, R. L. & Tache, Y. Intracisternal injection of a TRH analogue stimulates gastric luminal serotonin release in rats. *Am. J. Physiol. Liver Physiol.* **256**, 377–383 (2017).
162. Simreń, M. *et al.* Intestinal microbiota in functional bowel disorders: A Rome foundation report. *Gut* **62**, 159–176 (2013).
163. Turnbaugh, P. J. *et al.* An obesity-associated gut microbiome with increased capacity for energy harvest. *Nature* **444**, 1027–1031 (2006).
164. Depommier, C. *et al.* Supplementation with Akkermansia muciniphila in overweight and obese human volunteers: a proof-of-concept exploratory study. *Nature Medicine* **24**, 1096–1103 (2019).
165. Mertsalmi, T. H. *et al.* More than constipation – bowel symptoms in Parkinson's disease and their connection to gut microbiota. *Eur. J. Neurol.* **24**, 1375–1383 (2017).
166. Mayer, E. A., Padua, D. & Tillisch, K. Altered brain-gut axis in autism: Comorbidity or causative mechanisms? *BioEssays* **36**, 933–939 (2014).
167. Kelly, J. R. *et al.* Breaking down the barriers: the gut microbiome, intestinal permeability and stress-related psychiatric disorders. *Front. Cell. Neurosci.* **9**, 392 (2015).
168. Leclercq, S., Forsythe, P. & Bienenstock, J. Posttraumatic stress disorder: Does the gut microbiome hold the key? *Canadian Journal of Psychiatry* **61**, 204–213 (2016).
169. Barreau, F., Ferrier, L., Fioramonti, J. & Bueno, L. Neonatal maternal deprivation triggers long term alterations in colonic epithelial barrier and mucosal immunity in rats. *Gut* **53**, 501–506 (2004).
170. O'Mahony, S. M. *et al.* Early Life Stress Alters Behavior, Immunity, and Microbiota in Rats: Implications for Irritable Bowel Syndrome and Psychiatric Illnesses. *Biol. Psychiatry* **65**, 263–267 (2009).
171. Hemmings, S. M. J. *et al.* The Microbiome in Posttraumatic Stress Disorder and Trauma-Exposed Controls: An Exploratory Study. *Psychosom. Med.* **79**, 936–946 (2017).
172. Rincel, M. *et al.* Multi-hit early life adversity affects gut microbiota, brain and behavior in a

sex-dependent manner. *Brain. Behav. Immun.* **80**, 179–192 (2019).

173. McNulty, N. P. *et al.* The impact of a consortium of fermented milk strains on the gut microbiome of gnotobiotic mice and monozygotic twins. *Sci. Transl. Med.* **3**, 106 (2011).
174. Kelly, J. R., Clarke, G., Cryan, J. F. & Dinan, T. G. Brain-gut-microbiota axis: challenges for translation in psychiatry. *Annals of Epidemiology* **26**, 366–372 (2016).
175. Clarke, R. C. & Merlin, M. D. *Cannabis: Evolution and Ethnobotany*. *University of California* (2013). doi:10.5091/plecevo.2014.933
176. Merlin, M. D. COVER ARTICLE: Archaeological Evidence for the Tradition of Psychoactive Plant Use in the Old World. *Econ. Bot.* **57**, 295–323 (2003).
177. Russo, E. B. *et al.* Phytochemical and genetic analyses of ancient cannabis from Central Asia. *J. Exp. Bot.* **59**, 4171–4182 (2008).
178. Warf, B. High Points: An Historical Geography of Cannabis. *Geogr. Rev.* **104**, 414–438 (2014).
179. Adams, R. & Hunt, M. Structure of Cannabidiol, a Product Isolated from the Marihuana Extract of Minnesota Wild Hemp. I. *J. Am. Chem. Soc.* (1940). doi:10.1021/ja01858a058
180. Gaoni, Y. & Mechoulam, R. Isolation, Structure, and Partial Synthesis of an Active Constituent of Hashish. *J. Am. Chem. Soc.* **86**, 1646–1647 (1964).
181. Matsuda, L. A., Lolait, S. J., Brownstein, M. J., Young, A. C. & Bonner, T. I. Structure of a cannabinoid receptor and functional expression of the cloned cDNA. *Nature* **346**, 561–564 (1990).
182. Munro, S., Thomas, K. L. & Abu-Shaar, M. Molecular characterization of a peripheral receptor for cannabinoids. *Nature* **365**, 61–65 (1993).
183. Mechoulam, R. & Parker, L. The Endocannabinoid System and the Brain. *SSRN* **64**, 21–47 (2013).
184. Hashimotodani, Y., Kano, M., Ohno-Shosaku, T., Watanabe, M. & Uchigashima, M. Endocannabinoid-Mediated Control of Synaptic Transmission. *Physiol. Rev.* **89**, 309–380 (2009).
185. Marsicano, G. & Lutz, B. Expression of the cannabinoid receptor CB1 in distinct neuronal subpopulations in the adult mouse forebrain. *Eur. J. Neurosci.* **11**, 4213–4225 (1999).
186. Mackie, K. Cannabinoid receptor homo- and heterodimerization. *Life Sci.* **77**, 1667–1673 (2005).
187. Hermann, H., Marsicano, G. & Lutz, B. Coexpression of the cannabinoid receptor type 1 with dopamine and serotonin receptors in distinct neuronal subpopulations of the adult mouse forebrain. *Neuroscience* **109**, 451–460 (2002).
188. Degroot, A. *et al.* CB1 Receptor Antagonism Increases Hippocampal Acetylcholine Release: Site and Mechanism of Action. *Mol. Pharmacol.* **70**, 1236–1245 (2006).
189. Monory, K., Korte, M., Lutz, B., Remus, A. & Polack, M. Cannabinoid CB1 Receptor Calibrates Excitatory Synaptic Balance in the Mouse Hippocampus. *J. Neurosci.* **35**, 3842–3850 (2015).
190. Häring, M., Marsicano, G., Lutz, B. & Monory, K. Identification of the cannabinoid receptor

type 1 in serotonergic cells of raphe nuclei in mice. *Neuroscience* **146**, 1212–1219 (2007).

191. Stempel, A. V. *et al.* Cannabinoid Type 2 Receptors Mediate a Cell Type-Specific Plasticity in the Hippocampus. *Neuron* **90**, 795–809 (2016).
192. Erdozain, A. M., Meana, J. J. & Callado, L. F. Implicación del sistema cannabinoide endógeno en el alcoholismo. *Trastornos Adictivos* (2009). doi:10.1016/S1575-0973(09)72056-2
193. Devane, W. A. *et al.* Isolation and structure of a brain constituent that binds to the cannabinoid receptor. *Science (80-.).* **258**, 1946–1949 (1992).
194. Mechoulam, R. *et al.* Identification of an endogenous 2-monoglyceride, present in canine gut, that binds to cannabinoid receptors. *Biochem. Pharmacol.* **50**, 83–90 (1995).
195. Gonsiorek, W. *et al.* Endocannabinoid 2-arachidonyl glycerol is a full agonist through human type 2 cannabinoid receptor: antagonism by anandamide. *Mol. Pharmacol.* **57**, 1045–1050 (2000).
196. Marsicano, G. *et al.* CB1 cannabinoid receptors and on-demand defense against excitotoxicity. *Science (80-.).* **302**, 84–88 (2003).
197. Piomelli, D. The molecular logic of endocannabinoid signalling. *Nat. Rev. Neurosci.* **4**, 873–884 (2003).
198. Ligresti, A., Cascio, M. & Marzo, V. Endocannabinoid Metabolic Pathways and Enzymes. *Curr. Drug Target -CNS Neurol. Disord.* **4**, 615–623 (2005).
199. Maccarrone, M. Metabolism of the Endocannabinoid Anandamide: Open Questions after 25 Years. *Front. Mol. Neurosci.* **10**, 166 (2017).
200. Bisogno, T. *et al.* Cloning of the first sn1-DAG lipases points to the spatial and temporal regulation of endocannabinoid signaling in the brain. *J. Cell Biol.* **163**, 463–468 (2003).
201. Dinh, T. P., Freund, T. F. & Piomelli, D. A role for monoglyceride lipase in 2-arachidonoylglycerol inactivation. *Chem. Phys. Lipids* **121**, 149–158 (2002).
202. Blankman, J. L., Simon, G. M. & Cravatt, B. F. A Comprehensive Profile of Brain Enzymes that Hydrolyze the Endocannabinoid 2-Arachidonoylglycerol. *Chem. Biol.* **14**, 1347–1356 (2007).
203. Kozak, K. R. *et al.* Metabolism of the endocannabinoids, 2-arachidonylglycerol and anandamide, into prostaglandin, thromboxane, and prostacyclin glycerol esters and ethanolamides. *J. Biol. Chem.* **277**, 44877–44885 (2002).
204. Cravatt, B. F. *et al.* Molecular characterization of an enzyme that degrades neuromodulatory fatty-acid amides. *Nature* **384**, 83–87 (1996).
205. Di Marzo, V. & De Petrocellis, L. Endocannabinoids as Regulators of Transient Receptor Potential (TRP) Channels: a Further Opportunity to Develop New Endocannabinoid-Based Therapeutic Drugs. *Curr. Med. Chem.* **17**, 1430–1449 (2010).
206. Nevalainen, T. & J. Irving, A. GPR55, a Lysophosphatidylinositol Receptor with Cannabinoid Sensitivity? *Curr. Top. Med. Chem.* **10**, 799–813 (2010).
207. Rouse, S., Gilmor, M. & Levey, A. Differential presynaptic and postsynaptic expression of m1–m4 muscarinic acetylcholine receptors at the perforant pathway/granule cell synapse.

Neuroscience **86**, 221–232 (1998).

208. O'Sullivan, S. E. & Kendall, D. A. Cannabinoid activation of peroxisome proliferator-activated receptors: Potential for modulation of inflammatory disease. *Immunobiology* **215**, 611–616 (2010).
209. Sigel, E. *et al.* The major central endocannabinoid directly acts at GABAA receptors. *Proc. Natl. Acad. Sci.* **108**, 18150–18155 (2011).
210. Südhof, T. C. & Malenka, R. C. Understanding Synapses: Past, Present, and Future. *Neuron* **60**, 469–476 (2008).
211. Katona, I. & Freund, T. F. Multiple functions of endocannabinoid signaling in the brain. *Annual Review of Neuroscience* **35**, 529–558 (2012).
212. Alkadhi, K. A., Al-Hijailan, R. S., Malik, K. & Hogan, Y. H. Retrograde carbon monoxide is required for induction of long-term potentiation in rat superior cervical ganglion. *J. Neurosci.* (2001).
213. Carta, M. *et al.* Membrane lipids tune synaptic transmission by direct modulation of presynaptic potassium channels. *Neuron* **81**, 787–799 (2014).
214. Regehr, W. G., Carey, M. R. & Best, A. R. Activity-Dependent Regulation of Synapses by Retrograde Messengers. *Neuron* **63**, 154–170 (2009).
215. Maejima, T., Ohno-Shosaku, T. & Kano, M. Endogenous cannabinoid as a retrograde messenger from depolarized postsynaptic neurons to presynaptic terminals. *Neurosci. Res.* **40**, 205–210 (2001).
216. Wilson, R. I., Kunos, G. & Nicoll, R. A. Presynaptic specificity of endocannabinoid signaling in the hippocampus. *Neuron* **31**, 453–462 (2001).
217. Ohno-Shosaku, T. *et al.* Presynaptic cannabinoid sensitivity is a major determinant of depolarization-induced retrograde suppression at hippocampal synapses. *J. Neurosci.* **22**, 3864–3872 (2002).
218. Kreitzer, A. C. & Regehr, W. G. Retrograde inhibition of presynaptic calcium influx by endogenous cannabinoids at excitatory synapses onto Purkinje cells. *Neuron* **29**, 717–727 (2001).
219. Castillo, P. E., Younts, T. J., Chávez, A. E. & Hashimotodani, Y. Endocannabinoid signaling and synaptic function. *Neuron* **76**, 70–81 (2012).
220. Gao, Y. *et al.* Loss of Retrograde Endocannabinoid Signaling and Reduced Adult Neurogenesis in Diacylglycerol Lipase Knock-out Mice. *J. Neurosci.* **30**, 2017–2024 (2010).
221. Chávez, A. E., Chiu, C. Q. & Castillo, P. E. TRPV1 activation by endogenous anandamide triggers postsynaptic long-term depression in dentate gyrus. *Nat. Neurosci.* **13**, 1511–1518 (2010).
222. Gulyas, A. I. *et al.* Segregation of two endocannabinoid-hydrolyzing enzymes into pre- and postsynaptic compartments in the rat hippocampus, cerebellum and amygdala. *Eur. J. Neurosci.* **20**, 441–458 (2004).
223. Reguero, L. *et al.* Subcellular localization of NAPE-PLD and DAGL-α in the ventromedial

nucleus of the hypothalamus by a preembedding immunogold method. *Histochem. Cell Biol.* **141**, 543–550 (2014).

224. Losonczy, A., Biro, A. A. & Nusser, Z. Persistently active cannabinoid receptors mute a subpopulation of hippocampal interneurons. *Proc. Natl. Acad. Sci.* **101**, 1362–1367 (2004).
225. Ohno-Shosaku, T. & Kano, M. Endocannabinoid-mediated retrograde modulation of synaptic transmission. *Current Opinion in Neurobiology* **29**, 1–8 (2014).
226. Chevaleyre, V. *et al.* Endocannabinoid-Mediated Long-Term Plasticity Requires cAMP/PKA Signaling and RIM1α. *Neuron* **54**, 801–812 (2007).
227. Mato, S., Lafourcade, M., Robbe, D., Bakiri, Y. & Manzoni, O. J. Role of the cyclic-AMP/PKA cascade and of P/Q-type Ca++ channels in endocannabinoid-mediated long-term depression in the nucleus accumbens. *Neuropharmacology* **54**, 87–94 (2008).
228. Rey, A. A., Purrio, M., Viveros, M. P. & Lutz, B. Biphasic effects of cannabinoids in anxiety responses: CB1 and GABA B receptors in the balance of gabaergic and glutamatergic neurotransmission. *Neuropsychopharmacology* **37**, 2624–2634 (2012).
229. Chevaleyre, V. & Castillo, P. E. Endocannabinoid-mediated metaplasticity in the hippocampus. *Neuron* **43**, 871–881 (2004).
230. Kirkham, T. & Tucci, S. Endocannabinoids in Appetite Control and the Treatment of Obesity. *CNS Neurol. Disord. - Drug Targets* **5**, 272–292 (2008).
231. Lutz, B., Marsicano, G., Maldonado, R. & Hillard, C. J. The endocannabinoid system in guarding against fear, anxiety and stress. *Nature Reviews Neuroscience* **16**, 705–718 (2015).
232. Hill, M. N. *et al.* Functional Interactions between Stress and the Endocannabinoid System: From Synaptic Signaling to Behavioral Output. *J. Neurosci.* **30**, 14980–14986 (2010).
233. Thompson, Z., Argueta, D., Garland, T. & DiPatrizio, N. Circulating levels of endocannabinoids respond acutely to voluntary exercise, are altered in mice selectively bred for high voluntary wheel running, and differ between the sexes. *Physiol. Behav.* **170**, 141–150 (2017).
234. Tantimonaco, M. *et al.* Physical activity and the endocannabinoid system: An overview. *Cellular and Molecular Life Sciences* **71**, 2681–2698 (2014).
235. Pertwee, R. G. The pharmacology of cannabinoid receptors and their ligands: An overview. *International Journal of Obesity* **30**, 13–18 (2006).
236. Bellocchio, L., Cervino, C., Pasquali, R. & Pagotto, U. The endocannabinoid system and energy metabolism. *Journal of Neuroendocrinology* **20**, 850–857 (2008).
237. Klein, C., Hill, M. N., Chang, S. C. H., Hillard, C. J. & Gorzalka, B. B. Circulating Endocannabinoid Concentrations and Sexual Arousal in Women. *J. Sex. Med.* **9**, 1588–1601 (2012).
238. MacCarrone, M., Guzmán, M., MacKie, K., Doherty, P. & Harkany, T. Programming of neural cells by (endo)cannabinoids: From physiological rules to emerging therapies. *Nat. Rev. Neurosci.* **15**, 786–801 (2014).

239. Prenderville, J. A., Kelly, Á. M. & Downer, E. J. The role of cannabinoids in adult neurogenesis. *British Journal of Pharmacology* **172**, 3950–3963 (2015).
240. Tart, C. T. Marijuana intoxication: Common experiences. *Nature* **226**, 701–704 (1970).
241. Gates, P., Jaffe, A. & Copeland, J. Cannabis smoking and respiratory health: Consideration of the literature. *Respirology* **19**, 655–662 (2014).
242. Kelly, T. H., Foltin, R. W., Emurian, C. S. & Fischman, M. W. Multidimensional behavioral effects of marijuana. *Prog. Neuropsychopharmacol. Biol. Psychiatry* **14**, 885–902 (1990).
243. Varvel, S. A. 9-Tetrahydrocannbinol Accounts for the Antinociceptive, Hypothermic, and Cataleptic Effects of Marijuana in Mice. *J. Pharmacol. Exp. Ther.* **314**, 329–337 (2005).
244. Farah, A. Cannabis Induced Psychopathology. *J. Addict. Res. Ther.* 11–19 (2017). doi:10.4172/2155-6105.s11-019
245. Hall, W. & Babor, T. F. Cannabis use and public health: Assessing the burden. *Addiction* **95**, 485–490 (2000).
246. Hall, W. & Pacula, R. *Cannabis Use and Dependence*. (2003).
247. Campos, A. C. *et al.* Plastic and neuroprotective mechanisms involved in the therapeutic effects of cannabidiol in psychiatric disorders. *Frontiers in Pharmacology* **8**, 269 (2017).
248. Monory, K. *et al.* The Endocannabinoid System Controls Key Epileptogenic Circuits in the Hippocampus. *Neuron* **51**, 455–466 (2006).
249. Khaspekov, L. G. *et al.* Involvement of brain-derived neurotrophic factor in cannabinoid receptor-dependent protection against excitotoxicity. *Eur. J. Neurosci.* **19**, 1691–1698 (2004).
250. Aguado, T. *et al.* The CB 1 cannabinoid receptor mediates excitotoxicity-induced neural progenitor proliferation and neurogenesis. *J. Biol. Chem.* (2007). doi:10.1074/jbc.M700678200
251. Sachs, J., McGlade, E. & Yurgelun-Todd, D. Safety and Toxicology of Cannabinoids. *Neurotherapeutics* **12**, 735–746 (2015).
252. Aviram, J. & Samuelly-Leichtag, G. Efficacy of Cannabis-Based Medicines for Pain Management: A Systematic Review and Meta-Analysis of Randomized Controlled Trials. *Pain Physician* **20**, E755-796 (2017).
253. Koppel, B. S. *et al.* Systematic review: Efficacy and safety of medical marijuana in selected neurologic disorders: Report of the Guideline Development Subcommittee of the American Academy of Neurology. *Neurology* **82**, 1556–1563 (2014).
254. O'Neil, M. E. *et al.* Benefits and harms of plant-based Cannabis for posttraumatic stress disorder a systematic review. *Annals of Internal Medicine* **167**, 332–340 (2017).
255. Burstein, O., Shoshan, N., Doron, R. & Akirav, I. Cannabinoids prevent depressive-like symptoms and alterations in BDNF expression in a rat model of PTSD. *Prog. Neuro-Psychopharmacology Biol. Psychiatry* **84**, 129–139 (2018).
256. Calabrese, E. J. & Rubio-Casillas, A. Biphasic effects of THC in memory and cognition. *European Journal of Clinical Investigation* **48**, e12920 (2018).
257. Grotenhermen, F. & Müller-Vahl, K. The Therapeutic Potential of Cannabis and

Cannabinoids. *Dtsch. Aerzteblatt Online* **109**, 495–501 (2012).

258. Borgelt, L. M., Franson, K. L., Nussbaum, A. M. & Wang, G. S. The pharmacologic and clinical effects of medical cannabis. *Pharmacotherapy* **33**, 195–209 (2013).
259. Aizpurua-Olaizola, O. *et al.* Targeting the endocannabinoid system: future therapeutic strategies. *Drug Discovery Today* (2017). doi:10.1016/j.drudis.2016.08.005
260. Donvito, G. *et al.* The Endogenous Cannabinoid System: A Budding Source of Targets for Treating Inflammatory and Neuropathic Pain. *Neuropsychopharmacology* **43**, 52–79 (2018).
261. Bonomo, Y., Souza, J. D. S., Jackson, A., Crippa, J. A. S. & Solowij, N. Clinical issues in cannabis use. *British Journal of Clinical Pharmacology* **84**, 2495–2498 (2018).
262. Schultz, C. & Engelhardt, M. Anatomy of the hippocampal formation. in *The Hippocampus in Clinical Neuroscience* 6–17 (2014). doi:10.1159/000360925
263. Amaral, D., Lavenex, P. & Andersen, P. Hippocampal neuroanatomy. in *The hippocampus book* (2007).
264. Knierim, J. J. The hippocampus. *Current Biology* **25**, 1116–1121 (2015).
265. Poppenk, J., Evensmoen, H. R., Moscovitch, M. & Nadel, L. Long-axis specialization of the human hippocampus. *Trends Cogn. Sci.* **17**, 230–240 (2013).
266. Robinson, J. L. *et al.* Neurofunctional topography of the human hippocampus. *Hum. Brain Mapp.* **36**, 5018–5037 (2015).
267. Scarante, F. F. *et al.* Cannabinoid Modulation of the Stressed Hippocampus. *Front. Mol. Neurosci.* **10**, 411 (2017).
268. Jacob, W., Marsch, R., Marsicano, G., Lutz, B. & Wotjak, C. T. Cannabinoid CB1 receptor deficiency increases contextual fear memory under highly aversive conditions and long-term potentiation in vivo. *Neurobiol. Learn. Mem.* **98**, 47–55 (2012).
269. Marsicano, G. *et al.* The endogenous cannabinoid system controls extinction of aversive memories. *Nature* **418**, 530–534 (2002).
270. Steindel, F. *et al.* Neuron-type specific cannabinoid-mediated G protein signalling in mouse hippocampus. *J. Neurochem.* **124**, 795–807 (2013).
271. Massa, F. *et al.* Alterations in the Hippocampal Endocannabinoid System in Diet-Induced Obese Mice. *J. Neurosci.* **30**, 6273–6281 (2010).
272. Hagihara, H., Toyama, K., Yamasaki, N. & Miyakawa, T. Dissection of hippocampal dentate gyrus from adult mouse. *J. Vis. Exp.* **33**, 1543 (2010).
273. Farzi, A., Reichmann, F. & Holzer, P. The homeostatic role of neuropeptide Y in immune function and its impact on mood and behaviour. *Acta Physiologica* **213**, 603–627 (2015).
274. Ketchesin, K. D., Stinnett, G. S. & Seasholtz, A. F. Corticotropin-releasing hormone-binding protein and stress: from invertebrates to humans. *Stress* **20**, 449–464 (2017).
275. Ambrosini, A., Bresciani, L., Fracchia, S., Brunello, N. & Racagni, G. Metabotropic glutamate receptors negatively coupled to adenylate cyclase inhibit N-methyl-D-aspartate receptor activity and prevent neurotoxicity in mesencephalic neurons in vitro. *Mol. Pharmacol.* (1995).

276. Batish, M., Van Den Bogaard, P., Kramer, F. R. & Tyagi, S. Neuronal mRNAs travel singly into dendrites. *Proc. Natl. Acad. Sci. U. S. A.* **109**, 4645–4650 (2012).
277. Andreassi, C., Crerar, H. & Riccio, A. Post-transcriptional processing of mRNA in neurons: The vestiges of the RNA world drive transcriptome diversity. *Frontiers in Molecular Neuroscience* (2018). doi:10.3389/fnmol.2018.00304
278. Gaidatzis, D., Burger, L., Florescu, M. & Stadler, M. B. Analysis of intronic and exonic reads in RNA-seq data characterizes transcriptional and post-transcriptional regulation. *Nat. Biotechnol.* **33**, 722–729 (2015).
279. Ruehle, S., Rey, A. A., Remmers, F. & Lutz, B. The endocannabinoid system in anxiety, fear memory and habituation. *J. Psychopharmacol.* **26**, 23–39 (2012).
280. Yoon, Y. J. *et al.* Glutamate-induced RNA localization and translation in neurons. *Proc. Natl. Acad. Sci. U. S. A.* **113**, E6877–E6886 (2016).
281. Chen, Y., Wang, Y., Modrusan, Z., Sheng, M. & Kaminker, J. S. Regulation of neuronal gene expression and survival by basal NMDA receptor activity: A role for histone deacetylase 4. *J. Neurosci.* **34**, 15327–15339 (2014).
282. Ativie, F. *et al.* Cannabinoid 1 Receptor Signaling on Hippocampal GABAergic Neurons Influences Microglial Activity. *Front. Mol. Neurosci.* **11**, 295 (2018).
283. Gaidatzis, D., Burger, L., Florescu, M. & Stadler, M. B. Analysis of intronic and exonic reads in RNA-seq data characterizes transcriptional and post-transcriptional regulation. *Nat. Biotechnol.* **33**, 722–729 (2015).
284. Pulecio, J., Verma, N., Mejía-Ramírez, E., Huangfu, D. & Raya, A. CRISPR/Cas9-Based Engineering of the Epigenome. *Cell Stem Cell* **21**, 431–447 (2017).
285. Lorsch, Z. S. *et al.* Stress resilience is promoted by a Zfp189-driven transcriptional network in prefrontal cortex. *Nat. Neurosci.* **22**, 1413–1423 (2019).
286. Crocq, M. A. & Crocq, L. From shell shock and war neurosis to posttraumatic stress disorder: a history of psychotraumatology. *Dialogues Clin. Neurosci.* **2**, 47–55 (2000).
287. Pinel, P. *Nosographie Philosophique*. (1798).
288. Ellis, P. S. The origins of the war neuroses. *J. R. Nav. Med. Serv.* **70**, 168–177 (1985).
289. Salmon, T. W. *The care and treatment of mental diseases and war neuroses ("Shell Shock") in the British Army*. *Mental Hygiene* (1917).
290. Kardiner, A. & Spiegel, H. *War Stress and Neurotic Illness*. *American Journal of Psychiatry* (1947). doi:10.1176/ajp.104.11.749-b
291. Harris, S. L. DSM-III. *Child Behav. Ther.* (1979). doi:10.1300/j473v01n01_05
292. Naftolowitz, D. F., Donovan, S. & Frances, A. DSM-IV. *CNS Drugs* (1995). doi:10.2165/00023210-199504010-00001
293. Guina, J. *et al.* Should Posttraumatic Stress Be a Disorder or a Specifier? Towards Improved Nosology Within the DSM Categorical Classification System. *Current Psychiatry Reports* **19**, 10 (2017).
294. Stein, J. Y., Wilmot, D. V. & Solomon, Z. Does one size fit all? Nosological, clinical, and scientific implications of variations in PTSD Criterion A. *Journal of Anxiety Disorders* **43**,

106–117 (2016).

295. Steel, Z. *et al.* Association of torture and other potentially traumatic events with mental health outcomes among populations exposed to mass conflict and displacement: A systematic review and meta-analysis. *JAMA - Journal of the American Medical Association* **302**, 537–549 (2009).
296. Afifi, T. O., Asmundson, G. J. G., Taylor, S. & Jang, K. L. The role of genes and environment on trauma exposure and posttraumatic stress disorder symptoms: A review of twin studies. *Clinical Psychology Review* (2010). doi:10.1016/j.cpr.2009.10.002
297. Richter-Levin, G., Stork, O. & Schmidt, M. V. Animal models of PTSD: a challenge to be met. *Mol. Psychiatry* **24**, 1135–1156 (2018).
298. Mahan, A. L. & Ressler, K. J. Fear conditioning, synaptic plasticity and the amygdala: Implications for posttraumatic stress disorder. *Trends in Neurosciences* **35**, 24–35 (2012).
299. Rau, V., DeCola, J. P. & Fanselow, M. S. Stress-induced enhancement of fear learning: An animal model of posttraumatic stress disorder. *Neurosci. Biobehav. Rev.* **29**, 1207–1223 (2005).
300. Armario, A., Escorihuela, R. M. & Nadal, R. Long-term neuroendocrine and behavioural effects of a single exposure to stress in adult animals. *Neuroscience and Biobehavioral Reviews* **32**, 1121–1135 (2008).
301. Liberzon, I., Krstov, M. & Young, E. A. Stress-restress: Effects on ACTH and fast feedback. *Psychoneuroendocrinology* **22**, 443–453 (1997).
302. Zoladz, P. R., Conrad, C. D., Fleshner, M. & Diamond, D. M. Acute episodes of predator exposure in conjunction with chronic social instability as an animal model of post-traumatic stress disorder. *Stress* **11**, 259–281 (2008).
303. Richter-Levin, G. Acute and long-term behavioral correlates of underwater trauma-potential relevance to stress and post-stress syndromes. *Psychiatry Res.* **79**, 73–83 (1998).
304. McGuire, J., Herman, J. P., Horn, P. S., Sallee, F. R. & Sah, R. Enhanced fear recall and emotional arousal in rats recovering from chronic variable stress. *Physiol. Behav.* **101**, 474–482 (2010).
305. Malikowska-Racia, N. & Salat, K. Recent advances in the neurobiology of posttraumatic stress disorder: A review of possible mechanisms underlying an effective pharmacotherapy. *Pharmacological Research* **142**, 30–49 (2019).
306. Girgenti, M. J., Hare, B. D., Ghosal, S. & Duman, R. S. Molecular and Cellular Effects of Traumatic Stress: Implications for PTSD. *Curr. Psychiatry Rep.* **19**, 85 (2017).
307. de Kloet, C. S. *et al.* Elevated plasma corticotropin-releasing hormone levels in veterans with posttraumatic stress disorder. *Progress in Brain Research* **167**, 287–291 (2007).
308. Baker, D. G. *et al.* Serial CSF corticotropin-releasing hormone levels and adrenocortical activity in combat veterans with posttraumatic stress disorder. *Am. J. Psychiatry* **156**, 585–588 (1999).
309. Flandreau, E. *et al.* Cell type-specific modifications of corticotropin-releasing factor (CRF)

and its type 1 receptor (CRF1) on startle behavior and sensorimotor gating. *Psychoneuroendocrinology* **53**, 16–28 (2015).

310. Thoeringer, C. K. *et al.* Consolidation of remote fear memories involves corticotropin-releasing hormone (CRH) receptor type 1-mediated enhancement of AMPA receptor GluR1 signaling in the dentate gyrus. *Neuropsychopharmacology* **37**, 787–796 (2012).
311. Ströhle, A., Scheel, M., Modell, S. & Holsboer, F. Blunted ACTH response to dexamethasone suppression-CRH stimulation in posttraumatic stress disorder. *J. Psychiatr. Res.* **42**, 1185–1188 (2008).
312. de Kloet, C. S., Vermetten, E., Rademaker, A. R., Geuze, E. & Westenberg, H. G. M. Neuroendocrine and immune responses to a cognitive stress challenge in veterans with and without PTSD. *Eur. J. Psychotraumatol.* **3**, 16206 (2012).
313. Olff, M., Güzelcan, Y., de Vries, G. J., Assies, J. & Gersons, B. P. R. HPA- and HPT-axis alterations in chronic posttraumatic stress disorder. *Psychoneuroendocrinology* **31**, 1220–1230 (2006).
314. Sriram, K., Rodriguez-Fernandez, M. & Doyle, F. J. Modeling cortisol dynamics in the neuro-endocrine axis distinguishes normal, depression, and post-traumatic stress disorder (PTSD) in humans. *PLoS Comput. Biol.* **8**, e1002379 (2012).
315. Michopoulos, V. *et al.* Dexamethasone facilitates fear extinction and safety discrimination in PTSD: A placebo-controlled, double-blind study. *Psychoneuroendocrinology* **83**, 65–71 (2017).
316. Luther, J. A. *et al.* Neurosecretory and non-neurosecretory parvocellular neurones of the hypothalamic paraventricular nucleus express distinct electrophysiological properties. *J. Neuroendocrinol.* **14**, 929–932 (2002).
317. Ramot, A. *et al.* Hypothalamic CRFR1 is essential for HPA axis regulation following chronic stress. *Nat. Neurosci.* **20**, 385–388 (2017).
318. Jiang, Z., Rajamanickam, S. & Justice, N. J. Local corticotropin-releasing factor signaling in the hypothalamic paraventricular nucleus. *J. Neurosci.* **38**, 1874–1890 (2018).
319. Manteghi, A. A., Hebrani, P., Mortezania, M., Haghighi, M. B. & Javanbakht, A. Baclofen add-on to citalopram in treatment of posttraumatic stress disorder. *J. Clin. Psychopharmacol.* **34**, 240–243 (2014).
320. Drake, R. G. *et al.* Baclofen treatment for chronic posttraumatic stress disorder. *Ann. Pharmacother.* **37**, 1177–1181 (2003).
321. Cole, R. L. & Sawchenko, P. E. Neurotransmitter regulation of cellular activation and neuropeptide gene expression in the paraventricular nucleus of the hypothalamus. *J. Neurosci.* **22**, 959–969 (2002).
322. Trousselard, M. *et al.* Is plasma GABA level a biomarker of Post-Traumatic Stress Disorder (PTSD) severity? A preliminary study. *Psychiatry Res.* **241**, 273–279 (2016).
323. Vaiva, G. *et al.* Relationship between posttrauma GABA plasma levels and PTSD at 1-year follow-up. *Am. J. Psychiatry* **163**, 1446–1448 (2006).
324. Vaiva, G. *et al.* Low posttrauma GABA plasma levels as a predictive factor in the

development of acute posttraumatic stress disorder. *Biol. Psychiatry* **55**, 250–254 (2004).

325. Wamsteeker, J. I., Kuzmiski, J. B. & Bains, J. S. Repeated stress impairs endocannabinoid signaling in the paraventricular nucleus of the hypothalamus. *J. Neurosci.* **30**, 11188–11196 (2010).
326. Ziegler, D. R., Cullinan, W. E. & Herman, J. P. Organization and regulation of paraventricular nucleus glutamate signaling systems: N-methyl-D-aspartate receptors. *J. Comp. Neurol.* **484**, 43–56 (2005).
327. Ramaswamy, S., Madabushi, J., Hunziker, J., Bhatia, S. C. & Petty, F. An open-label trial of memantine for cognitive impairment in patients with posttraumatic stress disorder. *J. Aging Res.* **2015**, 934162 (2015).
328. Hartberg, J., Garrett-Walcott, S. & De Gioannis, A. Impact of oral ketamine augmentation on hospital admissions in treatment-resistant depression and PTSD: a retrospective study. *Psychopharmacology (Berl).* **135**, 393–398 (2018).
329. Brewin, C. R., Gregory, J. D., Lipton, M. & Burgess, N. Intrusive Images in Psychological Disorders: Characteristics, Neural Mechanisms, and Treatment Implications. *Psychol. Rev.* **117**, 210–232 (2010).
330. Tse, Y. C. *et al.* A longitudinal study of stress-induced hippocampal volume changes in mice that are susceptible or resilient to chronic social defeat. *Hippocampus* **24**, 1120–1128 (2014).
331. Gilbertson, M. W. *et al.* Smaller hippocampal volume predicts pathologic vulnerability to psychological trauma. *Nat. Neurosci.* **5**, 1242–1247 (2002).
332. Logue, M. W. *et al.* Smaller Hippocampal Volume in Posttraumatic Stress Disorder: A Multisite ENIGMA-PGC Study: Subcortical Volumetry Results From Posttraumatic Stress Disorder Consortia. *Biol. Psychiatry* **83**, 244–253 (2018).
333. Acheson, D. T., Gresack, J. E. & Risbrough, V. B. Hippocampal dysfunction effects on context memory: Possible etiology for posttraumatic stress disorder. *Neuropharmacology* (2012). doi:10.1016/j.neuropharm.2011.04.029
334. Zhang, Y., Zheng, Y., Xu, Y., Sheng, H. & Ni, X. Corticotropin-releasing hormone suppresses synapse formation in the hippocampus of male rats via inhibition of CXCL5 secretion by glia. *Endocrinology* **159**, 622–638 (2018).
335. Zhe, D., Fang, H. & Yuxiu, S. Expressions of hippocampal mineralocorticoid receptor (MR) and glucocorticoid receptor (GR) in the single-prolonged stress-rats. *Acta Histochem. Cytochem.* **41**, 89–95 (2008).
336. Lakshminarasimhan, H. & Chattarji, S. Stress leads to contrasting effects on the levels of brain derived neurotrophic factor in the hippocampus and amygdala. *PLoS One* **7**, e30481 (2012).
337. Stansley, B. J. *et al.* Contextual fear extinction induces hippocampal metaplasticity mediated by metabotropic glutamate receptor 5. *Cereb. Cortex* **28**, 4291–4304 (2018).
338. Riedel, G., Casabona, G., Platt, B., MacPhail, E. M. & Nicoletti, F. Fear conditioning-induced time- and subregion-specific increase in expression of mGlu5 receptor protein in

rat hippocampus. *Neuropharmacology* **39**, 1943–1951 (2000).

339. Rosenberg, N., Gerber, U. & Ster, J. Activation of group II metabotropic glutamate receptors promotes LTP induction at schaffer collateral-CA1 pyramidal cell synapses by priming NMDA receptors. *J. Neurosci.* **36**, 11521–11531 (2016).
340. Morena, M. *et al.* Enhancing Endocannabinoid Neurotransmission Augments the Efficacy of Extinction Training and Ameliorates Traumatic Stress-Induced Behavioral Alterations in Rats. *Neuropsychopharmacology* **43**, 1284–1296 (2018).
341. Hill, M. N., Campolongo, P., Yehuda, R. & Patel, S. Integrating Endocannabinoid Signaling and Cannabinoids into the Biology and Treatment of Posttraumatic Stress Disorder. *Neuropsychopharmacology* **43**, 80–102 (2018).
342. Koch, S. B. J. *et al.* Aberrant resting-state brain activity in posttraumatic disorder: a meta-analysis and systematic review. *Depression and Anxiety* **33**, 592–605 (2016).
343. Díaz-Mataix, L. *et al.* Characterization of the amplificatory effect of norepinephrine in the acquisition of Pavlovian threat associations. *Learn. Mem.* **24**, 432–439 (2017).
344. Jolkkonen, E. & Pitkänen, A. Intrinsic connections of the rat amygdaloid complex: Projections originating in the central nucleus. *J. Comp. Neurol.* **395**, 53–72 (1998).
345. Tzanoulinou, S. *et al.* Long-term behavioral programming induced by peripuberty stress in rats is accompanied by gabaergic- related alterations in the amygdala. *PLoS One* **9**, e94666 (2014).
346. Wilensky, A. E., Schafe, G. E., Kristensen, M. P. & LeDoux, J. E. Rethinking the fear circuit: The central nucleus of the amygdala is required for the acquisition, consolidation, and expression of pavlovian fear conditioning. *J. Neurosci.* **26**, 12387–12396 (2006).
347. Geuze, E. *et al.* Reduced GABAA benzodiazepine receptor binding in veterans with post-traumatic stress disorder. *Mol. Psychiatry* **13**, 74–83 (2008).
348. Ramikie, T. S. & Patel, S. Endocannabinoid signaling in the amygdala: Anatomy, synaptic signaling, behavior, and adaptations to stress. *Neuroscience* **204**, 38–52 (2012).
349. Azad, S. C. *et al.* Circuitry for associative plasticity in the amygdala involves endocannabinoid signaling. *J. Neurosci.* **24**, 9953–9961 (2004).
350. Fidelman, S., Mizrachi Zer-Aviv, T., Lange, R., Hillard, C. J. & Akirav, I. Chronic treatment with URB597 ameliorates post-stress symptoms in a rat model of PTSD. *Eur. Neuropsychopharmacol.* **28**, 630–642 (2018).
351. Neumeister, A. *et al.* Elevated brain cannabinoid CB 1 receptor availability in post-traumatic stress disorder: A positron emission tomography study. *Mol. Psychiatry* **18**, 1034–1040 (2013).
352. Shoshan, N. & Akirav, I. The effects of cannabinoid receptors activation and glucocorticoid receptors deactivation in the amygdala and hippocampus on the consolidation of a traumatic event. *Neurobiol. Learn. Mem.* **144**, 248–258 (2017).
353. Berardi, A., Schelling, G. & Campolongo, P. The endocannabinoid system and Post Traumatic Stress Disorder (PTSD): From preclinical findings to innovative therapeutic approaches in clinical settings. *Pharmacol. Res.* **111**, 668–678 (2016).

354. Landmann, N. *et al.* The reorganisation of memory during sleep. *Sleep Medicine Reviews* **18**, 531–541 (2014).
355. Landmann, N. *et al.* REM sleep and memory reorganization: Potential relevance for psychiatry and psychotherapy. *Neurobiology of Learning and Memory* **122**, 28–40 (2015).
356. Harada, K., Yamaji, T. & Matsuoka, N. Activation of the serotonin 5-HT2C receptor is involved in the enhanced anxiety in rats after single-prolonged stress. *Pharmacol. Biochem. Behav.* **89**, 11–16 (2008).
357. Baratta, M. V. *et al.* Stress Enables Reinforcement-Elicited Serotonergic Consolidation of Fear Memory. *Biol. Psychiatry* **79**, 814–822 (2016).
358. Bremner, J. D. & Vermetten, E. Neuroanatomical changes associated with pharmacotherapy in posttraumatic stress disorder. in *Annals of the New York Academy of Sciences* 154–157 (2004). doi:10.1196/annals.1314.012
359. Wade, D. M. *et al.* Intrusive memories of hallucinations and delusions in traumatized intensive care patients: An interview study. *Br. J. Health Psychol.* **20**, 613–631 (2015).
360. González-Maeso, J. *et al.* Identification of a serotonin/glutamate receptor complex implicated in psychosis. *Nature* **452**, 93–97 (2008).
361. Buffalari, D. M. & Grace, A. A. Noradrenergic modulation of basolateral amygdala neuronal activity: Opposing influences of α-2 and β receptor activation. *J. Neurosci.* **27**, 12358–12366 (2007).
362. Pidoplichko, V. I., Prager, E. M., Aroniadou-Anderjaska, V. & Braga, M. F. M. α7-Containing nicotinic acetylcholine receptors on interneurons of the basolateral amygdala and their role in the regulation of the network excitability. *J. Neurophysiol.* **110**, 2358–2369 (2013).
363. Vallejo, A. G. *et al.* Propofol-induced deep sedation reduces emotional episodic memory reconsolidation in humans. *Sci. Adv.* **5**, eaav3801 (2019).
364. Williams, L. M. *et al.* Trauma modulates amygdala and medial prefrontal responses to consciously attended fear. *Neuroimage* **29**, 347–357 (2006).
365. Bremner, J. D. *et al.* Decreased benzodiazepine receptor binding in prefrontal cortex in combat-related posttraumatic stress disorder. *Am. J. Psychiatry* **157**, 1120–1126 (2000).
366. Kugaya, A. *et al.* Cerebral benzodiazepine receptors in depressed patients measured with [123I]iomazenil SPECT. *Biol. Psychiatry* **54**, 792–799 (2003).
367. Geracioti, T. D. *et al.* Effect of traumatic imagery on cerebrospinal fluid dopamine and serotonin metabolites in posttraumatic stress disorder. *J. Psychiatr. Res.* **47**, 995–998 (2013).
368. Birnbaum, S., Gobeske, K. T., Auerbach, J., Taylor, J. R. & Arnsten, A. F. T. A role for norepinephrine in stress-induced cognitive deficits: α-1-Adrenoceptor mediation in the prefrontal cortex. *Biol. Psychiatry* **46**, 1266–1274 (1999).
369. Sun, X. R. *et al.* Amelioration of oxidative stress-induced phenotype loss of parvalbumin interneurons might contribute to the beneficial effects of environmental enrichment in a rat model of post-traumatic stress disorder. *Behav. Brain Res.* **312**, 84–92 (2016).

370. Müller, I., Obata, K., Richter-Levin, G. & Stork, O. GAD65 haplodeficiency conveys resilience in animal models of stress-induced psychopathology. *Front. Behav. Neurosci.* **8**, 265 (2014).
371. Lguensat, A., Bentefour, Y., Bennis, M., Ba-M'hamed, S. & Garcia, R. Susceptibility and Resilience to PTSD-Like Symptoms in Mice Are Associated with Opposite Dendritic Changes in the Prelimbic and Infralimbic Cortices Following Trauma. *Neuroscience* **418**, 166–176 (2019).
372. Naegeli, C. *et al.* Locus Coeruleus Activity Mediates Hyperresponsiveness in Posttraumatic Stress Disorder. *Biol. Psychiatry* **83**, 254–262 (2018).
373. Bangasser, D. A., Wiersielis, K. R. & Khantsis, S. Sex differences in the locus coeruleus-norepinephrine system and its regulation by stress. *Brain Research* **1641**, 177–188 (2016).
374. Roelofs, K. Freeze for action: Neurobiological mechanisms in animal and human freezing. *Philosophical Transactions of the Royal Society B: Biological Sciences* **372**, (2017).
375. Morey, R. A. *et al.* Fear learning circuitry is biased toward generalization of fear associations in posttraumatic stress disorder. *Transl. Psychiatry* **5**, e700 (2015).
376. Siegmund, A. & Wotjak, C. T. A mouse model of posttraumatic stress disorder that distinguishes between conditioned and sensitised fear. *J. Psychiatr. Res.* **41**, 848–860 (2007).
377. Lerner, R. *et al.* Simultaneous lipidomic and transcriptomic profiling in mouse brain punches of acute epileptic seizure model compared to controls. *J. Lipid Res.* **59**, 283–297 (2018).
378. Lerner, R., Cuadrado, D. P., Post, J. M., Lutz, B. & Bindila, L. Broad lipidomic and transcriptional changes of prophylactic pea administration in adult mice. *Front. Neurosci.* **13**, 527 (2019).
379. Hoppen, T. H. & Morina, N. The prevalence of PTSD and major depression in the global population of adult war survivors: a meta-analytically informed estimate in absolute numbers. *Eur. J. Psychotraumatol.* **10**, 1578637 (2019).
380. Dai, W. *et al.* Comorbidity of post-traumatic stress disorder and anxiety in flood survivors. *Med. (United States)* **96**, 79–94 (2017).
381. Ginzburg, K., Ein-Dor, T. & Solomon, Z. Comorbidity of posttraumatic stress disorder, anxiety and depression: A 20-year longitudinal study of war veterans. *J. Affect. Disord.* **123**, 249–257 (2010).
382. Strange, B. A., Witter, M. P., Lein, E. S. & Moser, E. I. Functional organization of the hippocampal longitudinal axis. *Nature Reviews Neuroscience* **15**, 655–669 (2014).
383. Janak, P. H. & Tye, K. M. From circuits to behaviour in the amygdala. *Nature* **517**, 284–292 (2015).
384. LeDoux, J. The amygdala. *Current Biology* **17**, 868–874 (2007).
385. Floresco, S. B. The Nucleus Accumbens: An Interface Between Cognition, Emotion, and Action. *Annu. Rev. Psychol.* **66**, 25–52 (2015).

386. Han, Y. & Lu, L. The Other Face of the Nucleus Accumbens: Aversion. *Neurosci. Bull.* **32**, 569–571 (2016).
387. Müller, C. P. *et al.* Brain membrane lipids in major depression and anxiety disorders. *Biochimica et Biophysica Acta - Molecular and Cell Biology of Lipids* **1851**, 1052–1065 (2015).
388. Schneider, M. *et al.* Lipids in psychiatric disorders and preventive medicine. *Neuroscience and Biobehavioral Reviews* **76**, 336–362 (2017).
389. Parekh, A., Smeeth, D., Milner, Y. & Thuret, S. The Role of Lipid Biomarkers in Major Depression. *Healthcare* **5**, 5 (2017).
390. Furuyashiki, T., Akiyama, S. & Kitaoka, S. Roles of multiple lipid mediators in stress and depression. *Int. Immunol.* **31**, 579–587 (2019).
391. Bluett, R. J. *et al.* Endocannabinoid signalling modulates susceptibility to traumatic stress exposure. *Nat. Commun.* **8**, (2017).
392. Jenniches, I. *et al.* Anxiety, Stress, and Fear Response in Mice with Reduced Endocannabinoid Levels. *Biol. Psychiatry* **79**, 858–868 (2016).
393. Torres-Fuentes, C., Schellekens, H., Dinan, T. G. & Cryan, J. F. The microbiota–gut–brain axis in obesity. *The Lancet Gastroenterology and Hepatology* **2**, 747–756 (2017).
394. Maruvada, P., Leone, V., Kaplan, L. M. & Chang, E. B. The Human Microbiome and Obesity: Moving beyond Associations. *Cell Host and Microbe* **22**, 589–599 (2017).
395. Johnson, E. L., Heaver, S. L., Walters, W. A. & Ley, R. E. Microbiome and metabolic disease: revisiting the bacterial phylum Bacteroidetes. *Journal of Molecular Medicine* **95**, 1–8 (2017).
396. Pascale, A., Marchesi, N., Govoni, S., Coppola, A. & Gazzaruso, C. The role of gut microbiota in obesity, diabetes mellitus, and effect of metformin: new insights into old diseases. *Current Opinion in Pharmacology* **49**, 1–5 (2019).
397. Vuong, H. E., Yano, J. M., Fung, T. C. & Hsiao, E. Y. The Microbiome and Host Behavior. *Annu. Rev. Neurosci.* **40**, 21–49 (2017).
398. Rook, G. A. W., Raison, C. L. & Lowry, C. A. Microbiota, immunoregulatory old friends and psychiatric disorders. *Adv. Exp. Med. Biol.* **817**, 319–356 (2014).
399. McGaughey, K. D. *et al.* Relative abundance of Akkermansia spp. and other bacterial phylotypes correlates with anxiety- and depressive-like behavior following social defeat in mice. *Sci. Rep.* **9**, 3281 (2019).
400. Lopetuso, L. R., Scaldaferri, F., Petito, V. & Gasbarrini, A. Commensal Clostridia: Leading players in the maintenance of gut homeostasis. *Gut Pathogens* **5**, 23 (2013).
401. Zhang, K. *et al.* Abnormal composition of gut microbiota is associated with resilience versus susceptibility to inescapable electric stress. *Transl. Psychiatry* **9**, 231 (2019).
402. Shalev, A., Liberzon, I. & Marmar, C. Post-traumatic stress disorder. *N. Engl. J. Med.* **376**, 2459–2460 (2017).
403. Kessler, R. C. *et al.* Trauma and PTSD in the WHO World Mental Health Surveys. *European Journal of Psychotraumatology* **8**, (2017).

404. Van Meer, G., Voelker, D. R. & Feigenson, G. W. Membrane lipids: Where they are and how they behave. *Nature Reviews Molecular Cell Biology* **9**, 112–124 (2008).
405. Abdullah, L. *et al.* Lipidomic profiling of phosphocholine containing brain lipids in mice with sensorimotor deficits and anxiety-like features after exposure to gulf war agents. *NeuroMolecular Med.* (2012). doi:10.1007/s12017-012-8192-z
406. Faria, R. *et al.* Alterations in phospholipidomic profile in the brain of mouse model of depression induced by chronic unpredictable stress. *Neuroscience* **273**, 1–11 (2014).
407. Oliveira, T. G. *et al.* The impact of chronic stress on the rat brain lipidome. *Mol. Psychiatry* **21**, 80–88 (2016).
408. Ghasemi, R., Dargahi, L. & Ahmadiani, A. Integrated sphingosine-1 phosphate signaling in the central nervous system: From physiological equilibrium to pathological damage. *Pharmacological Research* **104**, 156–164 (2016).
409. Huston, J. P. *et al.* A sphingolipid mechanism for behavioral extinction. *J. Neurochem.* **137**, 589–603 (2016).
410. Czubowicz, K., Jęśko, H., Wencel, P., Lukiw, W. J. & Strosznajder, R. P. The Role of Ceramide and Sphingosine-1-Phosphate in Alzheimer's Disease and Other Neurodegenerative Disorders. *Molecular Neurobiology* **56**, 5436–5455 (2019).
411. Pujol-Lereis, L. M. Alteration of Sphingolipids in Biofluids: Implications for Neurodegenerative Diseases. *Int. J. Mol. Sci.* **20**, 3564 (2019).
412. Hellhammer, J., Vogt, D., Franz, N., Freitas, U. & Rutenberg, D. A soy-based phosphatidylserine/ phosphatidic acid complex (PAS) normalizes the stress reactivity of hypothalamus-pituitary-adrenal-axis in chronically stressed male subjects: A randomized, placebo-controlled study. *Lipids Health Dis.* **13**, 121 (2014).
413. Leo, L. M. *et al.* GPR55-mediated effects on brain microvascular endothelial cells and the blood-brain barrier. *Neuroscience* **414**, 88–98 (2019).
414. Dlugos, A., Childs, E., Stuhr, K. L., Hillard, C. J. & De Wit, H. Acute stress increases circulating anandamide and other n-acylethanolamines in healthy humans. *Neuropsychopharmacology* **37**, 2416–2427 (2012).
415. Bassir Nia, A., Bender, R. & Harpaz-Rotem, I. Endocannabinoid System Alterations in Posttraumatic Stress Disorder: A Review of Developmental and Accumulative Effects of Trauma. *Chronic Stress* **3**, (2019).
416. Rizzatti, G., Lopetuso, L. R., Gibiino, G., Binda, C. & Gasbarrini, A. Proteobacteria: A common factor in human diseases. *BioMed Research International* **9**, 1–7 (2017).
417. Méndez-Salazar, E. O., Ortiz-López, M. G., Granados-Silvestre, M. D. L. Á., Palacios-González, B. & Menjivar, M. Altered gut microbiota and compositional changes in firmicutes and proteobacteria in mexican undernourished and obese children. *Front. Microbiol.* **9**, 2494 (2018).
418. Hechler, C. *et al.* Association between Psychosocial Stress and Fecal Microbiota in Pregnant Women. *Sci. Rep.* **9**, 4463 (2019).
419. Everard, A. *et al.* Cross-talk between Akkermansia muciniphila and intestinal epithelium

controls diet-induced obesity. *Proc. Natl. Acad. Sci. U. S. A.* **110**, 9066–9071 (2013).

420. Dao, M. C. *et al.* Akkermansia muciniphila and improved metabolic health during a dietary intervention in obesity: Relationship with gut microbiome richness and ecology. *Gut* **65**, 426–36 (2016).

421. Foster, J. A., Rinaman, L. & Cryan, J. F. Stress & the gut-brain axis: Regulation by the microbiome. *Neurobiology of Stress* **7**, 124–136 (2017).

7. Appendix

7.1 List of abbreviations

A ……

2-AG	2-arachidonoylglycerol
AA	Arachidonic acid
ABHD6/12	α-β hydrolase 6 / 12
AC	Adenylyl cyclase
ACN	Acetonitrile
ACTH	Adrenocorticotropic hormone
AEA	Anandamide
AMPA	α-amino-3-hydroxy-5-methyl-4-isoxazolepropionic acid receptor
APA	American psychiatry association
ASR	Acoustic startle response
ATAC	Assay for transposase-accessible chromatin

B ……

BDNF	Brain-derived neurotrophic factor
BLA	Basolateral nucleus of the amygdala
BNST	Bed nucleus of the stria terminalis

C ……

C1P	Ceramide-1-phosphate
CA	Cornu ammonis
CA^{2+}	Calcium
cAMP	Cyclic adenosine monophosphate
CB1	Cannabinoid receptor type-1
CB2	Cannabinoid receptor type-2
cDNA	Complementary DNA
CeA	Central nucleus of the amygdala
CER	Ceramide
CF	Contextual fear
CNS	Central nervous system
COX-2	Cyclooxygenase-2
CRH	Corticotropin-releasing hormone
CRH_1R	CRH receptor-1
CRH_2R	CRH receptor-2
CRISPR	Clustered regularly interspaced short palindromic repeats
CSF	Cerebrospinal fluid

D ……

DAG	Diacylglycerol
DAGL-α/β	Diacylglycerol lipase-α / –β
DEG	Differentially expressed gene
DG	Dentate gyrus
DGE	Differential gene expression
DHEA	Dehydroepiandrosterone
DSE	Depolarization-induced suppression of excitation
DSI	Depolarization-induced suppression of inhibition
DSM	Diagnostic and statistical manual

E ……

eCB	Endocannabinoids

eCB-LTD	Endocannabinoid-mediated long-term depression
eCB-STD	Endocannabinoid-mediated short-term depression
ECS	Endocannabinoid system
EGR	Early growth response family
EISA	Exon-intron split analysis

F ……

FAAH	Fatty acid amide hydrolase
FS	Foot-shock

G ……

GABA	γ-aminobutyric acid
$GABA_AR$	GABA receptor type A
$GABA_BR$	GABA receptor type B
GAD	Generalized anxiety disorder
GAD67	Glutamate decarboxylase (67 kDa)
GC	Glucocorticoid hormones
GDNF	Glia-derived neurotrophic factor
GIRK	G protein-activated inwardly rectifying K^+ channel
GluR2/3	AMPA receptor subunit 2/3
GPCR	G-protein coupled receptor
GR	Glucocorticoid receptor

H ……

$5\text{-}HT_{1A/2A/2C}$	Serotonin receptor 1A/2A/2C
HbT	Holeboard test
HPA	Hypothalamic-pituitary-adrenal

I ……

IEG	Immediate early gene
ISTD	Internal standards

K ……

K^+	Potassium ion
KEGG	Kyoto encyclopedia of genes and genomes

L ……

LA	Lateral amygdala
LC	Locus coeruleus
LC/MS	Liquid chromatography / mass spectrometry
LPA	Lysophosphatidic acid
LPC	Lysophosphatidylcholine
LTD	Long-term depression
LTP	Long-term potentiation

M ……

MAGL	Monoacylglycerol lipase
MAPK	MAP kinase
MDD	Major depressive disorder
MeOH	Methanol
mGluR	Metabotropic glutamate receptor
mGluR5	Metabotropic glutamate receptor 5
MR	Mineralocorticoid receptor
mRNA	Messenger RNA
MTBE	Methyl tert-butyl ether

N ……

NAc	Nucleus accumbens
NAPE-PLD	*N-acyl* phosphatidylethanolamine-selective phospholipase D
NArPE	*N*-arachidonoyl phosphatidylethanolamine
NMDA	N-methyl-D-aspartate receptor

NMDAR	N-methyl-D-aspartate receptor
NPY	Neuropeptide Y
Nur	Nuclear receptor family

O ……

OTU	Operational taxonomical unit

P ……

PA	Phosphatidic acid
PAG	Pperiaqueductal gray
PBS	Phosphate-buffered saline
PC	Phosphatidylcholine
PE	Phosphatidylethanolamine
PEA	Palmitoylethanolamide
PFC	Prefrontal cortex
PG	Phosphatidylglycerol
PI	Phosphatidylinositol
PKA	Proteinkinase A
PL	Phospholipid
PPAR	Peroxisome proliferator-activated receptor
PS	Phosphatidylserine
PTSD	Posttraumatic stress disorder
PUFA	Polyunsaturated fatty acid
PVN	Paraventricular nucleus (hypothalamus)

R ……

R-	Phenotype vulnerable to stress
R+	Phenotype resilient to stress
RT	Room-temperature

S ……

S1P	Sphingosine-1-phosphate
SAM	Sympathoadrenal-medullary axis
sfGFP	Superfolder GFP
SIT	Social interaction test
SM	Sphingomyelin
SNS	Sympathetic nervous system
SPH	Sphingosine
SPT	Sucrose preference test
SSRI	Selective serotonin reuptake inhibitor

T ……

Δ^9-THC	Δ^9-tetrahydrocannabinol
TAM	Tamoxifen
TEA	Triethylamine
TRPV1	Transient receptor potential vanilloid 1

V ……

VACC	Voltage-gated Ca^{2+} channel
vmPFC	Ventromedial prefrontal cortex
VTA	Ventral tegmental area

7.2 List of figures

7.3 List of tables

"Nothing in life is to be feared, it is only to be understood.
Now is the time to understand more, so that we may fear less"

Maria Skłodowska-Curie